FOTOKÉMIAI ENERGIAVESZTÉSI ÉS ELEKTRONÁTADÁSI FOLYAMATOK KINETIKÁJA

Tézisszerű doktori értekezés

BICZÓK LÁSZLÓ

MTA KÖZPONTI KÉMIAI KUTATÓINTÉZET

BUDAPEST

1997

TARTALOMJEGYZÉK

I. BEVEZETÉS ÉS CÉLKITŰZÉS

A mindennapi életben egyre inkább tért hódítanak a fotokémiai reakciókon alapuló eljárások és termékek. A modern nyomdatechnikai és mikroelektronikai ipar, integrált áramkörök, kompakt lemezek gyártása, polimerek fotostabilizálása, fény hatására megkeményedő anyagok, optikai fehérítők, fluoreszcenciás érzékelő-berendezések tervezése elképzelhetetlen lenne fotokémiai ismeretek nélkül. A fototerápiás módszerek és a lézerek sebészeti alkalmazása új utakat nyit az orvostudományban is. Ígéretes eredmények születnek a rákos sejtek fénnyel történő elpusztítására alkalmas és a DNS-t meghatározott helyen hasító fotoszenzibilizátorok fejlesztése terén. Széleskörű kutatások folynak nem lineáris optikai sajátságokkal rendelkező szerves anyagok és gyors optikai kapcsolók előállítására.

A fotokémiai reakciók számos kedvező tulajdonsággal rendelkeznek. Alacsony hőmérsékleten is nagy reakciósebességgel játszódnak le, szelektivitásuk sokszor lényegesen jobb, mint a termikus reakcióké. A fotolizáló hullámhossz megválasztásával esetenként a fotokémiai átalakulás iránya is befolyásolható és gyakran közvetlenül előállíthatók olyan termékek, melyek egyébként csak több lépésben nyerhetők. Mindezek az előnyök azonban csak a reakciómechanizmus ismeretében, optimálisan megválasztott körülmények között kivitelezett reakciókkal realizálhatók. Ezért az elemi fotofizikai, fotokémiai folyamatok kutatása, a gerjesztett molekulák és rövid élettartamú köztitermékek szerkezete és reakciókészsége közötti kapcsolat feltárása nemcsak elméleti, hanem gyakorlati szempontból is igen fontos.

Értekezésemben a fotokémiai rendszerek két legfontosabb reakciótípusának, az energiavesztéssel járó reakcióknak és az elektronátadási folyamatoknak a szisztematikus kinetikai vizsgálatával szeretnék hozzájárulni olyan általános törvényszerűségek

felismeréséhez, melyek segíthetik a fény hatására lejátszódó átalakulások hatásfokának növelését. A modellrendszerek kiválasztásánál elsődleges szempontnak tartom, hogy valamilyen módon kapcsolódjanak már meglevő vagy potenciális alkalmazási lehetőségekhez és széleskörű érdeklődésre tartsanak számot.

Természetesen az elektronátadások és energiavesztéssel járó folyamatok nem határolhatók el élesen egymástól. Hiszen a gerjesztett molekulák és komplexek nemcsak fotofizikai átalakulással kerülhetnek alacsonyabb energiájú elektronállapotba, hanem a gerjesztési energia hővé alakulhat két egymást gyorsan követő, egymással ellentétes irányú elektronátadási reakcióban is. Ennek elkerülése a napenergia-hasznosítás egyik kulcsproblémája. A fotokémiai elektronátadási folyamatok és a gerjesztett állapotú komplexek (exciplexek) tanulmányozása is csak nehezen különíthető el, mert az elektronátvitel sok esetben exciplexeken keresztül, azok gyökionokra történő disszociálásával megy végbe. Poláros oldószerekben azonban az exciplexek élettartama általában oly rövid, hogy a rendelkezésre álló kísérleti technikákkal nem különböztethetők meg a különböző módon szolvatált gyökionpároktól.

Disszertációm első részében a fluorenonszármazékok példáján mutatom be, hogy a gerjesztett molekulák energiáját és élettartamát befolyásoló tényezők vizsgálata hogyan vezethet új, az eddigieknél több információt adó jelzőanyag felfedezéséhez. A fluorenont azért választom modellvegyületként, mert kedvező elnyelési színképe miatt származékait gyakran alkalmazzák fotopolimerizáció iniciálására és már a 60-as évek vége óta ismert, hogy reakcióinak kvantumhatásfoka erősen oldószerfüggő. Feltételeztem, hogy a fotofizikai folyamatok sebessége is jelentősen változni fog a közeg polaritásával, amit kihasználhatunk a gerjesztett fluorenon molekula mikrokörnyezetének jellemzésére. A korlátozott terjedelem miatt nem kerülhettek bele ebbe a fejezetbe a naftálimidek fotofizikai sajátságaival kapcsolatos vizsgálataink,

melyek eredményeként talált új fluoreszcenciás jelzőanyag tulajdonságait mikrokörnyezetének "viszkozitása" határozza meg.

Disszertációm második részében megmutatom, hogy hidrogénhídkötéssel vagy van der Waals kölcsönhatásokkal összekapcsolt gerjesztett állapotú dimerek fotofizikai sajátságai jelentősen eltérnek a monomer tulajdonságaitól. A másodlagos kötőerőkkel összetartott adduktumok fotofizikai és fotokémiai sajátságairól elég kevés ismeret áll rendelkezésre az irodalomban, pedig nagy fontosságúak lehetnek például biológiai rendszerekben és a fotoszintézis során.

Mivel a fluorenon fluoreszcenciás sajátságai alkoholokban és hidrogénhídkötés létesítésére nem képes oldószerekben teljesen eltérőek, ezért ígéretesnek látszik a fluorenon - alkohol és a fluorenon - fenolszármazék komplexek rendszeres vizsgálata. Tanulmányozom a hidrogénhídkötés erőssége és a fotofizikai folyamatok sebessége közötti kapcsolatot, valamint a fenolszármazékok által okozott kioltás mechanizmusát.

A van der Waals erőkkel összekapcsolt adduktumok közül a fluorenon-ciklodextrin komplexek fotofizikáját derítem fel. Kimutatom, hogy a fluorenon lényegesen jobb jelzőanyag a lokális polaritás érzékelésére, mint az eddig alkalmazottak. Segítségével ugyanis megkülönböztethető a hidrogénhíd-kölcsönhatás az oldószerrel történő egyéb, nem specifikus kölcsönhatásoktól. Választ keresek arra a kérdésre is, hogy a különböző fluoreszcenciás jelzőanyagokkal a ciklodextrin üregének lokális polaritására kapott irodalmi eredmények miért oly ellentmondásosak.

Az értekezésem harmadik, befejező részében fotokémiai elektronátadási folyamatok kinetikáját tanulmányozom. Az ilyen típusú vizsgálatok iránt jelenleg széles érdeklődés nyilvánul meg, mert az elektronátadási reakciók alapvető szerepet játszanak a fényenergia tárolása és kémiai energiává alakítása terén. Elsősorban triplett gerjesztett molekulákat (^{3}A) alkalmazok elektronakceptorként és az alapállapotú elektrondonor reakciópartner (Q) szerkezetét változtatva tanulmányozom a reakciósebességet és a gyökionképződés kvantumhatásfokát befolyásoló tényezőket. A fotokémiai

elektronátadási folyamatok alkalmazásakor a legfontosabb cél, hogy minél nagyobb hatásfokkal sikerüljön a töltésszeparációt (1a) megvalósítani.

$$^3A + Q \longrightarrow {}^3(A^{\bullet-}\, Q^{\bullet+}) \longrightarrow {}^3A^{\bullet-} + Q^{\bullet+} \qquad (1a)$$

$$\searrow \quad A + Q \qquad (1b)$$

Ez nem könnyű feladat, mert a primer folyamatban keletkező gyökionok között, amíg azok nem távolodnak el elegendő mértékben egymástól, az eredetivel ellentétes irányú elektronvándorlás is lejátszódhat (1b). Ha triplett gerjesztett molekula reagál a primer folyamatban, akkor a fordított irányú, másodlagos elektronátadás (1b) spintiltott folyamat, így sebessége várhatóan lényegesen kisebb lesz, mint szingulett gerjesztett molekula reakciója esetén. Feltételezésem szerint minden változás, mely csökkenti azt az időt, amit a primer folyamat termékei egymás közelében töltenek, jelentősen javíthatja a töltésszeparálódás hatásfokát. Munkám során a következő öt lehetőséget fogom megvizsgálni:

$$^3A^{++} + Q \longrightarrow {}^3(A^{\bullet+}\, Q^{\bullet+}) \longrightarrow {}^3A^{\bullet+} + Q^{\bullet+} \qquad (2)$$

$$\searrow \quad A^{++} + Q$$

$$^3A + QH \longrightarrow {}^3(A^{\bullet-}\, QH^{\bullet+}) \longrightarrow {}^3A^{\bullet-} + Q^{\bullet} + H^{+} \qquad 3a)$$

$$\searrow \quad A + QH \qquad (3b)$$

$$^3A + (QH\text{--}B) \longrightarrow {}^3(A^{\bullet-}\, QH^{\bullet+}\text{--}B) \longrightarrow {}^3A^{\bullet-} + Q^{\bullet} + H^{+}B \qquad (4)$$

$$\searrow \quad A + QH + B$$

$$^3A + Q^{-} \xrightarrow{Q^{-}} {}^3(A^{\bullet-}\, Q^{\bullet}) \longrightarrow {}^3(A^{\bullet-}\, Q_2^{\bullet-}) \longrightarrow {}^3A^{\bullet-} + Q_2^{\bullet-} \qquad (5)$$

$$\searrow \quad A + 2\,Q^{-}$$

$$^3A + Q \xrightarrow{H^{+}} {}^3(A^{\bullet+}\, Q^{\bullet-}) \longrightarrow {}^3(A^{\bullet+}\, QH^{\bullet}) \longrightarrow A^{\bullet+} + QH^{\bullet} \qquad (6)$$

$$\searrow \quad A + Q + H^{+}$$

A (2) reakció szerint triplett gerjesztett dikation ($^3A^{++}$) reagál alapállapotú elektrondonor molekulával (Q) és gyökkationpár keletkezik. A pozitív töltések elektrosztatikus taszítása miatt várhatóan a gyökkationpár gyorsabban disszociál és a szabad gyökkationok rekombinációja is lassabb, mint az ellentétes töltésekkel rendelkezőké. Az ilyen típusú vizsgálatokhoz triplett tetrafenilporfirin-dikationt és aromás aminokat használok.

A (3) reakcióban a fordított irányú, másodlagos elektronátadás jelentősége csökkenhet, ha a $Q^{\bullet+}$ gyökkation gyors, kompetitív folyamatban protont ad le. Ha az elektrondonorból képződő gyökkation nagyon erős sav, akkor a gyors protonleadás (3a) hatékonyan versenyezhet a spintiltott (3b) folyamattal. A fenolszármazékok bizonyultak legalkalmasabb elektrondonornak az ilyen reakciókban, mert gyökkationjuk élettartama nagyon rövid, azonnal protont ad le a környezetnek.

Az előző bekezdésben vázolt elképzelésnek egy módosított változata a (4) reakció, melyben a protonleadást és feltehetőleg a primer elektronátadási folyamatot is azzal tesszük gyorsabbá, hogy az elektrondonor hidrogénhíddal kötődik egy jó proton-akceptorhoz (B). A protonleadással ez esetben is megszűnik a gyökionpárt összetartó Coulomb-kölcsönhatás és könnyebbé válhat a disszociáció.

A (5) reakció is, csakúgy mint a (2), az egyforma töltésű gyökionok közötti taszítással próbálja növelni a töltéselkülönülés sebességét. Azonban az (5) folyamatban a gyökanionpár két lépésben keletkezik. Először a triplett gerjesztett molekula vesz át elektront egy aniontól, majd a létrejövő gyökanion-gyök pár reagál tovább egy másik anionnal. Ha a Q^- koncentrációja elég nagy, akkor $^3(A^{\bullet-}\ Q^{\bullet})$ kvantitatívan $^3(A^{\bullet-}\ Q_2^{\bullet-})$-vé alakítható. A halogenid és pszeudohalogenid ionok jól használhatók ilyen reakciókban, mert a

$$Q^{\bullet} + \ Q^{-} \rightleftharpoons Q_2^{\bullet -}$$

átalakulás egyensúlyi állandója a dimerizálódásnak kedvez. A disszertációmban bemutatok egy példát, melyben a triplett gerjesztett molekulák nagy hatékonysággal gyökionokká alakíthatók e módszerrel.

A (6) folyamatban az elsődleges elektronátadás során képződő gyökionpáron belüli fordított irányú elektronátadást azzal akadályozzuk meg, hogy a gyökaniont gyors reakcióban protonáljuk. Az eredmények összehasonlíthatósága érdekében a (3), (4), (5) és (6) reakciókat egy közös triplett gerjesztett molekulával célszerű tanulmányozni.

A fenti szkémáknak megfelelő modellreakciók megtalálása nem könnyű feladat, mert biztosítani kell, hogy a választott anyagok csak fotokémiai elektronátadási folyamatban reagáljanak. Az elektrondonort vagy az elektronakceptort szelektíven kell gerjeszteni, a triplett gerjesztett molekulák, gyökionok és gyökök azonosítását és követését is meg kell oldani a rendelkezésre álló kísérleti technikával (időben felbontott elnyelési spektroszkópia). Sok esetben a rövid élettartamú köztitermékek színképe, moláris elnyelési együtthatója, várható élettartama is teljesen ismeretlen, pedig ezek a tervezett vizsgálatokhoz nélkülözhetetlenek. A fent említett követelményeken kívül az is fontos, hogy a fényelnyelő anyag triplettképződési kvantumhatásfoka és elektronaffinitása elég nagy legyen, de proton-donor-akceptor folyamatokban vagy hidrogénhídkötésben ne vehessen részt. E sokféle elvárásnak kiválóan megfelel a C_{60} , melynek előállítását először Krätschmer és munkatársai publikálták 1990-ben. A fullerének felfedezése által okozott lelkesedés ránk is hatott, és az elsők között kezdtük használni azokat fotokémiai elektronátadási reakciók iniciálására. A C_{60} oldat jellegzetes lilás színe mindjárt azt sugallja, hogy széles színképtartományban képes fényelnyelésre, így szelektív gerjesztése könnyen megoldható. Hidrofób jellege pedig a (3) és (4) reakciók tanulmányozásakor nagyon kedvező. Szabályos, gömb alakja és jól

definiált mérete nagy segítséget jelenthet a diffúziós vagy elektronátadási folyamatok elméletének tesztelésekor. Mindezek az előnyök kompenzálták azt a hátrányt, hogy vizsgálataink kezdetekor a C_{60} spektroszkópiai és fotokémiai sajátságairól csak nagyon kevés ismeret állt rendelkezésre.

Disszertációm végén megmutatom, hogy a C_{60} hatékony fotokatalizátor lehet olyan reakciókban, melyek a látható fénnyel nem, vagy csak kis hatékonysággal valósíthatók meg. Részletesen vizsgálom a fotokatalízis okát, feltárom az elemi reakciókat és azok kinetikáját.

II. VIZSGÁLATI MÓDSZEREK

A szingulett gerjesztett molekulákat elnyelési és fluoreszcencia spektroszkópiás módszerekkel tanulmányoztam. A fluoreszcencia kvantumhatásfokát házi építésű, fotonszámlálásos detektálást alkalmazó spektrofluoriméterrel mértem. A fluoreszcenciaintenzitás időfüggésének meghatározása időkorrelált egyfotonszámláló készülékkel történt. A lecsengési paramétereket nem-lineáris legkisebb négyzetek iteratív rekonvolúciós módszerrel számítottam. A triplett gerjesztett molekulák, szabad gyökök és gyökionok azonosítására és reakcióinak vizsgálatára lézer-villanófény fotolízises módszereket alkalmaztam. A rövid élettartamú köztitermékeket általában időben felbontott fényelnyelésváltozás méréssel követtem. Néhány esetben lehetőség nyílott a Massachusetts Egyetemen Bostonban rendelkezésre álló időben felbontott elektronparamágneses rezonancia detektálást végző berendezés használatára is. Az oxidációs és redukciós potenciálokat a Brandeis Egyetemen (Waltham, USA) ciklikus voltammetriás módszerrel határoztam meg.

III. EREDMÉNYEK ÉS ÉRTELMEZÉSÜK

III. 1. Fluorenon és származékainak fotofizikai sajátságai

Kimutattam, hogy a fluorenonszármazékok fotofizikai sajátságainak nagymértékű függését az oldószer polaritástól és a szubsztituenstől az egyes energiaszintek egymáshoz viszonyított helyzetének változása okozza.

Megfigyeléseim szerint a fluorenon fluoreszcenciás sajátságai akkor változnak a legnagyobb mértékben, ha a szubsztituenst 2-helyzetben csatlakoztatjuk a gyűrűhöz, ezért részletes vizsgálatokat csak az ilyen származékokkal végeztem. Elektronszívó csoportként fluor-, elektronküldő csoportként pedig metoxi- és aminocsoportot használtam. Széles hőmérséklettartományban, különböző oldószerekben mértem a legalacsonyabb szingulett gerjesztett állapot élettartamát (τ_F), valamint a triplettképződés ($^3\Phi$) és a fluoreszcencia kibocsátás kvantumhatásfokát (Φ_F), majd e mennyiségekből meghatároztam az egyes fotofizikai folyamatok sebességi együtthatóját.

A. Kimutattam, hogy a fluorenon valamint apoláros és mérsékelten poláros oldószerekben a 2-fluorofluorenon legkisebb energiájú szingulett gerjesztett állapotának legfontosabb átalakulási módja a triplettképződés, melynek sebességi együtthatója (k_{ISC}) erősen oldószer- és hőmérsékletfüggő. A belső konverzió (k_{IC}) és a fluoreszcencia kibocsátás (k_F) sebességi együtthatóját azonban a kísérleti körülmények alig befolyásolják.

B. A k_{ISC} hőmérsékletfüggése alapján arra következtettem, hogy a triplettképződés apoláros és mérsékelten poláros oldószerekben aktiválási energiát

igénylő (S_1 -T_3) folyamatban és hőmérsékletfüggetlen sebességű (S_1 - T_2, illetve S_1 - T_1) átmenetekben egyaránt végbemehet. Az S_1 és T_3 szintek közötti energiakülönbséget a hőmérsékletfüggő sebességű szingulett-triplett átmenet aktiválási energiája (E_{ISC}) alapján becsültem. A kapott értékek igazolják, hogy E_{ISC} az oldószer polaritás növekedésekor egyre nagyobbá válik. A fluorenon esetén ez a növekedés nagyobb mértékű, mint a 2-fluorofluorenon esetén. Poláros oldószerekben azonban már mindkét vegyület S_1 és T_3 szintje közötti energiakülönbség oly nagy, hogy szobahőmérséklet környékén a termikus energia nem elegendő az átmenet megvalósításához, így ekkor csak az aktiválási energiát nem igénylő S_1 - T_2 és S_1 - T_1 átalakulásokban keletkezhetnek triplett gerjesztett molekulák.

C. Ellentétben a fluorenon és 2-fluorofluorenon vizsgálata során tapasztaltakkal, a triplett gerjesztett 2-metoxifluorenon képződés sebességi együtthatóját oldószer- és hőmérsékletfüggetlennek találtam. Ezt azzal magyaráztam, hogy az elektronküldő metoxicsoport jelentősen növeli az S_1 és T_3 állapotok közötti energiakülönbséget, aminek következtében triplettképződés csak az aktiválási energiát nem igénylő átmenetekben lehetséges.

D. A szingulett gerjesztett 2-metoxifluorenon k_{IC} sebességi együtthatójának logaritmusa és a különböző oldószerekben mért fluoreszcencia maximum energiája között lineáris összefüggést találtam. Megállapítottam, hogy az oldószerrel való kölcsönhatás csökkenti a gerjesztett állapot energiáját, és ezáltal hatékonyabb rezgési csatolás jöhet létre az alap- és a gerjesztett állapot között, ami k_{IC} növekedését okozza.

E. Kimutattam, hogy metilciklohexán és toluol oldószerben a szingulett gerjesztett 2-metoxifluorenon belső konverziójának sebességi együtthatója (k_{IC}) jól leírható egy hőmérsékletfüggetlen és egy hőmérsékletfüggő sebességi együttható

összegeként ($k_{IC} = k^0_{IC} + A_{IC} \exp(- E_{IC} /RT)$). Mivel A_{IC} jelentősen csökken az oldószer polaritás növekedésekor, ezért toluolnál polárosabb oldószerekben hőmérsékletfüggést nem tapasztaltam.

III. 2. Gerjesztett állapotú dimerek vizsgálata

III.2. 1. Gerjesztett fluorenon kioltás alkoholokkal

Kimutattam, hogy a fluorenon fotofizikai sajátságai alkoholokban és hidrogénhídkötés létesítésére nem képes oldószerekben élesen különböznek, ami lehetővé teszi új típusú jelzőanyagként való alkalmazását. Igazoltam, hogy a triplettképződés sebességi együtthatója a nem-specifikus (dipól-dipól és dipól-indukált dipól) oldószer-fluorenon kölcsönhatásokra érzékeny, míg a belső konverzió sebességi együtthatója az oldószerrel létrejövő hidrogénhídkötés erősségének jelzésére alkalmas. Ez a felismerés nagy jelentőségű, mert a szakirodalomban eddig használt fluoreszcenciás jelzőanyagokkal nem különböztethetők meg kellőképpen a különböző típusú oldószer - oldott anyag kölcsönhatások.

A. Időben felbontott mérésekkel igazoltam, hogy a fluorenon fluoreszcencia kioltás alkoholokkal dinamikus folyamatban, gerjesztett állapotú, hidrogénhíddal kötött komplexen keresztül történik. A kioltás sebességének jelentős csökkenését tapasztaltam a hidrogénhídkötés erősségének csökkenésekor.

B. Megállapítottam, hogy a gerjesztett komplex nagyon gyengén fluoreszkál, legfontosabb reakciója a gyors belső konverzió; tripletté alakulása vagy szingulett gerjesztett fluorenonná és alapállapotú alkohollá disszociálása egyaránt elhanyagolható sebességű.

C. A fluorenon szingulett gerjesztett állapotban sokkal erősebb hidrogénhíd-

akceptor mint alapállapotban, mivel alkoholokkal még dimetilformamidban is megfigyeltem fluoreszcencia kioltást, de alapállapotban hidrogénhídkötést ebben az oldószerben nem tapasztaltam.

III.2. 2. Gerjesztett fluorenon kioltás fenolokkal

Kimutattam, hogy a fluorenon és fenolok közötti fotokémiai reakció nemcsak elektronátadási mechanizmus szerint játszódhat le, hanem gerjesztett, hidrogénhíddal kötött komplexen keresztül is.

A. Megállapítottam, hogy a gerjesztett molekula kioltás sebességi együtthatójának oldószerfüggése alapján jól megkülönböztethetők az elektronátadási mechanizmus szerinti és a gerjesztett, hidrogénhíddal kötött komplexen keresztül végbemenő folyamatok. Az előbbiek sebessége ugyanis jelentősen nő, míg az utóbbiaké nagymértékben csökken az oldószer polaritás növelésével.

B. Igazoltam, hogy a 4-helyzetben szubsztituált fenolszármazékok közül az elektronküldő csoportot (például CH_3O vagy OH) tartalmazók oxidációs potenciálja a legalacsonyabb, így ezek a vegyületek túlnyomórészt elektronátadási folyamatban reagálnak a gerjesztett fluorenonnal. A többi fenolszármazék esetén energetikai okok miatt az elektronátadás nem kedvezményezett, ezért gerjesztett, hidrogénhíddal kötött komplexen keresztül történik a reakció.

C. A gerjesztett hidrogénhíd-komplexen keresztül lejátszódó kioltás deutérium effektust mutat, ha a folyamat nem a diffúzió által meghatározott sebességű.

D. Széntetraklorid oldószerben 2,4,6-trimetilpiridin adalék hatására a triplett gerjesztett fluorenon és 3-cianofenol közötti reakció sebességének nagymértékű csökkenését

figyeltem meg. E jelenséget azzal értelmeztem, hogy a 2,4,6-trimetilpiridin - 3-cianofenol hidrogénhíd-komplex lényegesen kisebb sebességgel reagál a triplett fluorenonnal, mint a szabad, komplexbe nem kötött 3-cianofenol.

III.2. 3. Szingulett gerjesztett fluorenon - ciklodextrin komplexek sajátságai

Kimutattam, hogy vizes közegben a szingulett gerjesztett fluorenon sokkal alkalmasabb a β-ciklodextrin üreg polaritásának vizsgálatára, mint a szakirodalomban eddig használt fluoreszcenciás jelzőanyagok, mert segítségével megkülönböztethető a hidrogénhíd kölcsönhatás a nem specifikus (dipól-dipól, dipól-indukált dipól) kölcsönhatásoktól.

A. Oldékonyság méréssel, valamint elnyelési és fluoreszcencia spektroszkópiás módszerrel igazoltam, hogy vizes közegben a fluorenon beékelődési komplexet képez β-ciklodextrinnel és annak metilezett származékaival.

B. Megállapítottam, hogy a szingulett gerjesztett fluorenon-β-ciklodextrin-származék komplexek belső konverziója mindig nagyon gyors, a sebességi együttható értékét ($k_{IC} = 7.9 - 2.9 * 10^8\ s^{-1}$) a glükozid-OH csoportok metilezése alig befolyásolja. E tények alapján arra következtettem, hogy a ciklodextrin üregben a komplex képződés után is maradnak vízmolekulák.

C. A triplett gerjesztett fluorenon - β-ciklodextrin-származék komplexek képződésének sebességi együtthatóját ($k_{ISC} = 2.3 - 3.8 * 10^7\ s^{-1}$) összehasonlítva a fluorenon különböző oldószerekben mért k_{ISC} értékeivel, kimutattam, hogy a ciklodextrin üreg "polaritása" lényegesen nagyobb mint a dioxáné vagy a tetrahidrofuráné és közel van az etanoléhoz. Eredményeim alapján elemeztem, hogy mi lehet az oka a szakirodalomban a ciklodextrin üreg "effektív ekvivalens dielektromos

állandójára" közölt értékek rendkívül nagy eltérésének. (A különböző szerzők által megadott értékek 2.2 és 55 között változnak).

D. Kimutattam, hogy dimetilformamid és dimetilszulfoxid oldószerben a fluorenon alapállapotban nem képez komplexet ciklodextrin-származékokkal, szingulett gerjesztett állapotban azonban a ciklodextrin OH-csoport és a fluorenon CO-csoportja közötti kölcsönhatás hatékony belső konverziót eredményez.

III.3. Fény hatására végbemenő elektronátadási folyamatok kinetikája

III.3.1. Triplett tetrafenilporfirin-dikation fotoredukciója

Megállapítottam, hogy a tetrafenilporfirin fotofizikai és fotokémiai sajátságai semleges és savas közegben alapvetően különböznek. Aromás aminokkal és hidrokinonokkal csak a tetrafenilporfirin-dikation fotoredukálható.

A. Kimutattam, hogy a tetrafenilporfirin trifluorecetsav jelenlétében két protont vesz fel és dikationná alakul, mely jellegzetes elnyelési (maximumok: 436 és 654 nm) és fluoreszcencia spektruma (maximumok 697 és 750 nm) alapján könnyen azonosítható. A porfiringyűrű protonálódása jelenősen csökkenti szingulett gerjesztett állapot élettartamát (13.6 ns-ról 1.05 ns-ra) és a triplettképződés kvantumhatásfokát (0.67-ről 0.31-re), annak következtében, hogy a belső konverzió sebessége megnő.

B. Tetrafenilporfirin-dikation foszforeszenciát még a C_{60} esetén jól bevált, nehézatomot tartalmazó közegekben 77 K-en sem tudtam megfigyelni (kvantumhatásfok kisebb mint $5 * 10^{-6}$), így a triplett energiát az energiaátadási kísérletek alapján becsültem (1.44 ± 0.06 eV).

C. Kimutattam, hogy a tetrafenilporfirin sav jelenlétében azért fotoredukálható, mert a protonálódás nagymértékben csökkenti a porfirin redukciós potenciálját.

D. Megállapítottam, hogy aromás amin és hidrokinonszármazék típusú elektrondonorokkal lejátszódó reakciók esetén az elektronátadás sebessége és a reakció során fellépő szabadentalpia-változás közötti kapcsolat ugyanazzal a függvénnyel írható le.

E. A fotoredukcióban a gyökképződés kvantumhatásfoka (Φ_R) csak csekély mértékben függött a molekula szerkezetétől; aromás aminokkal $\Phi_R = 0.38$ hidrokinonokkal $\Phi_R = 0.32$ körüli értékeket mértem.

III.3.2. C_{60} fotofizikai és fotokémiai folyamatai

III.3.2.1 Fotofizikai átalakulások

A szakirodalomban elsőként sikerült C_{60} foszforeszenciát kimutatnom és igazolnom, hogy a triplett C_{60} moláris elnyelési együtthatója nagyobb mint az irodalomban addig elfogadott érték.

A. Megállapítottam, hogy 77 K-en metilciklohexánban illetve metilciklohexán, 2-metiltetrahidrofurán és etiljodid 2:1:1 arányú elegyéből készített üvegben az emissziós spektrum alapvetően különbözik. Az etiljodidot tartalmazó üvegben a C_{60} fluoreszcencia intenzitása elhanyagolhatóvá válik és a spektrumban 796 nm illetve 812 nm-nél két új emissziós maximum mutatható ki, melyet C_{60} foszforeszenciaként azonosítottam.

B. A foszforeszencia spektrum alapján közvetlenül meg tudtam határozni a triplett C_{60} energiáját. (1.574 ± 0.010 eV), mely korábban csak meglehetősen pontatlanul volt becsülhető.

C. Lézer-villanófénnyel történő gerjesztést alkalmazva jó egyezést találtam a triplett C_{60} fényelnyelés és a foszforeszenciaintenzitás időbeni változása között. A triplett lecsengés

sebességi együtthatója metilciklohexánban (5.3 * 10^3 s^{-1}) csak kis mértékben bizonyult lassabbnak, mint etiljodidot tartalmazó oldószerelegyben (2.3 * 10^4 s^{-1}). Megállapítottam, hogy a nehézatom-hatás a foszforeszencia kibocsátás sebességét több mint két nagyságrenddel növeli és ezáltal teszi lehetővé a foszforeszencia észlelését.

E. Energiaátadáson alapuló, nagypontosságú módszert dolgoztam ki a triplett C_{60} moláris elnyelési együtthatójának (ε) meghatározására és megállapítottam, hogy a szakirodalomban rendelkezésre álló adat módosításra szorul. Több gondosan kivitelezett mérés eredményének átlagaként ε = 16100 ± 700 dm^3 mol^{-1} cm^{-1} -et javasoltam a triplett C_{60} 750 nm-nél levő elnyelési maximumában a moláris elnyelési együttható értékére.

F. Benzofenont használva referenciaként, melynek triplettképződés kvantumhatásfoka megbízhatóan ismert (Φ_T=1), a C_{60} triplettképződés kvantumhatásfokát 0.93 ± 0.07 -nek találtam.

III.3.2.2. Triplett gerjesztett C_{60} redukciója

Megállapítottam, hogy a trifenilamin- és hidrokinonszármazékok valamint egyes szervetlen anionok elektronátadási folyamatban reagálnak a triplett C_{60}–nal. Kimutattam, hogy a $C_{60}^{\bullet-}$ gyökanion képződés kvantumhatásfoka nagymértékben függ az oldószertől és az elektrondonortól.

A. A triplett gerjesztett C_{60} és tritoluoilamin közötti reakció időben felbontott elnyelési spektroszkópiás vizsgálata során megállapítottam, hogy toluol oldószerben a folyamat sebességi együtthatója (k_q) (8.5±0.8)*10^7 dm^3 mol^{-1} s^{-1} és a kioltás termékképződést nem eredményez. Benzonitrilben azonban a reakciósebesség lényegesen nagyobb (k_q = (3.5 ± 0.3) *10^9 dm^3 mol^{-1} s^{-1}) és 0.32 kvantumhatásfokkal szabad gyökionpár keletkezik.

B. Kimutattam, hogy a hidrokinon sokkal kisebb sebességi együtthatójú elektronátadási folyamatban ($k_q = (1.2 \pm 0.1) * 10^7$ dm^3 mol^{-1} s^{-1} benzonitrilben) reagál a triplett C_{60}-nal, mint a tritoluoilamin. Mivel az elsődleges reakcióban keletkező hidrokinon gyökkation nagyon erős sav, protonleadással szinte azonnal szemikinon gyökké alakul, így az elektronátadás és a protonvesztés egymással csatolt folyamatban történik. Valószínűleg a hidrokinon gyökkation gyors protonvesztése az oka annak, hogy a C_{60} gyökanion képződés kvantumhatásfoka nagyobb, ha aminok helyett hidrokinont használunk redukálószerként.

C. Időben felbontott elektronparamágneses rezonancia (EPR) spektroszkópiás vizsgálataink megerősítették az elnyelési spektroszkópiás módszerrel kapott eredményeket és hozzájárultak a triplett C_{60} EPR jelének azonosításához.

D. Eredményeim szerint a triplett C_{60} elektronfelvételének sebessége és a reakció következtében fellépő szabadentalpia-változás közötti kapcsolat lényegesen eltér hidrokinonszármazékok esetén a más aromás elektrondonor vegyületekkel tapasztalt korrelációtól.

E. Megállapítottam, hogy benzonitril oldószerben a triplett C_{60} nagysebességű folyamatban reagál NO_2^- anionnal és 0.73 kvantumhatásfokkal $C_{60}^{\bullet -}$ gyökanion keletkezik. Amikor nitrition helyett tiocianátiont használtam reaktánsként, akkor a gyökionképződés kvantumhatásfokát nagymértékben koncentrációfüggőnek találtam.

III.3.3. Gerjesztett molekulák kioltása hidrogénhíd-komplexekkel

Kimutattam, hogy a gerjesztett molekulák és fenolok közötti elektronátadási reakció sebessége több nagyságrenddel is növekedhet, ha a fenol hidrogénhíd-komplexbe van kötve. A fenolok piridinszármazékokkal alkotott komplexei egy új-típusú elektronátadási folyamatban reagálnak, melynek jellemzője, hogy az elektron és a proton mozgása egymással csatoltan megy végbe, és ezért jelentős kinetikai izotóphatás figyelhető meg.

A. Megállapítottam, hogy a triplett gerjesztett C_{60} és fenolok között lejátszódó reakció jelentősen felgyorsul piridinszármazékok jelenlétében. Poláros oldószerben a reakciósebesség a piridin koncentráció függvényében kezdetben meredeken növekszik, majd határértéket ér el. A kísérleti eredmények kinetikai elemzésével igazoltam, hogy a reakciósebesség növekedés a fenol-piridin hidrogénhíd-komplexek nagyobb reaktivitásából ered. E megállapítás helyességét alátámasztja többek között az is, hogy a hidrogénhíd-komplex képződésének egyensúlyi állandójára (K) kinetikai és elnyelési spektroszkópiás mérésekből kapott értékek jó egyezést mutatnak. A különböző kísérleti körülmények között meghatározott K értékek igazolják, hogy az oldószer polaritás csökkenése, illetve a piridinszármazék bázicitásának növelése elősegíti a hidrogénhíd-komplex képződését.

B. Ciklikus voltammetriás mérésekkel igazoltam, hogy hidrogénhíd-komplex képződés hatására a fenolok oxidációs potenciálja jelentősen csökken. Minél bázikusabb a komplexet alkotó piridinszármazék, annál nagyobb oxidációs potenciál csökkenést tapasztaltam.

C. A triplett gerjesztett C_{60} és a hidrogénhíd-komplexek közötti reakció során fellépő szabadentalpia-változás ($\Delta G°$) és a reakció sebességi együtthatója (k) között jó korrelációt találtam. Ha $\Delta G°$ erősen negatív, a reakció sebességi együtthatója az oldószer polaritástól függetlenül közel diffúziókorlátozott. Ezzel szemben, ha $\Delta G° \approx 0$ eV, akkor az oldószer polaritás csökkenésével k is nagymértékben csökken. Ebben az esetben a triplett kioltás sebességének függése a piridinszármazék koncentrációjától apoláros oldószerben nem írható le telítési típusú görbével. A reakciósebesség a piridinszármazék koncentrációjának növelésekor egyre meredekebben növekszik. E jelenséget azzal értelmeztem, hogy a fenol szolvátburkában a piridinszármazék feldúsul, így a szolvátburok polaritása jelentősen növekszik, ami gyorsítja az elektronátadási reakciót.

D. A triplett gerjesztett C_{60} és 1-naftol–2,4,6-trimetilpiridin komplex közötti reakció példáján bemutattam, hogy apoláros széntetraklorid oldószerben a $C_{60}^{\bullet-}$ gyökanion képződés kvantumhatásfoka (Φ_R) a 2,4,6-trimetilpiridin koncentráció növekedésével mintegy tízszeresére növekszik, poláros benzonitril oldószerben azonban a trimetilpiridin koncentrációtól függetlenül Φ_R=0.8 körüli érték. A széntetraklorid közegben megfigyelt nagymértékű Φ_R változás szintén a szolvátburok polaritásának növekedésére utal.

E. Megállapítottam, hogy olyan reakciók esetén, melyek nem diffúziókorlátozott sebességgel játszódnak le, a fenolok OH-csoportjának deuterálása lassítja a gerjesztett molekulák hidrogénhíd-komplexekkel történő kioltását. E kinetikai izotóphatás egyértelműen bizonyítja, hogy újtípusú elektronátadási folyamatot találtunk. A szokásos elektronátadási folyamatok ugyanis nem mutatnak nehézatom-hatást. A gerjesztett molekula és az alapállapotú hidrogénhíd-komplex kölcsönhatásakor három molekulából összetevődő gerjesztett komplex keletkezik, melyben az elektron és proton mozgás egymással csatoltan megy végbe. Kimutattam, hogy ezek az elektronátadási folyamatok nagyon gyakoriak, például aromás vegyületek fluoreszcenciájának kioltása is ilyen módon megy végbe, ha fenolszármazékok hidrogénhíd-komplexeit használjuk elektrondonorként.

III.3.4. A reakciósebesség és a gyökionképződési kvantumhatásfok növelés egyéb lehetőségei

III.3.4.1. Hidroxilcsoportot tartalmazó vegyületek hatása a kinonok fotokémiai elektronátvételi reakcióiban

A triplett gerjesztett C_{60} és klórozott kinonok közötti elektronátadási reakció példáján kimutattam, hogy erős hidrogénhídkötés létesítésére képes OH-vegyületek által okozott reakciósebesség növekedés mértékét elsősorban az OH-vegyület hidrogénhídkötő

képessége, a gyökionképződés kvantumhatásfokának növekedését pedig az OH-vegyület saverőssége határozza meg.

Megállapítottam, hogy a diklórmetán oldószerben a triplett gerjesztett C_{60} kinonokkal történő oxidációja jelentősen felgyorsul erős hidrogénhídkötés létesítésére képes fluórozott alkoholok, nitrofenolok vagy trifluorecetsav jelenlétében. E reakciósebesség-növekedést azzal magyaráztam, hogy a hidrogénhídkötés elősegíti a kinon szolvátburkában az OH-vegyület feldúsulást és ezáltal nagyobb lokális polaritás alakul ki. Ha a kinon szolvátburka erős savat tartalmaz, akkor a triplett C_{60} -ról a kinonra történő elektronátadás során keletkező kinon gyökanion gyorsan protonálódik. Ennek következtében csökken az elsődleges folyamatban keletkező ($C_{60}^{\bullet+}$ kinon$^{\bullet-}$) gyökionpáron belüli fordított irányú elektronvándorlás esélye és ezáltal jelentősen nő a $C_{60}^{\bullet+}$ képződés kvantumhatásfoka.

III.3.4.2. C_{60} által katalizált gyökionképződés fotokémiai elektronátviteli reakciókban

Kimutattam, hogy a C_{60} kedvező fényelnyelési és redox sajátságai valamint stabilitása miatt hatékony fotokatalizátorként működhet elektronátadási reakciókban. Kísérleti módszereket dolgoztam ki a $C_{60}^{\bullet-}$ gyökanion moláris elnyelési együtthatójának (ε) meghatározására, mivel az irodalomban közölt adatok ellentmondásosak voltak. A három független eljárással kapott eredmények alapján 1080 nm-en $\varepsilon = 18300 \pm 1100$ dm^3 mol^{-1} cm^{-1} értéket javasoltam a $C_{60}^{\bullet-}$ moláris elnyelési együtthatójára.

A. Megállapítottam, hogy a triplett gerjesztett C_{60} és klóranil között végbemenő reakció lassú, sebességi együtthatója benzonitrilben $2 * 10^7$ dm^3 mol^{-1} s^{-1} .

B. Perilén vagy tritoluoilamin hozzáadásának hatására azonban a folyamat sebességének és a klóranil-gyökanion képződés kvantumhatásfokának jelentős növekedését tapasztaltam. Időben felbontott kísérleti módszerekkel kimutattam, hogy a két adalék hatásmechanizmusa alapvetően különbözik és meghatároztam az elemi reakciók sebességi együtthatóját.

C. Benzonitrilben a triplett gerjesztett C_{60} perilénnel két egymással versengő folyamatban reagál. E folyamatok közül a $^3C_{60}$ -ról a perilénre történő energiaátadás a domináló, sebességi együtthatója $k_{NT} = (1.1 \pm 0.2) * 10^9$ dm^3 mol^{-1} s^{-1}, a $C_{60}^{\bullet-}$ és perilén$^{\bullet+}$ gyökiont eredményező elektronátadás sebességi együtthatója ennél kisebb ($k_{LT} = (3.6 \pm 0.4) * 10^8$ dm^3 mol^{-1} s^{-1}). Ha az oldat klóranilt is tartalmaz, akkor az elsődleges fotokémiai folyamatokban keletkezett triplett perilén és a $C_{60}^{\bullet-}$ gyökanion is nagy sebességgel redukálja a klóranilt, és 0.62 ± 0.04 hatásfokkal keletkezik klóranil gyökanion.

D. Tritoluoilamin adalék jelenlétében az elsődleges fotokémiai reakció a triplett gerjesztett C_{60} redukciója tritoluoilaminnal. E gyors folyamatban képződött $C_{60}^{\bullet-}$ gyökanion közel diffúziókorlátozott sebességgel ad át elektront a klóranilnak.

IV. AZ EREDMÉNYEK GYAKORLATI HASZNOSÍTÁSA

A fluorenonszármazékok fotofizikai sajátságainak feltárása során elért eredményeim jól hasznosíthatók fotoiniciátorok és fotostabilizátorok hatásfokának növelésére. A fluorenon felhasználható jelzőanyagként, mivel fotofizikai sajátságai nagymértékben függnek a mikrokörnyezetétől.

A ciklodextrinekkel kapcsolatos felismeréseim hasznosak lehetnek ciklodextrin komplexek tervezésekor. Ugyanis alapvető fontosságú, hogy ismerjük a ciklodextrin-származékok üregének polaritását, mivel ez határozza meg a komplex képződés

egyensúlyi állandóját. A gyógyszer-, élelmiszer- és kozmetkai-iparban, széleskörben alkalmaznak ciklodextrineket, mert viszonylag apoláros üregükbe hidrofób molekulák beékelődhetnek, és ezáltal fokozható az anyagok oldhatósága, megszüntethető kellemetlen ízük vagy szaguk, csökkenthető illékonyságuk vagy bomlásuk sebessége.

A fény hatására végbemenő elektronátadási folyamatok sebességét és hatásfokát befolyásoló tényezők tanulmányozása terén elért eredményeim felhasználhatók napenergia-hasznosítási és fotokatalítikus eljárások hatásfokának növeléséhez.

A hidrogénhídkötésnek az elektronátadási folyamatok sebességére és mechanizmusára gyakorolt hatását feltáró vizsgálataim hozzájárulnak az élő szervezetekben lejátszódó oxidációs-redukciós folyamatok illetve a napsugárzás által biológiai rendszerekben okozott változások megértéséhez. Ugyanis a hidrogénhídkötés alapvető szerepet játszik biológiai rendszerekben például a DNS és a fehérjék másodlagos szerkezetének kialakításában, enzim reakciókban, biológiailag aktív anyagok kötődésekor.

V. KÖZLEMÉNYEK ÉS ELŐADÁSOK

AZ ÉRTEKEZÉS ALAPJÁT KÉPEZŐ KÖZLEMÉNYEK

1. L. Biczók, T. Bérces
   Temperature dependence of the rates of photophysical processes of fluorenone
   J. Phys. Chem. 92, 3842 (1988)

2. L. Biczók, T. Bérces
   Study of the photophysical processes of fluorenone derivatives
   Advances in Photochemistry, Eds.: Zhang Bao-wen, Tung Chen-ho, Wu Shi-kang;
   International Acad. Publ., Pergamon Press 1989.

3. L. Biczók, H. Linschitz, R. I. Walter
Extinction coefficients of C_{60} triplet and anion radical and one - electron reduction of the triplet by aromatic donors
Chem. Phys. Lett. 195, 339 (1992)

4. Y. Zeng, L. Biczók, H. Linschitz
External heavy atom induced phosphorescence emission of fullerenes: The energy of triplet C_{60}
J. Phys. Chem. 96, 5237 (1992)

5. C. A. Steren, P. R. Levstein, H. van Willigen, H. Linschitz, L. Biczók
FT - EPR study of triplet state C_{60}. Spin dynamics and electron transfer quenching
Chem. Phys. Lett. 204, 23 (1993)

6. L. Biczók, T. Bérces, F. Márta
Substituent, solvent and temperature effects on radiative and nonradiative processes of singlet excited fluorenone derivatives
J. Phys. Chem. 97, 8895 (1993)

7. L. Biczók, H. Linschitz, R. I. Walter
Reduction of triplet tetraphenyl porphyrin dication by arylamines and hydroquinones: Kinetics and primary radical yields
Res. Chem. Intermediates 20, (1994) 939

8. L. Biczók, H. Linschitz, A. Treinin
One-electron reduction of triplet C_{60} by organic donors and simple anions: Kinetics and radical yields
Fullerenes - Recent Advances in the chemistry and physics of fullerenes and related materials, Ed. K. M. Kadish and R. S. Ruoff, The Electrochemical Society, Pennington, NJ, 1994. p. 909.

9. L. Biczók, L. Jicsinszky, H. Linschitz
Solvent - dependent radiationless transitions in fluorenone. A probe for hydrogen bonding interactions in the cyclodextrin cavity
J. Inclusion Phenom. 18, (1994) 237

10. L. Biczók, H. Linschitz
Concerted electron and proton movement in quenching of triplet C_{60} and tetracene fluorescence by hydrogen-bonded phenol-base pairs
J. Phys. Chem. 99, (1995) 1843

11. C. A. Steren, H. van Willigen, L. Biczók, N. Gupta, H. Linschitz
C_{60} as a photocatalyst of electron-transfer processes: Reactions of triplet C_{60} with chloranil, perylene and tritolylamine studied by flash photolysis and FT-EPR
J. Phys. Chem. 100, (1996) 8920

12. L. Biczók, L. Jicsinszky, H. Linschitz
Hydrogen bonding interactions with cyclodextrins: Utilization of fluorenone as a new probe
Proceedings of the 8th International Cyclodextrin Symposium, Kluwer Academic Publishers, 1996.

13. N. Gupta, H. Linschitz, L. Biczók
Reduction of triplet C_{60} by hydrogen-bonded 1-naphthol: Concerted electron and proton movement
Fullerene Sci. Technol. (közlésre elfogadva)

14. L. Biczók, T. Bérces, H. Linschitz
Kinetics and mechanism of excited fluorenone quenching by hydroxy-compounds
J. Phys. Chem. (előkészületben)

15. L. Biczók, N. Gupta, H. Linschitz
Triplet C_{60} quenching by hydrogen bonded phenols and quinones
J. Phys. Chem. (előkészületben)

AZ ÉRTEKEZÉS TÉMAKÖRÉHEZ KAPCSOLÓDÓ KÖZLEMÉNYEK

16. L. Biczók, S. Förgeteg, T. Bérces
Intermolecular primary processes of triplet 2-pentanone with tributylstannane and butyraldehyde
J. Photochem. 16, 267 (1981)

17. S. Förgeteg, T. Bérces, L. Biczók
Evaluation of quantum yields in the presence of an absorbing additive
React. Kinet. Catal. Lett. 18, 503 (1981)

18. L. Biczók, S. Förgeteg, T. Bérces
Triplett gerjesztett 2-pentanon reakciói hidrogéndonorokkal
Magyar Kémikusok Lapja, 36, 603 (1981)

19. L. Biczók, T. Bérces, S. Förgeteg, F. Márta
Excimer formation in the photochemistry of aliphatic ketones I. Concentration dependence of quantum yields
J. Photochem. 27, 41 (1984)

20. F. Márta, S. Förgeteg, B. László, L. Biczók, T. Bérces
Újabb felismerések az alifás ketonok fotolízisében
Kémiai Közlemények, 63, 34 (1985)

21. L. Biczók, T. Bérces, F. Márta
Structural effects in the decay kinetics of 1-naphthyl derivative / triethylamine exciplexes
J. Photochem. Photobiol. A. 48, 265 (1989)

22. S. Bakalova, L. Biczók, I. Kavrakova, T. Bérces
Photophysical and photochemical properties of 2,3-dihydro-4(1H)-quinolinones. Part I. Fluorescence properties
Z. Naturforsch. C. 45, 980 (1990)

23. S. Bakalova, L. Biczók, T. Bérces
Photophysical and photochemical properties of 2,3-dihydro-4(1H)-quinolinones. Part II. The rate and mechanism of primary processes
Z. Naturforsch. C. 46, 549 (1991)

24. M. Hugerat, H. Levanon, E. Ojadi, L. Biczók, H. Linschitz
Multiple decay pathways and electron transfer in excited ion paired zinc - copper porphyrins: Laser photolysis and time-resolved EPR spectroscopy
Chem. Phys. Lett. 181, 400 (1991)

25. P. Valat, V. Wintgens, J. Kossanyi, L. Biczók, A. Demeter, T. Bérces
Influence of geometry on the emitting properties of 2,3-naphthalimides
J. Am. Chem. Soc. 114, 946 (1992)

26. A. Demeter, L. Biczók, T. Bérces, V. Wintgens, P. Valat, J. Kossanyi
Laser photolysis studies of transient processes in the photoreduction of naphthalimides by aliphatic amines
J. Phys. Chem. 97, 3217 (1993)

27. J. Vágó, L. Biczók, G. Grabner, G. Köhler, R. M. Quint, N. Getoff
On the photochemical decomposition of aromatic α-azo-hydroperoxides
J. Photochem. Photobiol. A: Chem. 76, (1993) 69

28. V. Wintgens, P. Valat, J. Kossanyi, L. Biczók, A. Demeter, T. Bérces
Spectroscopic properties of aromatic dicarboximides. Part 1. N-H and N-methyl-substituted naphthalimides
J. Chem. Soc. Faraday Trans. 90, (1994) 411

29. A. Demeter, T. Bérces, L. Biczók, V. Wintgens, P. Valat, J. Kossanyi
Substituent effect on the photophysical properties of N-phenyl-1,2-naphthalimide
J. Chem. Soc. Faraday Trans. 90, (1994) 2635

30. Y. Dromzeé, J. Kossanyi, V. Wintgens, P. Valat, L. Biczók, A. Demeter, T. Bérces
Crystal and molecular structure of N-phenyl substituted 1,2-, 2,3- and 1,8-naphthalimides
Z. Kristallogr.210, (1995) 760

31. M. Hugerat, M., van der Est, A., Ojadi, E., Biczók, L., Linschitz, H., Levanon, H., Stehlik, D.
Transient EPR studies of ion paired metalloporphyrin heterodimers
J. Phys. Chem. 100, (1996) 495

32. A. Demeter, T. Bérces, L. Biczók, V. Wintgens, P. Valat, J. Kossanyi
Comprehensive model of the photophysics of N-phenyl-naphthalimides: The role of solvent- and rotational relaxation
J. Phys. Chem. 100,(1996) 2001

33. V. Wintgens, P. Valat, J. Kossanyi, A. Demeter, L. Biczók, T. Bérces
Spectroscopic properties of aromatic dicarboximides. Part 3: Substituent effect on the photophysical properties of N-phenyl-2,3- naphthalimides
J. Photochem. Photobiol. A: Chem. 93, (1996) 109

34. V. Wintgens, P. Valat, J. Kossanyi, A. Demeter, L. Biczók, T. Bérces
Spectroscopic properties of aromatic dicarboximides. Part 4. On the modification of the fluorescence and intersystem crossing processes of molecules by electron-donating methoxy group at different positions. The case of 1,8-naphthalimides
New J. Chem. 20, (1996) 1149

35. L. Biczók
Photophysical properties of 3-aza-fluorenone
React. Kinet. Catal. Lett. (előkészületben)

A DISSZERTÁCIÓ ANYAGÁBÓL KÉSZÍTETT ELÖADÁSOK ÉS POSZTEREK

1. Aromás ketonok és dikarboximidek fotofizikai, fotokémiai sajátságai
   Biczók L., Demeter A., László B., Bérces T.
   MTA Sugárhatáskémiai Munkabizottság, 1989, Budapest

2. Fluorenon származékok fotofizikai sajátságai
   Biczók L., Bérces T.
   XII. Országos Lumineszcemcia-spektroszkópiai Iskola, 1989, Komló

3. Electron-transfer reactions of triplet protonated porphyrin
   L. Biczók, H. Linschitz
   Gordon Research Conferences, Organic Photochemistry, 1991. július
   Andover, New Hampshire, USA

4. Kinetics and radical yields in the photoreduction of protonated tetraphenyl-porphyrin dication
   L. Biczók, H. Linschitz
   15th Department of Energy Solar Photochemistry Research Conference, 1991. június 2-6.
   Snowmass Village, Colorado, USA

5. Substituent, solvent and temperature effects on the photophysical processes of singlet excited fluorenone derivatives
   L. Biczók, T. Bérces, F. Márta
   16th International Conference on Photochemistry, 1993. augusztus 1 - 6.
   Vancover, Canada

6. One-electron reduction of triplet C_{60} by organic donors and simple anions: Kinetics and radical yields
   L. Biczók, H. Linschitz, A. Treinin
   185th Electrochemical Society Meeting, Fullerenes Session, 1994. május 22-27., San Francisco, USA

7. Concerted electron and proton movement in base-assisted reductions of triplet C_{60} by hydroquinone and p-methoxyphenol

   L. Biczók, H. Linschitz

   Electron-Donor-Acceptor Interactions Gordon Conference, 1994.augusztus 14-19. Newport, Rhode Island, USA

8. Mechanistic studies of excited state chemical reactions: Proton-linked photoredox processes

   L. Biczók, H. Wang, H. Linschitz, A. Treinin

   19th Department of Energy Solar Photochemistry Research Conference, 1994. június 4-8.

   Tamiment, Pennsylvania, USA

9. Hydrogen bonding interactions in the cyclodextrin cavity: Utilization of fluorenone as a new probe

   L. Biczók, L. Jicsinszky, H. Linschitz

   8th International Cyclodextrin Symposium, 1996. március 30 - április 2. Budapest

10. Hidrogénhíd kötés hatása a gerjesztett molekulák energiavesztési és elektronátadási folyamataiban

    Biczók László

    Reakciókinetikai és Fotokémiai Munkabizottság ülése, 1996. április, Gyöngyöstarján

11. Concerted electron-proton movement in quenching by hydrogen bonded phenols and quinones

    L. Biczók, N. Gupta, H. Linschitz

    16th IUPAC Symposium on Photochemistry, 1996. július 21-26.

    Helsinki, Finnország

12. Kinetics and mechanism of excited fluorenone quenching by hydroxy-compounds

    L. Biczók, T. Bérces, H. Linschitz

    16th IUPAC Symposium on Photochemistry, 1996. július 21-26.

    Helsinki, Finnország

13. Concerted electron-proton transfer in excited hydrogen-bonded systems. Quenching rates and radical yields
L. Biczók, N. Gupta, H. Linschitz
20th Department of Energy Solar Photochemistry Research Conference, 1996. június 8-12. French Lick, Indiana, USA

14. Triplet C_{60} és aromás vegyületek közötti kölcsönhatás kinetikája és mechanizmusa
Biczók László
Reakciókinetikai és Fotokémiai Munkabizottság ülése, 1996. november 7-8, Gyöngyöstarján

A DISSZERTÁCIÓ TÉMAKÖRÉHEZ KAPCSOLÓDÓ ELŐADÁSOK ÉS POSZTEREK

15. Effect of hydrogen bonding on the electronic spectra of methyldihydroquinolinones
Sn. Bakalova, L. Biczók, T. Bérces, I. Kavrakova
XXVI. Colloquium Spectroscopicum Internationale, 1989.
Szófia, Bulgária

16. Spectral and theoretical investigation of 2-methyl-dihydroquinolinone
Sn. Bakalova, V. Enchev, L. Biczók, T. Bérces
XXVI. Colloquium Spectroscopicum Internationale, 1989.
Szófia, Bulgária

17. Photophysics and photochemistry of aromatic dicarboximides 1. Spectroscopic properties
P. Valat, V. Wintgens J. Kossanyi, L. Biczók, A. Demeter, T. Bérces
13th IUPAC Symposium on Photochemistry, 1990. július 22-28.
Warwick, Anglia

18. Photophysics and photochemistry of aromatic dicarboximides 2. Electron-transfer between dicarboximides and amines
L. Biczók, A. Demeter, T. Bérces, V. Wintgens, P. Valat, J. Kossanyi
13th IUPAC Symposium on Photochemistry, 1990. július 22-28.
Warwick, Anglia

19. Biphotonic processes in concentrated alkali halide and pseudohalide solutions
L. Biczók, H. Linschitz
14th IUPAC Symposium on Photochemistry, 1992. július 19-25.
Leuven, Belgium

20. On the origins of the quadruple emission of N-aryl substituted naphthalimides
V. Wintgens, P. Valat, J. Kossanyi, A. Demeter, L. Biczók, T. Bérces
14th IUPAC Symposium on Photochemistry, 1992. július 19-25.
Leuven, Belgium

21. Influence of electron-donating and electron-withdrawing substituents on the fluorescence of N-aryl-2,3-naphthalimides
V. Wintgens, P. Valat, J. Kossanyi, A. Demeter, L. Biczók, T. Bérces
16th International Conference on Photochemistry, 1993. augusztus 1 - 6.
Vancover, Canada

22. Photophysical processes of the N-alkyl and N-aryl substituted naphthalimides
A. Demeter, L. Biczók, T. Bérces, V. Wintgens, P. Valat, J. Kossanyi
16th International Conference on Photochemistry, 1993. augusztus 1 - 6.
Vancover, Canada

23. Reaction through triplet-triplet encounter of carbonyl compounds
A. Demeter, L. Biczók, T. Bérces
Gordon Research Conferences, Organic Photochemistry, 1993. július
Newport, Rhode Island, USA

24. Photophysics and photochemistry of 1-nitronaphthalene: Triplet and radical yields, quenching rates and solvent effects in reductions by simple anions and aryl donors
L. Biczók, H. Linschitz, A. Treinin
18th Department of Energy Solar Photochemistry Research Conference, 1994. június 5-9.
Tahoe City, California, USA

25. Comprehensive model of the photophysics of N-phenyl-naphthalimides

A. Demeter, T. Bérces, L. Biczók

17th International Conference on Photochemistry, 1995. július 30-augusztus 4. London, Anglia

26. Study of the spectroscopic properties of N-alkyl-2,3-naphthalimides in view of ab initio calculations

V. Wintgens, F. Botal, P. Valat, J. Kossanyi, A. Demeter, L. Biczók, T. Bérces, P.Chaquin

17th International Conference on Photochemistry, 1995. július 30-augusztus 4. London, Anglia

27. Interaction of transition metal ions and cyanocomplexes with triplet benzophenone-4-sulfonate in aqueous solution: Kinetics and radical yields

J. Eloranta, J. Eloranta, L. Biczók, H. Linschitz

16th IUPAC Symposium on Photochemistry, 1996. július 21-26. Helsinki, Finnország

MELLÉKLETEK JEGYZÉKE

1. Melléklet: a III. 1. fejezethez
L. Biczók, T. Bérces
Temperature dependence of the rates of photophysical processes of fluorenone
J. Phys. Chem. 92, 3842 (1988)

2. Melléklet: a III. 1. fejezethez
L. Biczók, T. Bérces, F. Márta
Substituent, solvent and temperature effects on radiative and nonradiative processes of singlet excited fluorenone derivatives
J. Phys. Chem. 97, 8895 (1993)

3. Melléklet: a III.2.1. és III.2.2. fejezetekhez
Kinetics and mechanism of excited fluorenone quenching by hydroxy-compounds
L. Biczók, T. Bérces, H. Linschitz
16th IUPAC Symposium on Photochemistry, 1996. július 21-26.
Helsinki, Finnország

4. Melléklet: a III.2.3. fejezethez
L. Biczók, L. Jicsinszky, H. Linschitz
Solvent - dependent radiationless transitions in fluorenone. A probe for hydrogen bonding interactions in the cyclodextrin cavity
J. Inclusion Phenom. 18, (1994) 237

5. Melléklet: a III.2.3. fejezethez
L. Biczók, L. Jicsinszky, H. Linschitz
Hydrogen bonding interactions with cyclodextrins: Utilization of fluorenone as a new probe
Proceedings of the Eigth International Symposium on Cyclodextrons, Eds. J. Szejtli and L. Szente, Kluwer Academic Publishers, 1996. p. 255.

6. Melléklet: a III.3.1. fejezethez
L. Biczók, H. Linschitz, R. I. Walter
Reduction of triplet tetraphenyl porphyrin dication by arylamines and hydroquinones: Kinetics and primary radical yields
Res. Chem. Intermediates 20, (1994) 939

7. Melléklet: a III.3.2.1. fejezethez
Y. Zeng, L. Biczók, H. Linschitz
External heavy atom induced phosphorescence emission of fullerenes: The energy of triplet C_{60}
J. Phys. Chem. 96, 5237 (1992)

8. Melléklet: a III.3.2.2. fejezethez
L. Biczók, H. Linschitz, R. I. Walter
Extinction coefficients of C_{60} triplet and anion radical and one - electron reduction of the triplet by aromatic donors
Chem. Phys. Lett. 195, 339 (1992)

9. Melléklet: a III.3.2.2. fejezethez
L. Biczók, H. Linschitz, A. Treinin
One-electron reduction of triplet C_{60} by organic donors and simple anions: Kinetics and radical yields
Fullerenes - Recent Advances in the chemistry and physics of fullerenes and related materials, Ed. K. M. Kadish and R. S. Ruoff, The Electrochemical Society, Pennington, NJ, 1994. p. 909.

10. Melléklet: a III.3.2.2. fejezethez
C. A. Steren, P. R. Levstein, H. van Willigen, H. Linschitz, L. Biczók
FT - EPR study of triplet state C_{60}. Spin dynamics and electron transfer quenching
Chem. Phys. Lett. 204, 23 (1993)

11. Melléklet: a III.3.3. fejezethez
L. Biczók, H. Linschitz
Concerted electron and proton movement in quenching of triplet C_{60} and tetracene fluorescence by hydrogen-bonded phenol-base pairs
J. Phys. Chem. 99, (1995) 1843

12. Melléklet: a III.3.3. fejezethez
N. Gupta, H. Linschitz, L. Biczók
Reduction of triplet C_{60} by hydrogen-bonded 1-naphthol: Concerted electron and proton movement
Fullerene Sci. Technol. (közlésre elfogadva)

13. Melléklet: a III.3.3. és III.3.4.1. fejezetekhez
Concerted electron-proton movement in quenching by hydrogen bonded phenols and quinones
L. Biczók, N. Gupta, H. Linschitz
16th IUPAC Symposium on Photochemistry, 1996. július 21-26.
Helsinki, Finnország

14. Melléklet: a III.3.4.2. fejezethez
C. A. Steren, H. van Willigen, L. Biczók, N. Gupta, H. Linschitz
C_{60} as a photocatalyst of electron-transfer processes: Reactions of triplet C_{60} with chloranil, perylene and tritolylamine studied by flash photolysis and FT-EPR
J. Phys. Chem. 100, (1996) 8920

1. Melléklet

Reprinted from The Journal of Physical Chemistry, 1988, *92*, 3842.

Temperature Dependence of the Rates of Photophysical Processes of Fluorenone

László Biczók and Tibor Bérces*

Central Research Institute for Chemistry, Hungarian Academy of Sciences, P.O. Box 17, 1525 Budapest, Hungary *(Received: September 22, 1987; In Final Form: January 27, 1988)*

Fluorescence lifetimes, fluorescence quantum yields, and triplet yields have been measured as a function of temperature in five solvents of different polarity. The rate coefficients for the dominant photophysical processes depopulating the fluorescent state have been found to depend on the solvent and temperature. The solvent dependence is attributed to the different extent of energy shift for the various excited states involved in these processes. The experimental results require the assumption of temperature-dependent and -independent singlet–triplet intersystem crossing rates. The temperature-dependent process is identified as a thermoneutral or endothermic transition from the lowest excited singlet to a higher triplet state.

Introduction

The study of radiationless deactivation of the fluorescent state of aromatic compounds has received considerable attention. Most of these studies attempted to elucidate the effect of the solvent and temperature on the rates of photophysical processes[1] and to reveal the role played by higher triplet states in the nonradiative deactivation of the first excited singlet state.[2]

The photophysics of fluorenone in solution exhibits some unique features as a consequence of the location of excited states and their dependence on the solvent. Using picosecond time-resolved spectroscopy, Kobayashi and Nagakura[3] succeeded in outlining a consistent picture of the energy level diagram for fluorenone in polar and nonpolar solvents (Figure 1). The major feature apparent from this diagram is that S_1 is a $\pi\pi^*$ state in a polar solvent while it is of $n\pi^*$ character in nonpolar media. On this basis one expects solvent dependence for the rates and the mechanism of the photophysical processes occurring from the first excited singlet state. The room-temperature flash-photolytic measurements of the photophysical parameters of fluorenone by Linschitz and co-workers[4] confirmed indeed the expectations.

In order to reveal the nature of the solvent effect in the photophysics of fluorenone, we have determined the basic photophysical parameters as a function of temperature between 180 and 340 K in five different solvents. Fluorescence lifetimes, fluorescence quantum yields, and triplet yields were measured, and from these, rate coefficients for the elementary processes depopulating the first excited singlet state were derived.

Experimental Section

Fluorescence spectra were taken with a photon-counting spectrofluorimeter constructed in our laboratory. The instrument,

(1) Wu, K. C.; Ware, W. R. *J. Am. Chem. Soc.* **1979**, *101*, 5906.
(2) Tanaka, M.; Tanaka, I., Tai, S.; Hamanoue, K.; Sumitani, M.; Yoshihara, K. *J. Phys. Chem.* **1983**, *87*, 813.
(3) Kobayashi, T.; Nagakura, S. *Chem. Phys. Lett.* **1976**, *43*, 429.
(4) Andrews, L. J.; Deroulede, A.; Linschitz, H. *J. Phys. Chem.* **1978**, *82*, 2304.

0022-3654/88/2092-3842$01.50/0

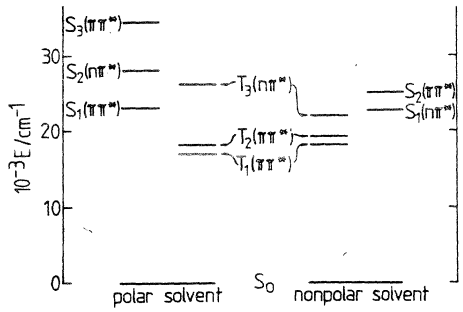

Figure 1. Energy level diagram for fluorenone in polar and nonpolar solvents.

TABLE I: Fluorescence Quantum Yields, Singlet Lifetimes, and Triplet Yields at 298 K

solvent	π^*	$^1\tau_0$, ns	$10^3\Phi_F$	Φ_T
methylcyclohexane	0.00	0.14[a]	0.52 ± 0.04	1.00
toluene	0.54	3.0 ± 0.2	9.7 ± 0.6	0.88 ± 0.08
tetrahydrofuran	0.58	2.7 ± 0.2	6.4 ± 0.6	0.87 ± 0.08
acetone	0.71	11.3 ± 0.5	21 ± 2	0.77 ± 0.07[b]
acetonitrile	0.75	18.7 ± 0.7	32 ± 2	0.46 ± 0.04

[a] Reference 8. [b] Reference 4.

which was equipped with a Princeton Applied Research type 1140 A/B photon-counting system, is described in detail elsewhere.[5] Spectra were corrected for the wavelength response of the photomultiplier. Fluorescence quantum yields were derived from relative measurements made against a reference sample of fluorenone in acetonitrile at 298 K. The fluorescence yield for the latter was taken from the literature.[4]

Singlet lifetimes were measured with a time-correlated single-photon-counting technique using a commercial Applied Photophysics SP-3 instrument. The nanosecond flash lamp was filled with hydrogen and operated at a frequency of 40 kHz. A high-intensity grating monochromator was used to select the 360-nm excitation wavelength, while a GG455 cutoff filter was placed in front of the "stop" multiplier (Mullard XP 2020 Q). Fluorescence decay data were analyzed by using a nonlinear least-squares reconvolution technique.[6] All measurements could be fitted well by assuming single-exponential decay.

Triplet yields were determined by laser flash photolysis and T–T absorption technique. The 308-nm light pulses from a Lambda Physik EMG 101 xenon chloride laser (15-ns duration at half-maximum points) were used for excitation, while triplet fluorenone decay was monitored by measuring transient absorption at 440 nm perpendicular to the laser excitation. Triplet yields were derived from initial absorbance ratios measured in comparison with a reference sample of fluorenone in methylcyclohexane at 298 K. For the reference quantum yield, $\Phi_T = 1$ was taken.[4]

All solutions used in this work were degassed by several freeze–pump–thaw cycles. Fluorenone (Fluka) was purified by repeated recrystallization from ethanol. Acetonitrile (Merck, HPLC grade) and acetone (Carlo Erba, spectroscopic grade) werre used without further purification. Methylcyclohexane (Carlo Erba), toluene (Reanal), and tetrahydrofuran (Reanal) were purified by methods described in the literature.[7]

Results

Some of the room-temperature results are given in Table I where the estimated error limits represent 1 standard deviation. In the table, the solvents are arranged, on the basis of their solvatochromic parameter π^*, in order of increasing polarity. The

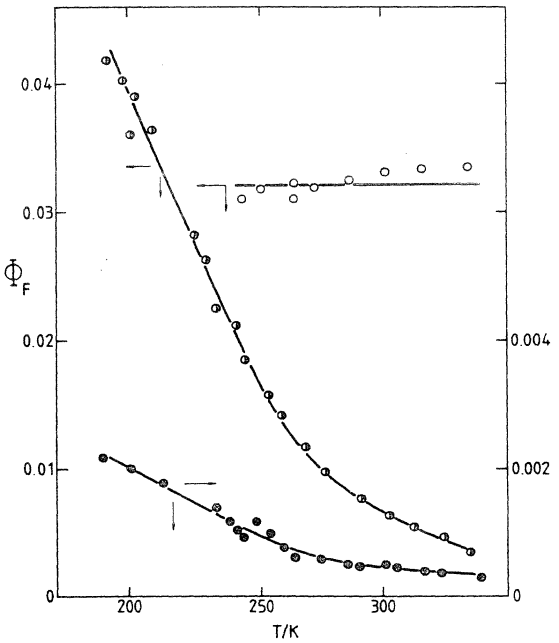

Figure 2. Temperature dependence of the fluorescence quantum yield in methylcyclohexane (●), tetrahydrofuran (◑), and acetonitrile (○).

π^* parameter was originally suggested by Taft and co-workers as an index of solvent dipolarity/polarizability which measures the ability of the solvent to stabilize a charge or a dipole by virtue of its dielectric effect.[9] In accordance with the results reported by Linchitz and co-workers[4] the data presented in Table I reveal a definite trend in the basic photophysical parameters with solvent polarity: The singlet lifetimes and the fluorescence yields increase while the triplet yields decrease with increasing polarity. The opposed changes of the singlet lifetimes and triplet yields indicate that the solvent influences the photophysical processes mainly by controlling the rate of singlet → triplet intersystem crossing.

In order to obtain more information, we extended our investigations to a wider temperatures range. Singlet lifetime, fluorescence quantum yield, and triplet yield determinations were made between 180 and 340 K in all solvents. In figure 2, the fluorescence quantum yields are shown as a function of temperature in three solvents. (Methylcyclohexane is a nonpolar solvent, tetrahydrofuran is chosen among the moderately polar solvents, and acetonitrile represents the polar solvents.) It can be seen that the fluorescence yields in polar acetonitrile are practically temperature-independent while in less polar tetrahydrofuran and in nonpolar methylcyclohexane the quantum yields increase considerably with decreasing temperature.

The temperature dependence of the singlet lifetimes was found to be analogous to the fluorescence quantum yields, i.e., temperature-independent lifetime in polar solvents and increasing lifetime with decreasing temperature in less polar and nonpolar media. However, the triplet yields measured under the same conditions showed no significant temperature dependence in the solvents investigated.

The photophysical parameters studied are related to the rate coefficients of the primary photophysical steps depopulating the excited singlet state by the relations

$$^1\tau_0 = 1/(k_F + k_{ISC} + k_{IC})$$

$$\Phi_F = k_F/(k_F + k_{ISC} + k_{IC})$$

$$\Phi_T = k_{ISC}/(k_F + k_{ISC} + k_{IC})$$

where k_F, k_{ISC}, and k_{IC} are the rate coefficients for fluorescence, singlet → triplet intersystem crossing, and internal conversion from

(5) László, B.; Förgeteg, S.; Bérces, T.; Márta, F. *J. Photochem.* **1984**, *27*, 49.
(6) O'Connor, D. V.; Phillips, D. *Time-Correlated Single Photon Counting*; Academic: London, 1984.
(7) Perrin, D. D.; Armarego, W. L. F.; Perrin, D. R. *Purification of Laboratory Chemicals*; 2nd ed.; Pergamon: Oxford, 1980.
(8) Singer, L. A. *Tetrahedron Lett.* **1969**, 923.
(9) Kamlet, M. J.; Abboud, J. L. M.; Abraham, M. H.; Taft, R. W. *J. Org. Chem.* **1983**, *48*, 2877.

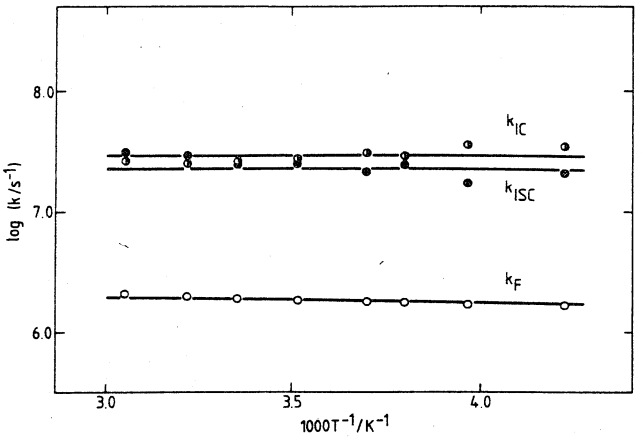

Figure 3. Arrhenius-type plots of photophysical rate coefficients in acetonitrile.

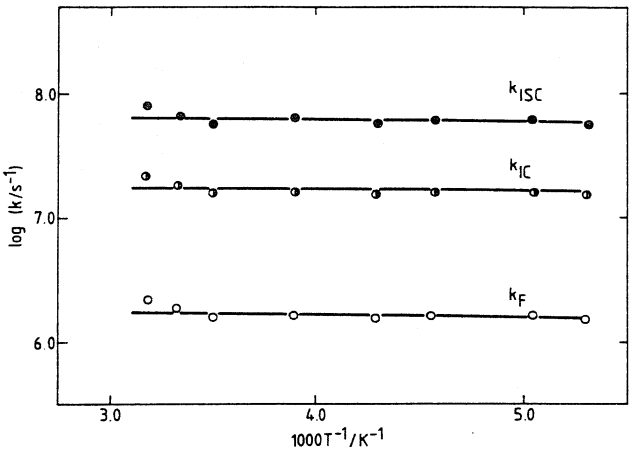

Figure 4. Arrhenius-type plots of photophysical rate coefficients in acetone.

the excited singlet to the ground state, respectively. From these relations the three elementary rate coefficients are easily derived:

$$k_F = \Phi_F/{}^1\tau_0$$

$$k_{ISC} = \Phi_T/{}^1\tau_0$$

$$k_{IC} = (1 - \Phi_T - \Phi_F)/{}^1\tau_0$$

Greater errors are expected in the value of k_{IC} since it is obtained as a difference.

In Figure 3, the rate coefficients determined for fluorescence, intersystem crossing, and internal conversion in acetonitrile are shown on an Arrhenius-type plot. In this polar solvent the rates of intersystem crossing and internal conversion are comparable and are more than an order of magnitude higher than the rate of radiative decay. It is important to stress that all three rate coefficients are temperature-independent within the limits of experimental error. Similar, temperature-independent behavior is observed also in acetone, as shown in Figure 4.

Data obtained for the rates of fluorescence and intersystem crossing in methylcyclohexane, toluene, and tetrahydrofuran are presented in Figures 5, 6, and 7, respectively. The qualitative picture in these nonpolar and moderately polar solvents is similar. The excited singlet lifetime is determined by the rate of singlet → triplet intersystem crossing. Clearly, two ranges have to be distinguished in the temperature dependence of the ISC process. Above about 220 K, a definite temperature dependence of the intersystem crossing rate coefficient is observed, while a limiting value is attained at low temperatures. It appears that transition from the lowest singlet state to the triplet state can occur via at

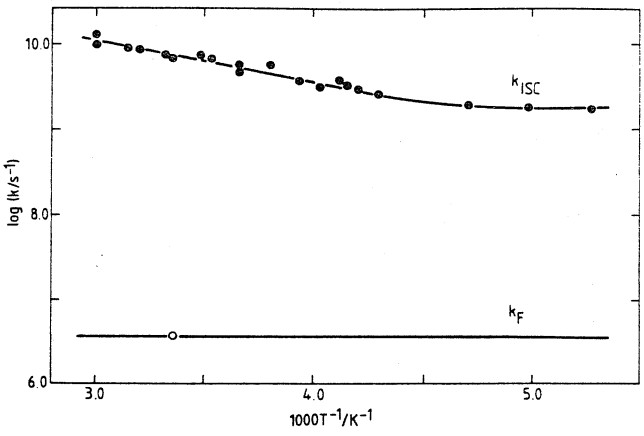

Figure 5. Arrhenius-type plots of photophysical rate coefficients in methylcyclohexane.

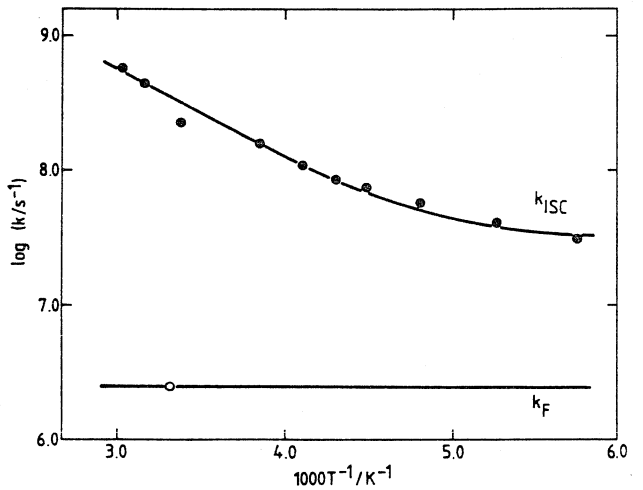

Figure 6. Arrhenius-type plots of photophysical rate coefficients in toluene.

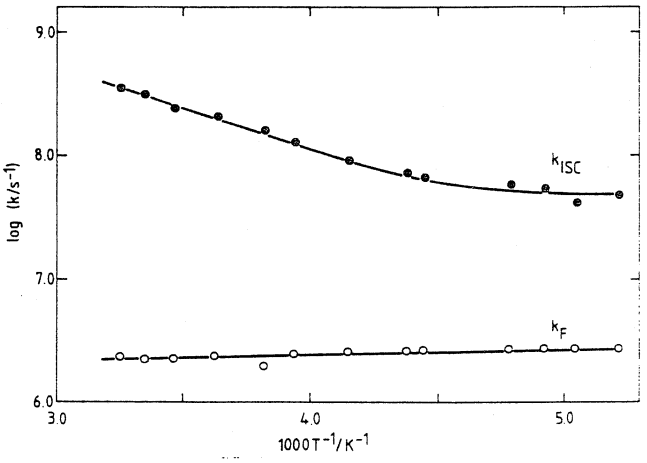

Figure 7. Arrhenius-type plots of photophysical rate coefficients in tetrahydrofuran.

least two routes: by a temperature-independent reaction with rate coefficient k°_{ISC} and by a thermally induced step with a rate coefficient k'_{ISC}, i.e., $k_{ISC} = k^\circ_{ISC} + k'_{ISC}$. In nonpolar and moderately polar solvents, the contribution of internal conversion to the depopulation of the first excited singlet state is relatively small. The data (especially those obtained in toluene) suggest a slight increase of k_{IC} with increasing temperature. However, since k_{IC} is derived as a small difference, the errors are comparable to the effect itself and so further confirmation is required. Finally,

TABLE II: Rate Parameters of Photophysical Processes of Singlet Fluorenone at Room Temperature

solvent	π^*	$10^{-7}k_{ISC}$, s^{-1}	$10^{-7}k°_{ISC}$, s^{-1}	$10^{-7}k'_{ISC}$, s^{-1}	$10^{-10}A'_{ISC}$, s^{-1}	E'_{ISC}, kcal mol^{-1}	$10^{-7}k_{IC}$, s^{-1}	$10^{-7}k_F$, s^{-1}
methylcyclohexane	0.00	710 ± 100	70 ± 30	620 ± 130	30 ± 18	2.3 ± 0.4		0.37 ± 0.09
toluene	0.54	29 ± 4	2.7 ± 0.4	29 ± 4	6.5 ± 2.1	3.2 ± 0.2	3.7 ± 2.0	0.32 ± 0.03
tetrahydrofuran	0.58	32 ± 4	2.9 ± 0.5	25 ± 5	7.9 ± 3.8	3.4 ± 0.3	4.8 ± 3.0	0.24 ± 0.03
acetone	0.71	6.8 ± 0.7	6.8 ± 0.7				1.8 ± 0.7	0.19 ± 0.02
acetonitrile	0.75	2.5 ± 0.2	2.5 ± 0.2				2.7 ± 0.3	0.17 ± 0.02

k_F is characterized by a small and practically constant rate coefficient.

Discussion

Room-temperature rate parameters are summarized in Table II. The rate coefficients k_{ISC} and k_F decrease with increasing solvent polarity. The tendencies indicate a change in the character of the lowest singlet state and a different shift in the energies of the excited states with change of the solvent.

Singlet → triplet intersystem crossing is most sensitive to changes in solvent and temperature. The overall room-temperature ISC rate coefficients as well as the specific rates for the constant and temperature-dependent transitions are listed in Table II. Kinetic data for the temperature-independent and for the thermally enhanced contributions to intersystem crossing were obtained from nonlinear least-squares fits to the experimental k_{ISC} temperature profiles described by

$$k_{ISC} = k°_{ISC} + A'_{ISC} \exp(-E'_{ISC}/RT)$$

The thermally enhanced contribution is most important at higher temperature in nonpolar media and is undetectable in the two polar solvents. The A factors derived in nonpolar and moderately polar solvents are of the order of 10^{10}–10^{11} s^{-1}, similar to those found by I. Tanaka and co-workers[2] for the thermally induced singlet → triplet intersystem crossing of meso-substituted bromoanthracenes in different solvents. The activation energies are in the range of 2–4 kcal mol^{-1}, which may be taken as a measure of the energy separation of the singlet and triplet states involved in the temperature-dependent transition.

One may attempt to explain our results on the rate of intersystem crossing by assuming competitive processes (both exothermic and endothermic ones) to occur from the lowest excited singlet state to adjacent triplet levels. The relative rate of the competitive transitions is expected to be temperature- and solvent-dependent. Such assumptions are in accordance with the interpretation of temperature and solvent effects in the photophysics of substituted anthracenes.[1,2,10]

We attribute the observed temperature-independent intersystem crossing to the exothermic transitions from the lowest excited singlet state to the lowest $T_1(\pi\pi^*)$ triplet and to the adjacent $T_2(\pi\pi^*)$ triplet levels (see Figure 1). Both T_1 and T_2 are $\pi\pi^*$ states, while S_1 is of $\pi\pi^*$ character in polar solvents and $n\pi^*$ in nonpolar media. Thus, one expects and finds, indeed, experimentally more efficient temperature-independent singlet → triplet transition in nonpolar than in polar media.

The temperature-dependent intersystem crossing can be identified as a thermoneutral or endothermic transition from the lowest excited S_1 singlet to the higher excited $T_3(n\pi^*)$ triplet state. In nonpolar and moderately polar solvents, where T_3 is adjacent to S_1, this thermally activated $S_1 \rightarrow T_3$ transition dominates the singlet-state depopulating processes and determines the photophysics of fluorenone. On the other hand, in strongly polar media where the T_3 level is located well above the S_1 state, thermal activation appears to be insufficient to induce $S_1 \rightarrow T_3$ transition and only exothermic intersystem crossing to the lower T_1 and T_2 triplet states occurs.

In polar solvents, internal conversion appears to play a significant role in depopulating the lowest singlet excited state and k_{IC} is practically temperature-independent. However, in less polar solvents a small temperature dependence of k_{IC} cannot be excluded. If the temperature effect is real, it may be an indication of the proximity effect[11,12] caused by the vibronic interaction between close-lying $n\pi^*$ and $\pi\pi^*$ singlet states in nonpolar and moderately polar media.

Fluorescence is a relatively insignificant excited singlet state process in all solvents. The results given in Table II show a decrease of k_F with increasing solvent polarity, which is related most probably to the change of the lowest excited singlet state character.

Our investigations show that the unique properties of fluorenone make this compound an excellent subject for both experimental and theoretical studies.

Registry No. Fluorenone, 486-25-9; methylcyclohexane, 108-87-2; tetrahydrofuran, 109-99-9; acetonitrile, 75-05-8; acetone, 67-64-1; toluene, 108-88-3.

(10) Bennett, R. G.; McLartin, P. J. *J. Chem. Phys.* **1966**, *44*, 1969.

(11) Wassam, W. A., Jr.; Lim, E. C. *J. Mol. Struct.* **1978**, *47*, 129.

(12) Wassam, W. A., Jr.; Lim, E. C. *J. Chem. Phys.* **1978**, *68*, 433.

2. Melléklet

J. Phys. Chem. 1993, 97, 8895–8899

Substituent, Solvent, and Temperature Effects on Radiative and Nonradiative Processes of Singlet Excited Fluorenone Derivatives

László Biczók, Tibor Bérces,* and Ferenc Márta

Central Research Institute for Chemistry, Hungarian Academy of Sciences, P.O. Box 17, 1525 Budapest, Hungary

Received: March 10, 1993; In Final Form: May 14, 1993

Fluorescence lifetimes, fluorescence quantum yields, and triplet yields have been measured for 2-fluorofluorenone and 2-methoxyfluorenone in different solvents having a wide range of polarities. The photophysical characteristics of the fluoro derivative were found to be similar to those of fluorenone itself. The dominating process in nonpolar and moderately polar solvents is singlet–triplet transition with temperature-independent and additional temperature-dependent components. However, the photophysics of the methoxy derivative is governed by internal conversion to the ground state, which gains in importance with increasing solvent polarity and shows a temperature-dependent rate in nonpolar solvent. The efficient internal conversion is explained by assuming the decay to occur from a charge-transfer-type excited state.

Introduction

It is well-known[1] that substituents and solvent polarity can greatly alter the photophysical and photochemical properties of molecules, especially of those which have closely located excited states of different character. The effect can often be explained in terms of the inversion of low-lying excited states caused by a change in solvent polarity or by electron-donating/withdrawing substituents. For instance, the effect of ring substituents on the photoreactivity of phenyl alkyl ketones has been extensively studied.[2] Futhermore, a characteristic solvent effect on the photophysics[3,4] of fluorenone and on its photoreduction by amines[5] has been observed.

In a previous paper,[4] we reported on the solvent and temperature dependence of the rates of the dominant photophysical processes depopulating the fluorescent state of fluorenone. In the present paper, we examine solvent and temperature effects on the photophysical processes of fluorenone derivatives with electron-donating and electron-withdrawing substituents, respectively, in position 2. 2-Fluorofluorenone (FF) and 2-methoxyfluorenone (MOF) are chosen as representatives of the two structures types.

Experimental Section

FF was obtained from Aldrich Chemical Co., and MOF was synthesized from 2-hydroxyfluorenone (Aldrich) by the method of Gray et al.[6] Compounds were purified by recrystallization and preparative thin-layer chromatography. Methylcyclohexane (Carlo Erba) was purified as described in the literature,[7] and all other solvents were of HPLC grade (Merck) and were used without further purification. Samples were deoxygenated by freeze–pump–thaw cycles and were sealed off under vacuum.

Corrected fluorescence spectra were recorded on a homemade spectrofluorimeter equipped with a Princeton Applied Research type 1140 A/B photon-counting system. Fluorescence quantum yields were determined relative to quinine sulfate in 1 N H_2SO_4 solution (reference yield: $\Phi_F = 0.546$).[8]

Fluorescence decay times were measured on an Applied Photophysics SP-3 instrument using a hydrogen lamp operated at 30 kHz. Data were analyzed by a nonlinear least-squares reconvolution method. All measurements could be fitted well by assuming single-exponential decay kinetics.

Room temperature triplet yields were determined by two different methods. For all samples prepared with different solvents, the "comparative method", with monochromatic laser flash excitation, was used. The principle of the method, as described,[9–13] is to compare the concentration of triplets formed on excitation of a solution of the compound investigated with the concentration of triplets formed by the same number of quanta from a solution of a standard with a known triplet yield (i.e., the compound and the standard having the same ground-state absorbency at the excitation wavelength). The original method depends on the knowledge and accuracy of the absorption coefficients of the compound and the standard. Here we used an improved version of the method[14] in which we eliminated this disadvantage by adding a common triplet energy acceptor to quench efficiently the triplet both in the solution of the compound investigated and in that of the standard. Thus, the triplet yield of the compound investigated was obtained as the ratio of the triplet–triplet absorption signal of the triplet energy acceptor, measured in the solution of the compound, to that of the standard multiplied by the known triplet yield of the standard.

Triplet yield determinations were performed with a laser flash photolysis apparatus using the 308-nm light from a Lambda Physik EMG 101 excimer laser (15-ns pulse width, 80 mJ/pulse). Fluorenone solution in methylcyclohexane, for which the triplet yield of $\Phi_T = 1$ is well established.[3b,15–17] was used as the standard. Moreover, 9,10-dibromoanthracene, with negligible absorption at the excitation wavelength and low triplet energy, was selected as an efficient triplet energy acceptor. The triplet–triplet absorption of the latter was monitored at 420 nm, perpendicular to the excitation light, using a Hitachi VC-6041 digital storage oscilloscope.

The other technique, used for room temperature triplet yield determinations in acetonitrile, was the "limiting slope" method[13] which also compares two samples. One of the cuvettes contained the solution of the fluorenone derivative while the other one contained the solution of the sensitizer and in small concentration the compound to be studied (i.e., benzophenone sensitizer plus 2×10^{-4} mol dm^{-3} fluorenone derivative). The two samples had matched absorbances at the excitation wavelength. Using the frequency-doubled 347-nm light of a Holobeam Q-switched ruby laser for excitation, the triplet–triplet absorbance of the fluorenone derivative was monitored at 450 nm both in the direct excitation sample (ΔA) and in the benzophenone-sensitized sample (ΔA^{sens}) as a function of laser energy (E). The triplet yield of the fluorenone

0022-3654/93/2097-8895$04.00/0

TABLE I: Fluorescence Quantum Yields, Singlet Lifetimes, and Triplet Yields at 298 K

solvent	τ_F, ns	λ_F^{max}, nm	$10^3\Phi_F$	Φ_T
		Fluorenone[a]		
methylcyclohexane	0.14	480	0.52 ± 0.04	>0.99
toluene	3.0 ± 0.2	490	9.7 ± 0.6	0.88 ± 0.08
tetrahydrofuran	2.7 ± 0.2	495	6.4 ± 0.6	0.87 ± 0.08
acetone	11.3 ± 0.5	513	21 ± 2	0.77 ± 0.07
acetonitrile	18.7 ± 0.7	520	32 ± 2	0.46 ± 0.04
		2-Fluorofluorenone		
methylcyclohexane	1.5 ± 0.1	508	3.0 ± 0.3	0.96 ± 0.04
toluene	10.8 ± 0.6	521	22 ± 2	0.72 ± 0.07
ethyl acetate	15.5 ± 0.8	525	36 ± 3	0.65 ± 0.07
acetone	11.7 ± 0.6	532	15 ± 2	0.52 ± 0.06
acetonitrile	10.7 ± 0.6	545	15 ± 2	0.16 ± 0.03
		2-Methoxyfluorenone		
methylcyclohexane	9.0 ± 0.5	522	24 ± 2	0.22 ± 0.03
dibutyl ether	4.5 ± 0.3	540	10 ± 1	0.14 ± 0.02
toluene	4.0 ± 0.2	554	9.2 ± 0.9	0.16 ± 0.02
ethyl acetate	3.4 ± 0.2	560	8.5 ± 0.8	0.10 ± 0.02
acetonitrile	1.4 ± 0.1	590	2.4 ± 0.2	0.05 ± 0.01

[a] Reference 4.

derivative was obtained from the equation

$$\Phi_T = \Phi_T^{sens}\left(\frac{d\Delta A/dE}{d\Delta A^{sens}/dE}\right)_{E\to 0}$$

using the benzophenone triplet yield $\Phi_T^{sens} = 1$. Again, the technique did not require the use of any absorption coefficients.

Both methods of triplet yield determination assume complete triplet energy transfer from and to the investigated fluorenone derivative, respectively. Provided that energy transfer is 100% between standard and 9,10-dibromoanthracene (which is probably realized here as a result of the large energy difference between donor and acceptor), an incomplete triplet energy transfer in the reactions of fluorenone derivatives would cause an underestimation in the triplet yield determination by the "comparative method" and an overestimation by the "limiting slope" method. The comparison of the data showed, however, no systematic deviations (only random errors), and the results from the two methods agreed within 15%.

Triplet yields for temperatures different from 298 K were derived from initial triplet–triplet absorbances relative to the room temperature values; Φ_T at 298 K served as the reference value.

Results

Wavelengths of fluorescence maxima (λ_F^{max}), fluorescence lifetimes (τ_F), fluorescence quantum yields (Φ_F), and triplet yields (Φ_T) in various solvents at room temperature are summarized in Table I for 2-fluorofluorenone (FF) and 2-methoxyfluorenone (MOF). For comparison photophysical properties of fluorenone (F) obtained in a previous study[4] are also included in the table.

The solvents are arranged in order of increasing polarity from the nonpolar methylcyclohexane to the highly polar acetonitrile. All three compounds exhibit considerable Stokes shifts of the fluorescence maximum, which increase with increasing solvent polarity. The shift is the greatest for MOF, indicating a significant difference between ground- and excited-state dipole moments. The singlet energies, obtained from the crossing points of the fluorescence and absorption curves in acetonitrile, are 63.5, 62.3, and 56.6 kcal mol^{-1} for F, FF, and MOF, respectively.

The photophysical properties of MOF and their dependence on the solvent polarity differ basically from those of F and FF. In the latter cases, the singlet lifetimes and the fluorescence quantum yields are much lower in methylcyclohexane than in medium and highly polar solvents, while for MOF, the τ_F and Φ_F values are highest in the nonpolar medium. Moreover, singlet lifetimes and fluorescence yields of MOF decrease with increasing solvent polarity, which is opposite to the tendency found[4] for F. FF appears to represent an intermediate case where an initial increase in τ_F and Φ_F is seen from the nonpolar to the medium polar solvents (similar to F); however, τ_F and Φ_F are lower in polar solvents (as found for MOF too).

TABLE II: Room Temperature Rate Coefficients of Photophysical Processes

solvent	$10^{-7}k_F$, s^{-1}	$10^{-7}k_{ISC}$, s^{-1}	$10^{-7}k_{IC}$, s^{-1}
	Fluorenone[a]		
methylcyclohexane	0.37 ± 0.09	710 ± 100	
toluene	0.32 ± 0.03	29 ± 4	3.7 ± 2.0
tetrahydrofuran	0.24 ± 0.03	32 ± 4	4.8 ± 3.0
acetone	0.19 ± 0.02	6.8 ± 0.7	1.8 ± 0.7
acetonitrile	0.17 ± 0.02	2.5 ± 0.2	2.7 ± 0.3
	2-Fluorofluorenone		
methylcyclohexane	0.20 ± 0.03	64 ± 6	
toluene	0.20 ± 0.02	6.7 ± 0.7	2.4 ± 0.7
ethyl acetate	0.23 ± 0.03	4.2 ± 0.5	2.0 ± 0.5
acetone	0.13 ± 0.02	4.4 ± 0.6	4.0 ± 0.6
acetonitrile	0.14 ± 0.02	1.5 ± 0.5	7.7 ± 0.6
	2-Methoxyfluorenone		
methylcyclohexane	0.27 ± 0.03	2.4 ± 0.4	8.4 ± 0.6
dibutyl ether	0.23 ± 0.03	3.5 ± 0.5	21 ± 2
toluene	0.22 ± 0.03	3.1 ± 0.5	19 ± 2
ethyl acetate	0.25 ± 0.02	3.2 ± 0.6	26 ± 1
acetonitrile	0.17 ± 0.02	3.6 ± 0.8	68 ± 5

[a] Reference 4.

The triplet yields decrease considerably with the increase of solvent polarity for all three fluorenones. In nonpolar and slightly polar solvents, the major singlet-state-depopulating process of F and FF is singlet–triplet intersystem crossing. However, in polar solvents internal conversion becomes dominant. (No photochemical decomposition is observed.) MOF behaves again in a different way. Its characteristic singlet reaction in all solvents is internal conversion to the ground state.

The photophysical parameters studied are related, as follows,

$$\tau_F = 1/(k_F + k_{ISC} + k_{IC}) \quad (1)$$

$$\Phi_F = k_F/(k_F + k_{ISC} + k_{IC}) \quad (2)$$

$$\Phi_T = k_{ISC}/(k_F + k_{ISC} + k_{IC}) \quad (3)$$

to the rate coefficients of the photophysical primary processes, i.e., to k_F, k_{ISC}, and k_{IC}, the rate coefficients for fluorescence, singlet–triplet intersystem crossing, and internal conversion, respectively. The rate coefficients derived from these relationships for different solvents are summarized in Table II.

The fluorescence rate coefficients are around $k_F = 2.5 \times 10^7$ s^{-1} for all three fluorenones, although a small decrease with solvent polarity can be observed. The main differences in the photophysical properties of F and substituted derivatives are due to the different rates of the nonradiative processes. For both F and FF, the dominating nonradiative process is singlet–triplet intersystem crossing, with the specific rate decreasing with increasing solvent polarity. The internal conversion rate is practically constant ($k_{IC} = 2$–4×10^7 s^{-1}). The only significant difference appears to be the higher intersystem crossing rate of F as compared with FF.

The dominating singlet-state process of MOF in all solvents and of FF in polar solvents is internal conversion to the ground state, with the rate coefficient increasing in importance with solvent polarity. Under these conditions, the intersystem crossing rate coefficient is around 2–4 × 10^7 s^{-1}.

The temperature dependence of the fluorescence spectra, fluorescence lifetimes, fluorescence quantum yields, and triplet yields of FF and MOF has been studied in the 180–320 K temperature range.

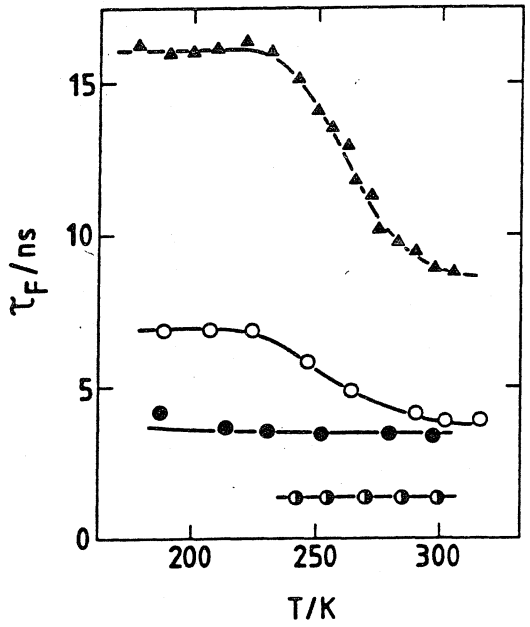

Figure 1. Temperature dependence of the fluorescence decay times of MOF in methylcyclohexane (▲), toluene (○), ethyl acetate (●), and acetonitrile (◑).

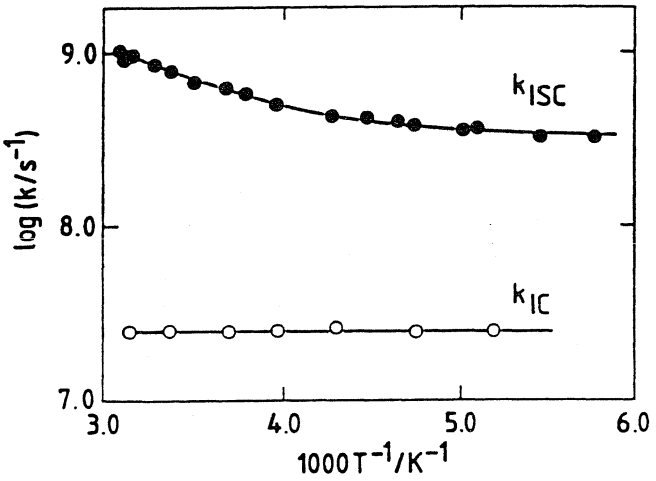

Figure 2. Arrhenius plots for rate constants of nonradiative processes of FF in methylcyclohexane.

The temperature dependence of the fluorescence decay times of MOF in different solvents is shown in Figure 1. The dependence of the fluorescence quantum yields was found to be similar. In addition to the temperature-independent yields of triplet formation measured in polar solvents, a small decrease of the triplet yields was found in toluene and a more significant decrease (by about a factor of 2) was obtained in methylcyclohexane as a result of temperature increase from 220 to 330 K. (No change of Φ_T occurred below 220 K.)

The variation of singlet lifetime and of fluorescence and triplet yields with temperature for FF was found to be similar to the temperature dependences of the photophysical properties of F[4] and therefore will not be presented here in detail. All photophysical properties of FF and MOF were found to be temperature independent in polar solvents; thus, the room temperature data given in Tables I and II are valid for the whole temperature range studied.

The Arrhenius plots of the rate coefficients of the nonradiative processes in methylcyclohexane are presented in Figures 2 and 3 for FF and MOF, respectively. Similar plots are obtained also in toluene. The most important facts regarding the observed temperature dependences of the photophysical properties of FF and MOF are as follows: (i) The temperature dependences of the fluorescence decay time, the fluorescence quantum yield, and

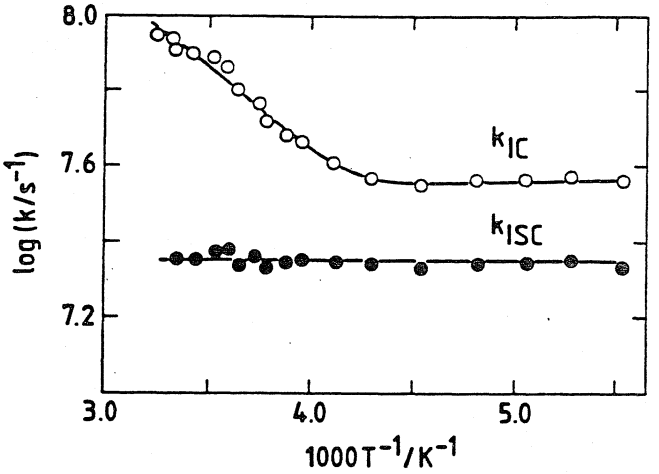

Figure 3. Arrhenius plots of rate constants of nonradiative processes of MOF in methylcyclohexane.

TABLE III: Rate Parameters[a] for Dominating Processes

process	$10^{-7}k^\circ$, s^{-1}	$10^{-7}k'$, s^{-1}	$10^{-10}A'$, s^{-1}	E', kcal mol^{-1}
intersystem crossing for F[b]				
in methylcyclohexane	70 ± 30	620 ± 130	30 ± 18	2.3 ± 0.4
in toluene	2.7 ± 0.4	29 ± 4	6.5 ± 2.1	3.2 ± 0.2
intersystem crossing for FF				
in methylcyclohexane	25 ± 4	39 ± 4	2.5 ± 0.6	2.4 ± 0.3
in toluene	2.1 ± 0.7	4.6 ± 0.6	0.2 ± 0.1	2.2 ± 0.3
internal conversion for MOF				
in methylcyclohexane	3.5 ± 0.6	4.9 ± 0.6	52 ± 10	5.4 ± 0.5
in toluene	11 ± 2	10 ± 2	3.9 ± 1.8	3.5 ± 0.4

[a] The k° and k', rate coefficients refer to the temperature-independent and thermally enhanced processes, respectively, at 298 K. [b] Reference 4.

the triplet yield are caused by the change of the rate coefficients of the singlet–triplet intersystem crossing and the singlet excited-state internal conversion to the ground state in the case of FF and MOF, respectively. (ii) The Arrhenius plots of the dominating processes are nonlinear, and the specific rates are temperature independent below about 210–230 K. However, at higher temperatures the rates of intersystem crossing of FF and those of internal conversion of MOF increase considerably with increasing temperature. (iii) The Arrhenius plots of the rate coefficients of the dominating photophysical processes in methylcyclohexane and toluene indicate that in nonpolar and moderately polar solvents temperature-independent and temperature-dependent intersystem crossing of FF can occur (just as observed[4] for F), while in the case of MOF, temperature-independent and temperature-dependent internal conversion is possible. Nonlinear least-squares fitting to the measured data, using eq 4

$$k = k^\circ + A' \exp(-E'/RT) \qquad (4)$$

gave the rate parameters summarized in Table III.

Discussion

The experimental data obtained for the photophysical properties of FF in this work closely resemble those found for F in a previous study.[4] The similarities of the solvent and temperature effects may be explained by assuming that fluoro substitution has little effect on the singlet and triplet energy levels, and consequently, the mechanism of the photophysical processes taking place subsequent to excitation of FF is the same as (or similar to) that established[4,15] for F. Thus, we assume that in methylcyclohexane, the first excited singlet state of FF is an $n\pi^*$ state with the second singlet of $\pi\pi^*$ character which is relatively close in energy to the lowest one. There are two $\pi\pi^*$ triplet states which are below and one $n\pi^*$ triplet level which lies just above the $S_1(n\pi^*)$ state. The temperature-independent singlet-triplet intersystem crossing can

be attributed to the "exothermic" transition from $S_1(n\pi^*)$ to $T_1(\pi\pi^*)$ and $T_2(\pi\pi^*)$. The relatively large k°_{ISC} rate coefficient found in methylcyclohexane can be explained by the strong $n\pi^*$–$\pi\pi^*$ spin–orbit coupling. One interpretation of the temperature-dependent intersystem crossing of FF could be a $S_1(n\pi^*)$–$T_3(n\pi^*)$ transition (as we previously suggested[4] for F). However, considering the high efficiencies and the relatively high A factors of the thermally enhanced intersystem crossing for both F and FF in methylcyclohexane compared to those measured in solvents of intermediate polarity (e.g., toluene or tetrahydrofuran), the indirect route of $S_1(n\pi^*) \rightarrow S_2(\pi\pi^*) \rightarrow T_3(n\pi^*)$ appears to be more probable in methylcyclohexane. This pathway of intersystem crossing consists of transitions which are favorable according to the El-Sayed rule.[18] Since both temperature-independent and temperature-dependent intersystem crossing processes are very fast, this leaves very little chance for the occurrence of fluorescence emission and internal conversion. Thus, the triplet yields are not far from unity in methylcyclohexane.

In the moderately polar toluene, the order of the singlet $n\pi^*$ and $\pi\pi^*$ states is probably reversed. The temperature-independent intersystem crossings, $S_1(\pi\pi^*) \rightarrow T_1(\pi\pi^*)$ and $S_1(\pi\pi^*) \rightarrow T_2(\pi\pi^*)$, are less efficient due to the weaker spin–orbit coupling between the singlet and triplet states involved in the transitions. If the lowest singlet state is of $\pi\pi^*$ character, the indirect route of the temperature-dependent intersystem crossing $S_1(\pi\pi^*) \rightarrow S_2(n\pi^*) \rightarrow T_3(n\pi^*)$ is not favorable, and triplet-state formation does occur by direct transition, $S_1(\pi\pi^*) \rightarrow T_3(n\pi^*)$, which is relatively slow due to the increased S_1–T_3 energy gap.

Increasing solvent polarity is known to increase the $n\pi^*$ and to decrease the $\pi\pi^*$ transition energies. In highly polar solvents (e.g., acetone and acetonitrile), the $S_1(\pi\pi^*) \rightarrow T_3(n\pi^*)$ energy gap is so large that thermal activation is insufficient to bring about the $S_1(\pi\pi^*) \rightarrow T_3(n\pi^*)$ transition. Thus, only the temperature-independent slow $S_1(\pi\pi^*) \rightarrow T_1(\pi\pi^*)$ and $S_1(\pi\pi^*) \rightarrow T_2(\pi\pi^*)$ intersystem crossing processes occur. The slow ISC rate of FF in highly polar solvents causes $S_1 \rightarrow S_0$ internal conversion to become the dominating photophysical process of the S_1 state.

The effect of ring substituents on the spectroscopy and photophysics of carbonyl compounds has been extensively studied, and detailed knowledge of the substituent effect, especially for phenyl ketones, has been accumulated (see for instance ref 2 and citations therein). Electron-donating substituents are known to lower $\pi\pi^*$ and raise $n\pi^*$ transition energies, which often causes an inversion of the lowest excited states. We assume that the general picture is similar in the case of fluorenone derivatives. Fluorenone with an inductively electron-donating methoxy substituent in ring position 2 has the lowest $\pi\pi^*$ singlet state, even in nonpolar methylcyclohexane. This is supported by the considerable red shift of the MOF absorption spectra compared to those of FF (35 nm) and F (45 nm) in methylcyclohexane and in other solvents.

The $\pi\pi^*$ character of the first excited singlet state explains at least one part of the differences in photophysical properties of MOF and those of F and FF. In methylcyclohexane (and even more in other solvents), the $T_3(n\pi^*)$ triplet state appears to lie so high above the $S_1(\pi\pi^*)$ of MOF that thermally enhanced intersystem crossing cannot occur. In any solvent, the triplet state of MOF is formed only by the temperature-independent $S_1(\pi\pi^*) \rightarrow T_1(\pi\pi^*)$ and $S_1(\pi\pi^*) \rightarrow T_2(\pi\pi^*)$ transitions. This identification of ISC is supported by the similarity of the intersystem crossing rate coefficients determined for MOF in different solvents and the k_{ISC} values obtained for F and FF in polar media. (All these transitions are exothermic and occur between two states of $\pi\pi^*$ character.)

Perhaps the most important feature of the observations made in this study is the significant decrease of fluorescence decay time, fluorescence yield, and triplet yield with solvent polarity in case of MOF in all solvents and of FF in polar media. All experimental results indicate that the observed interesting solvent effect is related to the dominating role played by internal conversion to the ground state which grows in importance with increasing solvent polarity. Understanding of the causes of the high internal conversion efficiency may be facilitated by identification of the excited state responsible for the fast nonradiative transition.

Fluorescence maxima, presented in Table I, indicate a large red shift of the luminescence spectra with increasing solvent polarity for MOF and in polar solvents for FF. The strong dependence of the emission energies on the polarity, together with the characteristic changes with the solvent of the quantum yields of radiative and nonradiative processes, is best explained by assuming that the excited state which dominates the photophysics of MOF in all studied solvents and of FF in acetonitrile is of highly polar character. For MOF, one expects electron delocalization developing a partial negative charge on the carbonyl oxygen and partial positive charge on the methoxy group.

The polar nature of the excited state is supported also by the Lippert–Mataga-type analysis of the absorption and fluorescence data.[19] Evaluation of the steady-state Stokes shifts yields for the change in the dipole moment upon excitation ($\Delta\mu = \mu_e - \mu_g$) approximately 5.9 and 10.2 D for FF and MOF, respectively. The difference between the dipole moments of ground and excited electronic states is seen to be considerably greater for MOF than for FF.

It has been found[20] for many nitrogen heterocyclic and aromatic carbonyl compounds that vibronic interaction between close-lying $n\pi^*$ and $\pi\pi^*$ singlet states may lead to a very efficient radiationless decay from the lower of the two excited states. This phenomenon is widely known as "proximity effect". The expected influence of the methoxy substitution and of the solvent effect on the location of the excited-state energy levels (as set forth above) excludes the possibility that the observed efficient internal conversion is due to the "proximity effect". The energy gap between the $n\pi^*$ and $\pi\pi^*$ singlet states of MOF in all solvents and of FF in highly polar solvents is probably so large that any interaction between these states is negligible.

However, the highly polar nature of the low-lying excited state responsible for the photophysics of MOF may explain the very efficient internal conversion. In an investigation of radiative and nonradiative processes of (*N*-arylamino)naphthalenesulfonates, Kosower and his co-workers suggested[21] that the return to the ground state from an excited charge-transfer state via an intramolecular electron-transfer process can occur. They also found that this decay process has a rate which is very dependent upon solvent polarity, and the major decay channel of the charge-transfer state in polar solvents is the electron-transfer process which produces vibrationally excited ground-state molecules. The striking similarity between the solvent dependence of the photophysical properties of MOF and those of (*N*-arylamino)-naphthalenesulfonates leads us to the conclusion that the efficient internal conversion observed for MOF occurs between a polar excited state and the ground state via intramolecular electron transfer with a rate strongly increasing with solvent polarity. Probably a similar mechanism holds at least one part of the radiationless decay of the excited state of FF in acetonitrile. In order to test the electron-transfer mechanism of radiationless transition to the ground state, a few experiments were carried out with 2-aminofluorenone (AF), i.e., with a fluorenone derivative having a stronger electron-donating substituent in position 2 than MOF. Shorter lifetime and higher IC yield were found for AF than for MOF, in accordance with the expectations.

The temperature dependence of MOF internal conversion observed in methylcyclohexane and toluene must be dealt with. Only very few well-documented cases of temperature-dependent internal conversions are known from the literature. An increase

in the $S_1 \rightarrow S_0$ internal conversion rate with increasing temperature was found by Lim and co-workers for N-heterocyclic compounds[22] and for psoralens.[20b] The strong temperature dependence was interpreted in terms of the "proximity effect" as a result of the thermal excitation of vibrationally active out-of-plane bending modes of molecules having closely spaced, lowest energy, $n\pi^*$ and $\pi\pi^*$ singlet states. Moreover, Schoof and Güsten[23] found a significant increase in the rate of radiationless deactivation by internal conversion above −10 C° for 9-methoxyanthracene in *n*-heptane and assumed[23b] that the photophysics is governed mainly by Franck–Condon factors involving coordinates with "ring-flapping" motions of the anthracene moiety.

This literature survey shows that various suggestions have been made regarding the nature of the temperature-dependent internal conversion, and further experimental and theoretical work is clearly required to solve this problem. This time, for the thermally enhanced IC of MOF we can only consider some possible explanations. Above we have argued against the role of the "proximity effect" in the photophysics of MOF. Therefore, we believe that the "proximity effect" is not the appropriate cause of the temperature-dependent internal conversion of MOF in methylcyclohexane and toluene. However, a similar explanation should be thoroughly considered. Thus, the dominant vibrationally active deactivating mode may be connected with the CH_3O group which by thermal excitation may considerably increase the vibrational overlap between the ground and excited states and thereby enhance the radiationless decay of the excited state.

Another interpretation of the temperature-dependent IC could be that in nonpolar and slightly polar solvents MOF has two low-lying singlet excited states: a charge-transfer state (identified in connection with the explanation of the solvent polarity effect) and a $\pi\pi^*$ state located below but close to the charge-transfer state. Thermal excitation from the $\pi\pi^*$ singlet state to the charge-transfer state and subsequent transition to the appropriate vibration level of the ground state could result in a temperature-dependent radiationless deactivation at higher temperatures, in nonpolar solvents. In polar solvents, where the inversion of these two states is expected, temperature-dependent IC is not found.

Finally, application of the energy gap law to the nonradiative decay processes of excited states of fluorenone derivatives will be examined. The energy gap law predicts[24] that the rate of nonradiative decay is determined by the vibrational coupling between the excited state and the ground state involved in the transition and that the value of k_{IC} decreases as the energy gap ΔE increases. The correlation is expressed in quantitative form in the equation derived for the low-temperature, weak vibrational coupling limit by Englman, Jortner, and Freed.[24] Using this equation, it can be shown that under certain conditions a linear correlation should hold in a given solvent for a series of compounds between log k_{IC} and the energy of fluorescence maxima. A similar linear correlation should describe for a given compound the effect of solvent changes on k_{IC}. A good linear correlation is obtained for the series of compounds consisting of F, FF, and MOF as indicated in Figure 4 by the broken line fitted to the data measured in acetonitrile. The predictions resulting from the energy gap law for the solvent effect are also established in the case of all three compounds investigated. The linear correlation for MOF is presented by the full line in Figure 4.

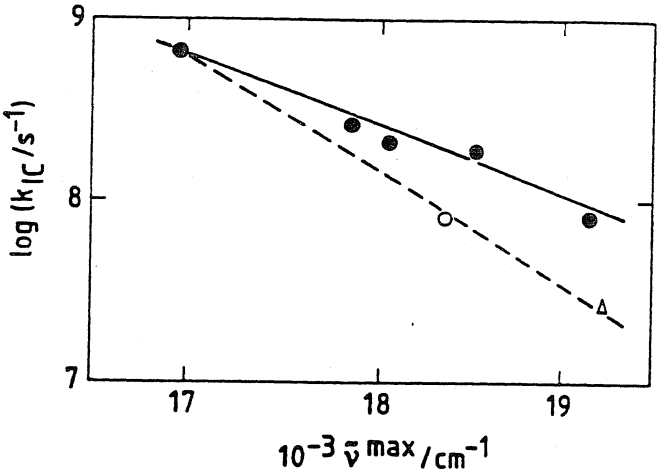

Figure 4. Plot of log k_{IC} vs $\tilde{\nu}_F^{max}$ for MOF (●), FF (○), and F (△). Full line refers to different solvents, broken line to acetonitrile.

Acknowledgment. Financial support from the Hungarian National Science Foundation (No. 1802) is gratefully acknowledged.

References and Notes

(1) Turro, N. *Modern Molecular Photochemistry*; Benjamin Cummings: New York, 1978.
(2) Wagner, P. J.; Siebert, E. J. *J. Am. Chem. Soc.* **1981**, *103*, 7329.
(3) (a) Caldwell, R. A. *Tetrahedron Lett.* **1969**, 2121. (b) Caldwell, R. A.; Gajewski, R. P. *J. Am. Chem. Soc.* **1971**, *93*, 533.
(4) Biczók, L.; Bérces, T. *J. Phys. Chem.* **1988**, *92*, 3842.
(5) Cohen, S. G.; Gutteplan, J. B. *Tetrahedron Lett. 1968*, 5353.
(6) Gray, G. W.; Hartley, J. B.; Ibbotson, A. *J. Chem. Soc. 1955*, 2686.
(7) Perrin, D. D.; Armarego, W. L. F.; Perrin, D. R. *Purification of Laboratory Chemicals*, 2nd ed.; Pergamon: Oxford, 1980.
(8) Eaton, D. F. *Pure Appl. Chem.* **1988**, *60*, 1107. Melhuish, W. H. *J. Am. Chem. Soc.* **1961**, *65*, 229.
(9) Richards, J. T.; Thomas, J. K. *Trans. Faraday Soc.* **1970**, *66*, 621.
(10) Amand, B.; Bensasson, R. *Chem. Phys. Lett.* **1975**, *34*, 44.
(11) Bensasson, R.; Goldschmidt, C. R.; Land, E. J.; Truscott, T. G. *Photochem. Photobiol.* **1978**, *28*, 277.
(12) Bensasson, R.; Land, E. J. In *Photochemical and Photobiological Revies*; Smith, K. C., Ed.; Plenum: New York, 1978; Vol. 3, p. 165.
(13) Hurley, J. K.; Sinai, N.; Linschitz, H. *Photochem. Photobiol.* **1983**, *38*, 9.
(14) A more detailed description of the method will be given in a forthcoming publication in *J. Photochem. Photobiol. A: Chemistry*.
(15) Kobayashi, T.; Nagakura, S. *Chem. Phys. Lett.* **1976**, *43*, 429.
(16) Lower, S. K.; El Sayed, M. A. *Chem. Rev.* **1966**, *66*, 199.
(17) Andrews, L. J.; Deroulede, A.; Linschitz, H. *J. Phys. Chem.* **1978**, *82*, 2304.
(18) El-Sayed, M. A. *J. Chem. Phys.* **1963**, *38*, 2834.
(19) Lakowicz, J. R. *Principles of Fluorescence Spectroscopy*; Plenum: New York, 1983.
(20) (a) Lim, E. C. *J. Phys. Chem.* **1986**, *90*, 6770. (b) Lai, T.-I.; Lim, B. T.; Lim, E. C. *J. Am. Chem. Soc.* **1982**, *104*, 7631. (c) Lim, E. C. In *Excited States*, Lim, E. C., Ed.; Academic: New York, 1977; Vol. 3, p. 305.
(21) Kosower, E. M.; Dodink, H.; Tanizawa, K.; Ottolenghi, M.; Orbach, N. *J. Am. Chem. Soc.* **1975**, *97*, 2167. Kosower, E. M.; Dodink, H.; Kanety, H. *J. Am. Chem. Soc.* **1978**, *100*, 4179.
(22) Lai, T.-I.; Lim, E. C. *Chem. Phys. Lett.* **1979**, *62*, 507.
(23) (a) Schoof, S.; Güsten, H. *J. Photochem.* **1978**, *9*, 246. (b) Schoof, S.; Güsten, H. *Ber. Bunsenges. Phys. Chem.* **1989**, *93*, 864.
(24) (a) Englman, R.; Jortner, J. *Mol. Phys.* **1970**, *18*, 145. (b) Freed, K. F.; Jortner, J. *J. Chem. Phys.* **1970**, *52*, 6272.

3. Melléklet

KINETICS AND MECHANISM OF EXCITED FLUORENONE QUENCHING BY HYDROXY-COMPOUNDS

L. Biczók, T. Bérces, H. Linschitz

Central Research Institute for Chemistry, Hungarian Academy of Sciences,
P.O. Box 17, H-1525 Budapest, Hungary
Department of Chemistry, Brandeis University, Waltham, MA 02254-9110, USA

The quenching reactions of excited carbonyl compounds have been of widespread interest for decades as these belong to the most fundamental processes of photochemistry. The primary step may involve (a) hydrogen abstraction, (b) electron transfer or (c) energy transfer. Numerous studies have established the major characteristics of these various reaction mechanisms. In the present paper, we report on a new type of deactivation pathway and demonstrate that hydrogen bonding of a ketone with alcohols or phenols in the excited state leads to efficient quenching via internal conversion directly to the ground state. Fluorenone was chosen as a model compound in these studies in order to reveal why its photophysical properties are entirely different in alcohols and non-hydroxylic solvents [1]. The well established $\pi\pi^*$ character of both the singlet and the triplet excited states in moderately polar and polar solvents excludes direct hydrogen atom abstraction as primary photochemical reaction of fluorenone.

Addition of alcohols to the fluorenone solution in CH_2Cl_2 shortens the lifetime of the excited singlet (τ_F) whose fluorescence decay can always be described by a single exponential function. These facts and the negligible variation of the ground state absorption spectra in the range of quencher concentrations used indicate that dynamic quenching occurs. The reciprocal fluorescence lifetimes are plotted as function of alcohol concentration in Fig.1. The quenching rate constants derived from the slopes exhibit good correlation with the hydrogen bonding ability of the alcohols. Thus, we infer that a short lived, non- or very weakly fluorescent hydrogen bonded complex is formed between singlet excited fluorenone and alcohols. The interaction is probably facilitated by enhancement of dipolemoment upon excitation of fluorenone. This mechanism is supported by the solvent dependence of the quenching rates (kq). Changing the CH_2Cl_2 solvent to dimethylformamide (DMF) decreases kq by ca. one order of magnitude (Table 1.) because the strength of hydrogen bonding between excited fluorenone and alcohols diminishes due to the higher polarity and hydrogen bonding ability of DMF.

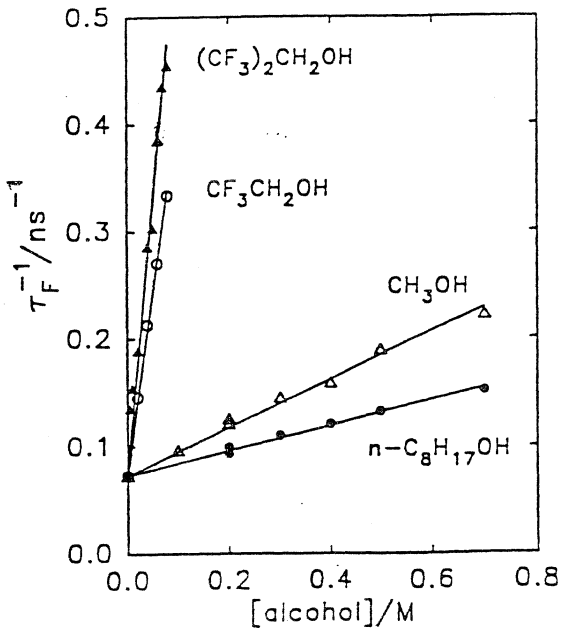

Fig. 1.

In order to explore the various competing processes depopulating the excited fluorenone - alcohol hydrogen bonded complexes, fluorescence and triplet yield

Table 1. Rate constants of singlet excited fluorenone quenching by alcohols and phenols in CH_2Cl_2 and DMF

Alcohol	CH_2Cl_2 k_q $10^8\ M^{-1}s^{-1}$	DMF k_q $10^8\ M^{-1}s^{-1}$	Phenol	CH_2Cl_2 k_q $10^8\ M^{-1}s^{-1}$	DMF k_q $10^8\ M^{-1}s^{-1}$
$(CF_3)_2CHOH$	46	2.8	4-NO_2	98	3.7
CF_3CH_2OH	32	0.8	4-CN	64	2.8
methanol	2.1		4-H	73	9.1
1-octanol	1.1		4-CH_3O	91	46

measurements were carried out as well. Both these yields showed parallel changes with the fluorescence decay time as function of alcohol concentration and the slopes of the Stern-Volmer plots based on the variation of these quantities agreed well within the limits of experimental error. Thus, we conclude that fast internal conversion is the dominant decay pathway of the short lived excited hydrogen bonded complex; the rates of its fluorescence and triplet formation are relatively negligible. The single exponential character of the free fluorenone fluorescence decay indicates that the dissociation of the hydrogen bonded complex to excited fluorenone and ground state alcohol is not feasible. Probably, the much lower energy of the complex hinders the back reaction.

To extend these results, we have studied the mechanism of excited fluorenone interaction with 4-substituted phenols, where both electron transfer and hydrogen bonding are conceivable. The quenching rate constants are summarized in Table 1. It is evident that the behavior of easily oxidized 4-methoxyphenol is entirely different from that observed for the unsubstituted phenol or for derivatives containing electron withdrawing substituents. In the former case, the reaction rate remains always close to diffusion controlled, independent of solvent, while in the latter case, much lower quenching rate constants are found in DMF, which is both more polar and more strongly hydrogen bonding. On the basis of this characteristic solvent dependence, we suggest that electron transfer is the dominant interaction between singlet excited fluorenone and 4-methoxyphenol, whereas the quenching occurs via an excited hydrogen bonded complex with the other phenols studied.

Experiments carried out in the presence of pyridine derivatives provide further evidence bearing on the quenching mechanism. For example, if hydrogen bonding is the major interaction, addition of pyridines results in a significant decrease of the pseudo-first-order rate constant as we have observed in the triplet fluorenone + cyanophenol reaction. Conversely, if the excited molecules react via electron transfer, a strong rate enhancement is expected due to formation of a strongly quenching phenol-pyridine hydrogen bonded complex, as was demonstrated in our recent paper [2].

[1] L. Biczók, L. Jicsinszky, H. Linschitz, J. Inclusion Phenom., **18**, (1994) 237
[2] L. Biczók, H. Linschitz, J. Phys. Chem. **99**, (1995) 1843

INTRODUCTION

The primary step in the quenching reactions of excited carbonyl compounds may involve (a) hydrogen abstraction, (b) electron transfer or (c) energy transfer. In the present paper, we report on a new type of deactivation pathway and demonstrate that hydrogen bonding of a ketone with alcohols or phenols in the excited state leads to efficient quenching via internal conversion directly to the ground state. Fluorenone was chosen as a model compound in these studies in order to reveal why its photophysical properties are entirely different in alcohols and non-hydroxylic solvents. The well established $\pi\pi^*$ character of both the singlet and the triplet excited states in moderately polar and polar solvents excludes direct hydrogen atom abstraction as primary photochemical reaction of fluorenone.

H-BONDING IN GROUND STATE

The equilibrium constants of hydrogen bond formation were derived from the redshift of fluorenone absorption caused by the addition of alcohols. Fig.1 illustrates the method. The intercept of plot shown in the insert gives -K. The following results were obtained in CH_2Cl_2:

alcohol	$(CF_3)_2CHOH$	CF_3CH_2OH	CH_3OH	$n\text{-}C_8H_{17}OH$
K, M^{-1}	3.5	0.7	<0.6	<0.6

No hydrogen bonding was found in dimethylformamid.

Fig.1 Variation of fluorenone absorption spectra on addition of $(CF_3)_2CHOH$ in methylene chloride. Insert is based on the absorbances measured at 336 nm.

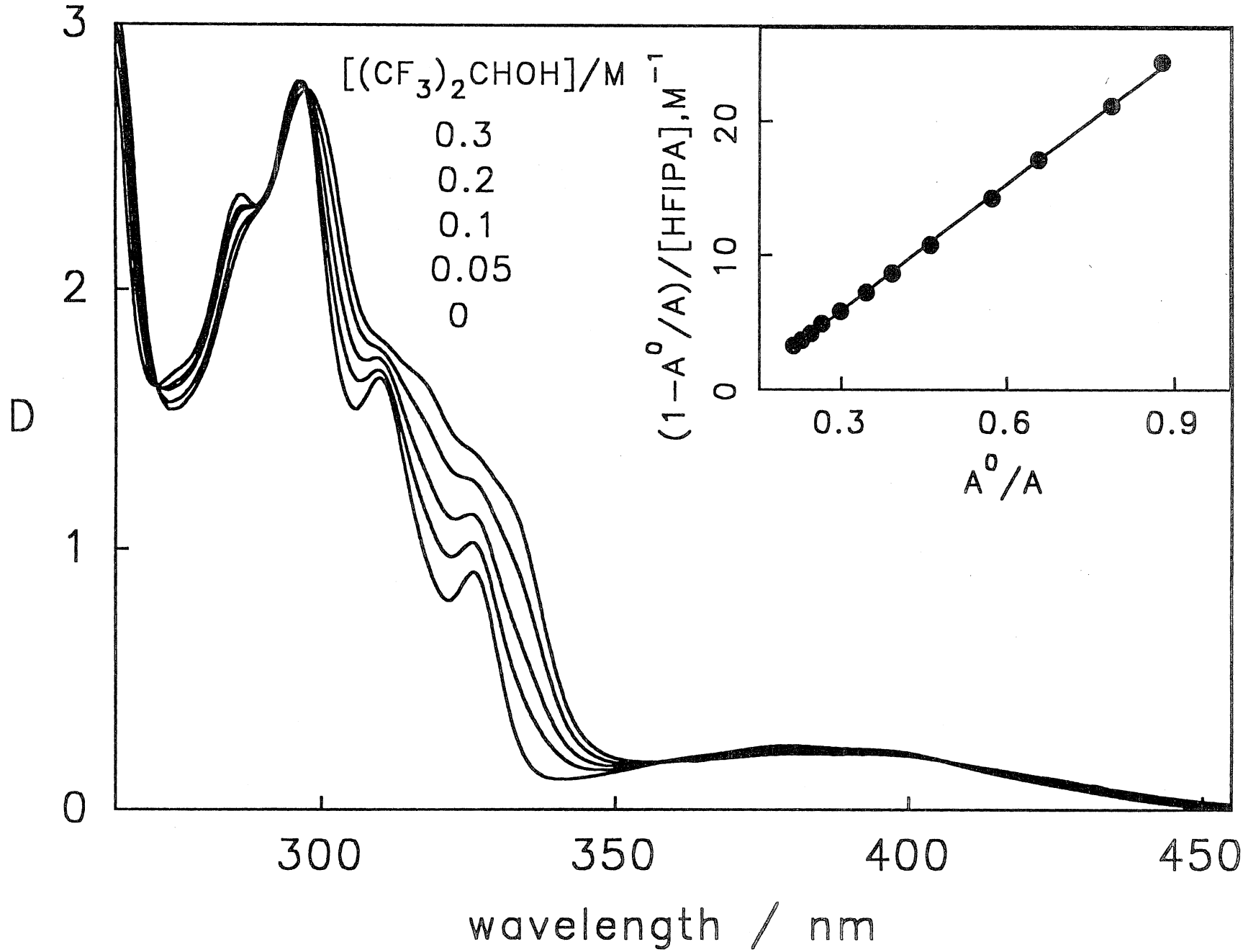
3
2
1
0
D
[(CF3)2CHOH]/M
0.3
0.2
0.1
0.05
0
300
350
400
450
wavelength / nm
(1−A°/A)/[HFIPA],M−1
0
10
20
0.3
0.6
0.9
A°/A

QUENCHING BY ALCOHOLS

Addition of alcohols to the fluorenone solution shortens the lifetime of the excited singlet (τ_F) whose fluorescence decay can always be described by a single exponential function. These facts and the negligible variation of the ground state absorption spectra in the range of quencher concentrations used indicate that **dynamic quenching** occurs. The reciprocal fluorescence lifetimes measured in CH_2Cl_2 are plotted as function of alcohol concentration in Fig.2. The quenching rate constants derived from the slopes (Table 1) exhibit good correlation with the hydrogen bonding ability of the alcohols. Fig.3 demonstrates that fluorescence and triplet yields show parallel changes with τ_F

Fig.2 Fluorenone quenching by alcohols

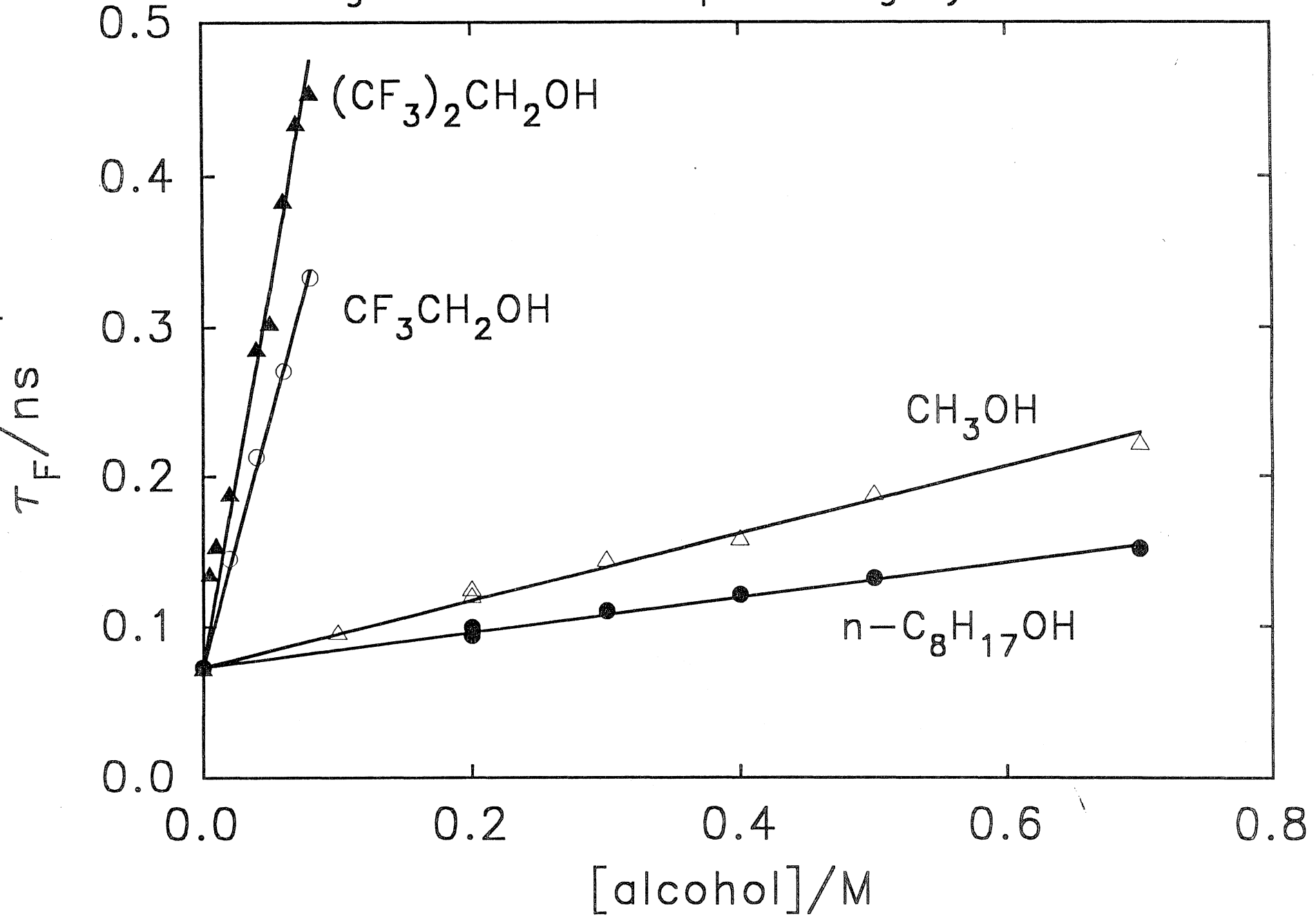

Table 1. Rate constants of singlet excited fluorenone quenching by alcohols in CH_2Cl_2 and DMF

Alcohol	CH_2Cl_2 k_q $10^8\ M^{-1}s^{-1}$	DMF k_q $10^8\ M^{-1}s^{-1}$
$(CF_3)_2CHOH$	46	2.8
CF_3CH_2OH	32	0.8
methanol	2.1	0.3
1-octanol	1.1	<0.3

Fig.3 Stern–Volmer plot of Φ_F (●), Φ_{ISC} (O) and τ_F (▲)
Fluorenone + $(CF_3)_2CHOH$ in CH_2CL_2

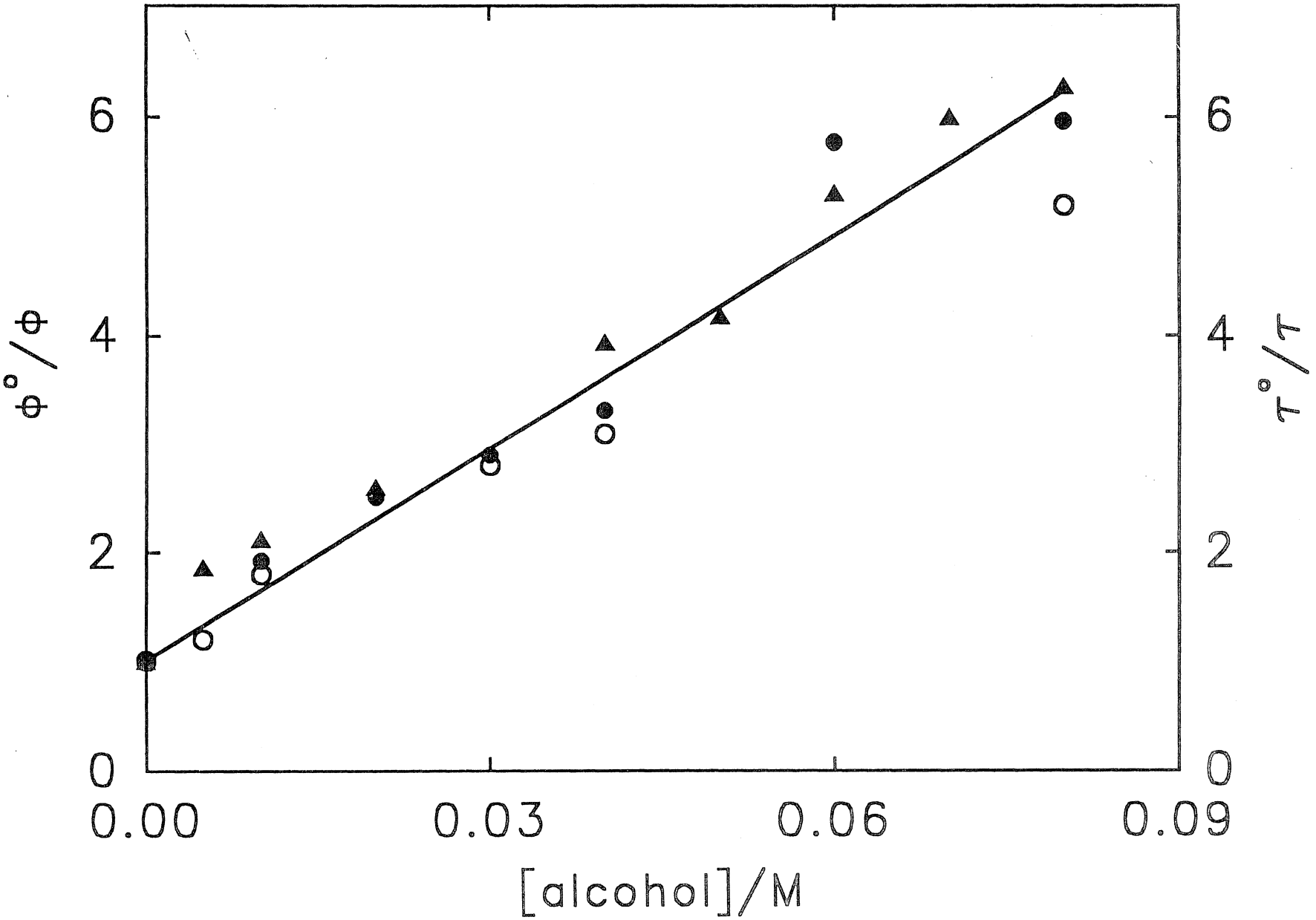

MECHANISM OF QUENCHING

$$^1F \longrightarrow {}^3F$$

$$^1F \longrightarrow F$$

$$^1F \longrightarrow F + h\nu$$

$$^1F + ROH \rightarrow {}^1(complex) \rightarrow F + ROH$$

Our results suggest that a short lived, non- or very weakly fluorescent hydrogen bonded complex is formed between singlet excited fluorenone and alcohols. The interaction is probably facilitated by enhancement of dipolemoment upon excitation of fluorenone. This mechanism is supported by the solvent dependence of the quenching rates (kq). Changing the

CH_2Cl_2 solvent to dimethylformamide (DMF) decreases kq by ca. one order of magnitude (Table 1.) because the strength of hydrogen bonding between excited fluorenone and alcohols diminishes due to the higher polarity and hydrogen bonding ability of DMF. Fast internal conversion is the dominant decay pathway of the excited hydrogen bonded complex; the rates of its fluorescence and triplet formation are relatively negligible. The single exponential character of the free fluorenone fluorescence decay indicates that the dissociation of the hydrogen bonded complex to excited fluorenone and ground state alcohol is not feasible. Probably, the much lower energy of the complex hinders the back reaction.

QUENCHING BY PHENOLS

The solvent dependence of quenching rate constants (Table 2) indicates that electron transfer is the dominant interaction between singlet excited fluorenone and the easily oxidizable 4-methoxyphenol, whereas the quenching occurs via an excited hydrogen bonded complex with the other phenols whose higher oxidation potentials make the electron transfer endothermic. Experiments carried out in the presence of pyridine derivatives provide further evidence bearing on the quenching mechanism. For example, if hydrogen bonding is the major interaction, addition of pyridines results in a significant decrease of the pseudo-first-order rate constant as we have observed in the triplet fluorenone + cyanophenol reaction (Fig.4).

Table 2. Rate constants of excited fluorenone quenching by phenols

Phenol	Singlet fluorenone		Triplet fluorenone	
	CH_2Cl_2	DMF	CH_2Cl_2	DMF
	k_q 10^8 $M^{-1}s^{-1}$	k_q 10^8 $M^{-1}s^{-1}$	k_q 10^8 $M^{-1}s^{-1}$	k_q 10^8 $M^{-1}s^{-1}$
4-NO_2	98	3.7		
4-CN	64	2.8	1.3	0.01
4-H	73	9.1	4.5	0.02
4-CH_3O	91	46	51	

Fig.4 Effect of 2,4,6-trimethylpyridine on the ^{3}fluorenone quenching by 3-cyanophenol in CCl_4

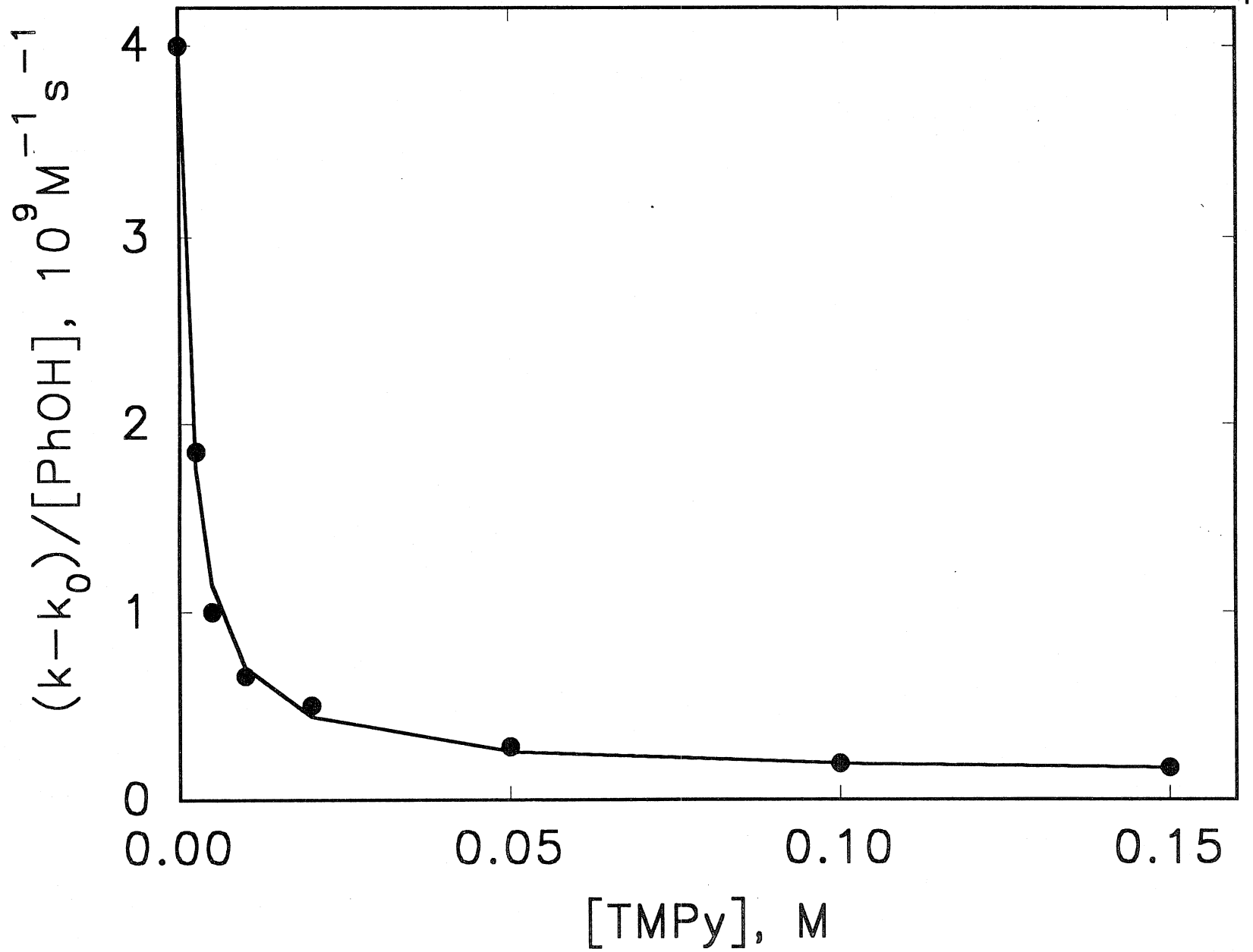

Reaction mechanism and kinetic parameters determined from the non-linear least-squares fit of eq 1 to the data presented in Fig. 4

$$^1F \longrightarrow {}^3F$$

$$^3F \xrightarrow{k_0} F \qquad k_0 = 30000\ s^{-1}$$

$$^3F + Q \xrightarrow{k_q} F + Q \qquad k_q = 4.0 \times 10^9\ M^{-1}s^{-1}$$

$$^3F + QPy \xrightarrow{k_{HB}} F + QPy \qquad k_{HB} = 1.4 \times 10^8\ M^{-1}s^{-1}$$

$$Q + Py \underset{}{\overset{K}{\rightleftharpoons}} QPy \qquad K = 560\ M^{-1}$$

$$\frac{k - k_0}{[PhOH]} = \frac{k_q}{1 + K\,[TMPy]} + \frac{k_{HB}\,K\,[TMPy]}{1 + K\,[TMPy]} \qquad (1)$$

4. Melléklet

Journal of Inclusion Phenomena and Molecular Recognition in Chemistry **18:** 237–245, 1994.

Solvent-Dependent Radiationless Transitions in Fluorenone: A Probe for Hydrogen Bonding Interactions in the Cyclodextrin Cavity

LÁSZLÓ BICZÓK
Central Research Institute for Chemistry, Hungarian Academy of Sciences, P.O. Box 17, 1525 Budapest, Hungary and Department of Chemistry, Brandeis University, Waltham, Massachusetts 02254–9110, U.S.A.

LÁSZLÓ JICSINSZKY
CYCLOLAB Research and Development Laboratory Ltd., P.O. Box 435, H–1525 Budapest, Hungary.

and

HENRY LINSCHITZ
Department of Chemistry, Brandeis University, Waltham, Massachusetts 02254–9110, U.S.A.

(Received: 2 February 1994; in final form: 17 May 1994)

Abstract. Fluorescence lifetimes, fluorescence quantum yields and triplet yields were measured for fluorenone in various hydroxylic and non-hydroxylic solvents, and in β-cyclodextrin complexes. The rate of singlet–triplet intersystem crossing, which decreases with increasing polarity, was found to be a good indicator of nonspecific solvent–solute interactions, while the rate of direct internal conversion from the singlet excited state was correlated with hydrogen bonding. The fast internal conversion of singlet excited fluorenone/β-cyclodextrin complexes shows that the probe molecule, while embedded within the cyclodextrin cavity, still remains hydrogen bonded.

Key words: Fluorescence lifetime, polarity, fluorenone, cyclodextrin.

1. Introduction

Cyclodextrins are water-soluble, torus-shaped cyclic oligosaccharides with a relatively apolar interior [1]. Their remarkable ability to form inclusion complexes with hydrophobic molecules which fit into the central cavity has led to widespread utilization of cyclodextrins in pharmaceutical, food, cosmetic and other chemical industrial areas [1,2]. Hydrophobic effects and van der Waals interactions are considered to be the major forces involved in such complex formation. Estimation of the local polarity of the cyclodextrin cavity helps to predict the kind of guest molecules which can be included in different cyclodextrin derivatives.

Fluorescence techniques have been widely used to examine the microenvironment of encapsulated molecules, since the fluorescence intensities, lifetimes and emission maxima of some fluorophores are very sensitive to, and reflect the nature of their solvation envelopes. Most of these fluorescent probes emit from twisted

* Dedicated to Professor Szejtli.

intramolecular charge transfer (TICT) states [3–7]. Fluorescence lifetime measurements of complexed 2-naphthol [7], or the spectral shifts shown by diphenylamine or exciplexes [8,9], have also been used to evaluate the polarity of the cyclodextrin cavity.

Earlier studies have reported on the solvent and temperature dependence of the rates of various competing photophysical processes depopulating the singlet excited state of fluorenone and its derivatives [10–13]. We now extend these studies to hydroxylic solvents (alcohols). These results are applied to the use of fluorenone as a probe for the investigation of specific hydrogen bonding interactions in the cyclodextrin cavity.

2. Experimental

Fluorenone (FLUKA) was purified by repeated recrystallization from ethanol. HPLC or spectroscopic grade organic solvents (dioxane, ethyl acetate, dichloromethane, acetone, acetonitrile, ethanol, water) were used as received; other solvents (methylcyclohexane, diethylether, tetrahydrofuran, dimethoxyethane, 1-pentanol, 1-octanol) were distilled. Purified β-cyclodextrin (βCD) and heptakis-(2,6-di-*O*-methyl)-β-cyclodextrin (DIMEB) were obtained from CYCLOLAB R&D Lab. Ltd., Hungary.

The inclusion complexes were prepared by adding fluorenone to 0.01M βCD or DIMEB in aqueous solution and warming to 60°C. The absorbances of all solutions were adjusted to 0.080 at the excitation wavelength and the samples were deoxygenated by purging with nitrogen for luminescence or flash photolysis studies.

Fluorescence lifetimes were measured on an Applied Photophysics SP-3 single photon counting apparatus using a hydrogen lamp operated at 30 kHz. Data were analyzed by a nonlinear least-squares deconvolution method.

Corrected fluorescence spectra were recorded on a homemade spectrofluorimeter equipped with a Princeton Applied Research type 1104A/B photon-counting system [14]. Fluorescence quantum yields were determined relative to fluorenone in acetonitrile ($\Phi_F = 0.032$) [10] following the usual procedure described in the literature [15]. 390 nm was chosen as the excitation wavelength, the slit widths of the excitation and emission monochromators were 3 nm and 5 nm, respectively.

Triplet yields were determined by the 'limiting slope' method [16] using fluorenone solution in methylcyclohexane as reference ($\Phi_{ISC}(MCH) = 1.00$). In this method, values of triplet yields are obtained by flash photolysis measurements of the relative slopes of triplet absorbance vs. flash energy plots, in the linear region. A frequency doubled ruby laser was used for excitation and the triplet-triplet absorption of fluorenone was monitored at 440 nm. The molar extinction coefficient of the triplet was taken to be the same for all solvents and in the cyclodextrin complexes. Further experimental details have been described [12].

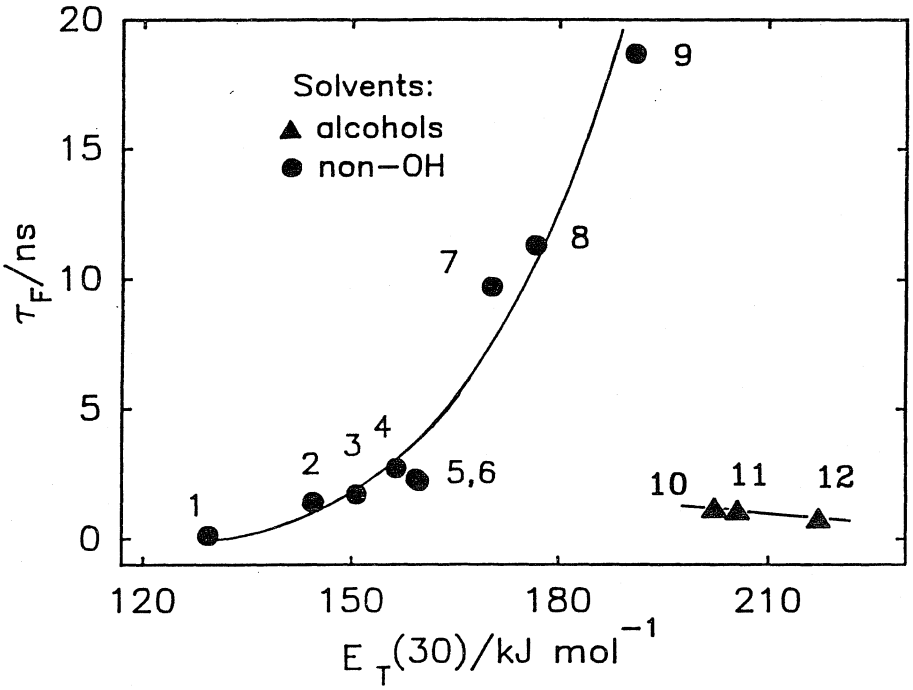

Fig. 1. Fluorescence lifetimes of fluorenone in hydroxylic ▲ and non-hydroxylic • solvents, as a function of $E_T(30)$ solvent polarity parameters. 1 methylcyclohexane, 2 diethylether, 3 dioxane, 4 tetrahydrofuran, 5 ethyl acetate, 6 dimethoxyethane, 7 dichloroethane, 8 acetone, 9 acetonitrile, 10 1-octanol, 11 1-pentanol, 12 ethanol.

3. Results and Discussion

3.1. Fluorescence lifetimes and triplet yields in organic solvents

The fluorescence quantum yield (Φ_F) and fluorescence lifetime (τ_F) of fluorenone showed parallel changes in a series of solvents of different polarity. As the accuracy of the fluorescence lifetimes is better (estimated error ±5%), we present here the solvent dependence of τ_F in more detail. Figure 1 gives the fluorescence lifetime of fluorenone as a function of the empirical solvent polarity parameter, $E_T(30)$ [17]. The plotted data clearly show two entirely distinct regions and polarity correlations. In non-hydroxylic (non-OH) solvents, τ_F increases by more than two orders of magnitude in going from methylcyclohexane to acetonitrile. However, in the alcohols, with $E_T(30)$ values higher than any of the non-OH media, the singlet lifetimes are very short, and decrease even further with increasing polarity (octanol → ethanol). Taking the dielectric constant as a general measure of polarity, the fluorescence lifetime in ethanol (0.8 ns) is much shorter than in acetone (11.3 ns) although the respective dielectric constants (24.3 and 20.7) are similar. Thus, it appears that a specific interaction between fluorenone and the hydroxylic solvents strongly affects the rate of deactivation of the fluorenone singlet. We take this to be hydrogen bonding.

TABLE I. Photophysical parameters of fluorenone in non-hydroxylic and hydroxylic solvents.

Solvent	$E_T(30)$ kJ/mol	Φ_{ISC}	Φ_F 10^{-3}	τ_F ns	k_{ISC} $10^7 s^{-1}$	k_{IC} $10^7 s^{-1}$
Non-hydroxylic						
Methylcyclohexane[a]	129	1.00	0.5	0.14	710	[b]
Diethyl ether	144	0.96	4.9	1.4	69	3
Dioxane	151	0.96	5.8	1.7	56	2
Tetrahydrofuran[a]	157	0.87	6.4	2.7	32	5
Ethyl acetate	160	–	5.5	2.3	–	–
Dimethoxyethane	160	–	5.3	2.2	–	–
Dichloromethane	170	–	20	9.7	–	–
Acetone[a]	177	0.77	21	11.3	6.8	1.8
Acetonitrile[a]	191	0.46	32	18.7	2.5	2.7
Hydroxylic						
1-Octanol	202	0.14	2.5	1.2	12	71
1-Pentanol	206	0.11	2.2	1.1	10	80
Ethanol	217	0.06	1.5	0.8	7	120

[a] References 10 and 12.

[b] Cannot be determined (see text).

In all media studied, the fluorescence quantum yield of fluorenone is low (Table I), so that deactivation proceeds mainly by radiationless processes. This may occur either by direct internal conversion of the singlet to the ground state, or by intersystem crossing to the triplet state. Proton transfer reactions of the singlet excited fluorenone leading rapidly to the ground state would be included in our k_{IC}, but there is no specific evidence for this pathway. Figure 2 (filled points) gives results of triplet yield measurements in various solvents. It is evident that, again, sharp differences appear between the alcohols and the non-OH solvents, the former showing very low values of Φ_{ISC}.

Table I summarizes experimental values of triplet yields (Φ_{ISC}) and singlet lifetimes (τ_F) for several solvents. Also listed are rate constants for singlet–triplet transitions (k_{ISC}) and direct internal conversion to the ground state (k_{IC}) derived from the relations:

$$k_{ISC} = \Phi_{ISC}/\tau_F$$

$$k_{IC} = (1 - \Phi_F - \Phi_{ISC})/\tau_F$$

The values of k_{ISC}, derived from the measured Φ_{ISC} and τ_F, are conservatively estimated to be reliable to $\pm 15\%$. However, the uncertainty in k_{IC} becomes quite large if Φ_{ISC} approaches unity. Thus, the differences in k_{IC} among the first three entries of Table I are within experimental error. For the opposite situation of

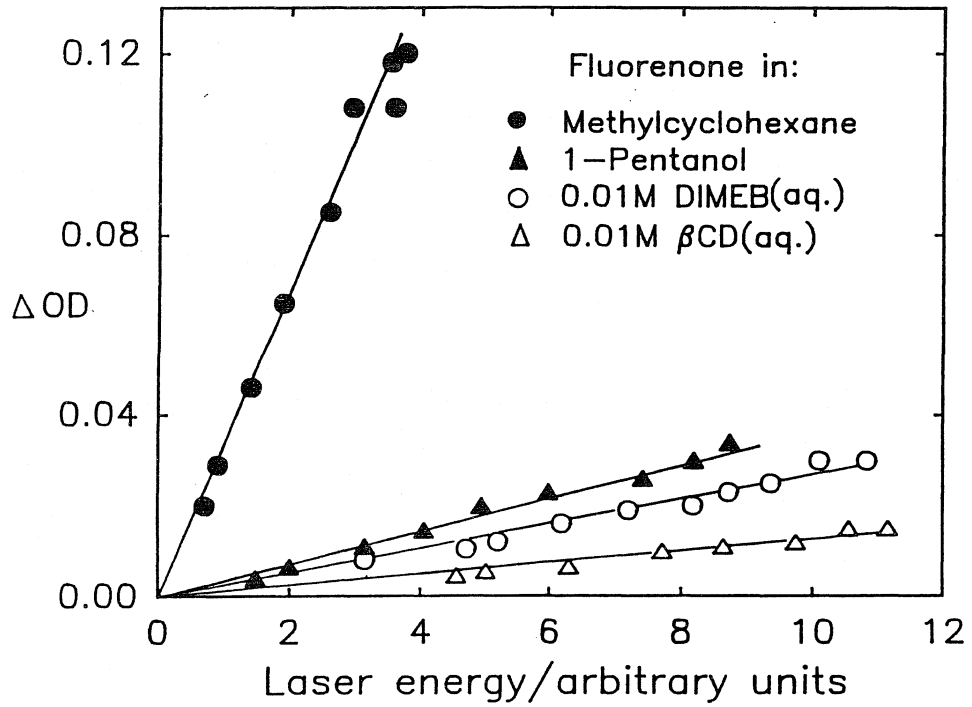

Fig. 2. Determination of triplet yields: triplet–triplet absorbance of fluorenone at 440 nm vs. laser energy in methylcyclohexane •, in 1-pentanol ▲, in 0.01 M aqueous DIMEB ○, in 0.01 M aqueous βCD △.

low Φ_{ISC}, k_{IC} is determined primarily by τ_F. We judge the uncertainty in k_{IC} in hydroxylic solvents and in cyclodextrin complexes to be about ±10%.

The data of Table I indicate that:

1. For the non-OH solvents, k_{IC} is relatively small, and is essentially independent of polarity; k_{ISC} is much larger, and decreases with polarity. It is mainly this process, singlet–triplet transition, which controls the solvent dependency of τ_F in these media.
2. For the alcohols, k_{ISC} is close to that of the non-OH solvents of comparable polarity, while k_{IC} is much greater. It is the OH-enhanced rate of internal conversion which results in a low triplet yield and a short singlet lifetime in this case. The rate decreases slightly with increasing chain length, as expected for a weakening hydrogen bonding interaction [17].

It is clear that the photophysical properties of fluorenone are sharply different in alcohols, where internal conversion is the main dissipative channel from the singlet, and in non-OH solvents, (particularly those of low polarity), where transition to the triplet is the dominant pathway. It is striking that hydrogen bonding interactions markedly increase the rate of internal conversion, while intersystem crossing is scarcely affected. Conversely, non-specific polarity-dependent interac-

TABLE II. Photophysical properties of fluorenone inclusion complexes.

Complex	τ_F ns	Φ_F 10^{-3}	Φ_{ISC}	k_{ISC} $10^7 s^{-1}$	k_{IC} $10^7 s^{-1}$
Fluorenone/βCD	1.2	2.4	0.04	3.3	79
Fluorenone/DIMEB	2.2	4.8	0.08	3.6	41

tions between singlet excited fluorenone and solvent do not influence the rate of internal conversion but do decrease intersystem crossing.

On the basis of its characteristic responses to different solvents, we may expect that fluorenone will provide a useful probe to study separately specific hydrogen bonding and non-specific dielectric interactions in the cyclodextrin cavity.

3.2. PHOTOPHYSICAL PROPERTIES OF FLUORENONE INCLUSION COMPLEXES

The formation of complexes between fluorenone and βCD or DIMEB is demonstrated unambiguously by cyclodextrin-enhanced solubility and very directly by the appearance of circular dichroism of fluorenone in the presence of βCD [19].

Table II presents photophysical properties of fluorenone embedded in βCD or DIMEB cavities. In both cases, fluorescence decays fit single exponential functions and lifetimes (1–2 ns) are quite short. In these measurements, interference from emission of uncomplexed fluorenone is negligible because of its low concentration and quantum yield. The results of triplet yield measurements are given in Figure 2 (open points). It is immediately evident that the yields for both complexes are low and close to those observed for alcohols. In accord with this, the derived rate constants k_{ISC} and k_{IC} (Table II) establish that direct internal conversion to the ground state is the dominant decay process in these complexes, and is mainly responsible for the short singlet lifetimes. This indicates that hydrogen bonding interactions with the fluorenone guest are significant.

In interpreting this result, we may exclude, on the basis of molecular dimensions and cavity geometry, the possibility that fluorenone is complexed equatorially, with the carbonyl group oriented toward water [19]. Indeed, an axially-bound complex is clearly demonstrated by the circular dichroism spectrum, which, assuming axial geometry, leads to the same spectroscopic assignments as are derived from crystal absorption and fluorescence polarization data [19]. Moreover, the qualitative similarity of the photophysical properties of βCD and DIMEB complexes indicates that no hydrogen bonds are formed between the fluorenone carbonyl and the OH groups of βCD. This agrees also with the expectation, based on the circular dichroism results, that fluorenone is probably symmetrically incorporated in βCD. Thus, we conclude that fluorenone while embedded in the cyclodextrin cavity still retains H-bonded water. This itself may be outside the cyclodextrin cavity. Additional sites for bonding water within the cavity may be provided by the cylindrically disposed,

central glycosidic oxygens, but the precise extent to which any such originally bound water is displaced, or stabilized, by complexed fluorenone is, of course, still uncertain.

As noted above, since both Φ_F and Φ_{ISC} are small, the derived values of k_{IC} in Table II depend primarily on the fluorescence lifetimes, which are measured with fairly good accuracy (±5%). We estimate that the uncertainty in the k_{IC}s are not greater than ±10%. Thus, the twofold difference observed in k_{IC} between the βCD and DIMEB complexes is well beyond the experimental error. This difference is matched by a corresponding reverse change in k_{ISC}, suggesting that the DIMEB cavity provides an environment somewhat closer to that of the non-OH solvents than does βCD. This may be related to a smaller content of internally bound water in the methylated case.

The values of both k_{ISC} and k_{IC} given in Table I and Table II support the following conclusions:

(i) If we take k_{ISC} values as indicators of the dielectric polarity (Table I), it is apparent that the cyclodextrin cavity is much more polar than dioxane or tetrahydrofuran and its polarity is close to that of ethanol.

(ii) However, the rates of internal conversion (k_{IC}) show that the strength of hydrogen bonding with the fluorenone is lower in the cavity of cyclodextrins than in ethanol and it is more similar to that found in 1-octanol.

There are extremely large discrepancies in the literature among the data on the polarity of the cyclodextrin cavity with 'effective equivalent dielectric constants' ranging from 2.2 to 55 [18,26]. From the fluorescence spectrum of exciplexes [20,21] or from the absorption spectrum of *p*-tert-butylphenol [22], it has been concluded that the polarity of the cyclodextrin cavity resembles that of dioxane. However, using pyrene-3-carboxaldehyde as a fluorescent probe, $\varepsilon = 55$ and $\varepsilon = 48$ has been derived for the dielectric constant of the γ-CD and β-CD cavity, respectively [23]. Other authors have found that the polarity of the cyclodextrin interior is like that of methanol [24], ethanol [7–9], 1-propanol [25], tert-butanol, ethylene glycol [5], 1-pentanol [26] or 1-octanol [27]. The discrepancies probably arise from any or all of the following factors: (a) some probes are not entirely encapsulated in the cyclodextrin, or are held in different configurations relative to the cavity wall [5]. (b) The number of water molecules inside the different cyclodextrin complexes may differ because of steric or energetic reasons. (c) The probes which have been used are able to respond primarily to the bulk polarity of the region; their sensitivity to the nonspecific solvent–solute interactions relative to their sensitivity to hydrogen bonding interactions varies considerably. The utilization of fluorenone as a molecular probe facilitates the study of nonspecific and hydrogen bonding interactions separately.

In connection with the above situation, the effect of complexation on the absorption spectrum of fluorenone is of interest. Figure 3 shows that the low energy band of fluorenone in βCD is red-shifted, broadened and loses fine-structure, compared

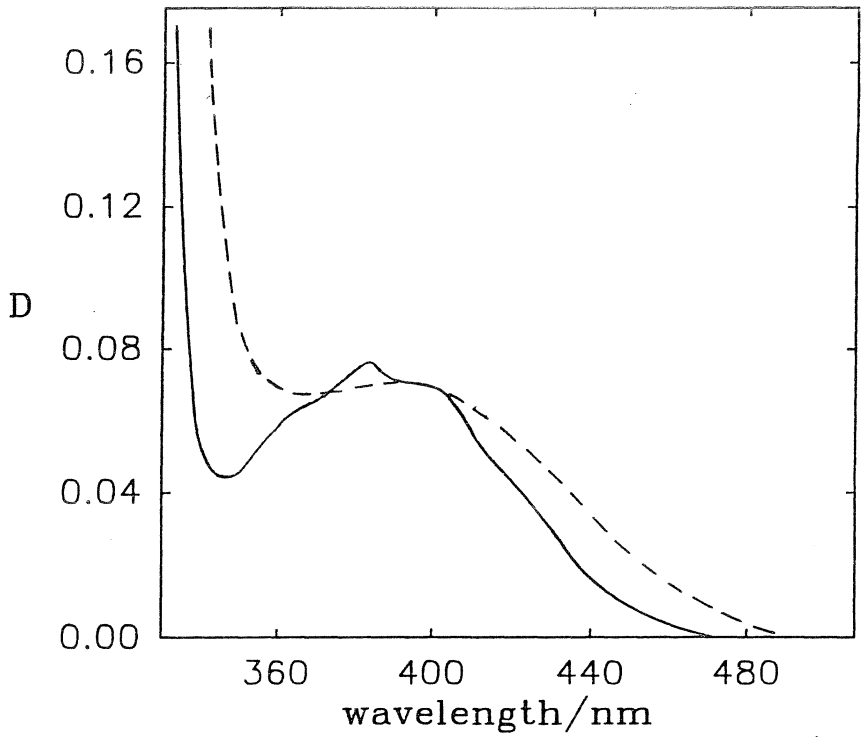

Fig. 3. Absorption spectrum of fluorenone in ethanol —— and in 0.01 M aqueous βCD solution – – – –.

to the spectrum in ethanol. The lowest energy transition of fluorenone is $\pi - \pi^*$ [13], which is characteristically red-shifted in polar media. While the observed effect may indeed indicate a highly polar cavity environment, other mechanisms may account for the effect. In particular, we suggest that especially strong van der Waals interactions with the cavity couple the $\pi - \pi^*$ transition more closely to the surroundings than is the case in the less structured geometry of liquid solutions. This would both lower the energy of the excited state and smear out vibrational structure.

4. Conclusions

Fluorescence decays fit single exponential functions and lifetimes (1–2 ns) are quite short when fluorenone is embedded in βCD or DIMEB cavities. The triplet yields for both complexes are low and close to those observed for alcohols. Excluding the possibility that fluorenone is complexed equatorially, with the carbonyl group oriented toward water, an axially-bound complex is clearly demonstrated as derived from crystal absorption and fluorescence polarization data. The fast internal conversion of singlet excited fluorenone/β-cyclodextrin complexes shows that the probe molecule embedded within the cyclodextrin cavity still remains hydrogen

bonded. Water within the cavity may be provided by the cylindrically disposed, central glycosidic oxygens.

Acknowledgement

We much appreciate support of this work by the Hungarian National Science Foundation (Grant No. 1802 to the Central Research Institute for Chemistry, Hungarian Academy of Sciences) and by the Division of Chemical Sciences, Office of Basic Energy Sciences, Office of Energy Research, U.S. Department of Energy (Grant No. DE–FG02–89ER14027 to Brandeis University).

References

1. J. Szejtli: *Cyclodextrins and Their Inclusion Complexes*, Akademiai Kiado, Budapest (1982).
2. J. Szejtli: *Cyclodextrin Technology*, Kluwer Academic Publishers, Dordrecht (1988).
3. A. Nag and K. Bhattacharyya: *Chem. Phys. Lett.* **151**, 474 (1988). A. Nag, R. Dutta, N. Chattopadhyay, and K. Bhattacharyya: *Chem. Phys. Lett.* **157**, 83 (1989). A. Nag and K. Bhattacharyya: *J. Chem. Soc. Faraday Trans.* **86**, 534 (1990).
4. A. Nag, T. Chakrabarty, and K. Bhattacharyya: *J. Phys. Chem.* **94**, 4203 (1990).
5. G. S. Cox, P. J. Hauptman, N. J. Turro: *Photochem. Photobiol.* **39**, 597 (1984).
6. F. V. Bright, G. C. Catena, and J. Huang: *J. Am. Chem. Soc.* **112**, 1343 (1990).
7. D. F. Eaton: *Tetrahedron* **43**, 1551 (1987).
8. A. Heredia, G. Requena, and F. G. Sanchez: *J. Chem. Soc. Chem. Commun.*, 1814 (1985).
9. G. S. Cox, N. J. Turro, N. C. Yang, and M.-J. Chen: *J. Am. Chem. Soc.* **106**, 422 (1984).
10. L. Biczok and T. Berces: *J. Phys. Chem.* **92**, 3842 (1988).
11. L. Biczok, T. Berces, and F. Marta: *J. Phys. Chem.* **97**, 8895 (1993).
12. L. J. Andrews, A. Deroulede, and H. Linschitz: *J. Phys. Chem.* **82**, 2304 (1978).
13. T. Kobayashi and S. Nagakura: *Chem. Phys. Lett.* **43**, 429 (1976).
14. B. Laszlo, S. Forgeteg, T. Berces, and F. Marta: *J. Photochem.* **27**, 49 (1984).
15. C. A. Parker: *Photoluminescence of Solutions*, Elsevier Publ. Co., Amsterdam (1968).
16. J. K. Hurley, N. Sinai, and H. Linschitz: *Photochem. Photobiol.* **38**, 9 (1983).
17. C. Reichardt: *Solvents and Solvent Effects in Organic Chemistry*, VCH: Weinheim (1988).
18. S. Li and W. C. Purdy: *Chem. Rev.* **92**, 1457 (1992).
19. H. Yamaguchi, K. Ninomiya, and M. Ogata: *Chem. Phys. Lett.* **75**, 593 (1980).
20. S. Hamai: *J. Phys. Chem.* **92**, 6140 (1988).
21. S. Hamai: *Bull. Chem. Soc. Jpn.* **55**, 2721 (1982).
22. R. L. Van Etten, J. F. Sebastian, G. A. Clowes, and M. L. Bender: *J. Am. Chem. Soc.* **89**, 3242 (1967).
23. K. W. Street Jr. and W. E. Acree: *Appl. Spectrosc.* **42**, 1315 (1988).
24. T. Soujanya, T. S. R. Krishna, and A. Samanta: *J. Phys. Chem.* **96**, 8544 (1992).
25. S. Hamai: *J. Phys. Chem.* **94**, 2595 (1990).
26. S. Hamai: *Bull. Chem. Soc. Jpn.* **64**, 431 (1991).
27. K. W. Street Jr.: *J. Liq. Chromatogr.* **10**, 655 (1987).

5. Melléklet

HYDROGEN BONDING INTERACTIONS WITH CYCLODEXTRINS: UTILIZATION OF FLUORENONE AS A NEW PROBE

LÁSZLÓ BICZÓK [1], LÁSZLÓ JICSINSZKY [2], HENRY LINSCHITZ [3]
[1] *Central Research Institute for Chemistry, Hungarian Academy of Sciences, P.O. Box 17. H-1525 Budapest, Hungary*
[2] *CYCLOLAB Research and Development Laboratory Ltd. P.O. Box 435. H-1525 Budapest, Hungary*
[3] *Brandeis University, Waltham, Massachusetts 02254-9110, USA*

ABSTRACT

The interaction of fluorenone with cyclodextrins (CD) was studied by fluorescence lifetime, fluorescence quantum yield and triplet yield measurements. In aqueous solutions, the fast internal conversion of the singlet excited inclusion complexes indicates that fluorenone, while embedded in the CD cavity, still retains hydrogen bonded water. In organic media, the dynamic quenching of fluorescence and singlet-triplet transition was attributed to formation of a short lived, non- or very weakly fluorescent excited fluorenone/CD hydrogen-bonded complex since the methylation of the glycosidic OH-groups significantly decreased the quenching rates.

1. INTRODUCTION

Fluorescence techniques have been widely used to examine the microenvironment of encapsulated molecules, since the fluorescence intensities, lifetimes and emission maxima of some fluorophores are very sensitive to, and reflect the nature of their solvation envelopes. However, the probes which have been used are unable to distinguish specific solvent-solute interactions from the effects of bulk polarity.

We have recently introduced a new molecular probe [1], the singlet excited fluorenone, which is able to selectively detect hydrogen bonding since the rate of its internal conversion markedly increases in the presence of alcohols, while the rate of transition to the triplet is scarcely affected. The singlet excited fluorenone was found to be a good indicator of non-specific interactions with solvents as well because the rate of its triplet formation increases more than two orders of magnitude in going from acetonitrile to hexane.

In the present studies, we exploit these unique photophysical properties to obtain more information on the major characteristics of fluorenone interaction with cyclodextrins and reveal how the methylation of the glycosidic OH-groups influences the structure of fluorenone / ß-cyclodextrin complexes. We also extend these studies to organic solvents and

demonstrate that dynamic quenching of the fluorenone singlet excited state in nonaqueous media takes place through short lived hydrogen-bonded complex formation with cyclodextrins.

2. MATERIALS AND METHODS

Fluorenone (FLUKA) was purified by repeated recrystallization from ethanol. Purified ß-cyclodextrin (ßCD), random methylated ß-cyclodextrin (RAMEB), heptakis-(2,6-di-O-methyl)-ß-cyclodextrin (DIMEB) and heptakis-(2,3,6-tri-O-methyl)-ß-cyclodextrin (TRIMEB) are products of CYCLOLAB R&D Lab. Ltd., Hungary. HPLC grade solvents were used as received. The samples were deoxygenated by purging with nitrogen.

Fluorescence lifetimes were measured on an Applied Photophysics SP-3 single photon counting apparatus using a hydrogen lamp operated at 30 kHz. Data were analyzed by a nonlinear least-squares deconvolution method. Corrected fluorescence spectra were recorded on a homemade spectrofluorimeter equipped with a Princeton Applied Research type 1104A/B photon-counting system. Fluorescence quantum yields were determined relative to fluorenone in acetonitrile ($\Phi_F = 0.032$) [1]. Triplet yields were obtained by the "limiting slope" method [2] using fluorenone solution in methylcyclohexane as reference (Φ_{ISC}(MCH)=1.00) [3]. In this method, values of triplet yields are obtained by flash photolysis measurements of the relative slopes of triplet absorbance vs. flash energy plots, in the linear region. A frequency doubled ruby laser or XeF excimer laser was used for excitation and the triplet-triplet absorption of fluorenone was monitored at 440 nm [3]. The molar extinction coefficient of the triplet was taken to be the same for all solvents and in the cyclodextrin complexes.

3. RESULTS AND DISCUSSION

3.1. Fluorenone inclusion complexes in aqueous solutions

In aqueous solution, inclusion of fluorenone in ßCD cavity is demonstrated unambiguously by cyclodextrin-enhanced solubility, absorption spectroscopy and very directly by the appearance of circular dichroism of fluorenone in the presence of ßCD [4]. In all cases, fluorescence decays fit single exponential functions and interference from emission of uncomplexed fluorenone is negligible because of its low solubility and fluorescence yield. Table I. presents the photophysical properties of fluorenone/ßCD complexes.

Table 1.Photophysical parameters of fluorenone

Media	τ_F ns	Φ_F 10^{-3}	Φ_{ISC}	k_{ISC} $10^7 s^{-1}$	k_{IC} $10^7 s^{-1}$
βCD	1.2	2.4	0.04	3.3	79
RAMEB	2.6	3.4	0.06	2.3	36
DIMEB	2.2	4.8	0.08	3.6	41
TRIMEB	3.0	3.6	0.12	3.8	29
THF	2.7	6.4	0.87	32	3
1-octanol	1.2	2.5	0.14	12	71

For comparison, the corresponding data in tetrahydrofuran (THF) and 1-octanol are included as well. It is apparent that the behavior of complexes is much closer to that observed in alcohols than in non-hydroxylic solvents. The short singlet lifetimes (τ_F), the very low values of triplet yields (Φ_{ISC}) and fluorescence yields (Φ_F) arise from the fast internal conversion (k_{IC}) as has been found for uncomplexed fluorenone in alcohols [1]. This indicates that hydrogen bonding interactions with the fluorenone guest are significant. We may exclude, on the basis of the circular dichroism spectrum [4], molecular dimensions and cavity geometry, the possibility that fluorenone is complexed equatorially, with the carbonyl group oriented toward water. The fact that the methylation of the glycosidic OH-groups does not affect significantly the major photophysical characteristics of the complexes suggests that hydrogen bonds do not form between the fluorenone carbonyl and the OH groups of ßCDs. Thus, we conclude that the fast internal conversion of singlet excited fluorenone must be assigned to the H-bonding interaction with water molecules still remaining in the cyclodextrin cavity after fluorenone inclusion.

3.2. Interactions between fluorenone and cyclodextrins in organic solvents

Addition of ßCD to the dimethylformamide (DMF) and dimethylsulfoxide (DMSO) solution of fluorenone leads to ca. 20 nm red-shift of the fluorescence maximum and substantial decrease in the fluorescence intensity but no significant change in the absorption spectra occurs. Fluorescence decaytimes and triplet yields exhibit parallel changes with fluorescence yield in the function of ßCD concentration. All of the three quantities provide linear Stern-Volmer plots. From the slopes $k_q = 9.0 \times 10^8\ M^{-1}\ s^{-1}$ and $3.0 \times 10^8\ M^{-1}\ s^{-1}$ is derived for the rate constant of singlet excited fluorenone quenching by ßCD in DMF and DMSO, respectively. The difference of these values probably reflects the higher hydrogen bonding ability of DMSO.

Table 2. Photophysical processes in the presence of 0.1 M additive in DMF

Additive 0.1 M	τ_F ns	Φ_F	Φ_{ISC}	k_{ISC} $10^7 s^{-1}$	k_q $10^8 M^{-1} s^{-1}$
αCD	7.0	0.013	0.28	4.0	7.7
γCD	6.0	0.011	0.25	4.2	10.1
βCD	6.5	0.012	0.26	4.0	9.0
RAMEB	10.3	0.019	0.41	4.0	3.2
DIMEB	14.2	0.025	0.59	4.2	0.5
TRIMEB	15.2	0.028	0.63	4.1	-
-	15.3	0.028	0.63	4.1	-
MeOH	14.8	0.028	0.63	4.1	0.3

In order to reveal the nature of the quenching process, the structure of cyclodextrins was systematically varied. Table 2. summarizes the photophysical parameters measured in the presence of 0.1 M additives in DMF. It is evident that the photophysical behavior of fluorenone is strikingly insensitive to the cavity size of CDs. In accord with the linearity of Stern-Volmer plots and the single exponential decay of fluorenone fluorescence, this suggests that no inclusion complex formation occurs. However, the fast dynamic quenching caused by CDs shows interaction between singlet excited fluorenone and CDs. Since the methylation of the glycosidic OH-groups significantly decreases the

quenching rates, we infer that short lived, non- or very weakly fluorescent hydrogen bonded complex forms between the singlet excited fluorenone and CDs. The interaction is probably facilitated by the enhancement of dipolmoment upon excitation of fluorenone. It is interesting to note that most of the CDs exhibit much higher quenching rate constants than alcohols. This may be attributed to the more efficient vibronic coupling between excited and ground states in the singlet excited fluorenone/CD complexes.

4. CONCLUSION

The interaction of fluorenone with CDs is sharply different in aqueous and organic solutions. In the former case, inclusion complex can be detected both in the ground and excited state. The fast internal conversion of the singlet excited complexes shows that fluorenone, while embedded in the CD cavity, still retains hydrogen bonded water. On the other hand, no intercalation of fluorenone in the CD cavity is observed in organic media. The dynamic quenching of fluorescence and triplet formation is assigned to short lived hydrogen bonded complex between the singlet excited fluorenone and CDs.

ACKNOWLEDGMENT

We much appreciate support of this work by the Division of Chemical Sciences, Office of Basic Energy Sciences, Office of Energy Research, US Department of Energy (Grant No. DE-FG02-89ER14027 to Brandeis University).

REFERENCES

[1] Biczók, L., Jicsinszky, L., Linschitz, H., Solvent dependent radiationless transitions in fluorenone: A probe for hydrogen bonding interactions in the cyclodextrin cavity, *J. Incl. Phen.*, **18**, 237-245 (1994)
[2] Hurley, J. K., Sinai, N., Linschitz, H., Actinometry in monochromatic flash photolysis: The extinction coefficient of triplet benzophenone and quantum yield of triplet zinc tetraphenyl porphyrin, *Photochem. Photobiol.* **38**, 9-14 (1983)
[3] Andrews, L. J., Deroulede, A., Linschitz, H. Photophysical processes in fluorenone, *J. Phys. Chem.* **82**, 2304-2309 (1978)
[4] Yamaguchi, H., Ninomiya, K., Ogata, M., Study of the electronic spectra of 9-fluorenone, Chem. *Phys. Lett.* **75**, 593-595 (1980)

6. Melléklet

Res. Chem. Intermed. Vol. 20, No. 9, pp. 939-951 (1994)

REDUCTION OF TRIPLET TETRAPHENYL-PORPHYRIN DICATION BY ARYL AMINES AND HYDROQUINONES: KINETICS AND PRIMARY RADICAL YIELDS

LÁSZLÓ BICZÓK[1†], HENRY LINSCHITZ*
Department of Chemistry, Brandeis University, Waltham, MA 02254-9110, U.S.A.

ROBERT I. WALTER
Department of Chemistry, University of Illinois at Chicago, Box 4348, Chicago, IL 60680, U.S.A.

Received 3 January 1994; accepted 15 February 1994

Abstract--The photophysics and one-electron reduction of triplet tetraphenylporphyrin dication by homologous series of substituted triphenylamines and hydroquinones in acetone solution have been studied by nanosecond flash photolysis. Triplet yield is ~0.3 and direct internal conversion from the singlet is a major decay pathway. Quenching rates (10^9 - 10^6 M^{-1} s^{-1}) for reductants covering a range of $\Delta G^{0'}$ ~0.4 V lead to reorganization energies λ ~0.6 ±0.1 eV. Radical yields (~0.38 for the amines) are remarkably constant for recombination free energies between 1.02 and 1.45 V. A rate-limiting step in the back reaction is suggested, involving spin-orbit relaxation of the primary radical pair.

INTRODUCTION

In view of the vast literature on the photochemistry and photophysics of porphyrins and metalloporphyrins, remarkably little systematic work has been done on the related properties of porphyrins protonated or deprotonated at the central nitrogens. Studies of these derivatives should give further information on the effects of such factors as molecular symmetry, central charge, orbital energies and redox potentials, without complications involving metal-related optical or charge-transfer processes. Extensive research on acid-base behavior of porphyrins has been reviewed [1] and some photophysical properties of porphyrin dications have been obtained [2-6]. The oxidation of triplet tetraphenylporphyrin dication ($TPPH_4^{2+}$) by quinones in acid media has recently been demonstrated by Gust and co-workers [7]. While much research has been done on photoreduction of porphyrins, including work in protic solvents [6], these studies are mainly concerned with overall two- or multi-electron processes leading to phlorins and other products [8] or with metal

[1]On leave from the Central Research Institute for Chemistry, Hungarian Academy of Sciences, Budapest, Hungary.

complexes [9]. We report here initial flash studies of the kinetics and primary radical yields in the one-electron reduction of triplet $TPPH_4^{2+}$ by a series of aryl donors (substituted triphenylamines and hydroquinones).

EXPERIMENTAL

Materials

Para-substituted triphenylamines were prepared and purified as described [10]. The corresponding amine cation radicals were made by treatment of the amine with $SbCl_5$ in methylene chloride or acetone solution [11], and spectra taken on a Cary-15 spectrophotometer. Durohydroquinone was prepared by $SnCl_2$ reduction of duroquinone [12] and recrystallized from ethanol. Tetraphenylporphyrin ($TPPH_2$, <0.1% chlorin) and trifluoroacetic acid (TFA), were from Aldrich and were used as received. To form the porphyrin dication, solutions of $TPPH_2$ were titrated spectrophotometrically with TFA, and acid concentrations were adjusted to be slightly in excess of that required for complete protonation (0.05 M in acetone). Perylene, reagent grade (Fluka, "purum") was recrystallized from benzene. Tetracene was zone-refined. Pure ferrocene was kindly provided by Professor M. Rosenblum of this Department. Solvents and $LiClO_4$ were reagent grade.

Apparatus and Procedure

Fluorescence lifetimes were obtained from direct emission vs. time traces, using a Hamamatsu microchannel plate photomultiplier, subnanosecond excitation at 532 nm from a mode-locked YAG laser, and associated data acquisition and analysis as described [13]. Steady state fluorescence quenching measurements were made on a Perkin-Elmer MPF-4 spectrofluorimeter, and quenching rate constants were derived from both lifetime data and good Stern-Volmer plots. Triplet states were studied by flash photolysis of N_2-purged solutions using a Q-switched ruby laser and associated equipment and procedures as in earlier work [14,15]. Photometer traces were recorded by a 200 MHz, 10-bit transient digitizer (Tektronix RTD 710A), interfaced to a PC computer. In porphyrin photoreduction experiments, laser flash excitation was at the ruby fundamental (694 nm, 30 ns FWHM), which falls at the red edge of $TPPH_4^{2+}$ absorption (see below). For determination of triplet yields relative to the benzophenone actinometer [16], laser excitation was frequency-doubled. Measurements were also made using a flashlamp-pumped dye laser (Candela ED-200, 0.2 μs pulse duration), tuned to the 656 nm peak absorption of $TPPH_4^{2+}$. Triplet spectra and extinction coefficients were determined by the method of total ground state depletion, using attenuating $CuSO_4$ filters in the laser beam to vary excitation energy at constant beam profile. Saturation conversion and good limiting ΔD values were readily obtained with no evidence of multiphoton processes. Triplet quenching rate constants (k_q) were obtained from excellent linear plots of pseudo-first order triplet decay rate constants (k_d) vs. reductant concentration [R], generally following the triplet absorption at 510 nm (see below) and using [R] values such that second order (T + T) decay was negligible. In

some cases, where k_q was low, k_d was derived from close-fitting computer resolution of pseudo-first and second order components of the triplet decay profile.

Cyclic voltammograms were obtained on a PAR Model 362 scanning potentiostat, with SCE reference and glassy carbon working electrodes, at sweep rates of 100 - 200 mV/s. Solutions were prepared in acetonitrile containing 0.2 M $LiClO_4$, 0.05 M TFA and ferrocene as internal standard. Triphenylamines, *para*-substituted by CH_3, F, Cl, Br, I or $COOCH_3$, gave reversible one-electron voltammograms. Polarographic oxidation potentials for these compounds agreed within ±0.02 V with those calculated by adding 0.33 V to values derived from reversible potentiometric titrations, referred to Ag, 0.01M $AgClO_4$ [17,18]. Cyclic voltammograms for the remaining amines and all hydroquinones were irreversible, even at higher TFA concentrations. For these cases, potentials were taken to be 30 mV less positive than the observed anodic peaks, or from the literature. Cathodic voltammograms for $TPPH_4^{2+}$ showed multi-step irreversible reductions. The reduction potential estimated from the first stage is -0.35 V vs. SCE, much higher than for the free base (-1.05 [19] V) as expected for the positively charged dication.

RESULTS AND DISCUSSION

Photophysics of $TPPH_4^{2+}$

Spectra and Excited State Lifetimes. Addition of TFA to $TPPH_2$ in acetone leads directly to the dication [20]. The spectrum (Fig. 1), with peaks at 654 and 436 nm agrees

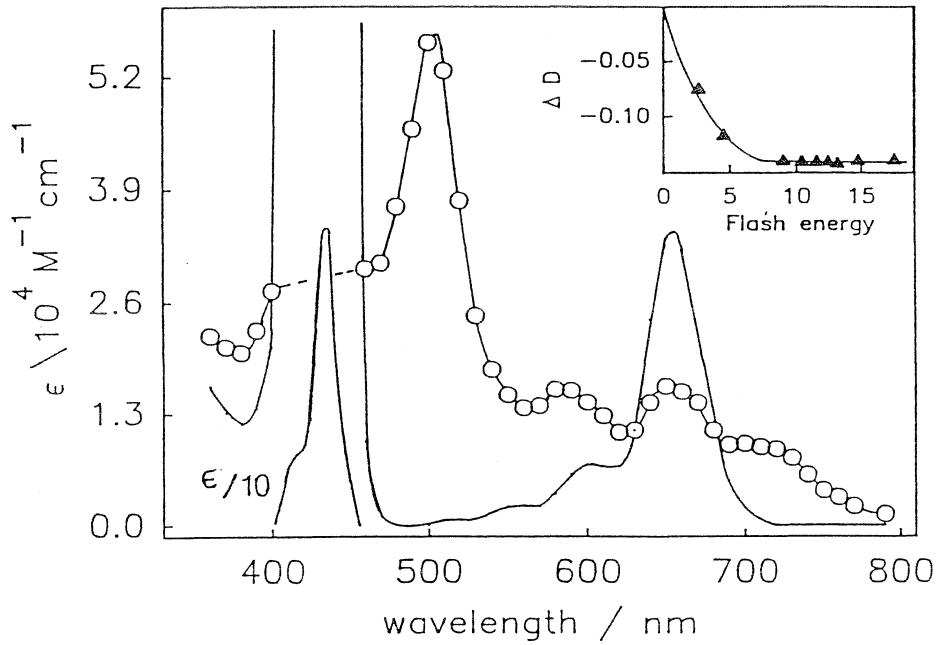

Figure 1. Absorption spectra of ground state (—) and triplet state (—O—) of $TPPH_4^{2+}$; insert, saturation of ground state conversion to triplet, λ = 650 nm, flash energy in arbitrary units.

with previous observations, taking account of solvent and anion dependent variations [3,21]. The excited singlet decayed exponentially with fluorescence lifetime, τ_F = 1.05 ±0.03 ns, independent of emission wavelength (697, 750 nm) [13]. This may be compared with the lifetime found in benzene (τ = 1.8 ns, and ϕ_F ~ 0.14) [5]. The triplet (ϵ_λ) absorption spectrum (Fig. 1) expands the more limited (ΔD) data of Gust, *et al.* [7]; absorption is generally similar to that of other porphyrin triplets, extending throughout the visible and into the near IR, with the most prominent band (here at 510 nm, ϵ = (5.3 ±0.4) x 10^4 M^{-1} cm^{-1}, see below) lying slightly to the red of the Soret peak [22]. Lesser bands in $TPPH_4^{2+}$ triplet also appear at 350 and 590 nm. The indicated band around 670 nm is reproducible, but its height is uncertain because of the large ground state bleaching correction. The spectrum remained quite constant when [TFA] was increased from 0.05 M (Fig. 1) to 2 M, and we conclude that $^3TPPH_4^{2+}$ does not lose protons under these conditions. In related dications, the main T-T band for protonated tetra-*p*-hydroxyphenylporphyrin lies also at 510 nm, with closely similar extinction (ϵ = 5.7 x 10^4 M^{-1} cm^{-1}), [23] and in tetra-*p*-pyridylporphyrin dication, T-T peaks are found at 720 and 930 nm [24]. The $TPPH_4^{2+}$ triplet recovers reversibly in acetone - 0.05 M TFA, via the usual mixed first and second-order kinetics [22]; k_1 ~8600 s^{-1} and k_2 = (2.1 ±0.1) x 10^9 M^{-1} s^{-1} (measured at two wavelengths), at room temperature.

Triplet Energy, E_T. The phosphorescence of $TPPH_4^{2+}$ has apparently not yet been observed, even with the aid of external heavy atom enhancement [2,25]. Limits for the triplet energy were therefore set by energy transfer experiments, using tetracene (E_T = 10,250 cm^{-1}) [26] and perylene (E_T = 12,370 cm^{-1}) [27] as acceptors. In toluene, tetracene quenched $^3TPPH_4^{2+}$ at close to diffusion-controlled rate, while perylene was ineffective; slight quenching by perylene at high concentrations was observed in acetone. We therefore take E_T of $^3TPPH_4^{2+}$ to be about 11,600 ±500 cm^{-1} (1.44 ±0.06 eV). This is supported by an estimate based on the S-T splitting (~3600 cm^{-1}) observed for octaethylporphyrin dication [2]. Applying this to $TPPH_4^{2+}$ (Q_{00} = 656 nm) gives E_T ~ 11,600 cm^{-1}.

Triplet Yield, ϕ_T. Results of measurements on $TPPH_4^{2+}$, using the limiting slope method [16], are shown in Fig. 2 and give ϕ_T = 0.31 ±0.03, for excitation at 347 nm. This is markedly less than that for the free base $TPPH_2$ (ϕ_T ~0.67 in benzene [23]). For the dication, ϕ_F in acetone-HCl solution is 0.11 [3]. Thus, the sum of ϕ_F + ϕ_T < 0.5 is evidently far below unity, contrary to what has been assumed [4]. Substantial internal conversion from the excited singlet to the ground state must occur, as indicated also by the short singlet lifetime. This may perhaps be associated with strong out-of-plane distortion of the porphyrin ring upon protonation [20] leading to enhanced crossings of the excited and ground state surfaces. A similar effect of protonation on ϕ_T has been observed in the case of tetra-*p*-hydroxyphenylporphyrin in methanol, in which the triplet yield falls from 0.65 to 0.29 on addition of TFA, and ϕ_F + ϕ_T is also low [23].

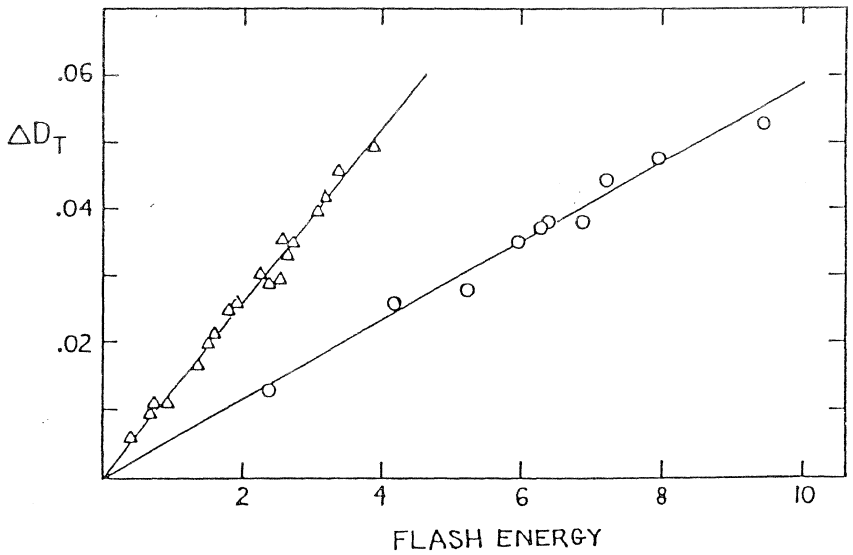

Figure 2. Determination of triplet yield, ϕ_T; limiting slopes of ΔD_T vs. flash energy (in arbitrary units) for benzophenone-in-benzene actinometer (—O—) and for $TPPH_4^{2+}$ in acetone -0.05 M TFA (—Δ—); absorbances = 0.051 at 347 nm.

Photochemistry of Triplet $TPPH_4^{2+}$

Interaction of $^3TPPH_4^{2+}$ with Reductants. The range of $^3TPPH_4^{2+}$ reductants that can be studied is evidently limited by the requirement that they be much weaker bases than $TPPH_2$ itself. This permits work with hydroquinones and diphenyl or triphenyl amines which are not protonated under conditions (0.05 M TFA in acetone) where $TPPH_2$ is fully protonated, and whose presence does not modify the absorption spectrum of the porphyrin dication.

Reaction Products. Flashing solutions of $TPPH_4^{2+}$ and reductants leads to biphasic transient decay profiles, with shortened triplet lifetime and formation of long-lived products (Fig. 3). Difference spectra following complete disappearance of the triplet are shown in Fig. 4, A and B, for solutions containing tri-*p*-tolylamine (TTA) and trimethyl hydroquinone (TMHQ), respectively. In spectrum A, the peak at 680 nm corresponds to the known absorption of TTA^+ radical and indicates that quenching proceeds via electron transfer to the triplet to form a radical pair. For quenching by hydroquinones, the H_2Q^+ radicals presumably formed by initial electron-transfers are strongly acidic [28] and will lose protons rapidly to give $HQ^\bullet$ species. These do not absorb above ~450 nm [29], so that at longer wavelengths, curve B, Fig. 4 should correspond only to the porphyrin radical-ground state difference spectrum. Thus, assuming comparable radical yields for amine and hydroquinone reduction (see below), subtracting B from A in Fig. 4 should isolate the TTA^+ spectrum, as is shown in Fig. 5A. Further, correcting curve B, Fig. 4 for ground state bleaching and taking account of incomplete reaction ($\phi_{Rad} < 1$, see below), we recover also the spectrum of the presumed reduced porphyrin radical as shown in Fig. 5B. This spectrum

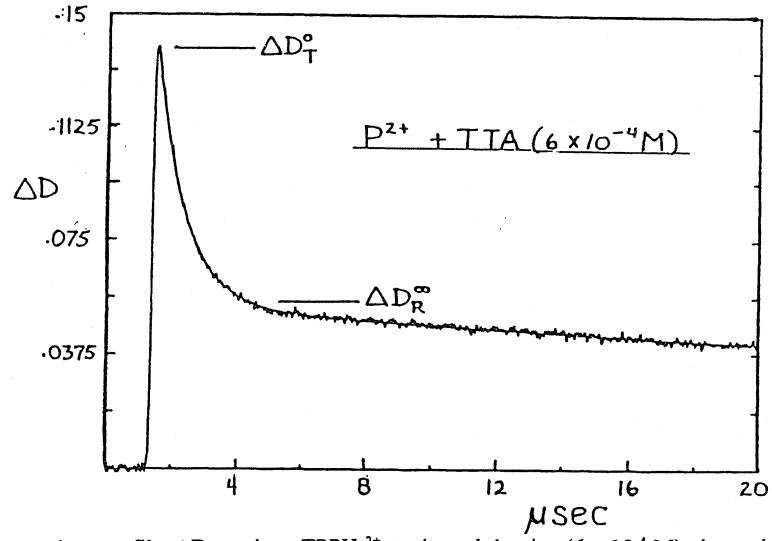

Figure 3. Flash transient profile, ΔD vs. time; $TPPH_4^{2+}$ + tri-*p*-tolylamine (6×10^{-4} M); determination of ΔD_T^0 and ΔD_R^∞ at λ = 580 nm.

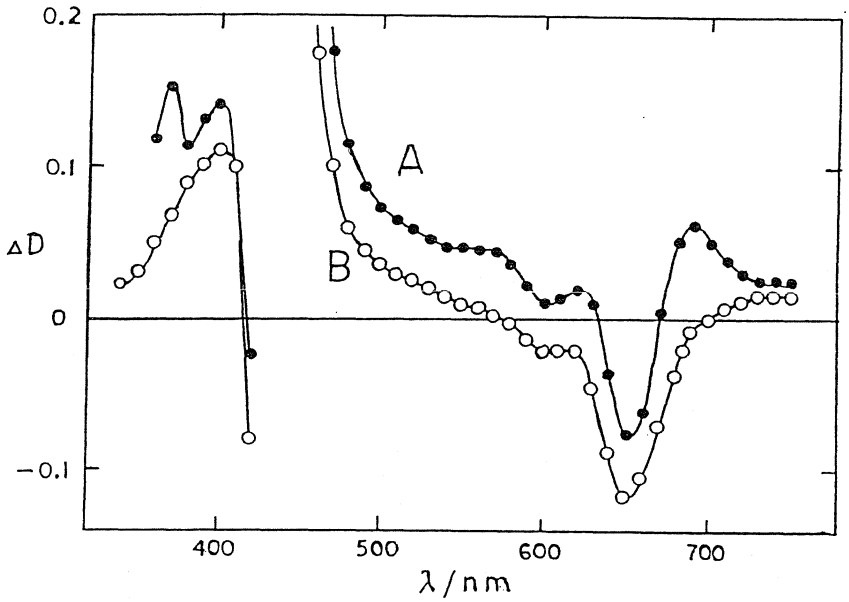

Figure 4. Transient difference spectra in acetone: A - $TPPH_4^{2+}$ + 10^{-3} M tri-*p*-tolylamine, 3 μs after flash; B - $TPPH_4^{2+}$ + 5 x 10^{-3} M trimethylhydroquinone, 2 μs after flash.

closely resembles that found by Neta and co-workers in pulse radiolytic reduction of $TPPH_2$ in neutral or basic isopropanol, and attributed by them to $TPPH_3^\bullet$ and $TPPH_2^{+\bullet}$ respectively [31]. In our case, under acidic conditions, formation of $TPPH_4^{+\bullet}$ is evidently possible. To clarify this situation, $TPPH_4^{2+}$-trimethylhydroquinone solutions in 2M TFA were flashed. The resulting transient spectra were indistinguishable from those observed with 0.05M TFA. This suggests that the porphyrin radical in Fig. 5B is $TPPH_4^{+\bullet}$. In any case, broad bands in the near IR and weakening of structure in the visible appear to be characteristics of reduced porphyrin radicals [31,32].

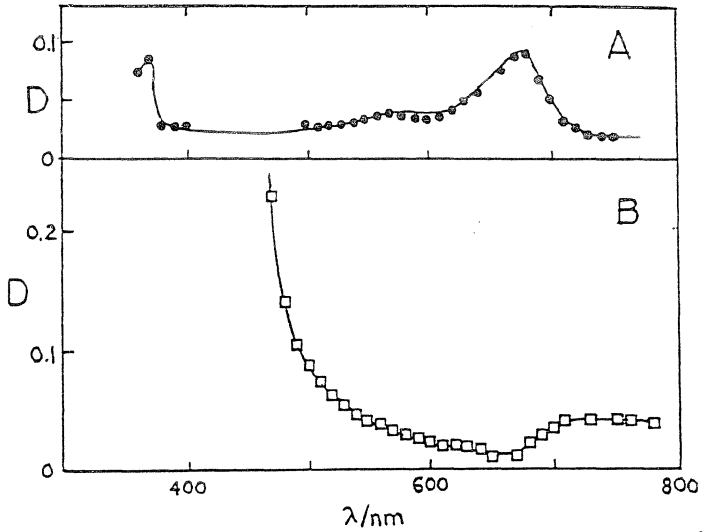

Figure 5. A) Identification of tri-*p*-tolylamine cation radical in photoreduction of $TPPH_4^{2+}$: (——) Spectrum of $TTA^{+\cdot}$ made by $SbCl_5$ oxidation. (——O——) Difference between spectra of Fig. 4, A - B. B) (——□——) Spectrum of $TPPH_4^{+\cdot}$ radical in acetone, corrected for ground state absorption. (See text for assignment of porphyrin radical.)

Kinetics of Reduction of $^3TPPH_4^{2+}$. The biphasic flash profiles observed in solutions of porphyrin dication and reductants were analyzed by a procedure which assumes pseudo-first order quenching of the triplet competing with normal triplet decay and overlapped by second order radical decay [33]. This provides values of both the "effective" first-order decay constant, k_d, and the total absorbance of the radicals formed. From the linear dependence of k_d on reductant concentration, [R], as seen in Fig. 6, we then obtain the triplet quenching rate constant, k_q, according to the relation $k_d = k_o + k_q[R]$.

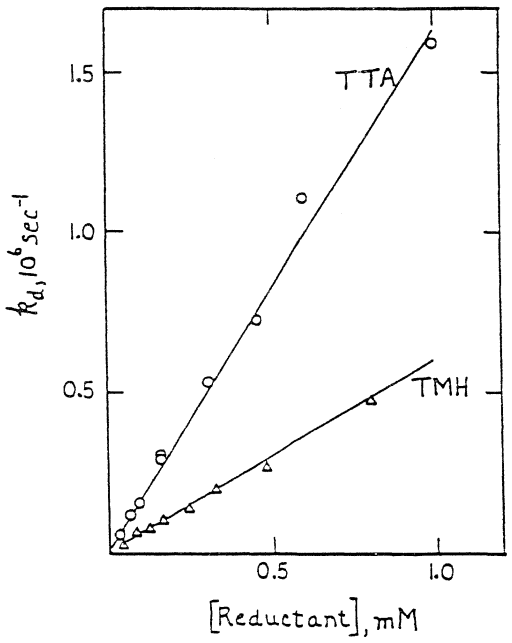

Figure 6. Determination of k_q for tri-*p*-tolylamine (——O——) and trimethylhydroquinone (——Δ——): pseudo-first order triplet decay constants, $k_o + k_q [Q] = k_d$ vs. [Q].

Table 1 summarizes these rate constants and the corresponding donor oxidation potentials, E_D^{0X} vs. SCE in acetonitrile. Table 1 also lists the values of $\Delta G^{0'}$, the free energy of the triplet-donor reaction in acetone, including the electrostatic contribution, as calculated from eqn. 1 [35].

$$\Delta G^{0'} = (E_D^{ox} - E_A^{red}) - E_T + e^2/\epsilon a \quad (1)$$

where a is the initial separation of the radical ion-pair. This was taken to be 8Å. In addition, the potentials in this equation must be corrected for the change in solvent (acetonitrile to acetone). This was done using the procedure of Weller [35], taking the radii of the reactants and radical separation to be 4Å and giving an overall correction (electrostatic and solvent) of +0.16 V.

Table 1
Reduction of $^3TPPH_4^{2+}$ by Hydroquinones and Aryl Amines: Rate Constants, Oxidation Potentials and Primary Radical Yields.

Reductant	k_q 10^7 M^{-1} s^{-1}	E_D^{OX} [a] vs. SCE	$\Delta G^{0'}$ [c] eV	ϕ_R
Hydroquinones				
1. 2,6-dimethoxy	110.	0.69	-0.24	0.28
2. tetramethyl	59.	0.75	-0.18	0.29
3. trimethyl (TMHQ)	57.	0.78	-0.15	0.33
4. 2,3-dimethyl	57.	0.85	-0.08	0.32
5. 2,5-di(*t*-amyl)	29.	0.82	-0.11	0.34
6. methyl-	30.	0.89	-0.04	0.34
7. phenyl-	9.5	0.90	-0.03	0.32
8. hydroquinone	5.9	0.94	0.01	0.34
9. pyrogallol	1.1	1.03	0.10	0.36
10. chloro-	0.53	1.07	0.14	0.28
Amines				
11. tri-*p*-tolyl (TTA)	150.	0.77[b]	-0.16	0.38
12. 3-methoxydiphenyl	14.	0.88	-0.05	0.35[d]
13. diphenyl-	8.2	0.90	-0.03	0.36[d]
14. triphenyl	6.8	0.92	-0.01	0.38
15. tri-*p*-fluorophenyl	1.7	1.00[b]	0.07	0.40
16. tri-*p*-iodophenyl	0.80	1.07[b]	0.14	0.40[d]
17. tri-*p*-chlorophenyl	0.36	1.09[b]	0.16	—
18. tri-*p*-bromophenyl	0.17	1.10[b]	0.17	—

[a] In acetonitrile

[b] Reversible potentials (polarographic and potentiometric).

[c] Taking $E^{red}(TPPH_4^{2+})$ = -0.35 V; E_T = 1.44 V, and total correction (for acetonitrile → acetone and $e^2/\epsilon a$) = + 0.16 V (see text).

[d] Quantum yields derived from absorbance ratios at 480 nm.

Fig. 7 shows the variation of log k_q with the calculated $\Delta G^{0'}$ for the several reductants studied here. No systematic difference appears between the behavior of the hydroquinone and the triphenylamine systems. Since electron-transfer quenching by the amines leads to singly charged radical cations (Figs. 4, 5) this indicates, as discussed above, that a similar reaction occurs in the primary quenching process for the hydroquinones as well, presumably followed by proton loss from the strongly acidic radical [34].

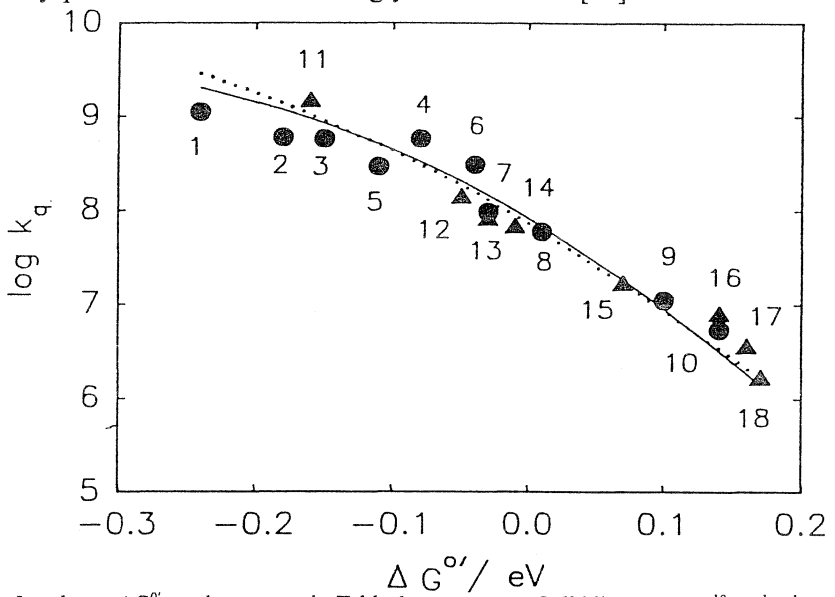

Figure 7. Log k_q vs $\Delta G^{0'}$: reductants as in Table 1; parameters: Solid line: $Z = 10^{10}$ M^{-1} s^{-1}, $\Delta G(0) = 0.123$. Dotted line: $Z = 10^{11}$ M^{-1} s^{-1}, $\Delta G(0) = 0.185$.

To interpret these kinetic results, we take $k_q = Z \exp(-\Delta G^{\ddagger}/RT)$ and make use of the Agmon-Levine relation (eqn. 2), which gives the activation energy of the quenching reaction, $\Delta G^{\ddagger}$, in terms of $\Delta G^{0'}$ and the "intrinsic activation energy," $\Delta G(0)$ [36,37,38]:

$$\Delta G^{*} = \Delta G^{0'} + \frac{\Delta G(0)}{\ln 2} \ln\left[1 + \exp\frac{(-\Delta G^{0'} \ln 2)}{\Delta G(0)}\right]$$

At $\Delta G^{0'} = 0$, $\Delta G^{\ddagger} = \Delta G(0)$ and from Fig. 7, log k ~ 7.9, whence log Z = 7.9 + $\Delta G(0)$/2.3 RT. A given value of Z then gives a corresponding value of $\Delta G(0)$ and thereby $\Delta G^{\ddagger}$ and log k_q as function of $\Delta G^{0'}$, for comparison with Fig. 7.

The best least squares fit is obtained with $Z = 10^{10}$ M^{-1} s^{-1}, and $\Delta G(0) = 0.123$ eV (Fig. 7, solid line). The corresponding Marcus reorganization energy, $\lambda = 4\Delta G(0)$, is 0.49 eV. However, within the spread of the data of Fig. 7, reasonable fits to the experimental points can also be obtained with values of Z and $\Delta G(0)$ as high as 10^{11} M^{-1} s^{-1} and 0.19 eV respectively (Fig. 7, dotted line). Z values lower than 10^{9} or higher than 10^{12} M^{-1} s^{-1} may definitely be excluded. We estimate λ to be 0.6 ±0.1 eV, from the spread of the rate data. Further uncertainties in these parameters must arise from the reduction potential of triplet $TPPH_2^{2+}$, derived from irreversible polarograms (E_A^{red} = -0.35V vs. SCE) and triplet energy transfer data (E_T = 1.44 eV).

In partitioning the reorganization energy, λ, between inner (λ_i) and outer (λ_o) components, it is generally assumed that λ_i is small for aromatic organic radicals with delocalized charge distributions [39,40]. However, for the case studied here, the possibility exists of large changes in shape upon reduction of the non-planar porphyrin dication[20], possibly associated with displacement of the central protons [41].

We note that the highest k_q found in this study, 1.5 x 10^9 M^{-1} s^{-1} for tritolylamine (TTA), is still significantly below the diffusion limit for these systems, as shown by the following values of $TPPH_4^{2+}$ fluorescence quenching rate constants (10^{10} M^{-1} s^{-1}): TTA, 3.0; diphenylamine, 2.5; trimethylhydroquinone, 2.3; hydroquinone, 1.1. Taking the S—T splitting (see above) to be about 3600 cm^{-1} (0.45 eV) and referring to Table 1, we expect that diffusion-limited rates of triplet quenching will be reached at polarographic E_D^{0X} vs. SCE values lower than about 0.5V.

Quantum Yields. These were obtained from the general relation

$$\phi_R = \frac{\Delta D_R^\infty}{\Delta D_T^0} \frac{(\epsilon_T - \epsilon_G)}{\sum(\epsilon_R - \epsilon_G)}$$

where ΔD_T^0 and ΔD_R^∞ are the transient absorbance changes corresponding respectively to the concentrations of initial triplet and total final radical products. These were evaluated from the flash profiles (Fig. 3) by the kinetic analysis which corrected for small amounts of untrapped triplets and any overlapping pseudo-first order radical formation and second order decay [33]. Radical extinction coefficients were derived from flash data at 480 and 580 nm as follows. As noted above, at wavelengths greater than 450 nm, the long-lived transient spectrum for the *hydroquinone* (TMHQ) quenched solutions is the difference between porphyrin radical and porphyrin ground state absorption. Moreover, at the isosbestic point, 580 nm, this difference is zero (Fig. 4B). Therefore, in the various solutions quenched by the *amines*, ΔD_{580}^0 represents only the initial porphyrin triplet and ΔD_{580}^∞ represents only the resulting amine radical. Quantum yields, ϕ_R's for the amine series (Table 1) are then obtained using the porphyrin triplet and amine radical extinctions at 580 nm (Table 2), and $(\Delta D_R^\infty/\Delta D_T^0)_{580}$ ratios measured on the same flash and sweep (Fig. 3). At 480 nm, the long-lived absorption in flashed porphyrin-TTA solutions (Fig. 4A) is due to both porphyrin and amine radicals. The contribution from TTA^+ is relatively small and is obtained from ΔD_{580}^∞ measured on the same solution, combined with the known TTA^+ spectrum ($\epsilon_{480}/\epsilon_{580} = 0.21$), thereby giving ΔD_{480}^∞ of the porphyrin radical alone. Putting the previously measured ϕ_R for this system back into eqn. 3 then gives $[(\epsilon_R-\epsilon_G)/(\epsilon_T-\epsilon_G)]_{480} = 0.88 \pm 0.05$ for the porphyrin (radical/triplet) extinction ratio. This value is finally used to obtain ϕ_R from measured $(\Delta D_R^\infty/\Delta D_T^0)_{480}$ ratios for the hydroquinone series, in which absorption at 480 nm is due solely to the two porphyrin transient species. The relevant extinction coefficients thus derived are listed in Table 2. Although this procedure is rather involved, ϕ_R values of reasonable precision are obtained (Table 1) owing to the good S/N levels of the transient profiles (Fig. 3) and the stability of the calibrating TTA^+ spectra. As an overall check, ϕ_R

for tri-*p*-fluorophenylamine was measured at both 480 and 580 nm, giving 0.39 ±0.02 and 0.41 ±0.02 respectively.

Table 2
Summary of Extinction Coefficients.

Compound	λ(max) nm	ϵ(max) 10^3 M^{-1} cm^{-1}	ϵ(480) 10^3 M^{-1} cm^{-1}	ϵ(580) 10^3 M^{-1} cm^{-1}
$(CH_3\text{-}\phi)_3N^{+\bullet}$ [a]	674	26.2	1.75	8.46
$(F\text{-}\phi)_3N^{+\bullet}$[a]	644	26.6	2.48	7.76
$(Cl\text{-}\phi)_3N^{+\bullet}$[a]	703	32.4	1.40	6.61
$(Br\text{-}\phi)_3N^{+\bullet}$[a]	726	36.0	1.05	5.41
$\phi_2NH^{+\bullet}$[b]	670	19.0	1.6	6.8
$TPPH_4^{2+}$	654	33.4	0.70	4.30
$^3TPPH_4^{2+}$ [c]	510	55.0	32.7	15.4
$TPPH_4^{+\bullet}$[d]	—	—	29.4	4.3

[a]Stable cation radicals of p-substituted triphenylamines, prepared by $SbCl_5$ oxidation in acetone.
[b]T. Shida and W. Hamill, J. Chem. Phys., 44 (1966) 2369; K. Kikuchi et al., J. Phys. Chem., 95 (1991) 38.
[c]Total conversion from ground state (Fig. 1).
[d]State of protonation is not certain; see text.

The radical yields listed in Table 1 are strikingly constant within each group of reductants, and within experimental error, are independent of $\Delta G^{0'}$, over a range of about 0.4 V. Thus, for the hydroquinones and triphenylamines, the average yields are 0.32 and 0.38 respectively, with mean deviations of ±0.02 for both groups. While the yields for amine reduction appear to be slightly higher than those for the hydroquinones, one may conclude that the same factors, controlling the ratio of cage escape to back reactions of the charge transfer intermediate, are operating to essentially the same extent in both cases.

The dependence of ϕ_R on $\Delta G^{0'}$ in an homologous reaction series can be understood in terms of a constant rate of cage escape of a primary radical pair competing with back transfer whose rate depends on the free energy of recombination, ΔG_{rec}, in general accord with theoretical expectations [42,43]. A situation in which ϕ_R is insensitive to ΔG_{rec} may arise if the recombination process happens to correspond to a region where the Marcus curve is flat, i.e., around the maximum in log k_{rec} vs. ΔG_{rec}. The range of variation of ΔG_{rec} for this reaction in Fig. 7 is about 0.4 V (1.02 to 1.45 V). Alternatively, one may suggest that another process, independent of ΔG_{rec} may be involved in the back reaction. For triplet quenching, this may be a spin-inversion step, in which the primary triplet radical pair relaxes to singlet, permitting the back transfer to occur [44]. The intervention of a rate-limiting step in the back reaction has been proposed by Hoffman, in connection with the radical yields in electron transfer quenching of excited Ru(II) complexes [45]. Further studies, including experiments over a wider range of ΔG_{rec} will help clarify the matter [41].

Acknowledgement

We much appreciate support of this work by the U.S. Department of Energy, Division of Chemical Sciences, Office of Basic Energy Sciences (Grant No. FG02-89ER14027, to Brandeis University).

REFERENCES AND NOTES

1. P. Hambright, In: Porphyrins and Metalloporphyrins, K.M. Smith, (Ed.), Ch. 6, Elsevier, Amsterdam (1975).
2. M. Gouterman and G. Khalil, J. Molec. Spectroscopy, **53**, 88 (1974).
3. E. Austin and M. Gouterman, Bioinorganic Chemistry, **9**, 281 (1978).
4. O. Ohno, Y. Kaizu, and H. Kobayashi, J. Chem. Phys., **82**, 1779 (1985).
5. R.S. Sinclair, D. Tait, and T.G. Truscott, J. Chem. Soc., Faraday I, **76**, 417 (1980).
6. A. Harriman and M. Richoux, J. Photochem., **27**, 205 (1984).
7. D. Gust, T.A. Moore, A.L. Moore, X.C. Ma, R.A. Nieman, G.R. Seely, R.E. Belford, and J.E. Lewis, J. Phys. Chem., **95**, 4442 (1991).
8. D. Mauzerall, In: The Porphyrins, D. Dolphin, (Ed.); Vol. V, Ch. 2, Academic Press, NY (1978).
9. M. Richoux, P. Neta, A. Harriman, S. Barel, and P. Hambright, J. Phys. Chem., **90**, 2462 (1986).
10 a) T.N. Baker, W.P. Doherty, W.S. Kelley, W. Newmeyer, J.E. Rogers, R.S. Spalding, and R.I. Walter, J. Org. Chem., **30**, 3714 (1985); b) R.I. Walter, J. Am. Chem. Soc., **77**, 5999 (1955).
11. F.A. Bell, A. Ledwith, and D.C. Sherrington, J. Chem. Soc. (C), 2719 (1969).
12. H.O. Huisman, Rec. Chim. Pays. Bas, **69**, 1133 (1950); Houben-Weyl, Methoden der Organischen Chemie, Band VI/1c. Teil 1, p. 567, Georg Thieme Verlag, Stuttgart.
13. J.S. Lindsey, J.K. Delaney, D.C. Mauzerall, and H. Linschitz, J. Am. Chem. Soc., **110**, 3610 (1988). We thank Professor David Mauzerall, of Rockefeller University, for these lifetime measurements.
14. L.J. Andrews, A. Deroulede, and H. Linschitz, J. Phys. Chem., **82**, 2304 (1978).
15. J.K. Hurley, H. Linschitz, and A. Treinin, J. Phys. Chem., **92**, 5151 (1988).
16. J.K. Hurley, N. Sinai, and H. Linschitz, Photochem. Photobiol., **38**, 9 (1983).
17. L. Hagopian, G. Kohler, and R.I. Walter, J. Phys. Chem., **71**, 2290 (1967).
18. This correction is obtained by combining the potential of (ferrocinium/ferrocene) in acetonitrile vs Ag, 0.01M $AgClO_4$ (+0.061V) with that vs SCE (+0.39V). See J.H. Wilford, M.D. Archer, J.R. Bolton, T.F. Ho, J.A. Schmidt, and A.C Weedon, J. Phys. Chem., **89** (1985); and A. Anne, P. Habiot, J. Moiroux, P. Neta, and J.M. Saveant, J. Phys. Chem., **95**, 2370 (1991).
19. R.H. Felton and H. Linschitz, J. Am. Chem. Soc., **8** , 113 (1966).
20. A. Stone and E.B. Fleischer, J. Am. Chem. Soc., **90**, 2735 (1968).
21. M. Meot-Ner and A.D. Adler, J. Am. Chem. Soc., **97**, 5107 (1975); 659 and 442 nm for the dication in DMF-$HClO_4$ solution, and (ref. 20), 661 and 445 nm in $CHCl_3$-HCl.
22. L. Pekkarinen and H. Linschitz, J. Am. Chem. Soc., **82**, 2407 (1960).
23. R. Bonnett, D.J. McGarvey, A. Harriman, E.J. Land, T.G. Truscott, and U.J. Winfield, Photochem. Photobiol., **48**, 271 (1988).
24. K. Kalyanasundaram, Inorg. Chem., **23**, 2453 (1984).
25. A careful search for this emission, using a N_2-cooled Ga-As photomultiplier and phase-sensitive detection likewise gave negative results. We thank Dr. L. Andrews and Ms. Barbara Thompson, of GTE Laboratories, Inc., for their assistance in these experiments.
26. S.P. McGlynn, T. Azumi, and M. Kasha, J. Chem. Phys., **40**, 507 (1964).
27. R.H. Clarke and R.M. Hochstrasser, J. Molec. Spectrosc., **32**, 309 (1969).
28. W.T. Dixon and D. Murphy, J. Chem. Soc., Faraday 2, **72**, 1221 (1976).
29. K.B. Patel and R.L. Willson, J. Chem. Soc., Faraday 1,814 (1973).

30. P. Neta, A. Scherz, and H. Levanon, J. Am. Chem. Soc., **101**, 3624 (1979), particularly Fig. 3.
31. S. Baral, P. Neta and P. Hambright, Radiat. Phys. Chem., **24**, 245 (1984); S. Baral and P. Hambright, J. Phys. Chem., **88**, 1595 (1984); D.M. Guldi, P. Hambright, D. Lexa, P. Neta, and J.M. Saveant, J. Phys. Chem., **96**, 4459 (1992).
32. V.S. Chernikov and S.L. Bondarev, Biofizika, **28**, 370 (1983).
33. L.J. Andrews, J.M. Levy, and H. Linschitz, J. Photochem., **6**, 355 (1976/77). The large difference between triplet and radical lifetimes (Fig. 3) simplifies calculation of the total radical absorbance and ϕ_R.
34. In this connection, see B.R. Eggins and J.Q. Chambers, Chem. Commun., 232 (1969).
35. A. Weller, Z. Phys. Chem. (Weisbaden), **133**, 93 (1982).
36. N. Agmon and R.D. Levine, Chem. Phys. Lett., **52**, 197 (1977).
37. R.D. Levine and H. Levanon, J. Phys. Chem., **83**, 259 (1979).
38. F. Scandola and V. Balzani, J. Am. Chem. Soc., **101**, 6140 (1979).
39. L. Eberson, Adv. Phys. Org. Chem., **18**, 79 (1982).
40. R.A. Marcus, J. Phys. Chem., **26**, 872 (1957).
41. A more detailed discussion of the kinetics and yields will be given in connection with temperature variation, deuteration and magnetic field studies now in progress.
42. I.R. Gould, D. Ege, J.E. Moser, and S. Farid, J. Am. Chem. Soc., **112**, 4290 (1990).
43. T. Ohno, A. Yoshimura, and N. Mataga, J. Phys. Chem., **90**, 3295 (1986).
44. N. Periasamy and H. Linschitz, Chem. Phys. Lett., **64**, 281 (1979).
45. M.Z. Hoffman, personal communication.

7. Melléklet

External Heavy Atom Induced Phosphorescence Emission of Fullerenes: The Energy of Triplet C_{60}

Yang Zeng, Laszlo Biczok,† and Henry Linschitz*

Department of Chemistry, Brandeis University, Waltham, Massachusetts 02254-9110 *(Received: May 6, 1992)*

The external heavy atom induced phosphorescence of C_{60} and C_{70} is obtained at 77 K in a glass containing ethyl iodide and gives 12 690 ± 30 cm^{-1} as a precise lower limit for the energy of triplet C_{60}. Triplet lifetime measurements show that the heavy atom effect is relatively much greater on the $S_1 \rightarrow T_1$ than on the $T_1 \rightarrow S_0$ radiationless transitions, as expected from the smaller Franck–Condon constraints in the former process.

As part of the intense research effort to establish the physical and chemical properties of the fullerenes,[1,2] fluorescence spectra of C_{60} and C_{70}, have been observed[3-5] as well as the phosphorescence of C_{70}.[3,4,6] However, the phosphorescence of C_{60}, which is evidently of fundamental spectroscopic and photochemical interest, has hitherto not been clearly identified, presumably because of a very long radiative lifetime compared to its radia-

† On leave from the Central Research Institute for Chemistry, Hungarian Academy of Sciences, Budapest II, Pusztaszeri ut 59-67, Hungary.

0022-3654/92/2096-5237$03.00/0

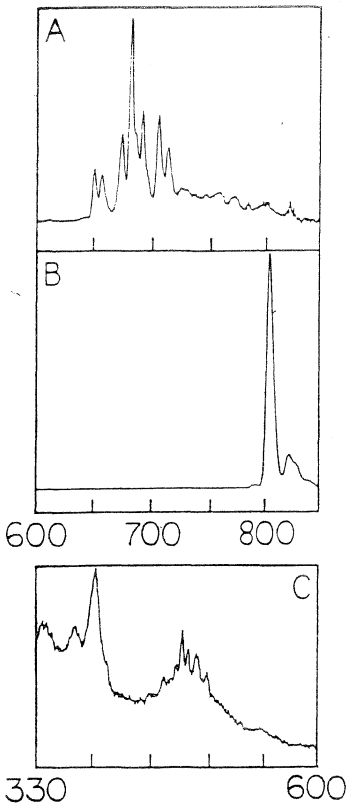

Figure 1. C_{70} at 77 K (concentration 3.2×10^{-5} M). (A) Emission spectrum in MCH (fluorescence). (B) Emission spectrum in HFI (phosphorescence). Excitation, in (A) and (B), λ = 470–490 nm; slit widths, 1.75 nm. Photometer gain in (A) is about 50 times greater than in (B). (C) Excitation spectrum of phosphorescence in HFI at λ = 804 nm; slit widths 1.75 nm for both excitation and emission. All spectra are uncorrected for photometer sensitivity.

tionless decay. We have now observed this emission unambiguously, using the external heavy atom effect[7,8] to enhance the triplet–singlet radiative rate.

Purified C_{60} and C_{70} preparations were obtained from the MER Corp. The very weakly emitting C_{60} was further refined by chromatography on neutral alumina developed with hexane.[9] Total emission and excitation spectra were taken on a Perkin-Elmer MPF-4 spectrofluorimeter, with a Hamamatsu R-928 photomultiplier detector. This has sufficient red response to establish clearly the 0–0 phosphorescence band, which is our main concern here. Fullerene emissions were measured in two solvents: (a) methylcyclohexane (MCH); (b) methylcyclohexane, 2-methyltetrahydrofuran, ethyl iodide, in 2:1:1 volume ratio ("HFI"). Both solvents formed clear noncracking glasses in liquid N_2. The decay of triplet C_{60} absorption at 750 nm[10-13] and 77 K, in both solvents, was followed by flash photolysis, using a frequency-doubled, Q-switched ruby laser for excitation at 347 nm, as described.[14]

Figure 1, A and B, shows emission spectra of C_{70} in MCH and HFI glass, respectively, at 77 K. The red fluorescence of C_{70} in MCH, which agrees well with that observed by Wang,[3] is completely eliminated in HFI solvent. Instead, there now appear a relatively weak threshold band at 794 nm and intense emissions at 804 and 823 nm, which are hardly seen in the MCH spectra under these conditions. The excitation spectra of the fluorescence in MCH or of the bands at 794 or 804 nm in HFI are all similar (Figure IC) and correspond to the absorption of C_{70}.[9] The HFI spectrum (Figure 1B) is identical with previous well-resolved observations in light atom media[3,4] and identified as $T \rightarrow S$ emission by ESR decay measurements.[6] Thus, the use of the iodide solvent does not shift the emitting triplet level appreciably.

Figure 2A–C shows similar results for C_{60}. Again, the fluorescence in MCH glass in the range 660–770 nm is totally abolished in HFI, where bands now appear at 796 and 812 nm. The onset of emission, using 1-nm slits, lies at 788 ± 2 nm. The

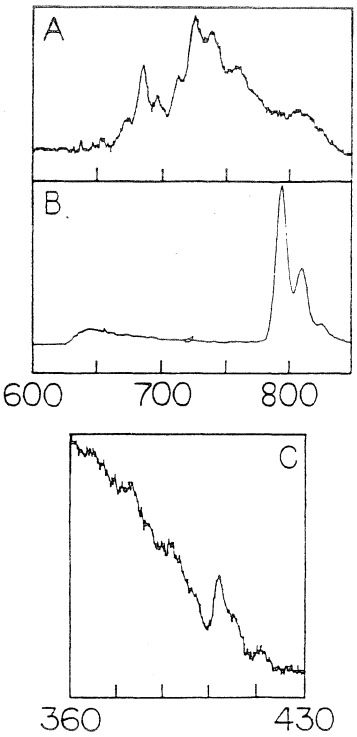

Figure 2. C_{60} at 77 K (concentration 1.0×10^{-4} M). (A) Emission spectrum in MCH (fluorescence), excitation, λ = 380–400 nm, slit, 4 nm. (B) Emission spectrum in HFI (phosphorescence), excitation, λ = 380–400 nm; slit, 2 nm. Photometer gain in (A) is about 5 times greater than in (B). (C) Excitation spectrum of phosphorescence in HFI, at λ = 790–800 nm; excitation slit, 2 nm.

excitation spectrum of the 796- or 812-nm band is accurately that of C_{60}[9] (Figure 2C).

Taking the emission threshold at 788 nm to be the O–O $T_1 \rightarrow S_0$ transition, the triplet energy of C_{60} is 12 690 ± 30 cm^{-1} or 36.3 ± 0.1 kcal/mol. This may be compared with the photoacoustic calorimetric result of Hung and Grabowski,[15] 12 600 ± 200 cm^{-1} in toluene, or of Terazima et al.,[12] 13 100 ± 300 cm^{-1} in benzene, in both of which the triplet quantum yield is assumed to be one. In turn, this value of ϕ_T is derived from measurements of sensitized singlet oxygen formation which in fact give ϕ_T values slightly less than one[12,16,17] or of the lifetime of singlet C_{60} in toluene, for which results are conflicting.[18,19]

Since the highest energy $T_1 \rightarrow S_0$ transition of C_{70} appears as a very weak emission, relative to the intense adjoining peak, much attention was given to the possibility of a similar close-lying high-energy band in C_{60} phosphorescence, rendered even weaker than the C_{70} band because of the higher orbital symmetry and overshadowed by the prominent peak at 796 nm (Figure 2B). This situation, involving an energy shift of less than 2%, would still be consistent with the photoacoustic energy and quantum yield data, within present experimental uncertainty of these values. However, many repeated spectral scans, at maximum possible C_{60} concentration, excitation flux, and spectral resolution, gave no clear indication of such high-energy emission, above noise levels.

The correct assignment of 0–0 levels in C_{60} is particularly complicated, since orbitally forbidden optical transitions involving the ground state become allowed only when coupled to appropriate vibrations. Reber, Zink, and co-workers have studied thin films of C_{60}, vacuum deposited on CaF_2, and find absorption and emission in the 700–1100-nm region.[20] On the basis of our observations (Figures 1 and 2) these may now be assigned with some confidence to singlet–triplet transitions as has been suggested by Leach et al.[21] From the overlap of the onset of absorption and emission, or by averaging peak absorption and emission energies, Reber et al. estimate 14 500 cm^{-1} as the O–O transition energy. Electronic interactions in these condensed films will of course introduce further uncertainties. Leach and co-workers[21] have assigned an extremely weak band system beginning at 14 660 cm^{-1} to $S_0 \rightarrow T_1$ transitions of C_{60} in solution and, on the basis of

oxygen-enhancement effects, have set E_T at least as low as 14 390 cm^{-1}. The photoacoustic results indicate that this is still too high. Thus, taking ϕ_T in light atom solvents to be as low as 0.95 and the calorimetric energy even as high as 13 300 cm^{-1} gives 14 000 cm^{-1} as an upper limit for E_T. We take the observed phosphorescence threshold, 12 690 ± 30 cm^{-1}, to be the lower limit. Vibrational quanta that may perhaps be associated with this transition are expected to be smaller than 500 cm^{-1}.[21] Calculated values of the lowest E_T of C_{60} are 2.23,[22] 2.06,[23] and 1.51 eV,[24] compared to the phosphorescence value 1.574 ± 0.01 eV found here.

In glassy solvents at 77 K, the decay of the C_{60} triplet absorption at 750 nm[10-12] was accurately first order, with rate constant $k = 5.3 \times 10^3$ s^{-1} in MCH and 2.3×10^4 s^{-1} in HFI. The relatively small change in triplet lifetime in passing from the light to heavy atom solvent is accompanied by what is evidently an exceedingly large change in the $T_1 \rightarrow S_0$ radiative rate, which we estimate very roughly to be at least a 100-fold. Since the phosphorescence yield, $\phi_P = k_{rad}/(k_{rad} + k_d)$, where the k's are radiative and radiationless transition rates, respectively, it is clear that failure to observe phosphorescence of C_{60} in light solvents must be due to the very low value of k_{rad}/k_d. The elimination of fluorescence of both C_{60} and C_{70} in HFI, with ϕ_T already close to one in light solvents, indicates also a large heavy atom effect on the rate of the radiationless $S_1 \rightarrow T_1$ transition,[25] compared to the small effect noted above on the triplet lifetime. Indeed, spin–orbit coupling would be expected to be more restrictive, relative to the Franck–Condon constraints, in the $S_1 \rightarrow T_1$ transition, where the splitting is small, than in the radiationless transition to the ground state, $T_1 \rightarrow S_0$, with a much larger energy gap.

Attempts to observe directly heavy atom induced absorption of C_{60} in the neighborhood of 780 nm[7,8] or emission activated bands in this region[26] have been indeterminate thus far.

Acknowledgment. We much appreciate support of this work by the U.S. Department of Energy, Division of Chemical Sciences, Office of Basic Energy Sciences (Grant 84ER13223, to Brandeis University).

References and Notes

(1) Kroto, H. W.; Heath, J. R.; O'Brien, S. C.; Curl, R. F.; Smalley, R. E. *Nature* **1985**, *318*, 162.

(2) Kratschmer, W.; Lamb, L. D.; Fostiropoulos, K.; Huffman, D. R. *Nature* **1990**, *347*, 354.

(3) Wang, Y. *J. Phys. Chem.* **1992**, *96*, 764.

(4) Sibley, S. P.; Argentine, S. M.; Francis, A. H. *Chem. Phys. Lett.* **1992**, *188*, 187.

(5) Verhoeven, J. W.; Scherer, T.; Heymann, D. *Recl. Trav. Chim. Pays-Bas* **1992**, *113*, 349.

(6) Wasielewski, M. R.; O'Neil, M. P.; Lykke, K. R.; Pellin, M. J.; Gruen, D. M. *J. Am. Chem. Soc.* **1991**, *113*, 2774.

(7) Kasha, M. *J. Chem. Phys.* **1952**, *20*, 71.

(8) McGlynn, S. P.; Azumi, T.; Kinoshita, M. *Spectroscopy of the Triplet State*; Prentice-Hall: Englewood Cliffs, NJ, 1969; Chapter 8.

(9) Ajie, H.; Alvarez, M. M.; Anz, S. A.; Beck, R. D.; Diederich, F.; Fostiropoulos, K.; Huffman, D. R.; Kratschmer, W.; Rubin, Y.; Schriver, K. E.; Sensharma, D.; Whetten, R. L. *J. Phys. Chem.* **1990**, *94*, 8630.

(10) Ebbeson, T. W.; Tanigaki, K.; Kuroshima, S. *Chem. Phys. Lett.* **1991**, *181*, 501.

(11) Sension, R. J.; Phillips, C. M.; Szarka, A. Z.; Romanow, W. J.; McGhie, A. R.; McCauley, J. P.; Smith, A. B.; Hochstrasser, R. M. *J. Phys. Chem.* **1991**, *95*, 6075.

(12) Terazima, M.; Hirota, N.; Shinohara, H.; Saito, Y. *J. Phys. Chem.* **1991**, *95*, 9080.

(13) Biczok, L.; Linschitz, H.; Walter, R. I. *Chem. Phys. Lett.*, in press.

(14) Andrews, L. J.; Deroulede, A.; Linschitz, H. *J. Phys. Chem.* **1978**, *82*, 2304.

(15) Hung, R. R.; Grabowski, J. J. *J. Phys. Chem.* **1991**, *95*, 6073.

(16) Arbogast, J. W.; Darmanyan, A. P.; Foote, C. S.; Rubin, Y.; Diederich, F. N.; Alvarez, M. M.; Whetten, R. B. *J. Phys. Chem.* **1991**, *95*, 11.

(17) We have also measured ϕ_T actinometrically, relative to benzophenone, with $\phi_T = 0.93 + 0.07$ (ref 13).

(18) To date, published values of the C_{60} singlet lifetime are 33,[6] 1200,[10] and 650 ps.[11]

(19) Triplet quantum yields less than one would raise proportionally the value of E_T computed from photoacoustic data.

(20) Reber, C.; Yee, L.; McKiernan, J.; Zink, J. I.; Williams, R. S.; Tong, W. M.; Ohlberg, D. A.; Whetten, R. L.; Diederich, F. *J. Phys. Chem.* **1991**, *95*, 2127.

(21) Leach, S.; Vervloet, M.; Desprès, A.; Brêheret, E.; Hare, J. P.; Dennis, T. J.; Kroto, H. W.; Taylor, R.; Walton, D. R. M. *Chem. Phys.* **1992**, *160*, 451.

(22) Laszlo, I.; Udvardi, L. *J. Mol. Struct.* **1989**, *183*, 271.

(23) Negri, F.; Orlandi, G.; Zerbetto, F. *Chem. Phys. Lett.* **1988**, *144*, 31.

(24) Feng, J.; Li, J.; Wang, Z.; Zerner, M. C. *Int. J. Quantum Chem.* **1991**, *39*, 331.

(25) Medinger, T.; Wilkinson, F. *Trans. Faraday Soc.* **1965**, *61*, 620.

(26) Kearns, D. R.; Case, W. A. *J. Am. Chem. Soc.* **1966**, *88*, 5087.

8. Melléklet

Extinction coefficients of C_{60} triplet and anion radical, and one-electron reduction of the triplet by aromatic donors

Laszlo Biczok [1], Henry Linschitz
Department of Chemistry, Brandeis University, Waltham, MA 02254-9110, USA

and

Robert I. Walter
Department of Chemistry, University of Illinois, Chicago, IL 60680, USA

Received 24 April 1992

The extinction coefficients of the triplet state of C_{60} are obtained by energy-transfer techniques in flash photolysis studies. The values permit actinometric measurement of the triplet quantum yield ($\phi_R = 0.93 \pm 0.07$) and give rates of T–T annihilation close to diffusion-controlled. Rates and radical quantum yields in reversible one-electron reduction of $^3C_{60}$ by tri-*p*-tolylamine, TTA, and hydroquinone are determined as well as extinction coefficients in the visible of the C_{60}^- anion radical. Back electron transfer from C_{60}^- to TTA^+ occurs at a distance markedly greater than van der Waals contact.

1. Introduction

Recent studies of the fullerenes [1,2] have contributed to the development of a systematic photochemistry of these fascinating new materials. With regard to establishing energy-flow pathways following excitation, an estimate of the triplet quantum yield of C_{60}, based on sensitized formation of singlet oxygen indicates that it is close to one [3]. The marked capacity of fullerenes to accept electrons [2,4,5] then suggests that a characteristic mode of photochemical reaction would be reduction of the triplet. Indeed, qualitative indications of this have been found by ESR studies using various aryl donors [6], and photochemically active charge-transfer complexes of C_{60} have been demonstrated [7,8]. In particular, Arbogast, Foote and Kao [9], in a letter which appeared during preparation of this report, have directly shown that cation radicals of aryl amine donors are formed accompanying quenching of $^3C_{60}$. We have been carrying out very similar studies, with the additional purpose of determining not only rates but also quantum yields of radical products resulting from $^3C_{60}$ reactions. Toward this end, we now report new measurements of the spectrum of $^3C_{60}$ including extinction coefficients together with actinometric studies which confirm the remarkably high triplet yield. From the accurately known spectrum of tri-*p*-tolylamine cation radical, we determine the extinction coefficients of C_{60}^- anion radical in the visible and the quantum efficiencies of $^3C_{60}$ reduction by the amine and hydroquinone.

Correspondence to: H. Linschitz, Department of Chemistry, Brandeis University, Waltham, MA 02254-9110, USA.
[1] On leave from the Central Research Institute for Chemistry, Hungarian Academy of Sciences, Budapest II, Pusztaszeri ut 59-67, Hungary.

2. Experimental

2.1. Materials

Purified C_{60} ($\approx 99\%$) was obtained from the MER Corporation. It formed magenta solutions, whose absorption spectrum closely matched that given for C_{60} [10], and was used as received. Toluene and benzonitrile were from Aldrich (HPLC grade), and

0009-2614/92/$ 05.00

zinc tetraphenyl porphyrin (ZnTPP, chlorine free) from Midcentury Chemicals. Tetracene (TET) was zone-refined. Tri-*p*-tolylamine (TTA) was synthesized as described [11]. Hydroquinone (H_2Q, Aldrich) was recrystallized from benzene and ethanol.

2.2. Apparatus and procedure

Solutions of C_{60} ($\approx 5\times10^{-5}$ M) containing appropriate reactants in toluene or benzonitrile were purged with N_2 and studied by flash photolysis, using a flashlamp-pumped dye laser (Candela, ED-200 with rhodamine 560; excitation at 555 nm, 0.3 μs fwhm) and a 10-bit transient digitizer (Tektronix, RTD-710 A) to record data. Auxiliary equipment and procedures were generally as described earlier [12].

Experiments involving $^3C_{60}$ in energy-transfer or redox processes were carried out at reagent concentrations such that more than 95% of the triplet was trapped and its disappearance followed pseudo-first-order kinetics. Total triplet or radical absorbances, corrected for any slight product decay during the reduction reaction were evaluated from the transient profiles by a computer analysis assuming sequential pseudo-first-order (quenching) and second-order (radical recombination) processes [13]. Extinction coefficients of $^3C_{60}$ were determined by a double energy-transfer technique [14], relative to ZnTPP, whose triplet extinction coefficient at 470 nm is reliably established by total ground state depletion [15]. TET, with no absorbance at the exciting laser wavelength, 555 nm, and $E_T = 10240$ cm^{-1} [16] was used as a common triplet acceptor from both $^3C_{60}$, $E_T = 12600$ cm^{-1} [17] and ^{3}ZnTPP, $E_T = 12800$ cm^{-1} [18]. Thus, for essentially complete transfer to TET from both systems, the extinction coefficient of $^3C_{60}$ is:

$$\epsilon_{\lambda_1}(^3C_{60}) = \frac{\Delta D_{\lambda_1}(C_{60})}{\Delta D_{\lambda_2}(\mathrm{TET})}\left(\frac{\Delta D(\mathrm{TET})}{\Delta D(\mathrm{ZnTPP})}\right)_{\lambda_2} \times \epsilon_{\lambda_2}(\mathrm{ZnTPP}), \quad (1)$$

where ΔD are initial donor (C_{60} and ZnTPP) and final acceptor (TET) triplet absorbances at suitable wavelengths, λ_1 and λ_2. In the first ratio, ΔD_{λ_1} (C_{60}) and ΔD_{λ_2} (TET) are measured on the same C_{60}–TET solution, at equal flash intensities. This technique exploits the convenient overlapping absorptions of ground-state C_{60} and ZnTPP at 555 nm, and of triplet ZnTPP and TET around 470 nm [15,18,19] [#1], and permits donor–acceptor absorbance ratios for the latter pair to be determined on the same flash. Measurements were made at $\lambda_1 = 750$ nm and $\lambda_2 = 465$ and 470 nm.

Bimolecular reaction rate constants for energy or electron transfer were derived from the linear dependence of the effective first-order triplet decay constant on quencher concentration (fig. 1).

Triplet yields were determined actinometrically by the "limiting slope" method, using benzophenone in benzene as the reference triplet [20]. Here,

$$\phi_T = \frac{\epsilon_{\mathrm{ref}}}{\epsilon_T}\left(\frac{\mathrm{d}\Delta D_T(\lambda_T)/\mathrm{d}E}{\mathrm{d}\Delta D_{\mathrm{ref}}(\lambda_{\mathrm{ref}})/\mathrm{d}E}\right)_{\lim E_{\lambda_0}\to 0}, \quad (2)$$

where E is the exciting flash energy at λ_0, ΔD are absorbances of $^3C_{60}$ at λ_T and triplet benzophenone at λ_{ref}, respectively, and both solution concentrations are adjusted for equal and low absorption at λ_0. For this purpose, a Q-switched frequency-doubled ruby laser ($\lambda_0 = 347$ nm) was used, as described [12]. Measurements were made at $\lambda_T = 750$ nm and

[#1] To avoid errors arising from the sharply peaked absorption of triplet TET [18], all measurements at λ_2 were made in sequence, at common monochromator settings and slit widths.

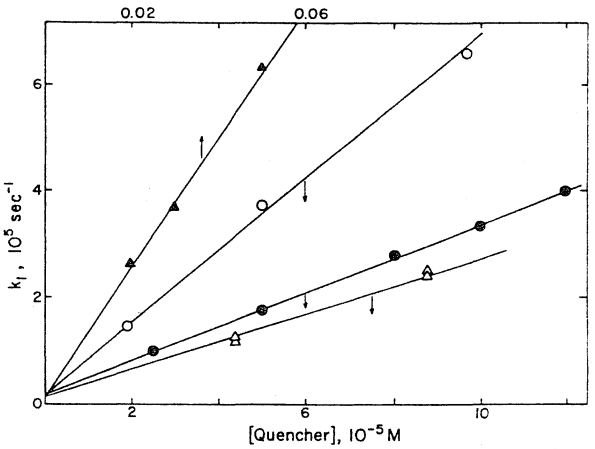

Fig. 1. Determination of quenching rate constants; variation of pseudo-first-order triplet decay constant with quencher concentration C_{60} (5×10^{-5} M) with: TET in toluene (○); TTA in benzonitrile (●); H_2Q in benzonitrile (▲); all $^3C_{60}$ data at 750 nm. ZnTPP with TET in toluene, at 470 nm (△).

$\lambda_{ref}=530$ nm; $\epsilon_{ref}=7220$ M^{-1} cm^{-1} [20].

3. Results and discussion

3.1. Triplet spectrum

Fig. 2 gives the difference spectrum, $\Delta\epsilon_\lambda=(\epsilon_T-\epsilon_g)_\lambda$ for $^3C_{60}$ in benzonitrile solution. The strong peak at 750 nm with shoulder at 680 and lesser bands at 510 and 400 nm are in good agreement with the difference spectra (ΔD_λ) obtained by others [21–24]. In establishing the extinction coefficient scale of fig. 2, rate constants for energy transfer in toluene from triplet C_{60} or ZnTPP to TET were 6.8×10^9 and 2.7×10^9 M^{-1} s^{-1} respectively (fig. 1). The difference may perhaps indicate a larger orientation restriction for transfer from the flat molecule. Measurements at $\lambda_2=465$ or 470 nm gave for $^3C_{60}$ $\epsilon_{750}=15800$ and 16300 M^{-1} cm^{-1}, respectively (eq. (1)). From the spread in ΔD ratios in several experiments, we take $\epsilon_{750}=16100\pm700$ M^{-1} cm^{-1} (fig. 2). This value falls substantially above the range 6000–9000 M^{-1} cm^{-1} given earlier [24].

3.2. Triplet decay kinetics

$^3C_{60}$ decayed by mixed first- and second-order kinetics, according to the well-known rate law: $-d\Delta D_\lambda/dt=k_1\Delta D_\lambda+(k_2/\Delta\epsilon)_\lambda\Delta D_\lambda$ [25]. The constants k_1 and $(k_2/\Delta\epsilon)_\lambda$ in toluene and benzonitrile were evaluated by an appropriate computer program and fitted the observed profiles very well. Representative values of k, listed in table 1, are reasonably constant across the spectrum and with $\Delta\epsilon_\lambda$ taken from fig. 2, k_2 are close to diffusion-controlled. In connection with this, we note that the ratio of the average k_2 in benzonitrile to that in toluene, $1.8/3.8=0.47$, is comparable to the inverse ratio of the corresponding solvent viscosities, $0.55/1.24=0.44$ [26].

3.3. Triplet yield

Fig. 3 gives results for determination of ϕ_T. The limiting slopes are in the ratio 0.1330/0.064, and taking $\epsilon_{750}=16100$, we obtain $\phi_T=0.93\pm0.07$, in excellent agreement with the value found by singlet oxygen sensitization [3]. It is gratifying also that our value of the product $\phi_T\epsilon_{750}=15000$ is in precise agreement with the result obtained by Ebbesen et al., using a similar method and slightly different λ_0 [21].

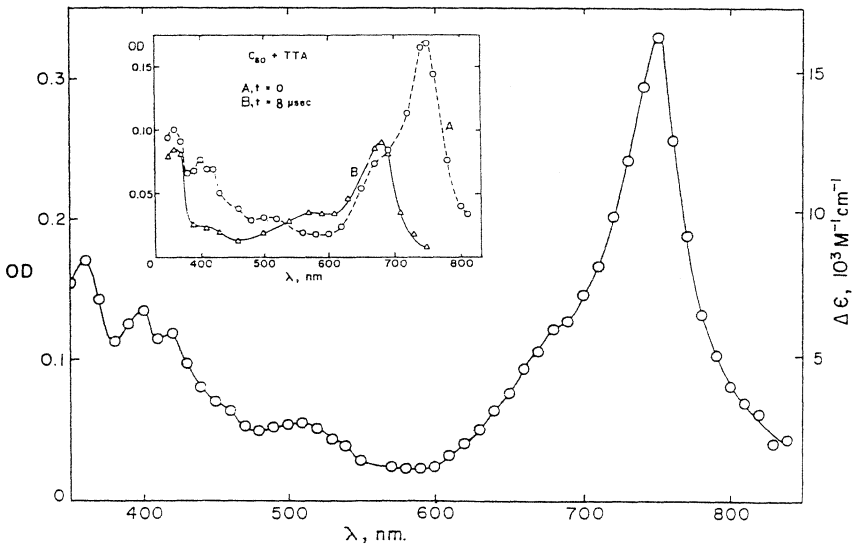

Fig. 2. Differential absorption spectrum ($\Delta\epsilon_\lambda$) of $^3C_{60}$ in benzonitrile (○); extinction coefficient scale is relative to ^{3}ZnTPP (see text). Insert: transient spectra of C_{60} (5×10^{-5} M) and TTA (10^{-4} M) in benzonitrile immediately ($^3C_{60}$ (A)) and 8 μs (radicals (B)) after flash.

Table 1
Decay kinetics of $^3C_{60}$

Solvent	λ (nm)	k_1 (10^4 s^{-1})	$(k_2/\Delta\epsilon)_\lambda$ (10^5 cm^{-1} s^{-1})	$\Delta\epsilon_\lambda$ (10^4 M^{-1} cm^{-1})	k_2 (10^9 M^{-1} s^{-1})
toluene	750	1.9	2.3	1.61	3.7
	680	1.3	6.3	0.60	3.8
	505	1.2	13.4	0.26	3.5
	400	1.6	6.6	0.66	4.4
benzonitrile	750	1.6	1.1	1.61	1.7
	680	1.5	2.7	0.60	1.6
	505	0.9	7.8	0.26	2.0
	400	1.1	3.0	0.66	2.0

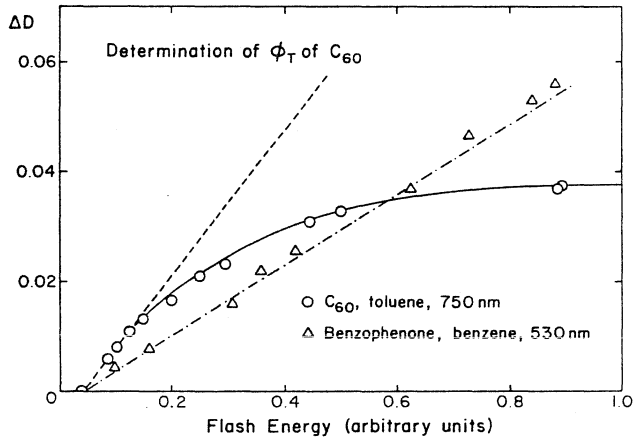

Fig. 3. Determination of ϕ_T of $^3C_{60}$ in toluene by "limiting slope" method, relative to benzophenone in benzene. Absorbance at 347 nm = 0.10.

However, further comment on the curves of fig. 3 is required.

It is expected that the $^3C_{60}$ absorbance (ground-state concentration $\approx 10^{-5}$ M; $\phi_T \approx 1$) will tend to saturation at much lower excitation flux than that of triplet benzophenone ($\approx 10^{-3}$ M), as is observed. While it is tempting to assign this to total ground-state depletion, the value of ϵ_{750} obtained from this assumption is far less than that given by energy transfer. The same effect, though much less pronounced, was also observed in attempted total ground-state conversion using the dye laser at 555 nm excitation. Thus, as has been noted [7,21] there is indication that at high excitation flux (multi-photon absorption) or high photon energy, new deactivation pathways become available for C_{60}. This effect does not appear in the limit of low flash energies (fig. 3) nor in our strongly quenched solutions where shortened triplet lifetime limits biphotonic processes [27].

3.4. Reaction with tri-p-tolylamine

3.4.1. Quenching rates and transient spectra

Addition of TTA to C_{60} solutions shortens the lifetime of the triplet at 750 nm and leads to further long-lived transients in benzonitrile, but not in toluene. The rate constants for quenching $^3C_{60}$ by TTA are $(3.5 \pm 0.3) \times 10^9$ M^{-1} s^{-1} in benzonitrile and $(8.5 \pm 0.8) \times 10^7$ M^{-1} s^{-1} in toluene (fig. 1). The polar solvent favors the charge-transfer intermediate and separation of ionic products.

Fig. 2 (insert) shows the difference spectra observed immediately after, and 8 μsec after, flashing C_{60}+TTA in benzonitrile (A and B, respectively). Spectrum B, obtained after complete disappearances of $^3C_{60}$, exhibits a prominent peak at 680 nm, which grows in at a rate matching that of triplet decay (fig. 4, insert) and which clearly corresponds to the known cation radical, TTA^+ [28]. The decay of spectrum B also follows excellent second-order kinetics (see below). We therefore assign this absorption to both TTA^+ and the C_{60}^- anion radical. Moreover, we take $\Delta\epsilon_{680} \approx \epsilon_{680}$ for TTA^+, since at this wavelength there is no ground-state correction, and any absorption by C_{60}^- is certainly very much less than that of the cation radical.

Fig. 4 gives spectrum B in more detail, including the absorption of TTA^+ itself, obtained by treating TTA with $SbCl_5$ in benzonitrile. The extinction coefficient scale of fig. 4, 26200 ± 200 M^{-1} cm^{-1} at 680

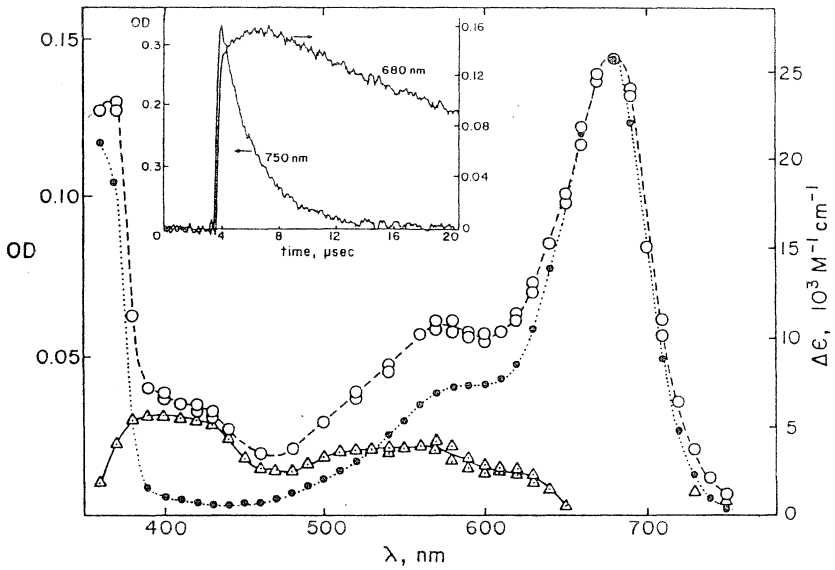

Fig. 4. C_{60} (5×10^{-5} M) + TTA (10^{-4} M) in benzonitrile: resolution of flash spectrum, ΔD_R (○) into TTA^+ (●) and C_{60}^- (△) absorptions; extinction coefficient scale based on ϵ_{680} of TTA^+. Insert: flash transient-time profiles; decay at 750 nm ($^3C_{60}$) and growing-in at 680 nm (TTA^+).

nm, is based on our measurement of TTA^+ and closely concordant literature values [28]. The residual absorption at shorter wavelengths ((△) in fig. 4) is then assigned to $\Delta\epsilon = \epsilon_{C_{60}^-} - \epsilon_{C_{60}}$. This difference spectrum shows broad bands around 520 and 420 nm, in general agreement with the results of Greaney and Gorun [29], and particularly of Kamat [30] [#2]. Other studies of C_{60}^- spectra show no structure in the visible [31,32].

3.4.2. Radical yields and recombination rates

Quantum yields are given by $\phi_R = (\Delta D_R/\Delta D_T)_\lambda \times (\Delta\epsilon_T/\Delta\epsilon_R)_\lambda f$, where ΔD_T is the initial triplet absorbance, ΔD_R is the total product absorbance, corrected for radical decay during its formation [13], and f is a correction factor for triplet which escapes reaction (< 10%), as estimated from quenched and initial unquenched lifetimes. Measurements of $(\Delta D_R/\Delta D_T)_\lambda$ were made at wavelengths corresponding to the absorption of TTA^+ essentially alone (680 nm), to that mainly of C_{60}^- (415 nm) and of both combined (500 nm). Quantum yields obtained with values of $\Delta\epsilon_T$ and total $\Delta\epsilon_R = \Delta\epsilon_{C_{60}^-} + \epsilon_{TTA^+}$ taken from figs. 2 and 4, are summarized in table 2, which gives average values of ϕ_R (± 10%) at each wavelength. From excellent linear plots of ΔD_λ^{-1} versus time (fig. 5), with slope $= k_{rec}/\Delta\epsilon_{R,\lambda}$, we obtain the radical recombination rate constants ($k_{rec} = (9.5\pm0.1)\times10^9$ M^{-1} s^{-1}) listed in table 2. The constancy, within experimental error, of both ϕ_r and k_{rec} at the several wavelengths validates the procedure and interpretation of fig. 4. We estimate conservatively that the values of $\Delta\epsilon$ in fig. 4 and table 2 are correct to better than ± 20%.

Table 2
C_{60} + TTA in benzonitrile: extinction coefficients (10^3 M^{-1} cm^{-1}), radical quantum yields and recombination rate constants (10^9 M^{-1} cm^{-1})

λ	$\Delta\epsilon_T$	ϵ_{TTA^+}	$\Delta\epsilon_{C_{60}^-}$	ϕ_R	k_{rec}
750	16.1	0.5			
680	6.0	26.2	–	0.31	10.1–8.3
500	2.6	2.1	3.2	0.30	9.2
415	5.8	0.80	5.5	0.33	10.0
400	6.6				

[#2] Applying the data of table 2 to the C_{60}^- spectrum given by Kamat indicates a small, uncertain $\Delta\epsilon_{680}$ of about 1000 M^{-1} cm^{-1}, which has been neglected in fig. 4. Correcting for this would raise $\Delta\epsilon$ of C_{60}^- and k_{rec} in table 2 by about 5%, and decrease ϕ_R to the same extent.

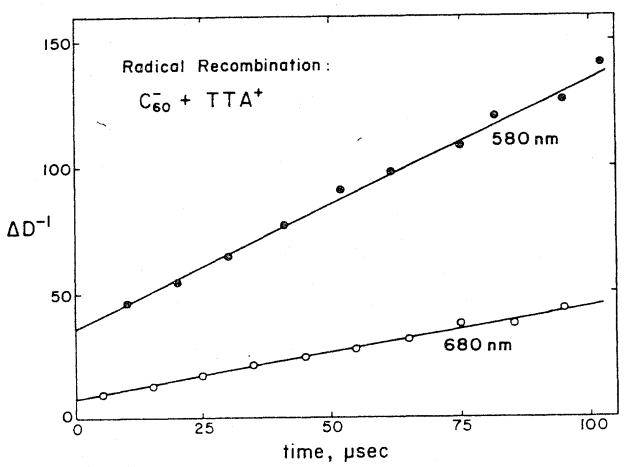

Fig. 5. Second-order radical recombination: ΔD_R^{-1} at 680 nm (○) and 580 nm (●) versus time; C_{60} (5×10^{-5} M) + TTA (10^{-4} M) in benzonitrile.

3.5. Reaction with hydroquinone: quenching rate and transient spectra

H_2Q quenches $^3C_{60}$ in benzonitrile with rate constant $(1.2\pm0.1)\times10^7$ M^{-1} s^{-1} (fig. 1), producing the long-lived transient spectrum shown in fig. 6. The peak at 415 nm corresponds to the absorption of the neutral radical, HQ$^\cdot$ [33]. (The cation radical, H_2Q^+ is a very strong acid with $pK_a \approx -0.8$ [34], and loses a proton immediately.) The HQ$^\cdot$ radical has $\epsilon_{415}=4300$ M^{-1} cm^{-1} [33] but does not absorb beyond 450 nm. This enables us again to check the spectral data by comparing yields based on the combined radical absorption at 415 nm ($\Delta\epsilon_R=4300+5500$ M^{-1} cm^{-1}) with those obtained only from C_{60}^- absorption at longer wavelengths. Measurements of $(\Delta D_R/\Delta D_T)_\lambda$ at 415 and 500 nm (fig. 6, insert) gave $\phi_R=0.44\pm0.04$ and 0.48 ± 0.04, respectively. The agreement further validates the extinction coefficients given here.

Decay of the product absorption following H_2Q reduction did not follow simple second-order kinetics, possibly because of competing HQ$^\cdot$ dimerization and dismutation reactions [35].

3.6. Remarks on rates and yields

For reduction of $^3C_{60}$ by TTA, ΔG^* is about -8.3 kcal/mol [#3]. The observed reaction rate, 3.5×10^9

[#3] This is based on E_T of $^3C_{60}=36$ kcal/mol [17], E^0_{red} of $C_{60}=-0.42$ V versus SCE [4,9], E^0_{ox} of TTA = 0.86 V versus SCE in benzonitrile (from our cyclic voltammetric measurement in acetonitrile (0.77 V), corrected to benzonitrile [9], and estimated transfer distance ≈ 7 Å.

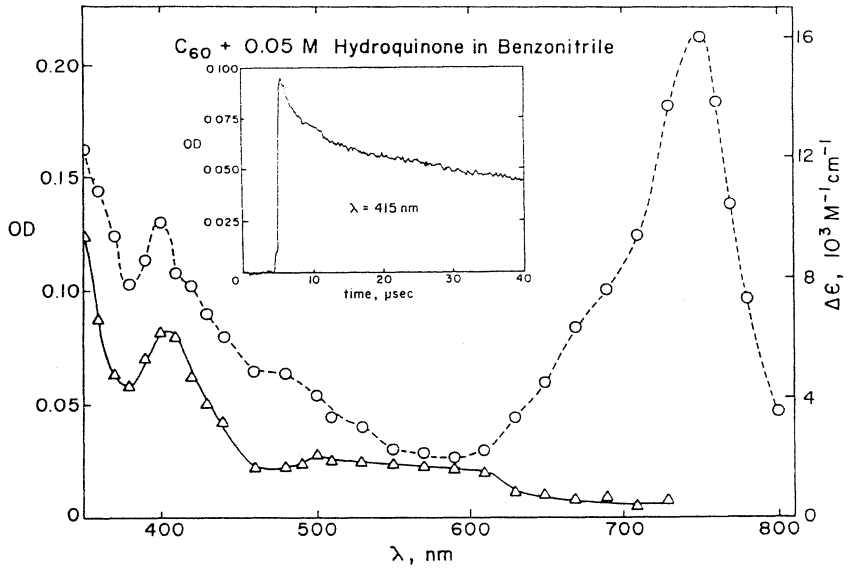

Fig. 6. C_{60} (5×10^{-5} M) + H_2Q (0.05 M) in benzonitrile ((○) $^3C_{60}$) and 8 μs ((△) $^3C_{60}$ + HQ$^\cdot$) after flash. Insert: flash transient-time profile, 415 nm.

M^{-1} cm^{-1} is in close accord with rates found for related reductants and similar ΔG^* values [9]. The quite appreciable radical yield in benzonitrile, despite the extremely high bulk recombination rate, is clearly attributable to the triplet origin of the radicals and the spin-relaxation condition for back transfer. In this connection, the fullerenes are evidently unique in that intra-molecular proton hyperfine interactions are not available to implement spin dephasing [36,37]. In addition, the rather small Onsager radius of benzonitrile, $r=21$ Å, also favors high escape yields [38]. The high value of k_{rec} is of interest also with regard to the recombination process itself. If we assume that this corresponds to a pure diffusion-controlled interaction of oppositely charged ions with uncorrelated spins, and in highly dilute solution, we may apply the Debye expression [39]:

$$k_{rec} = \frac{8RT}{3000\eta} \frac{b/r}{\exp(b/r) - 1},$$

where $b = z_D z_A e^2/DkT$. Setting $k_{rec} = 9.5 \times 10^9$ M^{-1} s^{-1}, with $D=26$ for benzonitrile, give $r=16$ Å for the transfer distance, a result well beyond contact.

Further results of quenching rate and product yield measurements of $^3C_{60}$ reactions, using parameters established here, will appear elsewhere.

Acknowledgement

We appreciate support of this research by the US Department of Energy, Division of Chemical Sciences, Office of Basic Energy Sciences (Grant No. FG02-89ER14072).

References

[1] H.W. Kroto, J.R. Heath, S.C. O'Brien, R.F. Curl and R.E. Smalley, Nature 318 (1985) 162.
[2] R.E. Haufler, J. Conceicao, L.P.F. Chibante, Y. Chai, N.E. Byrne, S.Flanagan, M.M. Haley, S.C. O'Brien, C. Pan, Z. Xiao, W.E. Billups, M.A. Ciufolini, R.H. Hauge, J.L. Margrave, L.J. Wilson, R.F. Curl and R.E. Smalley, J. Phys. Chem. 94 (1990) 8634.
[3] J.W. Arbogast, A.P. Darmanyan, C.S. Foote, Y. Rubin, F.N. Diederich, M.M. Alvarez, S.J. Anz and R.L. Whetten, J. Phys. Chem. 95 (1991) 11.
[4] D. Dubois, K.M. Kadish, S. Flanagan, R.E. Haufler, L.P.F. Chibante and L.J. Wilson, J. Am. Chem. Soc. 113 (1991) 4364.
[5] P.M. Allemand, A. Koch, F. Wudl, Y. Rubin, F. Diederich, M.M. Alvarez, S.J. Anz and R.L. Whetten, J. Am. Chem. Soc. 113 (1991) 1050.
[6] P.J. Krusic, E. Wasserman, B.A. Parkinson, B. Malone, E.R. Holler, P.N. Keizer, J.R. Morton and K.F. Preston, J. Am. Chem. Soc. 113 (1991) 6274.
[7] Y. Wang, J. Phys. Chem. 96 (1992) 764.
[8] R.J. Sension, A.Z. Szarka, G.R. Smith and R.M. Hochstrasser, Chem. Phys. Letters 185 (1991) 179.
[9] J.W. Arbogast, C.S. Foote and M. Kao, J. Am. Chem. Soc. 114 (1992) 2273.
[10] H. Ajie, M.M. Alvarez, S.A. Anz, R.D. Beck, F. Diederich, K. Fostiropoulos, D.R. Huffman, W. Krätschmer, Y. Rubin, K.E. Schriver, D. Sensharma and R.L. Whetten, J. Phys. Chem. 94 (1990) 8630.
[11] R.I. Walter, J. Am. Chem. Soc. 77 (1955) 5999.
[12] L.J. Andrews, A. Deroulede and H. Linschitz, J. Phys. Chem. 82 (1978) 2304.
[13] L.J. Andrews, J.M. Levy and H. Linschitz, J. Photochem. 6 (1976/77) 355.
[14] R. Bensasson and E.J. Land, Trans. Faraday Soc. 67 (1971) 1904.
[15] L. Pekkarinen and H. Linschitz, J. Am. Chem. Soc. 82 (1960) 2407.
[16] S.P. McGlynn, T. Azumi and M. Kasha, J. Chem. Phys. 40 (1964) 507.
[17] R.R. Hung and J.J. Grabowski, J. Phys. Chem. 95 (1991) 6073.
[18] D.J. Quimby and F.R. Longo, J. Am. Chem. Soc. 97 (1975) 5111.
[19] G. Porter and M. Windsor, Proc. Roy. Soc. A 245 (1958) 238.
[20] J.K. Hurley, N. Sinai and H. Linschitz, Photochem. Photobiol. 38 (1983) 9.
[21] T.W. Ebbesen, K. Tanigaki and S. Kuroshima, Chem. Phys. Letters 181 (1991) 501.
[22] R.J. Sension, C.M. Phillips, A.Z. Szarka, W.J. Romanow, A.R. McGhie, J.P. McCauley Jr., A.B. Smith III and R.M. Hochstrasser, J. Phys. Chem. 95 (1991) 6075.
[23] M. Terazima, N. Hirota, H. Shinohara and Y. Saito, J. Phys. Chem. 95 (1991) 9080.
[24] Y. Kajii, T. Nakagawa, S. Suzuki, Y. Achiba, K. Obi and K. Shibuya, Chem. Phys. Letters 181 (1991) 100.
[25] H. Linschitz and K. Sarkanen, J. Am. Chem. Soc. 80 (1958) 4826.
[26] International critical tables, Vol. VII, p. 218.
[27] L.W. Tutt and A. Kost, Nature 365 (1992) 225.
[28] I.R. Gould, D. Ege, J.E. Moser and S. Farid, J. Am. Chem. Soc. 112 (1990) 4290.
[29] M.A. Greaney and S.M. Gorun, J. Phys. Chem. 95 (1991) 7142.
[30] P.V. Kamat, J. Am. Chem. Soc. 113 (1991) 9705.
[31] T. Kato, T. Kodama, T. Shida, T. Nakagawa, Y. Matsui, S. Suzuki, H. Shiromaru, K. Yamauchi and Y. Achiba, Chem. Phys. Letters 180 (1991) 446.

[32] Z. Gasyna, L. Andrews and P.N. Schatz, J. Phys. Chem. 96 (1992) 1525.
[33] K.B. Patel and R.L. Willson, J. Chem. Soc. Faraday Trans. I (1973) 814.
[34] W.T. Dixon and D. Murphy, J. Chem. Soc. Faraday Trans. II 72 (1976) 1221.
[35] B.R. Eggins and J.Q. Chambers, Chem. Commun. (1969) 232.
[36] B.Brocklehurst, Chem. Phys. Letters 28 (1974) 357.
[37] A. Schulten and K. Schulten, J. Chem. Phys. 66 (1977) 4616.
[38] D. Mauzerall and S.G. Ballard, Ann. Rev. Phys. Chem. 33 (1982) 377.
[39] P. Debye, Trans. Electrochem. Soc. 82 (1942) 265.

9. Melléklet

ONE-ELECTRON REDUCTION OF TRIPLET C_{60} BY ORGANIC DONORS AND SIMPLE ANIONS: KINETICS AND RADICAL YIELDS

L. Biczók[†] and H. Linschitz
Department of Chemistry, Brandeis University, Waltham, MA 02254-9110
and
A. Treinin
Department of Physical Chemistry and the Farkas Center of Light Induced Processes, Hebrew University, Jerusalem, Israel

ABSTRACT

Rates and bulk radical yields are given for the interaction of triplet C_{60} with a series of hydroquinones and triphenylamines, and with tetrabutylammonium thiocyanate and nitrite in benzonitrile solution. Kinetic effects of added base or acid indicate that electron-transfer to $^3C_{60}$ by hydroquinone is coupled to proton-transfer to an ambient acceptor. The dependence of radical yield on anion identity and concentration is similar to that observed with other types of organic triplets, and is interpreted similarly in terms of anion-specific spin-orbit coupling in the reaction intermediates.

The remarkable ability of C_{60} to bind electrons, as established by its ground state electrochemistry (1-4) is manifest even more strongly in its excited states, where photoreduction is a characteristic mode of reaction (5-9). In this regard, we have previously described flash photolysis measurements of rates and bulk radical yields in quenching of $^3C_{60}$ by tritolylamine and hydroquinone, in toluene and benzonitrile solution (9). We now report further studies of reductions by a series of substituted triphenylamines, hydroquinones and related compounds. The relative dependence of rates on the free enthalpy of the excited state reduction, and the effects of added acids or bases indicate that quenching by the hydroquinones involves a proton-coupled intermediate. We also extend our earlier studies of triplet-anion interactions to C_{60}, and establish that characteristics of these reactions previously demonstrated for triplet carbonyl compounds apply also to the $^3C_{60}$ case.

[†] On leave from the Central Research Institute for Chemistry, Hungarian Academy of Sciences, Budapest, Hungary.

EXPERIMENTAL

Materials

C_{60}(>99.9%) was obtained from the SES Research Co. Substituted triphenylamines were prepared and purified as described (10). Hydroquinones (from Aldrich) were recrystallized from ethanol and benzene. Durohydroquinone was prepared by reduction of duroquinone with $SnCl_2$ (11). Solvents (benzonitrile, acetonitrile, pyridine) and inorganic salts were reagent grade.

Procedure

Redox potentials referred to SCE were obtained from cyclic voltammograms (PAR, Model 362) in acetonitrile solution containing 0.2 M $LiClO_4$ and ferrocene as internal standard. One-electron cyclic voltammograms of the triphenylamines substituted by CH_3, F, Cl or Br were reversible, in agreement with their potentiometric behavior (12), but those of the remaining amines and all hydroquinones were irreversible. For these latter cases, oxidation potentials were taken to be 30 mV less positive than the observed anodic peaks.

Values of $\Delta G^{0\prime}$ for the charge-transfer excited state quenching reaction in benzonitrile were calculated from eq. [1] (13)

$$\Delta G^{0\prime} = 23.06\,[E_D^{OX}(D^+/D) + 0.09 - E_A^{RED}(A^-/A) - E_T] - e^2/\epsilon a \qquad [1]$$

in which E_D^{OX} is the donor oxidation potential in acetonitrile; + 0.09 the change in potential of ferrocene in passing from acetonitrile to benzonitrile; $E_A^{RED}(A^-/A)$ = -0.42 for C_{60} in benzonitrile (2, 8); E_T = 1.574 eV is the energy of $^3C_{60}$ (14); a, the initial radical separation, is taken to be 8Å; ϵ = 25.2 is the static dielectric constant of benzonitrile.

Flash photolysis measurements were made using a flashlamp-pumped tunable dye laser (excitation at 590 nm; 0.3 μs fwhm) and associated equipment (9). Extinction coefficients of $^3C_{60}$ and C_{60}^- anion radical have been determined earlier (9) and those of the several triphenylamine radicals, prepared by $SbCl_5$ oxidation of the parent amines in acetone or dichloromethane, were obtained directly from their spectra (15).

RESULTS AND DISCUSSION

Reduction of $^3C_{60}$ by Triphenylamines and Hydroquinones

Reaction Kinetics. Flashing solutions of C_{60} and organic donors typically gives rise to absorption transients showing short-lived (triplet) and long-lived (radical) components (Fig. 1). Quenching rate constants and radical yields from the triplet were derived as in earlier studies, from the initial triplet and total integrated radical absorbances (9,16). Table I summarizes these quantities, together with the corresponding redox potential data, values of $\Delta G^{0\prime}$ for the excited state reaction, and ΔG_B^0 for the back reaction to the ground state.

Fig. 2 shows the variation of log k_q with the calculated $\Delta G^{0\prime}$ for these donors. Two clearly different curves appear, with the rates for the hydroquinones falling below those of the amines and 1,2,4 trimethoxybenzene. This supports the view that the difference between the two groups is related to the mobile protons of the hydroquinones. Indeed, the ESR spectra (17) of the radical transients establish unequivocally that the quenching of $^3C_{60}$ by hydroquinone itself leads, as suggested previously (9), to the neutral radical HQ· and not to the strongly acidic H_2Q^+ radical (18).

Table II gives the rates of quenching of $^3C_{60}$ by hydroquinone, in benzonitrile with added pyridine or trifluoroacetic acid. The rate is very sensitive to base, increasing 10-fold at pyridine concentration of 0.01 M in benzonitrile, and decreasing upon addition of trifluoroacetic acid (TFA).

In view of the lack of information regarding the detailed nature of the polarographic oxidation reaction of the hydroquinones, and the uncertainty in their oxidation potentials, the calculated $\Delta G^{0\prime}$ values for these systems in Table I and the corresponding plot in Fig. 2 must be considered to be simply formal representations of the experimental procedure and data. It is, of course, evident that the overall thermodynamic potential for the oxidation of hydroquinone to HQ· must involve a proton-transfer reaction (18), which relates also to the observed polarographic irreversibility. However, the dependence of the quenching rate on the presence of bases in the solvent is quite unambiguous, and requires that some type of proton-transfer process be coupled to the observed electron-transfer reaction. Several mechanisms may be proposed for this. These include electron transfer directly coordinated with proton transfer within a hydrogen-bonded hydroquinone-base complex, or an initial proton transfer equilibrium followed by quenching by the hydroquinone anion. Further studies are now in progress to test these, and other, hypotheses.

Table I. Electron-Transfer Quenching of Triplet C_{60} in Benzonitrile

	k_q 10^7 M^{-1} s^{-1}	E_D^{ox} V vs. SCE	$-\Delta G^{0\prime}$ eV	$-\Delta G_B^0$ eV	Φ_R [a]
Hydroquinones					
1. tetramethyl-	220	0.75	0.38	1.19	0.39
2. trimethyl-	200	0.78	0.35	1.22	0.37
3. 2,3-dimethyl-	86	0.85	0.28	1.29	0.38
4. methyl-	11	0.89	0.24	1.33	0.43
5. hydroquinone	1.2	0.94	0.19	1.38	0.44
Amines					
6. tri-p-tolyl-	350	0.77	0.36	1.21	0.32
7. 3-methoxydiphenyl-	155	0.88	0.25	1.32	0.36
8. triphenyl-	145	0.92	0.21	1.36	0.36
9. tri-p-fluorophenyl-	50	1.00	0.13	1.44	0.34
10. tri-p-chlorophenyl-	2.4	1.09	0.04	1.53	0.28
11. tri-p-bromophenyl-	1.7	1.10	0.03	1.54	0.28
12. Triphenylphosphine	17	0.98	0.15	1.42	0
13. 1,2,4-trimethoxy benzene	6	1.12	0.01	1.56	--

[a] ϕ_R is radical yield from the triplet.

Estimation of Marcus Parameters. The availability of authentic $\Delta G^{0\prime}$ values for the triphenylamine systems permits the determination of Marcus rate parameters for the corresponding electron-transfer reactions in Fig. 2. We take

$$k_q = A \exp(-\Delta G^{\ddagger}/RT) \qquad [2]$$

Table II. Effect of Base and Acid on Quenching of $^3C_{60}$ by Hydroquinone in Benzonitrile

$[H_2Q]$, M	[Pyridine], M	[TFA], M	k_q, 10^8 M^{-1} s^{-1} [a]
0.002	0.01		1.4
0.001	0.05		5.2
0.0003	0.20		12.7
0.0001	0.60		23.1
0.01		0.05	0.08
0.1		0.50	0.015

[a] Derived from pseudo-first order decay constant $k = k_q[H_2Q] + k_o$, where $k_o \sim 4 \times 10^4$ s^{-1} is first order decay constant in absence of H_2Q.

---

and use the Agmon-Levine relation (19) between $\Delta G^{\ddagger}$ and the "intrinsic activation energy," $\Delta G^{\ddagger}(0)$:

$$\Delta G^{\ddagger} = \Delta G^{0\prime} + \frac{\Delta G^{\ddagger}(0)}{\ln 2} \ln[1 + \exp(-\Delta G^{0\prime} \ln 2/\Delta G^{\ddagger}(0))] \qquad [3]$$

The best non-linear least squares fit, including the triphenylphosphine and trimethoxybenzene points, and shown by the line in Fig. 2, is obtained with $A = (5 \pm 2) \times 10^{10}$ M^{-1} s^{-1}, and $\Delta G^{\ddagger}(0) = (0.20 \pm 0.03)$ eV. The classical Marcus reorganization energy is $\lambda = 4\Delta G^{\ddagger}(0)$ (19, 20, 21) or, in this case 0.8 ± 0.1 eV. This is quite close to the value $\lambda = 0.6 \pm 0.1$ eV, found in the quenching of tetraphenyl porphyrin dication by the same series of triphenylamines (15), but is much lower than the value proposed for reductions by other aryl amines in methylcyclohexane (22).

Radical Yields. These were evaluated as in our previous work. For the hydroquinones, yields are based on the extinction coefficients of $^3C_{60}$ and C_{60}^-, while for the amines, we use the extinctions of $^3C_{60}$ and the amine cation radicals (9, 15).

Table I shows that within each group of donors, the yields are remarkably constant, and essentially independent of the forward or back

reaction free enthalpies, over the rather restricted range covered (~0.3V). It appears that the yields for the hydroquinones are systematically slightly higher than for the triphenylamines. This may reflect either a systematic error (±10%) in $\Delta\epsilon$ of C_{60}^- or a real effect caused by a slower back reaction involving proton movement within the exciplex, competing with a relatively constant rate of radical cage escape.

We assign the relative constancy of yield to a fairly constant rate of spin inversion within the exciplex, which controls the back reaction to the singlet ground state. Supporting this view is the low radical yield ($\phi_R \sim 0$) found in the case of triphenyl phosphine, presumably associated with stronger spin-orbit coupling at the heavier phosphorous center.

Interaction of $^3C_{60}$ with Simple Anions

Background. Previous work (23, 24, 25) on the interaction of anions with triplets, mainly of carbonyl compounds and some dyes, has shown that the anions fall generally into two groups. Group I anions (X^- = halides, pseudohalides) quench triplets at low [X^-] without separation of radicals while at concentrations higher than that required for (effectively) total quenching, organic and $X_2^{\cdot-}$ radicals appear. For Group II anions (NO_2^-; SO_3^{2-}) quenching is accompanied by radical formation at all [X^-]. These differences are interpreted (23-25) in terms of different spin-orbit coupling of the inorganic component X·, within the reaction exciplex, $^3(M^{\cdot-}...X\cdot)$, according to the following somewhat simplified scheme:

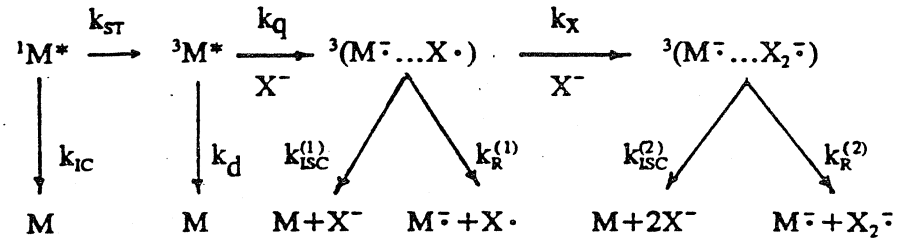

For Group I anions, the X· radical has non-zero orbital angular momentum and SO coupling may be strong, resulting in rapid spin relaxation of the exciplex ($k_{ISC}^{(1)} > k_R^{(1)}$), fast back-reaction within the exciplex to the singlet ground state and low radical yield. At high [X^-], this process is intercepted ($k_X[X^-] \geq k_{ISC}^{(1)}$) forming $X_2^{\cdot-}$ with low SO coupling, thus permitting radical separation from the second exciplex. In contrast, Group II anions form non-linear radicals with no overall orbital angular momentum, and relatively slow

spin relaxation, leading to radical separation already from the first exciplex. For Group II anions the limiting radical yield from the triplet, $\phi_R^\infty = k_R^{(1)}/(k_R^{(1)} + k_{ISC}^{(1)})$, is reached simply at salt concentrations at which the triplet is completely quenched. For long-lived triplets ($\tau > 10\mu s$) and efficient donors ($k_q > 10^7\ M^{-1}\ s^{-1}$), this is easily available. However, for Group I anions, ϕ_R^∞ can be attained only at such high salt concentrations that the short-lived primary triplet exciplex is itself completely trapped. The above reaction scheme leads to a linear double reciprocal plot for the Group I case:

$$\frac{1}{\phi_R} = \frac{1}{\theta}\left[1 + \frac{k_{ISC}^{(1)}}{k_X}\ \frac{1}{[X^-]}\right]$$

in which $\theta = k_R^{(2)}/(k_R^{(2)} + k_{ISC}^{(2)})$. The intercept and slope of this plot as $[X^-]^{-1} \rightarrow 0$ give ϕ_R^∞ and $k_{ISC}^{(1)}/k_X$.

Interaction of $^3C_{60}$ with Thiocyanate and Nitrite. The two anions, SCN^- and NO_2^- respectively exemplify typical Group I and Group II characteristics. Table III gives results of rate and yield measurements in benzonitrile solutions of C_{60} and the respective tetrabutylammonium salts. For thiocyanate, the radical yields are derived using the extinction coefficient of the well-known $(SCN)_2^{\cdot-}$ radical (26); for nitrite, there is no overlap in absorption of $NO_2\cdot$ and $C_{60}^{\cdot-}$ radicals, and the latter extinction is used directly.

Table III - Interaction of $^3C_{60}$ with $(Bu)_4NX$ Salts, in Benzonitrile.

X^-	k_q, $10^7\ M^{-1}\ s^{-1}$	ϕ_R^∞ [a]
SCN^-	3.1	1.0[b]
NO_2^-	240.	0.73[c]

[a] Quantum yield relative to the triplet.

[b] From Fig. 3.

[c] Extrapolated to complete triplet quenching.

For the nitrite salt, radicals appear concurrently with triplet quenching. At a nitrite concentration of 2 x 10^{-4} M, the triplet is 90% quenched and the radical yield is also 90% of its maximum value.

Fig. 3 shows in more detail the concentration dependence of ϕ_R in the case of Bu_4NSCN. The yield is essentially zero at $[X^-]$ below 10^{-3} M, but rises sharply at 10^{-2} M. This must be attributed to trapping of the primary exciplex since 90% of the triplet has already been quenched at this point. The further rise to $\phi_R^\infty = 1$ then occurs (Fig. 3) as the salt concentration is increased. The insert in Fig. 3 shows the corresponding linear plot of ϕ^{-1} vs $[SCN^-]^{-1}$, from which ϕ_R^∞ and $k_{ISC}^{(1)}/k_X$ are derived.

The sharp difference in behavior between the thiocyanate and nitrite salts clearly demonstrates that the characteristic grouping of the anions observed in their interactions with carbonyl and dye triplets is valid also for triplet C_{60}. More extensive data on other anions, solvent effects and kinetic interpretations will be given elsewhere.

ACKNOWLEDGEMENT

We appreciate support of this work by the Division of Chemical Sciences, Office of Basic Energy Sciences, U.S. Department of Energy (Grant No. FG02-89ER14072). The Farkas Center is supported by Bundenministerium für Forschung und Technologie and the Minerva Gesellschaft für die Forschung.

Keywords: Triplet C_{60}; Quenching Rates; Radicals; Quantum Yields; Reorganization Energy.

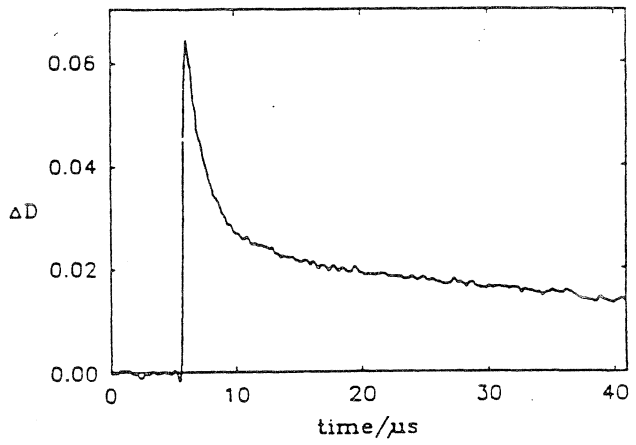

Fig. 1 - C_{60} triplet (short-lived) and radical anion (long-lived) transient absorption decay: C_{60} + 0.05 M hydroquinone in benzonitrile; λ = 460 nm.

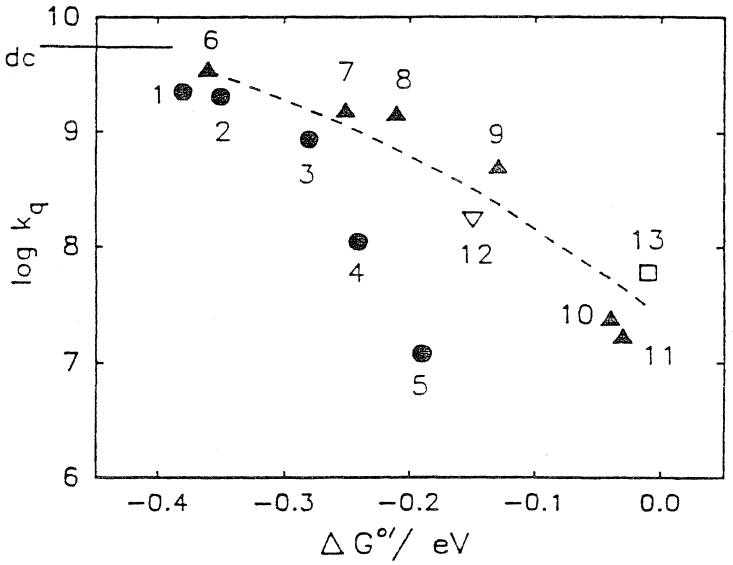

Fig. 2 - Kinetics of $^3C_{60}$ quenching by organic donors: log k_q vs $\Delta G^{0\prime}$. Numbering of points corresponds to Table I; dc = diffusion-controlled limit.

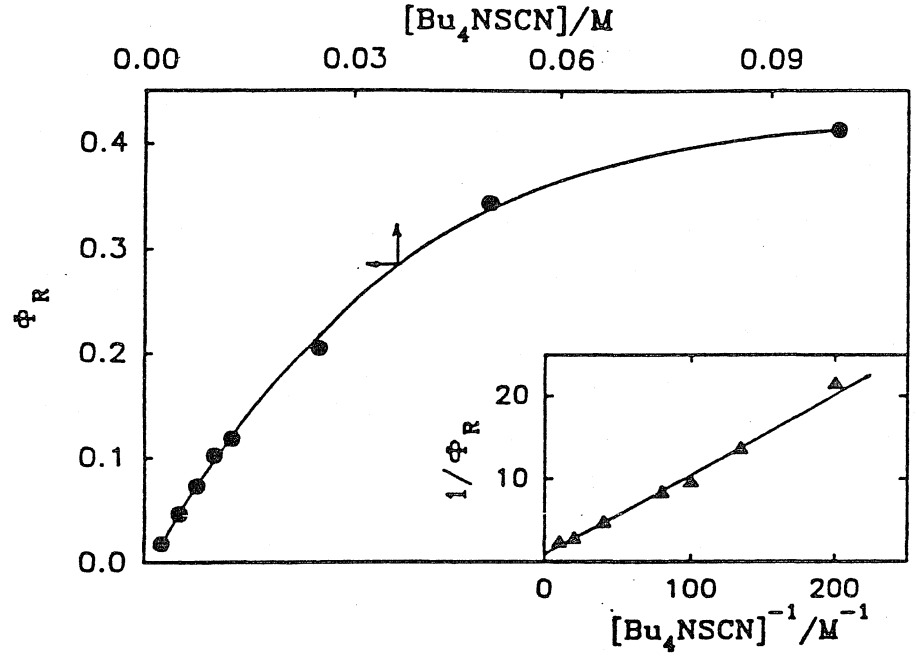

Fig. 3 - Interaction of $^3C_{60}$ with Bu_4NSCN in benzonitrile: ϕ_R vs salt concentration, upper scale; insert, ϕ_R^{-1} vs $[SCN^-]^{-1}$, giving $\phi_R^{\infty} \sim 1.0$.

REFERENCES

1. R. E. Haufler, J. Conceicau, L. P. F. Chibante, Y. Chai, N. E. Byrne, S. Flanagan, M. M. Haley, S. C. O'Brien, C. Pan, Z. Xiao, W. E. Billups, M. A. Ciufolini, R. H. Hauge, J. L. Margrave, L. J. Wilson, R. F. Curl and R. E. Smalley, J. Phys. Chem., **94**, 8634 (1990).

2. D. Dubois, K. M. Kadish, S. Flanagan, R. E. Haufler, L. P. F. Chibante and L. J. Wilson, J. Am. Chem. Soc., **113**, 4364 (1991).

3. P. M. Allemand, A. Koch, F. Wudl, Y. Rubin, F. Diederich, M. M. Alvarez, S. J. Anz and R. L. Whetten, J. Am. Chem. Soc., **113**, 1050 (1991).

4. M. A. Greaney and S. M. Gorun, J. Phys. Chem., **95**, 7142 (1991).

5. P. J. Krusic, E. Wasserman, B. A. Parkinson, B. Malone, E. R. Holler, P. N. Keizer, J. R. Morton and K. F. Preston, J. Am. Chem. Soc., **113**, 6274 (1991).

6. Y. Wang, J. Phys. Chem., **96**, 764 (1992).

7. R. J. Sension, A. Z. Szarka, J. R. Smith and R. M. Hochstrasser, Chem. Phys. Lett., **185**, 179 (1991).

8. J. W. Arbogast, C. S. Foote and M. Kao, J. Am. Chem. Soc., **114**, 2277 (1992).

9. L. Biczók, H. Linschitz and R. I. Walter, Chem. Phys. Lett., **195**, 339 (1992); **221**, 188 (1994).

10. R. I. Walter, J. Am. Chem. Soc., **77**, 5999 (1955); T. N. Baker, W. P. Doherty, Jr., W. S. Kelley, W. Newmeyer, J. E. Rogers, Jr., R. E. Spalding and R. I. Walter, J. Org. Chem., **30**, 3714 (1965). We thank Prof. Walter for kindly providing these compounds to us.

11. H. O. Huisman Rec. Chim. Pays Bas, **69**, 1133 (1950); Houben-Weyl, Methoden der Organischer Chemie, Band VI/IC, Georg Thieme Verlag, Stuttgart, p. 567.

12. L. Hagopian, G. Kohler and R. I. Walter, J. Phys. Chem., 71, 2290 (1967).

13. D. Rehm and A. Weller, Israel J. Chem., 8, 259 (1970).

14. Y. Zeng, L. Biczók and H. Linschitz, J. Phys. Chem., 96, 5237 (1992).

15. L. Biczók, H. Linschitz and R. I. Walter, Res. Chem. Intermed., in press (1994).

16. L. J. Andrews, J. M. Levy and H. Linschitz, J. Photochem., 6, 355 (1976/77).

17. C. A. Stern, P. R. Levstein, H. v. Willigen, H. Linschitz and L. Biczók,, Chem. Phys. Lett., 204, 23 (1993).

18. F. G. Bordwell and J. P. Cheng, J. Am. Chem. Soc., 113, 1736 (1991).

19. N. Agmon and R. D. Levine, Chem. Phys. Lett., 52, 197 (1977).

20. F. Scandola and V. Balzani, J. Am. Chem. Soc., 101, 6140 (1979).

21. L. Eberson, Adv. Phys. Org. Chem., 18, 79 (1982).

22. J. V. Caspar and Y. Wang, Chem. Phys. Lett., 218, 221 (1994).

23. A. Treinin, I. Loeff, J. K. Hurley and H. Linschitz, Chem. Phys. Lett., 95, 333 (1983).

24. I. Loeff, A. Treinin and H. Linschitz, J. Phys. Chem., 88, 4931 (1984).

25. J. K. Hurley, H. Linschitz and A. Treinin, J. Phys. Chem., 92, 5151 (1988).

26. G. L. Hug, Optical Spectra of Non-Metallic Inorganic Transient Species in Aqueous Solution; NSRDS-NBS 69, p. 56, 1981.

10. Melléklet

FT-EPR study of triplet state C_{60}. Spin dynamics and electron transfer quenching

Carlos A. Steren [1], Patricia R. Levstein [2], Hans van Willigen
Department of Chemistry, University of Massachusetts at Boston, Boston, MA 02125, USA

Henry Linschitz and Laszlo Biczok [3]
Department of Chemistry, Brandeis University, Waltham, MA 02254, USA

Received 21 December 1992

A FT-EPR study was made of paramagnetic species formed by pulsed-laser excitation of C_{60} in fluid solution. Earlier findings that photoexcitation of C_{60} in fluid solution gives rise to an EPR signal with narrow linewidth were confirmed. The lifetime of the signal corresponds to that of the C_{60} triplet as measured by flash photolysis. In the presence of donors, the rate of signal decay is increased and matches the growing in of EPR signals from oxidized donors. The time dependence of the FT-EPR spectra gives values for electron transfer rate constants which agree with those derived from flash photolysis measurements on the same systems. Based on these findings, we assign the narrow line signal to the triplet of C_{60}. The time evolution of the FT-EPR signal establishes that the triplets are born with less spin polarization than the thermal equilibrium value. As a result, signal growth is controlled by spin–lattice relaxation.

1. Introduction

The photoexcited triplet state of C_{60} has been the subject of a number of publications [1–15]. Several have been concerned with magnetic resonance studies of paramagnetic species generated by photoexcitation of C_{60} [2,9,10,14,15]. The EPR spectrum of $^3C_{60}^*$ randomly oriented in frozen solution is characterized by zero-field splitting parameters D and E of 0.0114 ($\approx$12.2 mT) and 0.00069 cm^{-1} ($\approx$0.74 mT), respectively [2,9].

Closs and co-workers [10] observed a narrow transient EPR signal (linewidth 0.014 mT over the temperature range from 300 to 200 K) upon UV irradiation of a solution of C_{60} in liquid methylcyclohexane. The signal was attributed to $^3C_{60}^*$. The assignment requires rotational averaging of the dipole–dipole interaction between the unpaired electrons in the triplet with a correlation time $\tau_c \approx 10^{-12}$ s even at 200 K. By contrast, $\tau_c \approx 10^{-11}$ s for ground state C_{60} in tetrachloroethane at room temperature [16]. Closs et al. [10] proposed that the unusually short correlation time stems from fast reorientation of the principal axes of the zfs tensor relative to the molecular axes because of a dynamic Jahn–Teller effect.

The same signal was apparently also observed in an FT-EPR study by Rübsam et al. [14], but this group assigned it to the C_{60}^- anion radical. Levanon et al. [15] report a transient EPR signal from photoexcited C_{60} in toluene near its freezing point similar to that found for solutions in methylcyclohexane [10]. However, these authors attribute the narrow peak to an unpaired electron delocalized on an aggregate of C_{60} [15].

Flash photolysis studies [7,11] have established that $^3C_{60}^*$ can undergo reversible electron transfer reactions with donor molecules. In benzonitrile, electron transfer quenching of the triplet with tri-*p*-to-

[1] On leave from Physics Department, FIQ, UNL, 3000 Santa Fe, Argentina.
[2] Present address: INTEC, Guëmes 3450, 3000 Santa Fe, Argentina.
[3] On leave from Central Research Institute for Chemistry, Hungarian Academy of Sciences, Pusztaszeri ut 59-67, Budapest II, Hungary.

lylamine (TTA) or hydroquinone (H_2Q) gives the free radicals C_{60}^- and TTA^+ or the neutral semiquinone radical $HQ^\cdot$ [11]. We now report a FT-EPR study of this quenching reaction by TTA and H_2Q. The study provides compelling evidence for the assignment of the narrow line signal to $^3C_{60}^*$. The high time resolution permits analysis of the spin dynamics of the triplets and the electron transfer kinetics [17,18].

2. Experimental

C_{60} purified by chromatography was obtained from SES Research and was used without further purification. Solvents (HPLC grade) were from Aldrich. TTA [19] was kindly provided by Professor R.I. Walter (University of Illinois/Chicago). H_2Q (Aldrich) was used as received. Solutions were degassed on a high-vacuum line by several freeze–pump–thaw cycles or by purging with argon.

FT-EPR spectra were recorded with a home-built spectrometer [20]. The nominal microwave pulsewidth used was 15 ns and the free induction decay (FID) was sampled, with quadrature detection, at 200 Msample/s. The measurements used a CYCLOPS phase-cycling routine; final spectra typically were the average of 2400 FIDs.

C_{60} was excited with the second harmonic (532 nm) of a Quanta Ray GCR12 Nd/YAG laser (up to 80 mJ/pulse, repetition rate 10 Hz). The time evolution of FT-EPR spectra was monitored by recording FIDs for a series of delay time (τ_d) settings between laser and microwave pulses. τ_d values ranged from 10 ns to 100 μs.

3. Results and discussion

Room temperature FT-EPR spectra from photoexcited C_{60} (0.1 to 0.5 mM) in benzonitrile, methylcyclohexane, and cyclohexane show a single, narrow absorption peak with $g=2.0012$ and 0.03 mT linewidth at half maximum ($T_2 \approx 0.5$ μs). The time dependence of signal intensity, determined with linear prediction–singular value decomposition (LP–SVD) analysis [21] of the FIDs given by a sample of C_{60} (1.4×10^{-4} M) in benzonitrile is displayed in fig. 1. The build-up kinetics is similar to that reported by Rübsam et al. [14]. For $\tau_d < 50$ ns signal

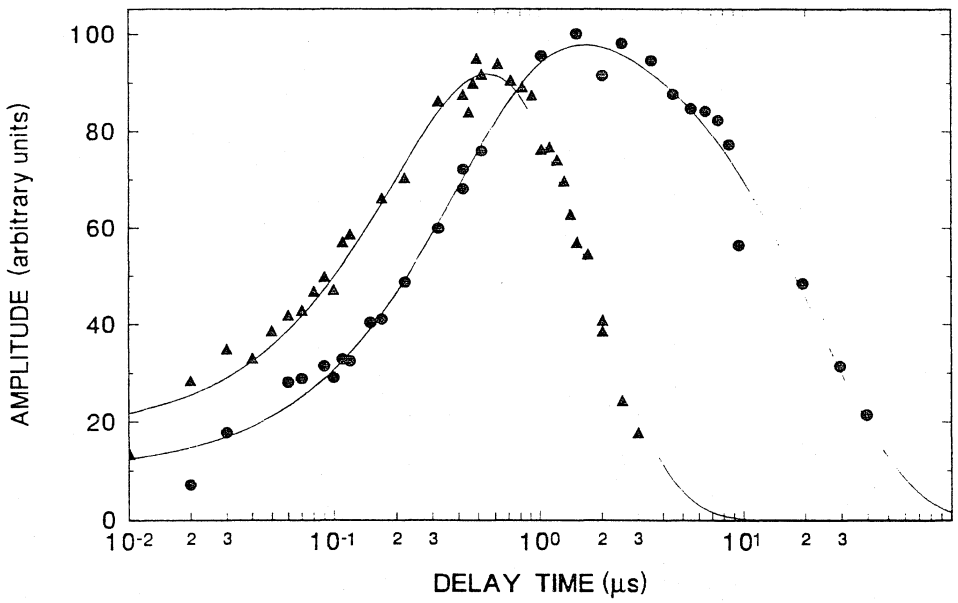

Fig. 1. Time evolution of the intensity of the FT-EPR signal generated by pulsed-laser excitation of a solution of C_{60} in benzonitrile at room temperature (●) with no TTA present and (▲) with [TTA] = 0.2 mM. The solid lines represent least-squares fits of the data to eq. (1). Note that the dependence of signal rise time on [TTA], apparent in the figure, results from overlapping growth and decay processes.

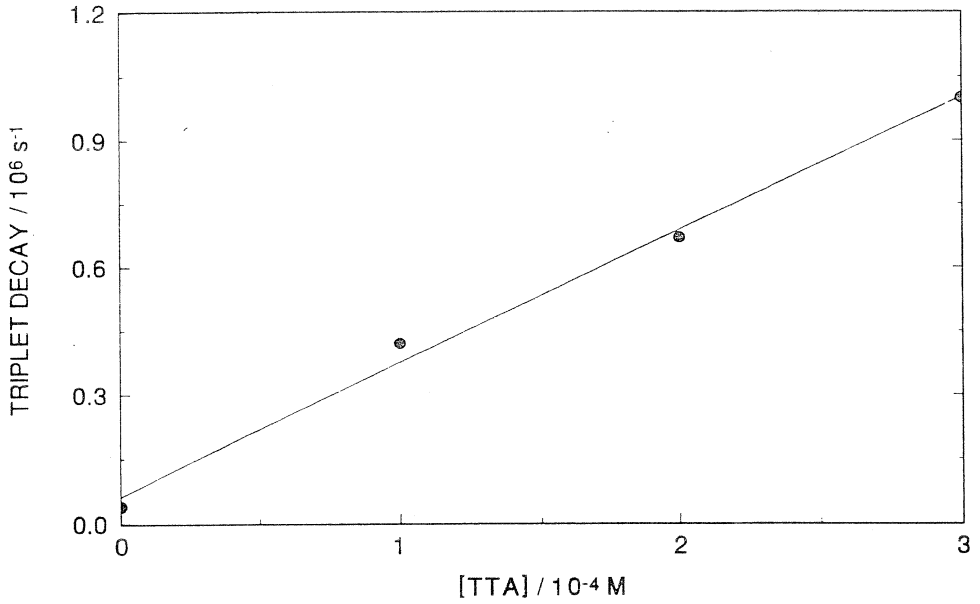

Fig. 2. [TTA] dependence of the rate of decay of the signal from photoexcited C_{60} in benzonitrile at room temperature.

growth is controlled by the instrument response time. Following this fast component, the intensity increases more slowly until it reaches a maximum around $\tau_d = 1$ μs. Signal decay is exponential with rate constant 4.0×10^4 s^{-1}.

As shown in fig. 1, addition of TTA increases the rate of decay of the photoinduced signal. The decay of the single-line signal is matched by the formation of a complex multi-line EPR signal that can be assigned to TTA^+ [22]. The dependence of decay rate of the single-line signal on TTA concentration is shown in fig. 2 and is represented by the equation

$$k_{obs} = \tau_T^{-1} + k_{et}[TTA] .$$

Here k_{obs} is the measured single-line decay rate, $\tau_T = 25$ μs is the lifetime of the species in the absence of quencher, and $k_{et} = 3.1 \times 10^9$ M^{-1} s^{-1} is the quenching rate constant.

Addition of H_2Q (1.0×10^{-2} M) to a solution of C_{60} in benzonitrile also increases the decay rate of the single peak, which is now accompanied by the appearance of the spectrum of the neutral semiquinone radical ($HQ^\bullet$). The spectrum obtained (cf. fig. 3) is characterized by the following hyperfine coupling constants: 0.59 (2H), 0.14 (1H), and 0.07 mT (2H); the g value is 2.0049. The unambiguous identification of the product radical $HQ^\bullet$, instead of the strongly acidic H_2Q^+ cation radical, confirms the assignment proposed earlier [11] which was based on the analysis of partially overlapping optical spectra of the transient species. Fig. 4 gives the delay time dependence of the intensity of a peak (marked with an arrow in fig. 3) in the central group of lines in the semiquinone radical spectrum. The peak initially is in emission and then turns into absorption as τ_d increases. This behavior is common to all lines found on the low-field (high-frequency) side of the signal from C_{60} (cf. fig. 3).

On the basis of linewidth and g values of the spectrum obtained from solutions of C_{60} alone, it is evident that we are seeing the signal reported previously by Closs et al. [10], Rübsam et al. [14], and Levanon et al. [15]. (It is noted that we could also detect the resonance with the direct-detection cw time-resolved EPR method employed by Closs and Levanon.) The lifetime of the species giving rise to this signal (25 μs) closely matches the lifetime of the triplet excited state of C_{60} (for $[C_{60}] \approx 0.1$–0.2 mM) determined with flash photolysis techniques [6]. (At the C_{60} concentration used in this study, the triplet lifetime is determined mainly by pseudo first-order quenching by ground state molecules [6] and no evidence is found for a second-order contribution [11].) Even so, the fact that it takes about a microsecond

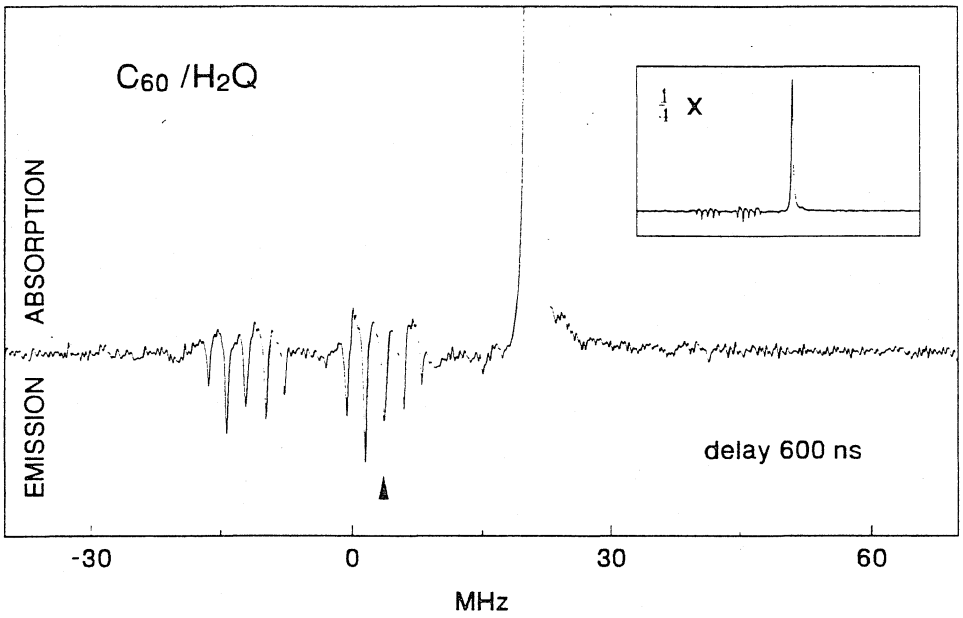

Fig. 3. FT-EPR spectrum generated by photoexcitation of C_{60} in the presence of H_2Q (0.01 M), solvent benzonitrile. The delay time between laser pulse and microwave pulse is 600 ns. The arrow marks the peak for which the time evolution of the intensity was analyzed (cf. fig. 4). The relative amplitudes of $^3C^*_{60}$ and HQ˙ signals are shown in the inset where the signal is attenuated by a factor of 4.

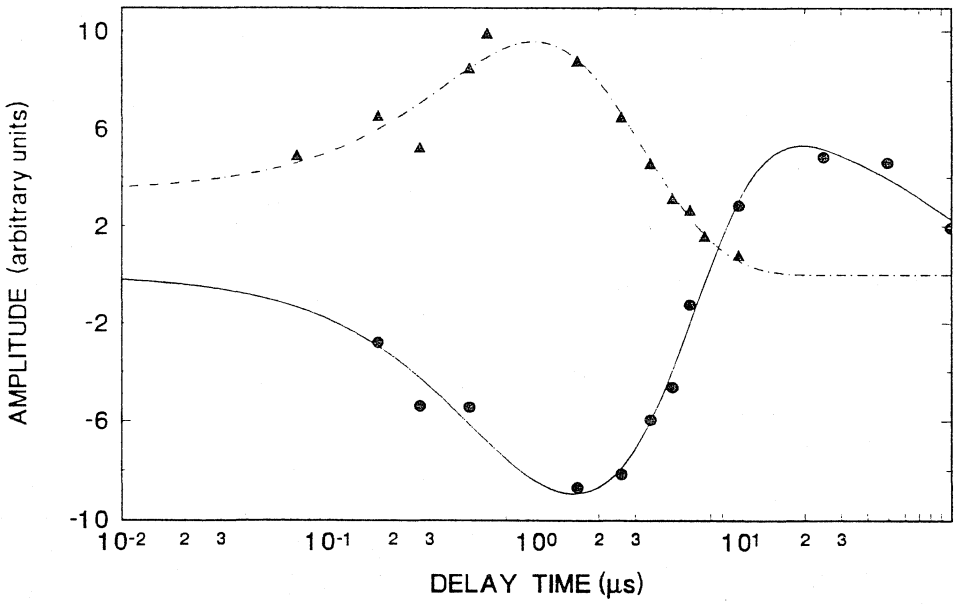

Fig. 4. Time dependence of the signal intensity of the peak (marked by the arrow in fig. 3) in the center of the spectrum from HQ formed by photoexcitation of C_{60} in the presence of H_2Q (0.01 M) (●), the solvent is benzonitrile. For comparison, the time dependence of the single-line signal from C_{60} is given also (▲). The dashed line represents a least-squares fit to the C^*_{60} data based on eq. (1). The solid line is a least-squares fit to the data from HQ˙ using the data analysis procedure outlined in ref. [23].

for the signal to reach its maximum amplitude appears to argue against its assignment to $^3C_{60}^*$. The rate of singlet–triplet intersystem crossing is 1.5×10^9 s^{-1} [3], so that the triplets are formed in a time which is an order of magnitude shorter than the instrument response time ($\approx$ 50 ns). This apparent conflict between signal rise time and rate of triplet formation can be resolved by taking into account that signal intensity is a function of spin state population difference. If the signal is assigned to C_{60} triplets, its growth must be due to the time evolution of the triplet spin state populations.

EPR spectra of $^3C_{60}^*$ in glassy matrices show enhanced absorption and emission peaks [2,9,10,15]. This establishes that intersystem crossing is spin state selective. However, if the short rotational correlation time limit ($\omega_0\tau_r \ll 1$) applies [10,14], the spin selectivity is not expected to generate significant spin polarization in $^3C_{60}^*$ in *fluid solution* [24,25]. Hence, signal growth can be due to relaxation of the triplets to thermal equilibrium. In that case, the time evolution of signal intensity can be represented by the equation

$$I(t) = C\{(n^0 - n_B^0)\exp[-(k_T + k_d)t] + n_B^0 \exp(-k_d t)\}, \quad (1)$$

which is based on the following premises. (1) The signal generated by photoexcitation of C_{60} is due to triplets formed instantaneously (that is, within the duration of the laser pulse). (2) At $t=0$ the difference in population of the triplet spin states n^0 is less than that obtained at thermal equilibrium n_B^0. C is a proportionality factor relating population difference to signal strength. k_T is the inverse of the triplet spin–lattice relaxation time T_1^T, and k_d is the rate of triplet decay. As noted earlier, the initial signal growth ($\tau_d < 50$ ns) reflects the instrument response time and the model does not take this into account. The data analysis does not consider data points for $\tau_d < 50$ ns.

The solid lines in fig. 1 represent least-squares fits of the experimental data to eq. (1). The analysis of the signal development of the sample with no TTA gives $T_1^T = 0.42$ μs, $k_d = 4.0\times10^4$ s^{-1}, and $n^0/n_B^0 = 0.15$. The value for the spin–lattice relaxation time differs considerably from the value of 8 μs derived from a least-squares analysis of the time dependence of the cw time-resolved EPR signal [10]. However, the latter value is from a measurement performed at 203 K [10] so that a direct comparison of the results is not possible. Our result is in good agreement with the value, also obtained from FT EPR measurements, quoted by Rübsam et al. [14]. Under the condition $\tau_c = 10^{-11}$ s (the short correlation time limit) $T_1^T = T_2$ [26]. Our finding that the signal rise time closely matches the decay time (T_2) of the FID, therefore, is consistent with the proposal that signal growth reflects relaxation of the triplet spin system. Work in progress is concerned with the temperature dependence of the spin–lattice relaxation time of C_{60} [27].

Support for the assignment of the single-line spectrum to $^3C_{60}^*$ is provided by the quenching data. A flash photolysis study of electron transfer quenching of C_{60} triplets by TTA in benzonitrile gives $k_{et} = 3.5\times10^9$ M^{-1} s^{-1} [11], in excellent agreement with the quenching rate constant $k_{et} = 3.1\times10^9$ M^{-1} s^{-1} obtained in the present work. The decay of the peak attributed to triplet C_{60} is accompanied by the formation of TTA^+. The FT-EPR spectra do not show a contribution from the C_{60}^- radical whose optical spectrum is observed in flash photolysis studies of these systems [11]. The absence of an anion radical signal can be attributed to its short T_2 [28]. As expected, the linewidth of the signal from $^3C_{60}^*$ increases with TTA concentration due to the reduction in triplet lifetime. In principle, this can be used to determine the quenching rate constant [23]. However, the uncertainty in the measurement was too large for the linewidth data to give reliable results.

An analysis of the time evolution of the intensity of a center line in the spectrum of HQ$^\cdot$ based on a model described earlier [23] provides a satisfactory fit to the data (given by the solid line in fig. 4). The analysis takes into account the initial population distribution in the triplet precursor, the triplet spin–lattice relaxation time, radical-pair mechanism (ST_0) of chemically induced electron polarization [#1] (CIDEP) generated by the electron transfer process, and spin–lattice relaxation (T_1^R) of the semiquinone radical. The least-squares analysis gives a value of 0.39×10^6 s^{-1} for the pseudo first-order electron transfer rate constant. By comparison, the decay of

[#1] For a recent review see ref. [29].

the C_{60} triplet signal gives 0.35×10^{6} s^{-1}. A value of 3.0 μs is derived for the spin–lattice relaxation time of $HQ^{\cdot}$. There is satisfactory agreement between the electron transfer quenching rates derived from triplet and doublet radical signals, However, the values give a second-order rate constant of $\approx4\times10^{7}$ M^{-1} s^{-1}, which differs somewhat from the value of 1.2×10^{7} M^{-1} s^{-1} obtained from flash photolysis [11]. Further measurements will be required to verify the value of the rate constant of triplet quenching by H_2Q.

In conclusion, this study establishes that the signal first reported by Closs et al. [10] is indeed due to $^{3}C_{60}^{*}$. The spectra show that the triplets are born with $\approx$ 15% of the Boltzmann spin polarization. The spin–lattice relaxation time is consistent with a rotational correlation of about 10^{-11} s [24]. To our knowledge, this is the first time that the rate constant of photoinduced electron transfer has been determined by monitoring the EPR signals of both the excited state precursor and one of the doublet radical products. The observation of the triplet signal simplifies the analysis of the time dependence of FT-EPR spectra of electron transfer products which exhibit pronounced CIDEP effects. Also, it offers an opportunity to study electron transfer quenching in non-polar solvents where no separated redox products may be formed.

Acknowledgement

We thank Dr. Dinse of the Technische Hochschule in Darmstadt (Ge) for communicating results of his FT-EPR study of triplet state C_{60} prior to publication. Financial support for this work was provided by the Division of Chemical Sciences, Office of Basic Energy Sciences of the US Department of Energy (DE-FG02-84ER-13242 and DE-FG02-89ER-14072). PRL thanks the Antorchas Foundation for financial support.

References

[1] J.W. Arbogast, A.P. Darmanyan, C.S. Foote, Y. Rubin, F.N. Diederich, M.M. Alvarez, S.J. Anz and R.L. Whetten, J. Phys. Chem. 95 (1991) 11.
[2] M.R. Wasielewski, M.P. O'Neil, K.R. Lykke, M.J. Pellin and D.M. Gruen, J. Am. Chem. Soc. 113 (1991) 2774.
[3] R.J. Sension, C.M. Phillips, A.Z. Szarka, W.J. Romanow, A.R. McGhie, J.P. McCauley Jr., A.B. Smith III and R.M. Hochstrasser, J. Phys. Chem. 95 (1991) 6075.
[4] M. Terazima, N. Hirota, H. Shinohara and Y. Saito, J. Phys. Chem. 95 (1991) 9080.
[5] R. Sension, A.Z. Szarka, G.R. Smith and R.M. Hochstrasser, Chem. Phys. Letters 185 (1991) 179.
[6] N.M. Dimitrijević and P.V. Kamat, J. Phys. Chem. 96 (1992) 4811.
[7] J.W. Arbogast, C.S. Foote and M. Kao, J. Am. Chem. Soc. 114 (1992) 2277.
[8] T. Andersson, K. Nilsson, M. Sundahl, G. Westman and O. Wennerström, J. Chem. Soc. Chem. Commun. (1992) 604.
[9] P.A. Lane, L.S. Swanson, Q.-X. Ni, J. Shinar, J.P. Engel, T.J. Barton and L. Jones, Phys. Rev. Letters 68 (1992) 887.
[10] G.L. Closs, P. Gautam, D. Zhang, P.J. Krusic, S.A. Hill and E. Wasserman, J. Phys. Chem. 96 (1992) 5228.
[11] L. Biczok, H. Linschitz and R.I. Walter, Chem. Phys. Letters 195 (1992) 339.
[12] Y. Zeng, L. Biczok and H. Linschitz, J. Phys. Chem. 96 (1992) 5237.
[13] D.K. Palit, A.V. Sapre, J.P. Mittal and C.N.R. Rao, Chem. Phys. Letters 195 (1992) 1.
[14] M. Rübsam, K.P. Dinse, M. Plüschau, J. Fink, W. Krätschmer, K. Fostiropoulos and C. Taliani, J. Am. Chem. Soc. 114 (1992) 10059.
[15] H. Levanon, V. Meiklyar, A. Michaeli, S. Michaeli and A. Regev, J. Phys. Chem. 96 (1992) 6128.
[16] R.D. Johnson, D.S. Bethune and C.S. Yannoni, Accounts Chem. Res. 25 (1992) 169.
[17] T. Prisner, O. Dobbert, K.-P. Dinse and H. van Willigen, J. Am. Chem. Soc. 110 (1988) 1622.
[18] M.K. Bowman, M. Toporowicz, J.R. Norris, T.J. Michalski and A. Angerhofer, Israel J. Chem. 28 (1988) 215.
[19] R.I. Walter, J. Am. Chem. Soc. 77 (1955) 5999.
[20] P.R. Levstein and H. van Willigen, J. Chem. Phys. 95 (1991) 900.
[21] R. De Beer and D. van Ormondt, in: Advanced EPR: applications in biology and biochemistry, ed. A.J. Hoff (Elsevier, Amsterdam, 1989) ch. 4.
[22] E.T. Seo, R.F. Nelson, J.M. Fritsch, L.S. Marcoux, D.W. Leedy and R.N. Adams, J. Am. Chem. Soc. 88 (1966) 3498.
[23] M.H. Ebersole, P.R. Levstein and H. van Willigen, J. Phys. Chem. 96 (1992) 9311.
[24] P.W. Atkins and G.T. Evans, Mol. Phys. 27 (1974) 1633.
[25] F.J. Adrian, J. Chem. Phys. 61 (1974) 4875.
[26] A. Carrington and A.D. McLachlan, Introduction to magnetic resonance (Harper & Row, New York, 1967) ch. 11.
[27] K.P. Dinse, C.A. Steren and H. van Willigen, (1992), unpublished results.
[28] A.J. Schell-Sorokin, F. Mehran, G.R. Eaton, S.S. Eaton, A. Viehbeck, T.R. O'Toole and C.A. Brown, Chem. Phys. Letters 195 (1992) 225.
[29] K.A. McLauchlan, in: Advanced EPR: applications in biology and biochemistry, ed. A.J. Hoff (Elsevier, Amsterdam, 1989) ch. 10.

11. Melléklet

Reprinted from The Journal of Physical Chemistry, 1995, 99.

Concerted Electron and Proton Movement in Quenching of Triplet C_{60} and Tetracene Fluorescence by Hydrogen-Bonded Phenol–Base Pairs

László Biczók and Henry Linschitz*

Department of Chemistry, Brandeis University, Waltham, Massachusetts 02254-9110, and Central Research Institute for Chemistry, Hungarian Academy of Sciences, P.O. Box 17, 1525 Budapest, Hungary

Received: January 4, 1995[⊗]

The quenching of triplet C_{60} and tetracene fluorescence by phenols is strongly enhanced by added pyridines. Evidence that this is due to quenching by hydrogen-bonded phenol–base pairs is given by the close agreement between equilibrium constants for hydrogen-bond formation derived from kinetic measurements and from independent spectroscopic data. The effect is attributed to a trimolecular transition state in which electron transfer from the phenol to the excited molecule is concerted with proton movement from the incipient strongly acidic phenol cation radical to the hydrogen-bonded base.

Extensive studies over the past several decades have shown that electron transfer may be coupled with proton movement in several ways. Thus, in reduction of ketone triplets by amines or alkylbenzenes, proton movement is facilitated by initial electron transfer, and overall reaction consists of H atom transfer within a bimolecular charge-transfer complex.[1,2] In other instances, fluorescence quenching results from reversible associated electron and proton movement within an excited hydrogen-bonded D–A pair,[3] or complete electron transfer between components of a carboxylic acid dimer occurs via a hydrogen-bond "interface".[4] In these cases, electron and proton displacements, whether reversible or not, are *coordinated* and follow the same path between the same donor and acceptor species. We now present evidence for another type of coupling, in which electron transfer occurs from donor to acceptor, *concerted* with proton transfer from donor to another associated (hydrogen-bonded) base in a trimolecular reaction complex.

We have previously shown that the reduction of triplet C_{60} by hydroquinone resulted in the $C_{60}^{\bullet-}$ anion and neutral phenoxy radicals.[5] Formation of the latter species was confirmed by time-resolved ESR measurements.[6] We have also noted the increase and decrease in hydroquinone quenching rate caused by addition of bases and acids, respectively, which suggested concurrent electron and proton movements in the rate-controlling step.[7] To clarify the situation further, we have measured rates of quenching of $^3C_{60}$ and tetracene fluorescence in several phenol–base systems, together with hydrogen-bond equilibria between the same phenol–base pairs.

Results of flash experiments on C_{60} using methods described earlier[5–7] are shown in Figure 1, for the case of hydroquinone and various solvents and pyridines. Here "k" is the effective pseudo-first-order rate constant for triplet decay at given quencher concentration, and k_0 is the corresponding rate constant in the solvent–base mixture in absence of quencher. For the several phenols (Q) and pyridine bases (B), equilibrium constants for hydrogen-bonded pair formation, $K = [QB]/[Q][B]$, were evaluated from the observed red shift in phenol absorption, using the treatment of Mataga et al.[3b,c] We now take the effective pseudo-first-order triplet decay constant, k, to be

$$k = k_0 + k_Q[Q] + k_{QB}[QB] \qquad (1)$$

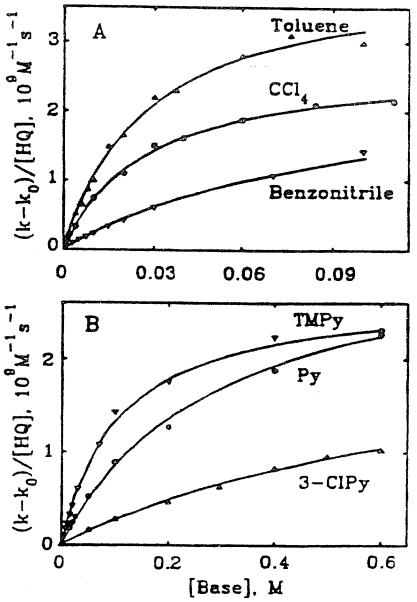

Figure 1. Effect of base concentration on pseudo-first-order decay rate of triplet C_{60}, quenched by hydroquinone. (A) Variation with solvent: toluene, CCl_4, benzonitrile; base = 2,4,6-trimethylpyridine (TMPy). (B) Variation with base: TMPy, Py, 3-Cl-Py; solvent = benzonitrile.

where the second and third right-hand terms represent contributions of free and hydrogen-bonded quenchers, respectively, and $[Q] + [QB] = [Q]_0$, the total quencher concentration. For the case that the total added base $[B]_0 \gg [Q]_0$, eq 1 then becomes

$$\frac{k - k_0}{[Q]_0} = \frac{k_Q}{1 + K[B]_0} + \frac{k_{QB}K[B]_0}{1 + K[B]_0} \qquad (2)$$

In the C_{60} studies, concentrations were adjusted so that the quenched lifetime ($\tau_Q \sim 1.0\ \mu s$) was much shorter than the unquenched value ($\tau_0 \sim 50\ \mu s$). The latter was only slightly affected by low concentrations of added pyridine components ($k_{py} \sim 10^5\ M^{-1}\ s^{-1}$, etc.),[8] and k_0 was taken to be essentially constant around $4 \times 10^4\ s^{-1}$. Values of k_Q for phenols in base-free solvents vary with their ease of oxidation. For example, in benzonitrile, k_Q ($M^{-1}\ s^{-1}$) is 2.2×10^9 for tetramethylhydroquinone ($E^0_{OX} = 0.75$V vs SCE) and falls to 1.2×10^7 for hydroquinone ($E^0_{OX} = 0.94$ V).[7] For *p*-methoxy- and 2,6-

[⊗] Abstract published in *Advance ACS Abstracts*, February 1, 1995.

0022-3654/95/2099-1843$09.00/0

TABLE 1: Summary of Kinetic Parameters

phenol	base	pK_a	solvent	k_{QB}, 10^9 M^{-1} s^{-1}	K, M^{-1} kinetic	K, M^{-1} spectroscopic
p-OH	TMPy[a]	7.43	toluene	4.1 ± 0.2	36 ± 3	43 ± 5
	TMPy	7.43	CCl_4	2.7 ± 0.2	37 ± 3	38 ± 3
	TMPy	7.43	benzonitrile	2.7 ± 0.1	9.5 ± 0.6	6 ± 3
	pyridine	5.25	benzonitrile	3.3 ± 0.4	3.4 ± 0.3	
	3-Cl-Py	2.84	benzonitrile	2.5 ± 0.4	1.2 ± 0.3	
p-CH_3O	TMPy	7.43	CCl_4	1.6 ± 0.1	86 ± 11	82 ± 5
2,6-diCH_3O	TMPy	7.43	CCl_4	3.1 ± 0.3	3.0 ± 0.5	2.0 ± 0.5

[a] TMPy = 2,4,6-trimethylpyridine.

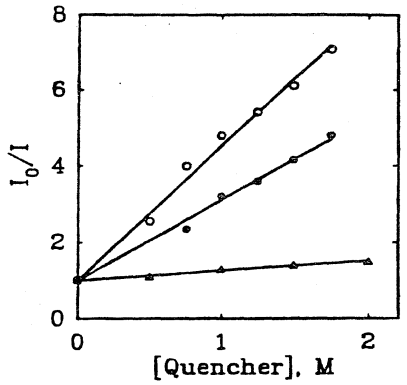

Figure 2. Stern–Volmer plots: base and isotope effects for tetracene fluorescence quenched by *p*-methoxyphenols. ▲, MeO–C_6H_4–OH in CH_2Cl_2; ○, MeO–C_6H_4–OH in 1:1 CH_2Cl_2/TMPy; ●, MeO–C_6H_4–OD in 1:1 CH_2Cl_2/TMPy.

dimethoxyphenol, no quenching at all is observed in CCl_4 in absence of added base ($k_Q < 10^4$). Thus, for these three latter phenols, the rate is dominated by the third term of eq 1. Nonlinear least-squares fit of eq 2 to the data, using points for which $[B]_0 \gg [Q]_0$, gives the curves of Figure 1 and corresponding best values of K and k_{QB}. Table 1 summarizes the kinetic and spectroscopic results.

We note first that, over a wide range, the equilibrium constants, K, obtained from the kinetic measurements (Figure 1) agree within experimental uncertainty with those derived from the phenol absorption spectra. This validates the assignment of "k_{QB}" to quenching by the hydrogen-bonded complex. In agreement with this, 1,2,4-trimethoxybenzene (E^0_{OX} = 1.12 V vs SCE) quenches $^3C_{60}$ in benzonitrile solution ($k_Q = 6 \times 10^7$ M^{-1} s^{-1}) but shows no effect of added pyridine. The magnitude of the base effect on the reaction rate and the relatively negligible quenching by the free phenols in Table 1 indicate that electron and proton movement from these donors is concerted in the phenol–base complex. Proton transfer from the very strongly acidic incipient phenol cation radical[9] evidently contributes not only to the overall driving force of the reaction but also to the structure and free energy of the transition state, which presumably involves proton displacement from the phenolic OH to the pyridine nitrogen. The quenching constants, k_{QB}, are quite insensitive to the strengths of the bases in Table 1, as measured by their aqueous pK_a values. We attribute this to the leveling effect resulting from the very high acidities of the phenol cation radicals, particularly as expressed in nonaqueous solvents.[9]

Similar effects of added bases on reaction rates are observed with singlet excited states. Figure 2 shows Stern–Volmer plots for the quenching of tetracene fluorescence by *p*-methoxyphenol in methylene chloride alone and in a 1:1 mixture with 2,4,6-trimethylpyridine (TMPy) of similar polarity.[10] Taking the singlet lifetime to be 6.4 ns,[11] the quenching rate constant (M^{-1} s^{-1}) increases from 4×10^7 to 5.5×10^8 on addition of the base. At the high quencher concentrations imposed by the short singlet lifetime, intermolecular hydrogen bonding may of course occur among the phenols themselves. Thus, the large rate increase in the presence of pyridine at concentrations at least 2-fold greater than the phenol clearly establishes the effect of relatively strong H-bond pairing. A marked isotope effect on replacement of OH by OD in *p*-methoxyphenol was found in the tetracene system (Figure 2) but not for the much faster $^3C_{60}$ reaction. In this latter case, the solvent (CCl_4) was saturated with H_2O or D_2O, respectively, to maintain isotopic compositions at low phenol concentrations.

The clear distinction drawn here between coordinated vs concerted electron–proton movements, in bimolecular vs trimolecular reaction complexes, respectively, becomes somewhat blurred in the interesting case where the loci of electron and proton displacements in a bimolecular reaction are distinct. This appears to occur, for example, in hydrogen transfer from ketyl radicals to ketones[12] or in a carotene–porphyrin–carboxyquinone triad.[13] Further studies are now in progress on the generality of these concerted proton-coupled electron transfer reactions, with regard to excited singlet or triplet substrates, various bases, and isotope effects. In this connection, it is interesting to note that the reduction of triplet fluorenone by 3-cyanophenol is *inhibited*, not assisted, by added TMPy. This presumably indicates competition between hydrogen bonding of the phenol directly to the ketone (leading to fast coordinated proton-coupled reduction) and bonding to the added base.

Acknowledgment. We much appreciate support of this work by the Division of Chemical Sciences, Office of Basic Energy Sciences, U.S. Department of Energy (Grant FG02-89ER14072, to Brandeis University).

References and Notes

(1) Cohen, S. G.; Parola, A.; Parsons, G. J. *Chem. Rev.* **1973**, *73*, 141.

(2) Wagner, P. J.; Truman, R. J.; Puchalski, A. E.; Wake, R. *J. Am. Chem. Soc.* **1986**, *108*, 7727.

(3) (a) Rehm, D.; Weller, A. *Isr. J. Chem.* **1970**, *8*, 259. (b) Miyasaka, H.; Tabata, A.; Ojima, S.; Ikeda, N.; Mataga, N. *J. Phys. Chem.* **1993**, *97*, 8222. (c) Mataga, N.; Tsuno, S. *Bull. Chem. Soc. Jpn.* **1957**, *30*, 368. (d) Tolbert, L. M.; Nesselroth, S. M. *J. Phys. Chem.* **1991**, *95*, 10331. (e) Herbich, J.; Waluk, J.; Thummel, R. P.; Hung, C. Y. *J. Photochem. Photobiol. A: Chem.* **1994**, *80*, 157.

(4) Turró, C.; Chang, C. K.; Leroi, G. E.; Cukier, R. I.; Nocera, D. G. *J. Am. Chem. Soc.* **1992**, *114*, 4013.

(5) Biczók, L.; Linschitz, H.; Walter, R. I. *Chem. Phys. Lett.* **1992**, *195*, 339; **1994**, *221*, 188.

(6) Steren, C. A.; Levstein, P. R.; van Willigen, H.; Linschitz, H.; Biczók, L. *Chem. Phys. Lett.* **1993**, *204*, 23.

(7) Biczók, L.; Linschitz, H.; Treinin, A. In *Fullerenes: Recent Advances in the Chemistry and Physics of Fullerenes and Related Materials*; Kadish, K. M., Ruoff, R. S., Eds.; The Electrochemical Society: Pennington, NJ; 1994; pp 909–920.

(8) Arbogast, J. W.; Foote, C. S.; Kao, M. *J. Am. Chem. Soc.* **1992**, *114*, 2277.

(9) (a) Bordwell, F. G.; Cheng, J. P. *J. Am. Chem. Soc.* **1991**, *113*, 1736. (b) Holton, D. M.; Murphy, D. J. *J. Chem. Soc., Faraday Trans. 2*

1979, *75*, 1637. (c) Land, E. J.; Porter, G.; Strachan, E. *Trans. Faraday Soc.* **1961**, *57*, 1885. (d) Nicholas, M.; Arnold, D. R. *Can. J. Chem.* **1982**, *60*, 2165.

(10) Kamlet, M. J.; Abboud, J. L.; Abraham, M. H.; Taft, R. W. *J. Org. Chem.* **1983**, *48*, 2877.

(11) Berlman, I. B. *Handbook of Flurescence Spectra of Aromatic Molecules*; Academic Press: New York, 1965; p 132.

(12) Naguib, Y. M. A.; Steel, C.; Cohen, S. G. *J. Phys. Chem.* **1988**, *92*, 6574.

(13) Moore, A. L.; Moore, T. A.; Gust, D.; Hung, S. C.; MacPherson, A. *Photochem. Photobiol.* **1994**, *59S*, 45S.

JP9500652

12. Melléklet

REDUCTION OF TRIPLET C_{60} BY HYDROGEN-BONDED NAPHTHOLS : CONCERTED ELECTRON AND PROTON MOVEMENT

by

Neeraj Gupta[a] , Henry Linschitz[a]* and László Biczók[b]

a) Department of Chemistry, Brandeis University, Waltham, MA, 02254, USA

b) Central Research Institute for Chemistry, Hungarian Academy of Science, 1025, Budapest, Hungary

Abstract

Hydrogen bonding equilibria, redox potentials and quenching of triplet C_{60} in naphthol solutions containing added pyridines are studied by absorption spectroscopy, nanosecond flash photolysis and cyclic-voltammetry. It is shown that the quenching reaction involves reduction of the triplet by a hydrogen bonded naphthol-pyridine pair, with formation of $C_{60}^{-\cdot}$, neutral naphthoxy radical and protonated base. Quenching rates increase with pyridine basicity, in parallel with decreased naphthol oxidation potential, and decrease with deuteration of the naphthol. It is concluded that electron and proton movement from the naphthol respectively to $^3C_{60}$ and to base is concerted. Bulk radical yield increases with pyridine basicity and solvent polarity.

---

* To whom correspondence should be addressed.

We have recently shown that the reductive quenching of triplet C_{60} by some phenols is enhanced by hydrogen bonding to pyridines[1]. This pairing permits proton transfer to participate directly in the redox reaction and thereby lowers the oxidation potential and increases the reducing power of the phenol. We now report in more detail a further example of this, the pyridine-assisted reduction of triplet C_{60} by 1-naphthol. Effects of solvent, pyridine basicity and deuteration are found which exemplify behavior typical of these systems. We conclude that such reactions involve a concerted movement of electron (from the phenol to triplet C_{60}) and proton (from the incipient phenol cation to the hydrogen-bonded pyridine).

It is appropriate to point out here some features which make triplet C_{60} a particularly useful substrate in flash photolysis studies of electron transfer processes. A full analysis and understanding of the reaction kinetics, including determination of both rate constants and product quantum yields, requires knowledge of the triplet state yield ($\Phi_T > 0.93$ [2]) and reversible redox potential (-0.44 V vs SCE in benzonitrile[3]), as well as the spectra and extinction coefficients of the triplet (750 nm, 16,100 ± 700 $cm^{-1}\ M^{-1}$ [2]) and corresponding anion radical (1080 nm, 18,300 ± 1100 $cm^{-1}\ M^{-1}$[4]; 555 nm, 3800 ± 500 $cm^{-1}\ M^{-1}$[2]). These main absorptions lie far in the red, thus providing a broad window for observation of other flash transients formed in excited state reactions. Similarly, the very broad absorption of C_{60} itself makes it convenient, with appropriate tunable sources, to choose excitation wavelengths which do not overlap the absorptions of added quenching reagents. Moreover, the almost ideal spherical shape and well established radius of C_{60} permits use, without approximation, of the simple expression for solvation energy given by electron-transfer theories[5]. Finally, with regards to the particular situation considered here, no complications arise from possible protonation of the C_{60} redox couple, since both C_{60} and $C_{60}^{-\cdot}$ anion radical are weak bases[6].

Experimental :

C_{60} (99.9%) was obtained from SES Research Inc. Solvents (HPLC grade), pyridine (Py) and 2,4,6-trimethylpyridine (TMP) were the best available grades from Aldrich, (>99%) and were used as received. 3-Chloropyridine (Cl-Py) was freshly redistilled. 1-naphthol and 2-naphthol were purified by sublimation before use.

Kinetic measurements were carried out on nitrogen purged solutions using a flashlamp pumped dye (rhodamine-590) laser, and associated gear as described[2]. Pseudo-first order rate constants, k, were derived from the decay of triplet C_{60} absorption at 750 nm which matched the growing-in of the $C_{60}^{-\cdot}$ anion radical at 1080 nm.

Since quencher concentrations were adjusted so that the triplet lifetimes in blank experiments without naphthol were very much longer (~ 50 μsec) than the quenched lifetimes (~1.0 - 2.0 μsec) and since essentially no quenching by naphthol (N) was observed in absence of added base, (B), we consider k to be due only to naphthol hydrogen-bonded to pyridine (NB). We thus have

$$k = k_{NB}[NB] \qquad (1) \quad \text{and}$$

$$K = \frac{[NB]}{[N][B]} \qquad (2)$$

For the case where total added pyridine, B_o, much exceeds total naphthol, N_o, corresponding to the conditions in these experiments :

$$[B]_o >> [N]_o = [N] + [NB],$$

we then have

$$\frac{k}{[N]_o} = \frac{k_{NB}K[B]_o}{1+K[B]_o} \qquad (3)$$

Fitting this expression to the observed kinetic data then permits determination of both the equilibrium constant, K, and the corresponding bimolecular quenching rate constant, k_{NB}.

Independent values of K were also obtained spectrophotometrically from the red shift in naphthol UV absorption with added pyridine. In this treatment, the function $(1-A_o/A)/[B]_o$ is plotted against A_o/A where A and A_o are the absorbances at given λ, respectively with and without pyridine, at total concentration $[B]_o$. Extrapolation of the ordinate to zero abscissa gives $-K$[7].

Polarographic oxidations of 1-naphthol were carried out in benzonitrile - $TBAPF_6$ solution using a platinum working electrode and ferrocene as internal reference.

Results and Discussion :

Figure 1 shows transient spectra, produced by flashing C_{60} - 2-naphthol - TMP solution in PhCN. The peaks at 750, 1080 and 353 and 475 nm correspond respectively to $^3C_{60}$, $C_{60}^{-\cdot}$ and the *neutral* 2-naphthoxy radical[8]. In other related reactions, which permit clear separation and identification of the transient peaks (the 7,8-benzoquinoline-assisted quenching of $^3C_{60}$ by 4-methoxyphenol), we have shown that protonated base is formed at the same time as the phenoxy radical[9]. We may thus write the overall quenching reaction as:

$$^3C_{60} + NOH\text{---}B \longrightarrow C_{60}^{-\cdot} + NO^{\cdot} + BH^{+}$$

Figure 2 gives representative data, showing the dependence of $k/[N_o]$ on total added base, $[B_o]$, for 1-naphthol with various pyridines and solvents. The plotted curves correspond to equation (3), using the best fitting values of k_{NB} and K. These

are listed in Table 1.

Figure 3 illustrates the spectrophotometric determination of K's for the H-bonding of 1-naphthol in similar solvent systems. These results are also given in Table 1.

The values of the K's increase with the basicity of the pyridine, as indicated by their pKa's in water (TMP = 7.43, Py = 5.25, Cl-Py = 2.84)[10], and decrease with solvent polarity. Thus in CH_2Cl_2, K (M^{-1}) is 30 for pyridine and 62 for TMP, and for pyridine, K increases from 5 in benzonitrile to 82 in CCl_4. These trends and values are in very good agreement with extensive observations in the literature[11]. It is especially noteworthy that, with the exception of pyridine in CCl_4 (see below) we find agreement between kinetically and spectroscopically measured equilibrium constants. *This establishes that the actual quenching species is the hydrogen-bonded naphthol-pyridine pair.*

This finding is closely related to the polarographic results given in Table 1. It is seen that the oxidation potential of 1-naphthol in benzonitrile decreases with addition of the pyridines. The limiting values listed in the Table are reached at quite low concentration of added base[9]. Moreover this decrease is more marked with increasing basic strength of the pyridine. Notwithstanding the irreversible nature of the electrode reaction, the general trend of increasing reducing power of the naphthol with basic strength of the pyridine is evident and is reflected also in the values of k_{NB}. We interpret this effect to indicate a proton-linked oxidation process, in which hydrogen bonding of the naphthol to an immediately available acceptor facilitates proton transfer from the increasingly acidic naphthol cation radical. This contributes to the overall free energy decrease in the electron transfer reaction and makes rapid quenching possible.

It is a fortunate circumstance that the first reduction potential of triplet C_{60} is

such that the decreased oxidation potential of 1-naphthol caused by hydrogen-bonding permits the observation of sharp changes in quenching rate.

Polarity Effect : We gain further insight into the factors controlling the quenching rate by comparing the effects of TMP and pyridine in CCl_4 solution, as shown in figure 4. Whereas the rate versus base concentration function for TMP is a convex curve, corresponding to the form of equation (3), the function for pyridine is concave and cannot conform to equation (3) (figure 4 and figure 4 insert). We believe that the added factor, exposed in the situation, is the local polarity of the medium, which is particularly sensitive to additives in the case of non-polar CCl_4. Thus, polar pyridine ($E_T(30)$ = 40.5[12]), clustering[13] around naphthol, introduces a local polar environment, favoring charge transfer. This added effect is less manifest for the much stronger base but less polar TMP ($E_T(30)$ = 36.4[12]), for which we find the convex curve. However, even here, the value of K, derived from figure 4, does not correspond with the spectroscopic value as well as in other cases of Table 1.

Isotope Effect : A direct indication of proton movement in the rate-controlling step is the observation of a deuterium effect. In the present case, such effect is expected to be small, since the bimolecular quenching rates are high, and approach diffusion control (Table 1). Nevertheless, we do find a significant effect, on the relatively slow rate constant, in the case of naphthol in presence of Cl-Py in CH_2Cl_2 as shown in figure 5. Here an excess of CH_3OD is added to the solution for exchange with the naphthol OH. Comparison with the blank containing CH_3OH leads to k_H/k_D = 1.26.

Radical Yields : Since radical decay is relatively slow, quantum yields of separated radicals are directly given by flash measurements of initial triplet and final $C_{60}^{-\cdot}$ peaks as shown in figure 1, together with the corresponding extinction coefficients listed above. Table 2 gives such yields for TMP-enhanced quenching in polar (PhCN) and non-polar (CCl_4) solution. In benzonitrile, the yield is rather remarkably high,

presumably in consequence of fast concerted proton movement to the strongly basic TMP combined with stabilization of charged products by solvation. In CCl_4 the yield measured at constant triplet quenching increases strongly with TMP concentration. This is in agreement with the 'clustering' effect proposed above in connection with figure 4. In this case segregation of TMP around the naphthol may contribute to stabilization of the protonated base, and thereby favor cage escape of the several products in competition with fast back reaction.

Conclusions :

Quenching of triplet C_{60} by naphthol solutions containing pyridine bases involves electron transfer to the triplet and proton transfer to the base. The quenching species in such systems is the hydrogen-bonded naphthol-pyridine pair. A significant deuterium isotope effect on the rate indicates that electron and proton movement to separate loci is concerted.

References:

1. Biczok, L. and Linschitz, H., *J. Phy. Chem.*, 1991, **99**, 1843.
2. Biczok, L.; Linschitz, H and Walter, R.I. *Chem. Phys. Lett.*, 1992, **195**, 339 ; 1994, **221**, 188.
3. Dubois, D.; Moninot, G.; Kutner, W.; Jones, M.T. and Kadish, K.M.; *J. Phy. Chem.*, 1992, **96**, 7137.
4. Steren, C.A.; van Willigen, H.; Biczok, L.; Gupta, N. and Linschitz, H.; *J. Phy. Chem.*, 1996, **100**, 8920.
5. (a) Marcus, R.A. and Sutin, N.; *Biochim. Biophys. Acta*, 1985, **811**, 265. (b) Ulstrup, J.; *Charge Transfer Processes in Condensed Media*, Springer-Verlog, Berlin, 1979.
6. (a) Cliffel, D.E. and Bard A.J; *J. Phy. Chem.*, 1994, **98**, 8140. (b) Niyazymbetov, M.E.; Evans, D.H.; Lerke, S.A.; Cahill, P.A. and Henderson, S.C., *J. Phy. Chem.*, 1993, **98**, 13093.
7. Mataga, N. and Tsuno, S.; *Bull. Chem. Soc. Japan*, 1957, **30**, 368.
8. Das, P.K.; Encinas, M.V.; Steenken, S. and Scaiano, J.C.; *J. Am. Chem. Soc.*, 1981, **103**, 4162.
9. Manuscript in preparation.
10. Abraham, M.H.; Duce P.P.; Prior, D.V; Barratt, D.G.; Morris J.J. and Taylor, J.; *J. Chem. Soc. Perkin Tran. II* , 1989, 1355.
11. Joesten, M.D. and Schaad, L.J.; *Hydrogen Bonding*, Marcel Dekker, 1974, p. 361.
12 Reichardt, C.; *Solvents and Solvent Effects in Organic Chemistry*, VCH Publishers, NewYork, 1988, p. 370.
13. (a) Doubal, A.; Lohmani, F. and Zewail, A.H.; *Chem. Phys.*, 1996, **207**, 477. (b) Kim, S.K.; Wang J.K. and Zewail A.H.; *Chem. Phys. Lett.*, 1994, **228**, 369.

Table 1 : Oxidation Potentials, Hydrogen-Bonding Equilibrium Constants and $^3C_{60}$ Quenching Rate Constants of 1-Naphthol - Pyridine - Solvent Systems.

Base	**Solvent**	**E^{ox}, V vs SCE**	**K, M^{-1} Spect.**	**K, M^{-1} Kinetic**	**$-\Delta G^{o}$, eV**	**$k_{NB} \times 10^7$ $M^{-1}s^{-1}$**
-	PhCN	1.13	-	-	0.09	0.25±0.03
Cl-Py	PhCN	0.93	-	3.3±0.2	0.29	55±5
Py	PhCN	0.90	5.0±0.5	4.4±0.2	0.32	200±20
TMP	PhCN	0.77	9.5±0.5	9.4±0.5	0.45	260±30
-	CH_2Cl_2	-	-	-	-	<0.2
Cl-Py	CH_2Cl_2	-	10±0.5	9.8±0.5	-	21±5
Py	CH_2Cl_2	-	30±2	25±2	-	300±20
TMP	CH_2Cl_2	-	62±2	58±5	-	450±40
-	CCl_4	-	-	-	-	<0.1
Cl-Py	CCl_4	-	22±2	-	-	<0.1
Py	CCl_4	-	82±8	a	-	a
TMP	CCl_4	-	220±30	170±30	-	140±40

a : Concave curve

Table 2 : Quantum Yields of $C_{60}^{\cdot -}$ in quenching of $^3C_{60}$ by 1-naphthol.

Solvent	Base	[Base], M	Φ_R [(a)]
PhCN	TMP	0.05	0.85±0.05
PhCN	TMP	0.50	0.80±0.03
CCl_4	TMP	0.03	0.02±0.01
CCl_4	TMP	0.30	0.18±0.02

(a) Φ_R measured at 95% quenched triplet.

Figure captions :

Figure 1 : Time resolved absorption spectra of a solution of ~ 0.3 mM C_{60} + 1.5 mM 2- Naphthol + 0.5 M TMP in PhCN immediately (0μs) and 3μs after the flash. Data with 2-naphthol are shown instead of 1-naphthol because of larger extinction coefficient and characteristic structure of its neutral radical .

Figure 2 : Effect of base strength and solvent polarity on the rate of reduction of $^3C_{60}$ by 1- naphthol : (A) in PhCN, (B) in CH_2Cl_2 .

Figure 3 : Spectroscopic determination of hydrogen-bond formation equilibrium constant : 1-naphthol + Cl-Py in CH_2Cl_2.

Figure 4 : Effect of base strength on the rate of reduction of $^3C_{60}$ by 1-naphthol in CCl_4. Insert : Expanded plot for Py curve to illustrate the concave behavior.

Figure 5 : Deuterium isotope effect on the rate of reductive quenching of $^3C_{60}$ by 1-naphthol in CH_2Cl_2 as function of added Cl-Py. Curve H : with 0.2 M CH_3OH, Curve D : with 0.2 M CH_3OD.

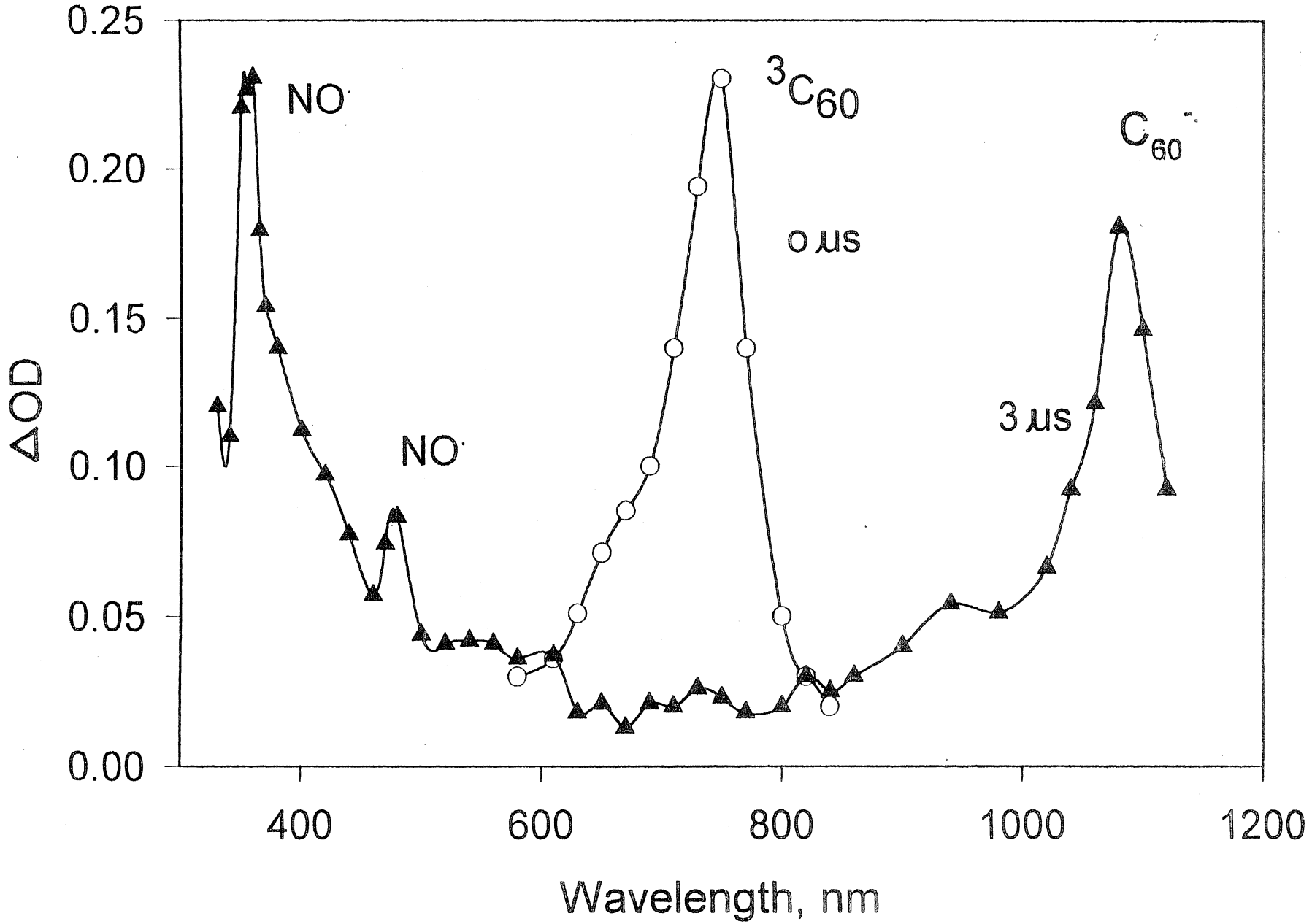
0.25
0.20
0.15
0.10
0.05
0.00
ΔOD
400
600
800
1000
1200
Wavelength, nm
NO·
NO·
$^3C_{60}$
0 μs
$C_{60}^{-\cdot}$
3 μs

Fig. 1

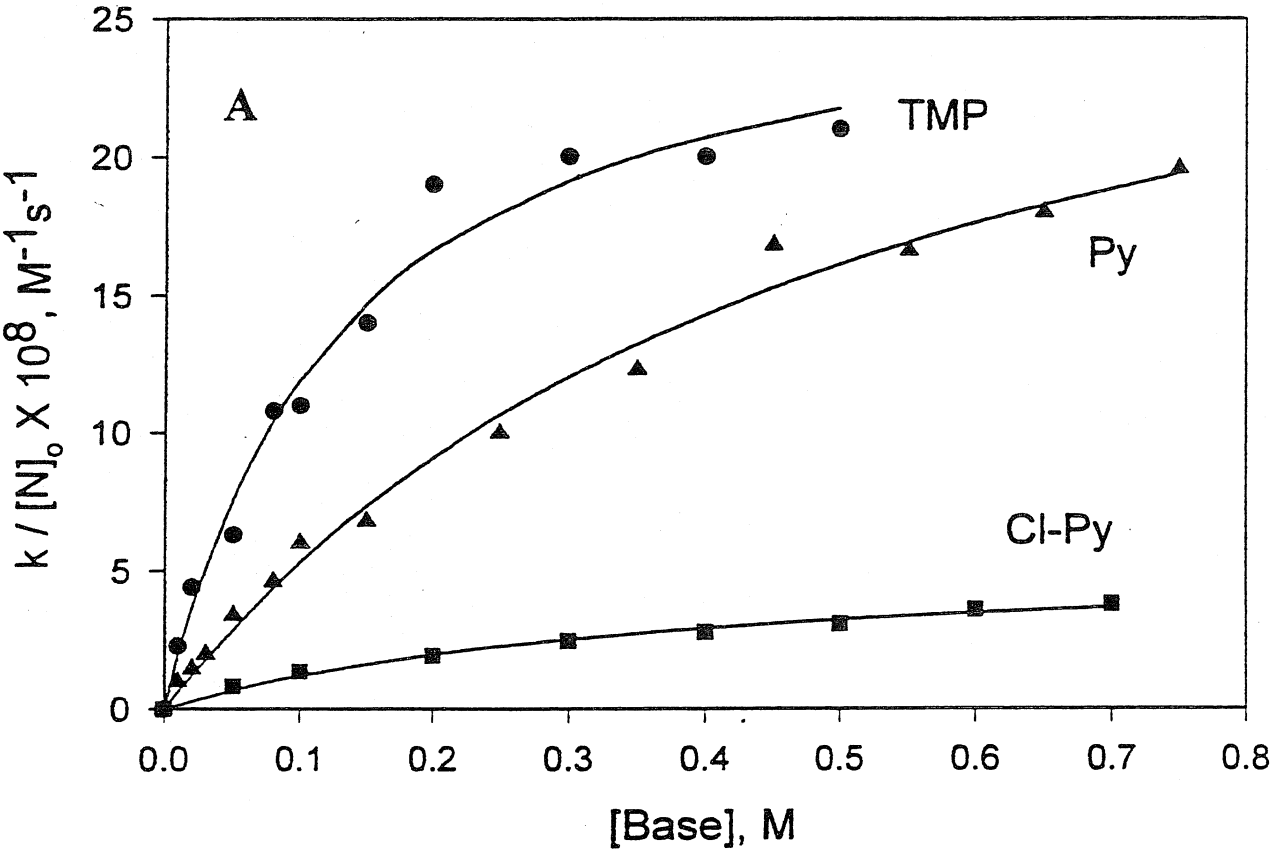
A
TMP
Py
Cl-Py
k / [N]o X 10^8, M^-1s^-1
[Base], M
0
5
10
15
20
25
0.0
0.1
0.2
0.3
0.4
0.5
0.6
0.7
0.8

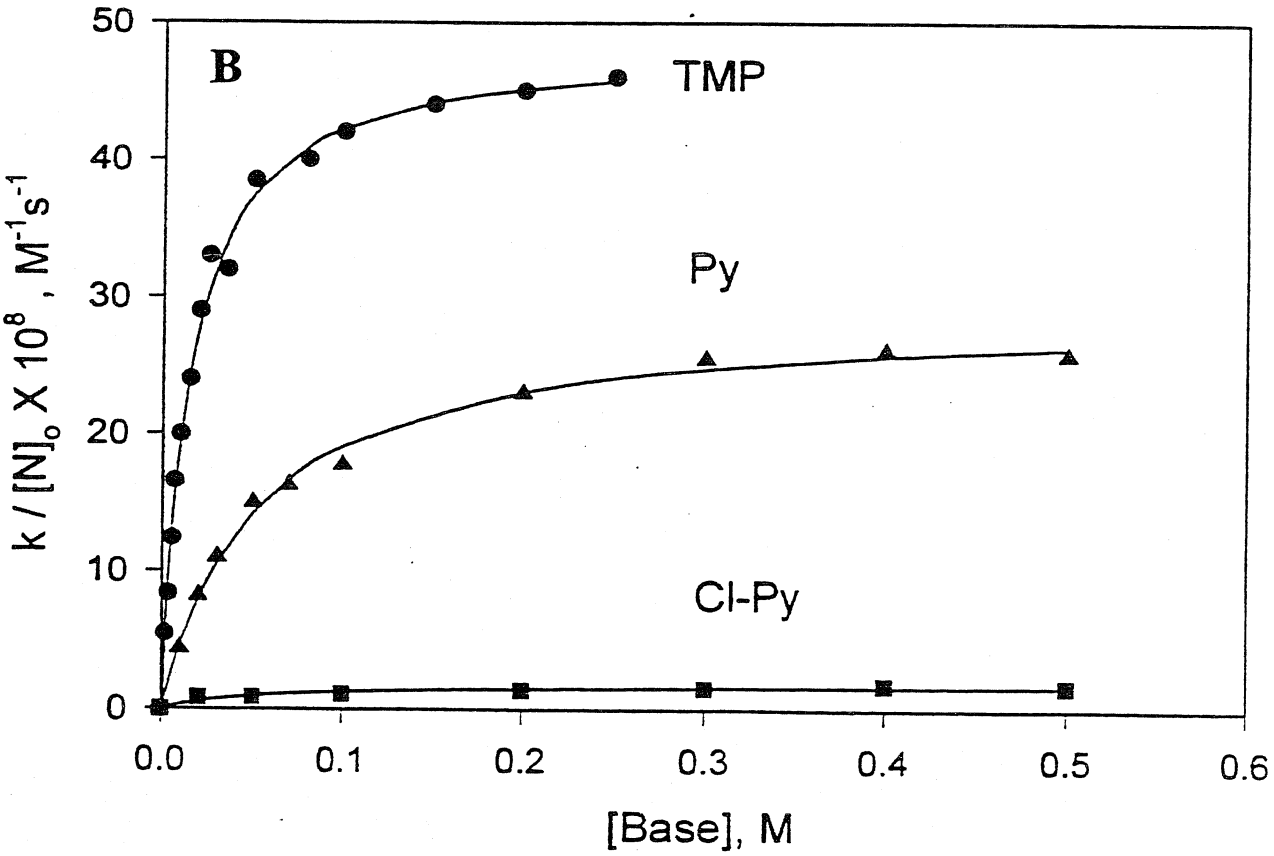
B
TMP
Py
Cl-Py
k / [N]o X 10^8, M^-1s^-1
[Base], M
0
10
20
30
40
50
0.0
0.1
0.2
0.3
0.4
0.5
0.6

Fig. 2

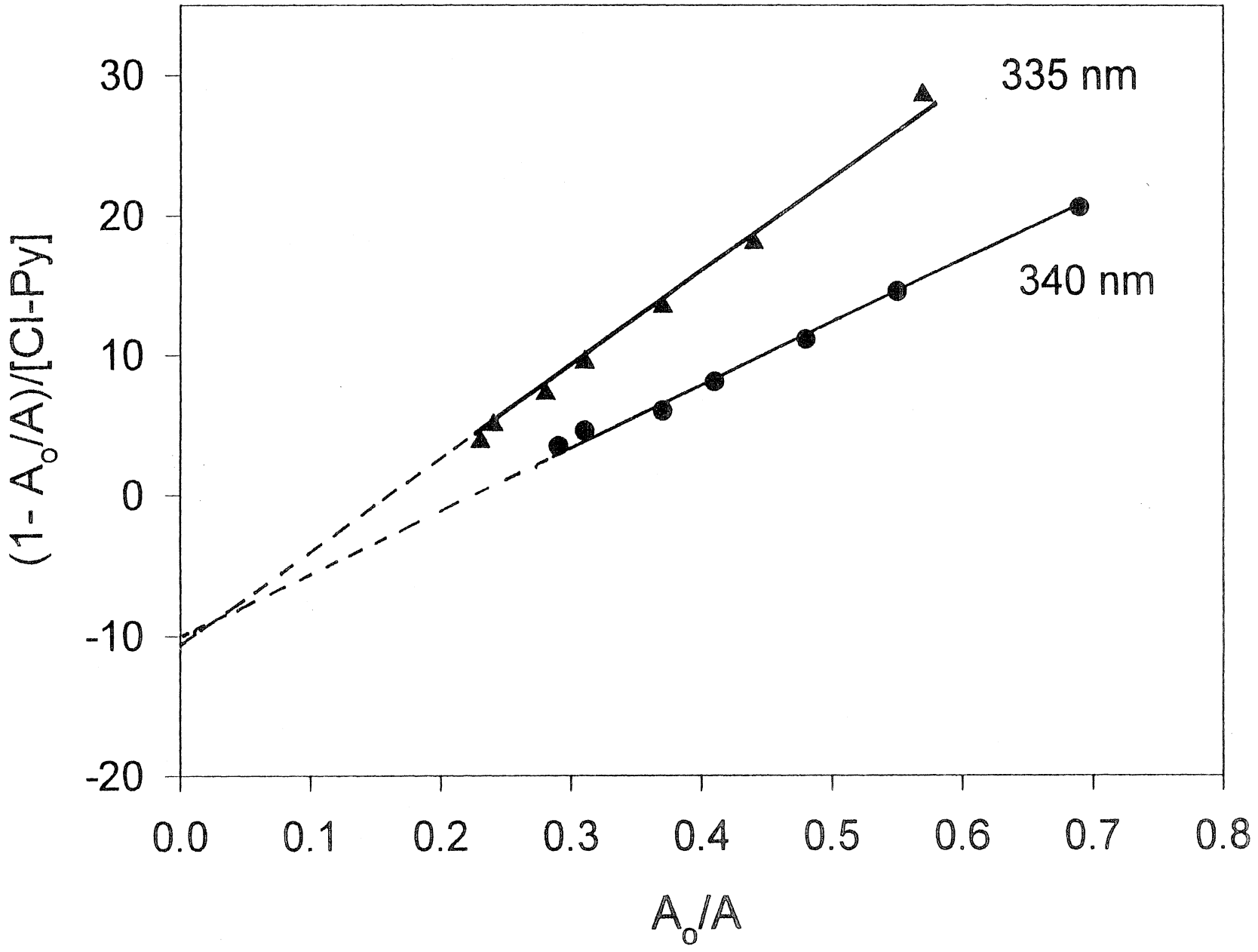
30
20
10
0
-10
-20
0.0
0.1
0.2
0.3
0.4
0.5
0.6
0.7
0.8
335 nm
340 nm
(1- A$_o$/A)/[Cl-Py]
A$_o$/A

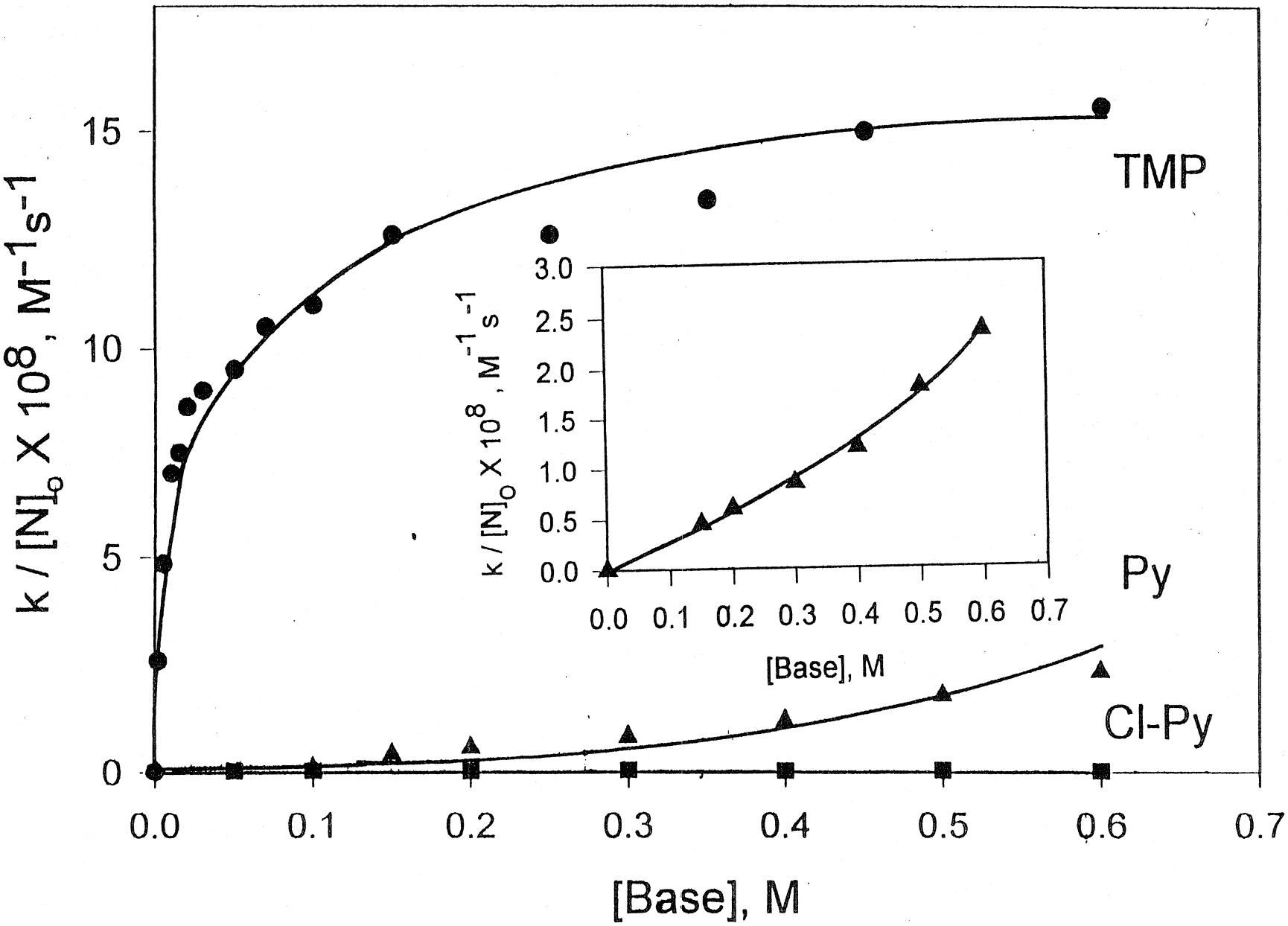
15
10
5
0
0.0
0.1
0.2
0.3
0.4
0.5
0.6
0.7
k / [N]$_o$ X 10^8, M^{-1}s^{-1}
[Base], M
TMP
Py
Cl-Py
3.0
2.5
2.0
1.5
1.0
0.5
0.0
k / [N]$_o$ X 10^8, M^{-1} s^{-1}
[Base], M

Fig 4

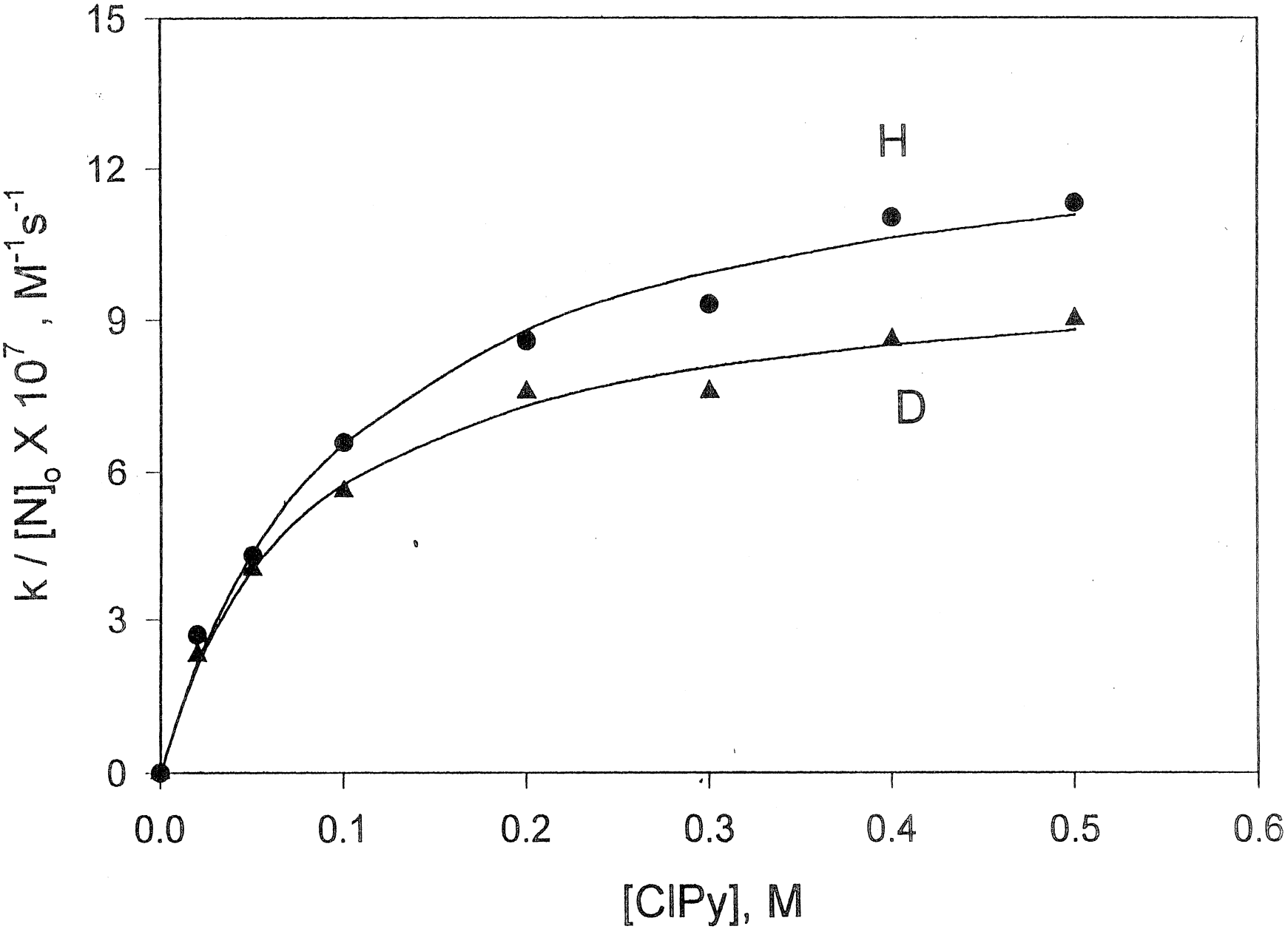

Fig. 5

13. Melléklet

Concerted electron-proton movement in quenching by hydrogen bonded phenols and quinones

L. Biczók, N. Gupta, H. Linschitz
16th IUPAC Symposium on Photochemistry, 1996. július 21-26.
Helsinki, Finnország

Introduction : The coupling of proton movement to electron transfer is of fundamental importance, particularly in biochemical processes. Nevertheless, much remains to be clarified regarding the detailed molecular mechanism of such reaction. Accordingly, we have studied excited-state electron transfer reactions in suitably structured model redox systems, in which the redox quencher is hydrogen-bonded to ***another*** molecule which functions as proton donor or acceptor. In such reactions, electrons and protons move to ***different*** loci in a ***trimolecular*** transition state complex. This is in sharp distinction to more familiar coupled electron-proton transfers, in which the two particles move over the ***same*** path and between the ***same*** loci, in a ***bimolecular*** hydrogen-bonded D-A pair.

The reactions reported here are :

1. Reductive quenching of excited substrates by phenols, hydrogen bonded to pyridines.
2. Oxidative quenching by quinones, hydrogen-bonded to alcohols or acids.

Our favorite substrate is triplet C_{60} which does not undergo hydrogen bonding interactions itself, and whose redox potentials are known. Moreover, the spectra and extinction coefficients of its triplet and radicals are known, thus permitting measurements of radical quantum yields. For the above systems, we determine rates and radical yields as function of quencher, hydrogen bonding agent and solvent, and correlate these results with redox potentials, hydrogen bonding equilibrium constants and deuterium kinetic isotope effects.

Experimental : Quenching rate constants and radical yields of triplet C_{60} were determined by laser flash photolysis, using a tunable flash-lamp driven dye laser. Effects of hydrogen bonding reagents on redox potentials of phenols and quinones were studied by cyclic voltammetry in benzonitrile - $TBAPF_6$ solution. Free energies of the excited state reactions were obtained from the Weller equation :

(Q = quencher ; E_T = triplet energy)

$$\Delta G^\circ = E^\circ_{ox}(Q) - E^\circ_{red}(C_{60}) - E_T - e^2/\epsilon a$$

	Hydrogen Bonding Reagents	**pKa**
For phenols :	3-chloropyridine (Cl-Py)	2.84
	pyridine (Py)	5.25
	2,4,6-trimethylpyridine (TMP)	7.43
For quinones :	hexafluoro-2-propanol (HFIP)	9.3
	p-nitrophenol (NP)	7.15
	trifluoroethanol (TFE)	12.39
	trifluoroacetic acid (TFA)	0.52

I- Quenching of $^3C_{60}$ by Phenols

A. Effect of hydrogen-bonding additives -

Figure 1 shows the enhancement of electron transfer quenching rate by addition of hydrogen bonding bases, for various phenol-pyridine-solvent systems.

B. Evaluation of hydrogen bonding formation constants-

1. From kinetics : (Fig. 1; Q = phenol quencher, B = base)

take $[Q] + [B] \approx [QB]$; $$K = \frac{[QB]}{[Q][B]} \qquad (1)$$

and effective pseudo-first order quenching constant k as

$$k = k_o + k_Q[Q] + k_{QB}[QB] \qquad (2)$$

for case that $[Q] + [QB] = [Q]_o << [B]_o$,

(1) and (2) becomes

$$\frac{k-k_o}{[Q]_o} = \frac{k_Q}{1+K[B]_o} + \frac{k_{QB}K[B]_o}{1+K[B]_o} \qquad (3)$$

We obtain both k_{QB} and K from the best fit to data (Fig. 1).

2. From spectra : Figure 2 illustrates method for spectroscopic determination of K. Intercept of this plot is -K.

Table 1 summarizes results on the C_{60}- phenol- pyridine systems.

For each phenol, data are arranged in order of increasing pyridine basicity and decreasing solvent polarity. We observe, for all phenols :

1. Potentials : The decrease in oxidation potential with added base parallels the pyridine basicity. The average maximum decrease (with TMP) is 0.36 ± 0.03 V. This is much less than that obtained with strong bases (~ 1.0 V with tetrabutylammonium hydroxide) and therefore corresponds to oxidation of hydrogen-bonded, *not* deprotonated, phenol.

2. Equilibrium Constants : K increases with pyridine basicity and with decreasing solvent polarity. The values obtained ***independently*** from spectra or kinetics agree closely. ***This establishes that the quenching species is the hydrogen-bonded phenol.***

3. Rates : Addition of hydrogen bonding agent greatly increases the quenching rate ($k_{QB} >> k_Q$). In benzonitrile, this increase parallels $-\Delta G^{o*}$, finally reaching diffusion controlled values.

4. Solvent Effect : Electron transfer is facilitated by polar media, while solvents of lower polarity favor hydrogen bonding. The net result depends on ***both*** the strength of the hydrogen-bonded base and solvent polarity, as shown in **Figure 3**. Hydrogen bonding to the strong base, TMP, permits reaction to occur, even in CCl_4, giving ***convex*** curves of Figure 3A, and correct values of K based on equation (3) (Table 1, 4MeOPhOH, etc.).

We attribute the ***concave*** behavior of **Figure 3B** to development of a *local* polar environment by segregation of polar pyridine, $E_T(30) = 40.5$, around the reaction complex, within non-polar CCl_4, $E_T(30) = 32.4$. This makes quenching possible, even with the weaker base, pyridine. In support of this interpretation, **Figure 3C** shows the change from concave to convex functional form, and increase in the rate with increasing solvent polarity, despite corresponding decrease in K.

5. Kinetic Isotope Effect:

The clearest demonstration of concerted electron-proton movement is the appearance of a primary isotope effect. This is best seen in the case where the rate is far from diffusion-controlled, as in the system shown in **Figure 4.** Note that the isotope effect in Fig. 4, upper, cannot be assigned to a change in K, since the final rates at the plateaus correspond to quenching by fully hydrogen bonded phenol. Moreover, even when the rate vs. [base] function is concave (Fig. 4, lower) and does not permit kinetic evaluation of K, a marked isotope effect is still observed. For other phenol-base-solvent systems(**Table 1.**) k_H / k_D approaches unity as the rate approaches diffusion controlled.

Results similar to those found for $^3C_{60}$ are obtained also for quenching of aromatic singlets by phenol-pyridine systems. The Stern-Volmer plot, **Figure 5,** for pyrene - 2,6-dimethoxyphenol - TMP in CH_2Cl_2 gives $k_H / k_D = 1.56$.

Table 1: Quenching of Triplet C_{60} by Phenol-Pyridine Systems: Oxidation potentials, Hydrogen Bonding Equilibria and Rate Constants.

Phenol	Base	Solvent	E^{ox} vs. SCE	K, M^{-1} Spectr.	K, M^{-1} Kinet.	-ΔG eV	k_{QB} 10^7 $M^{-1}s^{-1}$
H	-	PhCN	1.40			-0.18	-
	TMP	PhCN	1.13		6.7 ± 0.9	0.09	6.0 ± 0.3
4-Me	-	PhCN	1.36			-0.14	-
	ClPy	PhCN	1.33			-0.11	
	Py	PhCN	1.15		2.6 ± 0.3	0.07	19 ± 1
	TMP	PhCN	1.02	5.5 ± 0.6	6.9 ± 0.9	0.20	53 ± 3
	Py	CH_2Cl_2		16 ± 2	15 ± 3		4.4 ± 0.2
4-MeO	-	PhCN	1.11			0.11	0.44 ± 0.04
	ClPy	PhCN	1.07	0.9 ± 0.2	1.1 ± 0.2	0.15	96 ± 8
	Py	PhCN	0.96			0.26	230 ± 20
	TMPy	PhCN	0.77	6.0 ± 0.6	4.8 ± 0.5	0.45	250 ± 20
	Py	CCl_4		33 ± 3	a		a
	TMP	CCl_4		82 ± 5	86 ± 11		160 ± 10
2-MeO	-	PhCN	1.28			-0.06	
	ClPy	PhCN	1.24			-0.02	
	Py	PhCN	1.05		0.7 ± 0.3	0.17	210 ± 50
	TMP	PhCN	0.97			0.25	
	Py	CH_2Cl_2		2.4 ± 0.3	2.1 ± 0.2		6.7 ± 3
	TMP	CH_2Cl_2		2.4 ± 0.3	2.2 ± 0.2		190 ± 10
	Py	toluene					a
	Py	CCl_4		1.4 ± 0.3			a
	TMP	CCl_4		3.0 ± 0.5			b
2,6-DiMeO	-	PhCN	1.11			0.11	0.45 ± 0.03
	ClPy	PhCN	1.01		0.9 ± 0.2	0.21	170 ± 20
	Py	PhCN	0.87			0.35	250 ± 20
	TMP	PhCN	0.71			0.51	260 ± 20
	Py	CCl_4		1.5 ± 0.3	a		a
	TMP	CCl_4		2.0 ± 0.5	3.0 ± 0.5		310 ± 30
3-CN	TMP	PhCN	1.27			-0.05	0.35 ± 0.05
4-OH	-	PhCN	1.01			0.21	1.2 ± 0.2
	ClPy	PhCN			1.2 ± 0.3	0.35	250 ± 20
	Py	PhCN			3.4 ± 0.3	0.36	330 ± 40
	TMP	PhCN		6 ± 3	9.5 ± 0.6	0.61	270 ± 10
	TMP	toluene		43 ± 5	36 ± 3		410 ± 20
	TMP	CCl_4		38 ± 3	37 ± 3		270 ± 20
1-naphthol	-	PhCN	1.13			0.09	0.25 ± 0.03
	ClPy	PhCN	0.93		3.3 ± 0.2	0.29	55 ± 5
	Py	PhCN	0.90	5.0 ± 0.5	4.4 ± 0.2	0.32	200 ± 20
	Py	CH_2Cl_2		30 ± 2	25 ± 2		300 ± 20
	Py	CCl_4		82 ± 8	a		a
	TMP	PhCN	0.77	9.5 ± 0.5	9.4 ± 0.5	0.45	260 ± 30
	TMP	CH_2Cl_2		62 ± 2	58 ± 5		450 ± 40

a: Concave plot, see Fig.3.
b: Linear plot, see Fig. 3.

Table 2 - Quantum Yields of $C_{60}^{\cdot-}$ in Quenching of $^3C_{60}$ by 2-Methoxyphenol : Effect of Base and Solvent.

Solvent	Base	[Base], M	ϕ_R[(a)]
CCl_4	TMPy	0.05	<0.02
		0.3	0.07
		0.7	0.14
CCl_4	Py	0.3	0.15
		0.7	0.21
CH_2Cl_2	Py	0.2	0.46
		0.3	0.42
PhCN	Py	0.05	0.47
		0.5	0.42

(a) ϕ_R measured at 95% quenched triplet (i.e. at equal quenching rates). No reaction is observed in absence of added base (Fig. 3).

Figure 1

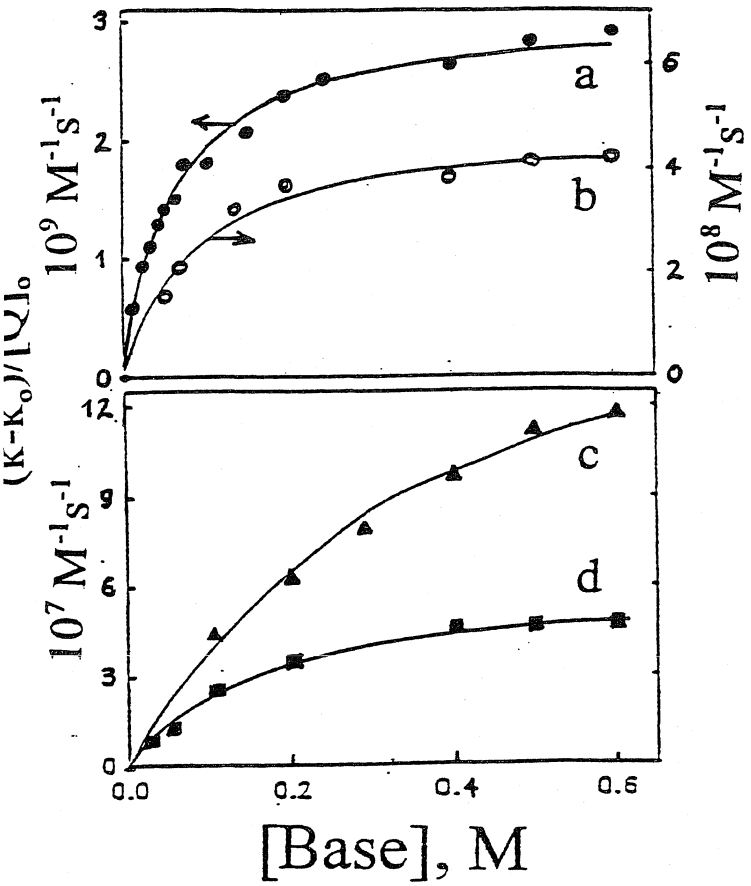

Figure 2

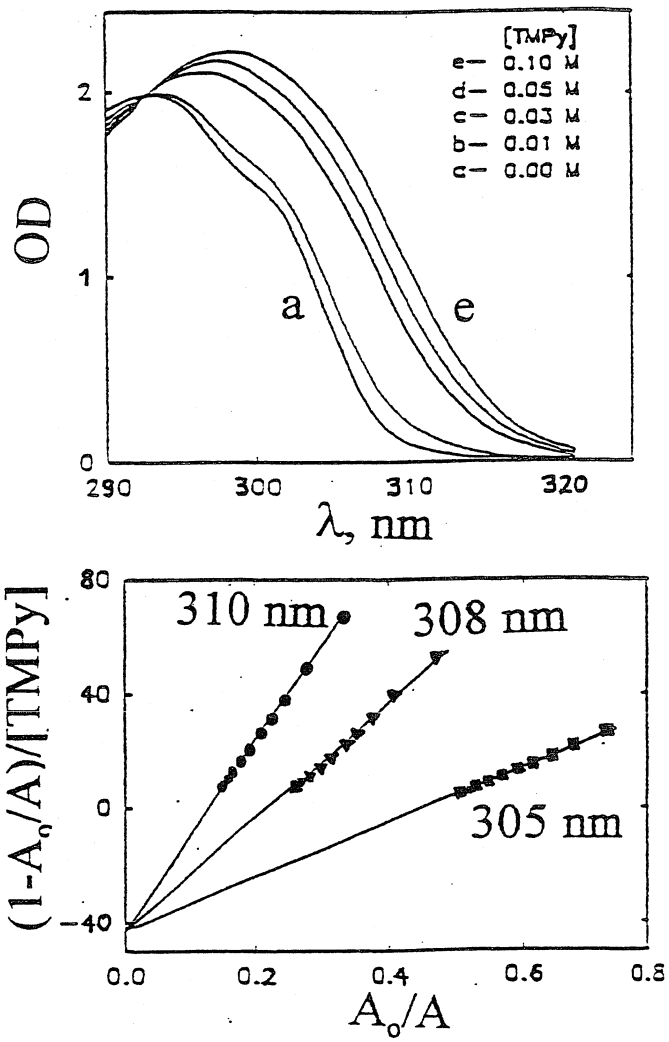

Figure 1 - Effect of Hydrogen-Bonding Additives on Rate of Quenching of $^3C_{60}$: "k" = Pseudo-First Order Decay Constant.

(a) 1- Naphthol + Py in CH_2Cl_2 (b) 4-Me-PhOH + TMP in PhCN

(c) 4-Me-PhOH + Py in PHCN (d) PhOH + TMP in PhCN

Figure 2 - Spectroscopic Determination of Hydrogen-Bond Formation Equilibrium Constant : Hydroquinone + TMP in Toluene

Figure 3 - Effect of Base Strength and Solvent Polarity :

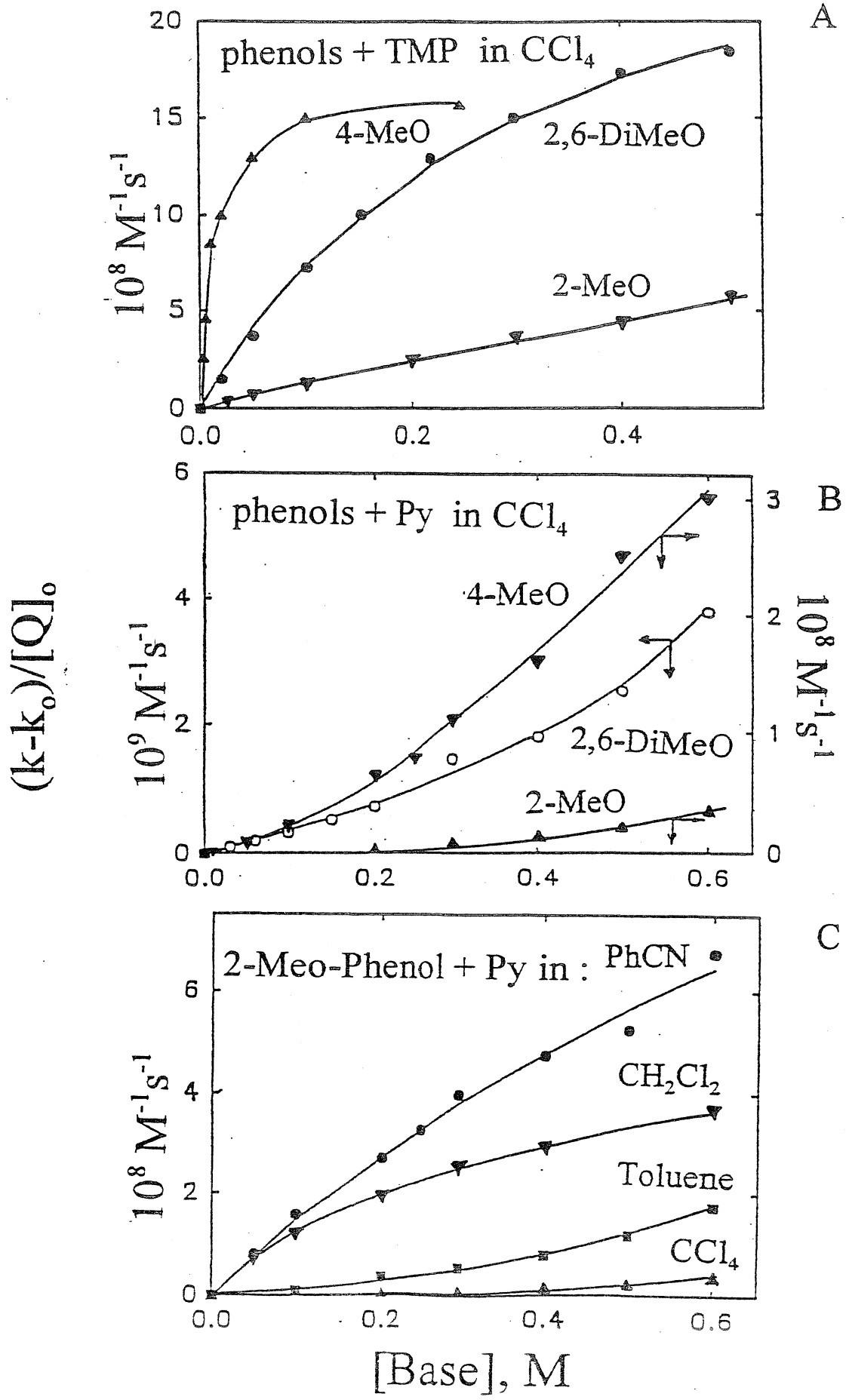

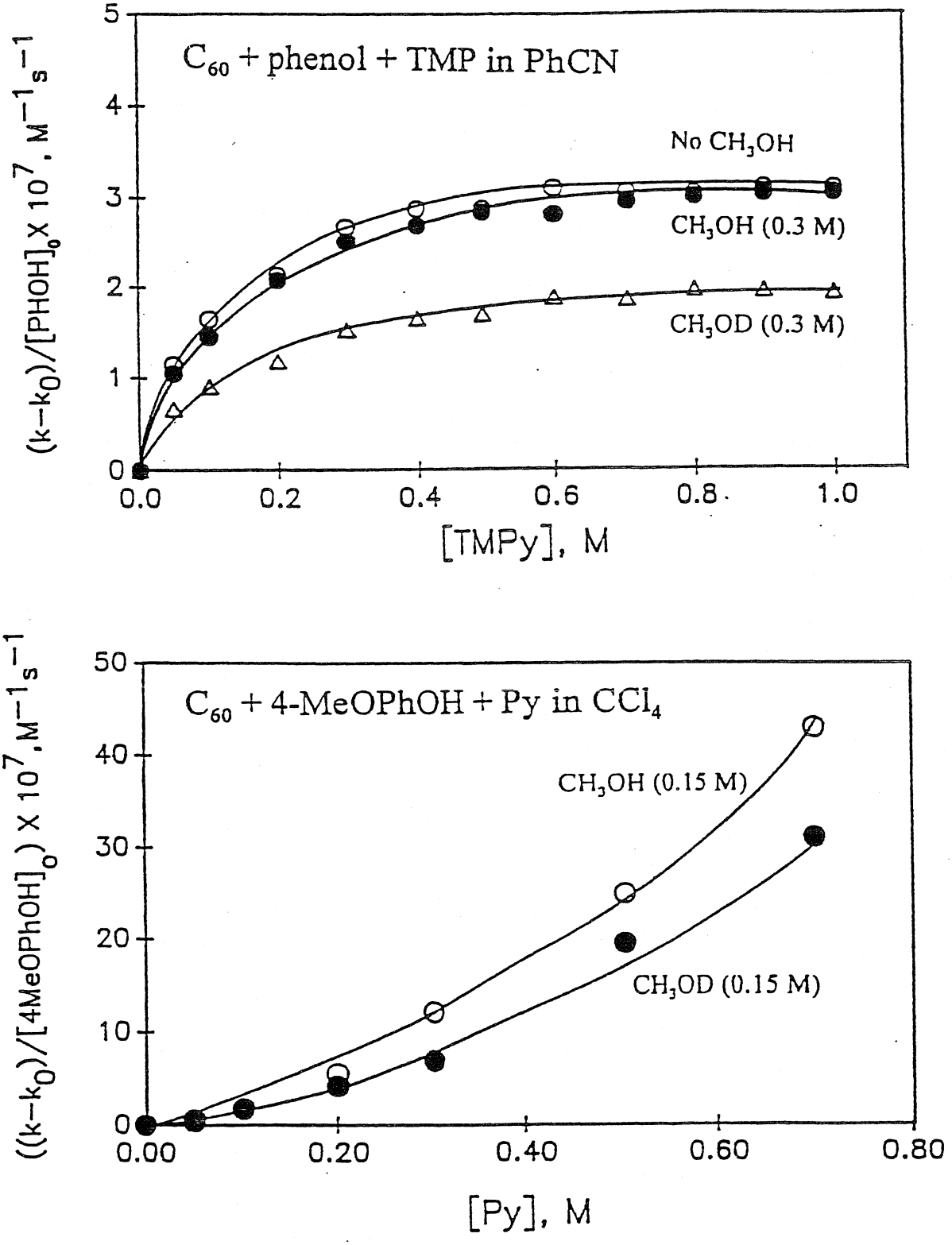

Figure 4 - Deuterium Isotope Effect in Reduction of Triplet C_{60} by Phenol + Py Systems.

Upper : Phenol + TMP in PhCN

Lower : 4-Methoxyphenol + Py in CCl_4

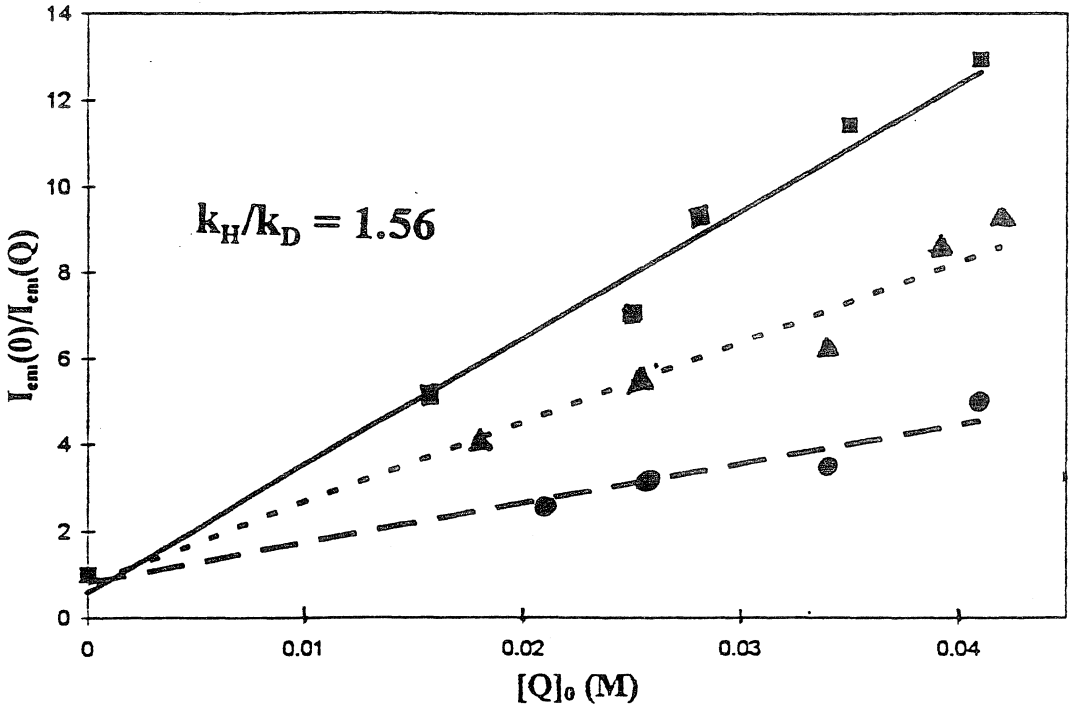

Figure 5 - Quenching of Pyrene Fluorescence by 2,6-Dimethoxyphenol

- **[EtOH] = 1 M; no added TMP**
- **[EtOH] = 1 M; [TMP] = 1 M**
- **[EtOD] = 1 M; [TMP] = 1 M**

II- Quenching of $^3C_{60}$ by Quinones

Triplet C_{60} and chloranil (Q) react very slowly if at all ($k < 10^6\ M^{-1}\ s^{-1}$) in CH_2Cl_2. However addition of hydrogen bonding or acidic reagents causes quenching of the triplet and formation of $C_{60}^{+\bullet}$ and either $Q^{-\bullet}$ or $QH^{\bullet}$. (The chloranil semiquinones are difficult to distinguish in absorption).

Rates : **Figure 6** shows the effect of various additives on quenching of $^3C_{60}$ by chloranil in CH_2Cl_2.

Deuterium Isotope Effect : It is significant that despite the results of Fig. 6, we find no isotope effects with TFA, HFIP or TFE.

Interpretations : Table 3 gives the relevant parameters. TFA and p-nitrophenol have similar kinetic effects, but their pKa's differ by about seven units ! However, their tendency to form hydrogen bonds, measured by "log kα" in Table 3, are similar. We assign the increase in rate to hydrogen bonding, leading to a local highly polar environment. The sharp differences between quenching by phenols and quinones may relate to the strongly acidic character of phenol cation radicals compared to the weakly basic character of quinone anion radical.

Yields : **Table 4** summarizes effects of TFA and HFIP concentrations on radical yields in oxidation of triplet C_{60}.

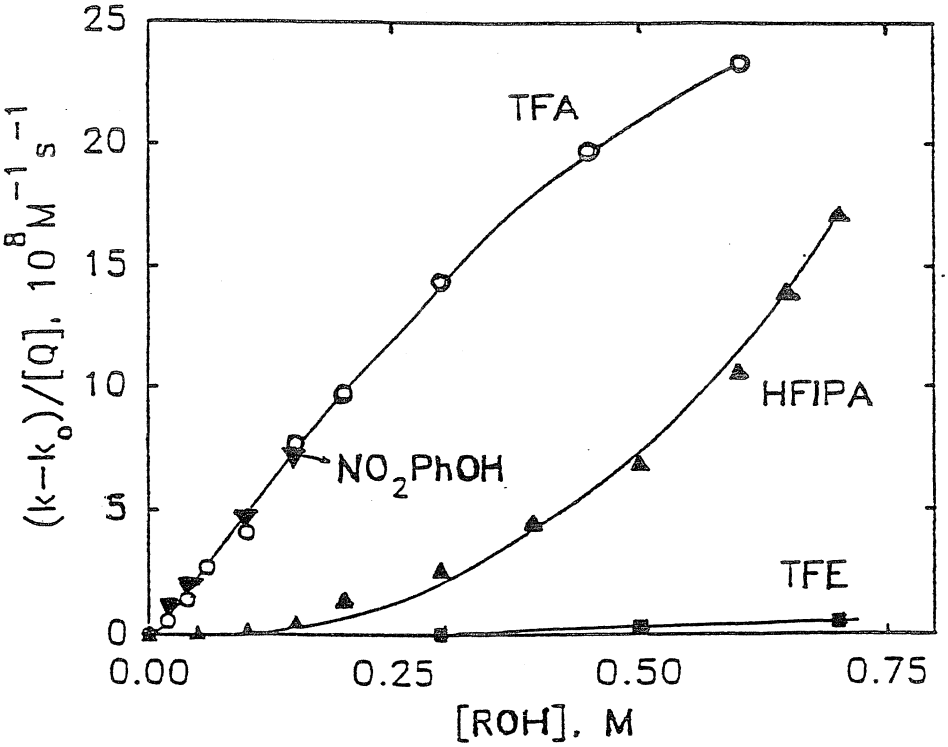

Figure 6 - Effect of Hydrogen-Bonding Additives on Rate of Oxidative Quenching of Triplet C_{60} by Chloranil in CH_2Cl_2. "k" = Pseudo-first Order Decay Constant

Table 3 - Oxidation of $^3C_{60}$ by Chloranil with 0.15 M Additives in CH_2Cl_2 :

Additives	logKα[(a)]	pKa (H_2O)	pKa (DMSO)	E^o_{Red} V vs SCE	$(k-k_o)/[Q]_o$ × 10^8, M^{-1} s^{-1}
-	-	-	-	-0.10	-
TFA	3.55	0.52	3.45	0.44[(b)]	7.7
4-NO_2-PhOH	3.12	7.15	10.8	0.01[(b)]	7.2
2-CN-PhOH	2.69	-	-	-	5.9
HFIP	2.83	9.3	-	0.02[(c)]	0.52
TFE	2.00	12.39	23.45	-0.07[(d)]	0.02
AcOH	2.04	4.76	12.3	-	< 0.01

(a) Hydrogen-bonding equilibrium constant towards a common acceptor, N-methylpyrrolidinone in 1,1,1-trichloroethane.
(b) Limiting value.
(c) Limiting value 0.10 V at 0.6 M HFIP.
(d) Data in PhCN. Limiting value 0.00 V at 0.7 M TFE.

Table 4 - Oxidation of Triplet C_{60} by Quinones in CH_2Cl_2 : Quantum yields of $C_{60}^{\bullet+}$[(a)].

Quinone M × 10^{-3}	Additive M	ϕ_R
2,5-dichloro	TFA	
5.0	0.015	0.23
1.3	0.050	0.44
0.25	0.50	0.51
tetra-chloro	TFA	
0.45	0.30	0.76
0.38	0.40	0.72
0.30	o.50	0.80
tetra-chloro	HFIP	
5.0	0.20	0.15
1.0	0.40	0.15
0.30	0.70	0.15

(a) ϕ_R measured at 95% quenched triplet (i.e., at equal quenching rates). No reaction is observed in absence of acid or alcohol addition (Fig. 5).

Conclusions

1. Electron transfer may be coupled to proton movement by use of redox reagents which are hydrogen-bonded to appropriate proton acceptors or donors.

2. Kinetic deuterium effects in such reactions establish that electron and proton movement are ***concerted***, and occur within a trimolecular transition state complex.

3. Proton movement, facilitated by hydrogen-bonded structures, particularly in quenching by phenols, contributes to redox potentials and enhances rates of concerted electron transfer reactions. The effect increases with the strength of the bond (reflected in the redox potentials) and the local polarity around the reaction complex.

4. In these systems, primary radical yields in homogeneous solution are enhanced because improved charge separation and reorganization following electron transfer restricts rate of back reaction. Such reorganization may involve the solvate structure (quinones) as well as proton transfer (phenols).

14. Melléklet

The Journal of
Physical Chemistry

C_{60} as a Photocatalyst of Electron-Transfer Processes: Reactions of Triplet C_{60} with Chloranil, Perylene, and Tritolylamine Studied by Flash Photolysis and FT-EPR

Carlos A. Steren, Hans van Willigen, Laszlo Biczók, Neeraj Gupta, and Henry Linschitz

Departments of Chemistry, University of Massachusetts at Boston, Boston, Massachusetts 02125; Brandeis University, Waltham, Massachusetts 02254; and Central Research Institute for Chemistry, Hungarian Academy of Sciences, P.O. Box 17, 1525, Budapest, Hungary

Reprinted from
J. PHYS. CHEM., Volume 100, Number 21, Pages 8920–8926

C_{60} as a Photocatalyst of Electron-Transfer Processes: Reactions of Triplet C_{60} with Chloranil, Perylene, and Tritolylamine Studied by Flash Photolysis and FT-EPR

Carlos A. Steren,[†,‡] Hans van Willigen,[*,†] Laszlo Biczók,[§,⊥] Neeraj Gupta,[§] and Henry Linschitz*[,§]

Departments of Chemistry, University of Massachusetts at Boston, Boston, Massachusetts 02125; Brandeis University, Waltham, Massachusetts 02254; and Central Research Institute for Chemistry, Hungarian Academy of Sciences, P.O. Box 17, 1525, Budapest, Hungary

Received: February 29, 1996[⊗]

Photoprocesses in benzonitrile solutions of C_{60} and chloranil (CA) have been studied by complementary techniques of nanosecond laser photolysis and Fourier transform EPR. Direct oxidation of $^3C_{60}$ by CA is slow ($k = (2.0 \pm 0.3) \times 10^7$ M^{-1} s^{-1}), consistent with the high oxidation potential of $^3C_{60}$. However, the formation rate and yield of CA^- are much increased by addition of perylene (Pe) or tritolylamine (TTA) via the fast reactions $^3C_{60} + Pe \rightarrow C_{60} + {}^3Pe$, followed by $^3Pe + CA \rightarrow Pe^+ + CA^-$, or $^3C_{60} + TTA \rightarrow C_{60}^- + TTA^+$, followed by $C_{60}^- + CA \rightarrow C_{60} + CA^-$. These reactions utilize the broad absorption and initial high triplet yield of C_{60}, as well as the low oxidation potential of ^3Pe or high reduction potential of $^3C_{60}$, to catalyze efficient formation of CA^- and enhance separation of radicals. Triplet C_{60} also reacts with Pe by electron transfer, forming Pe^+ and C_{60}^- with rate one-third that of energy transfer. However, the CA^- formed in the Pe-catalyzed reaction is strongly spin-polarized, indicating that it is formed primarily via the ^3Pe pathway. The extinction coefficient of C_{60}^- at 1080 nm is measured ($\epsilon = 18\,300 \pm 1100$ M^{-1} cm^{-1}) using the TTA reaction.

Introduction

Triplet state C_{60} may react by reversible electron transfer with either donors (arylamines,[1,2] phenols[2]) or acceptors such as tetracyanoquinodimethane (TCNQ),[3] tetracyanoethylene (TCNE),[3−5] and chloranil (CA).[6] We have previously studied reductive reactions, including formation and decay of cage-escape radical products, by complementary flash photolysis and Fourier transform electron paramagnetic resonance (FT-EPR).[7] These combined techniques are well-suited for such study since the optical absorption spectrum of $^3C_{60}$[8] is clearly separated from that of C_{60} and its anion[9,10] or cation[10,11] radicals, and the unique narrow-line EPR spectrum of the triplet[7,12] is easily distinguished from the highly resolved spectra of radical products. In addition to information on chemical kinetics, the FT-EPR data provide detailed information on spin dynamics.

Here we extend an earlier FT-EPR study of the C_{60}/chloranil (CA) system[6] and demonstrate the function of C_{60} as a photocatalyst for other electron-transfer reactions. It is shown that in solutions of perylene (Pe) or tritolylamine (TTA) with CA and C_{60}, a fast and efficient electron-transfer reaction between Pe or TTA and CA can be initiated by photoexcitation of C_{60}. In these reactions, C_{60} functions as a harvester of visible light and an efficient channel to triplet states ($\phi_T > 0.9$).[8] In the case of C_{60}/Pe/CA, triplet−triplet energy transfer, $^3C_{60} + Pe \rightarrow C_{60} + {}^3Pe$, leads to efficient production of perylene triplets which are oxidized by CA to yield Pe^+ and CA^-. That this is the primary route of CA^- formation is directly demonstrated by flash photolysis and is also deduced from the spin polarization (CIDEP) of the anion radicals. An alternative catalytic pathway is illustrated by the C_{60}/TTA/CA system. Reductive quenching of the triplet by TTA, $^3C_{60} + TTA \rightarrow C_{60}^- + TTA^+$, yields C_{60} anion radicals, which then transfer the electron to CA. A similar catalytic sequence involving C_{60}^- as intermediate also plays a role, but to a lesser extent, in the C_{60}/Pe/CA system, leading to Pe^+ and CA^- radicals. The facts that light absorption by C_{60} covers a broad range of the visible spectrum and radicals formed from triplet precursors avoid immediate back-reaction suggest its possible application in solar-driven photochemical reactions.

In this work, we measure also the extinction coefficient of the C_{60}^- anion radical and give rates and quantum yields of reactions involved in these catalytic sequences.

Experimental Section

C_{60} (99.9%, SES Research), Pe (Gold label, Aldrich), and benzonitrile (99.9% HPLC grade, Aldrich) were used as received. CA (Aldrich) was purified by vacuum sublimation. TTA was kindly donated by Professor R. I. Walter of the University of Illinois—Chicago. Studies were carried out on freshly prepared solutions freed of oxygen by purging with nitrogen or argon. Photochemical degradation over the course of an experiment was found to be minimal and did not affect the results.

Flash photolysis studies utilized a flash lamp driven dye laser (Candela ED-200) giving 0.2 μs pulses at 590 nm (rhodamine 6G). Initial triplet absorbance on flashing $[C_{60}] \sim 7 \times 10^{-5}$ M in benzonitrile ($\Delta D_{750} \sim 0.6$) corresponded to $[^3C_{60}]_0 \sim 4 \times 10^{-5}$ M. Transient absorption spectra were followed by conventional means,[13] using a photomultiplier to 800 nm and an InGaAs photodiode and fast amplifier (New Focus, 1811) for the near-IR. Quenching rate constants were determined from the linear dependence of pseudo-first-order decay constants on quencher concentration. In averaging transient absorbances, ΔD values measured on each flash were corrected for flash energy variations by plotting ΔD's vs energy and reading off the absorbance at a given flash energy.

† University of Massachusetts at Boston.
‡ Present address: FAMAF, Universidad Nacional de Córdoba, 5000 Córdoba, Argentina.
§ Brandeis University.
⊥ CRIC, Hungarian Academy of Sciences.
* To whom correspondence should be addressed.
⊗ Abstract published in *Advance ACS Abstracts*, May 1, 1996.

S0022-3654(96)00640-5 CCC: $12.00

Reversible polarographic potentials of perylene (oxidation) and C_{60} (reduction) were measured in the same benzonitrile solution vs SCE, using an E.G.G. "Versastat" potentiostat, glassy carbon working electrode, and 0.1 M tetrabutylammonium hexafluorophosphate (TBAHP) electrolyte.

FT-EPR measurements were performed with a home-built spectrometer.[14] The nominal microwave pulse width used in the measurements was 15 ns, and the free induction decay (FID) was sampled, with quadrature detection, at 200 Msamples/s. A CYCLOPS phase-cycling routine was used in the measurements. Final spectra typically were the average of 2400 FIDs. C_{60} was excited with the second harmonic (532 nm) of a Quanta Ray GCR12 Nd:YAG laser (~20 mJ/pulse, 10 Hz repetition rate). Measurements in which ^{3}Pe was generated by direct excitation (440 nm, ~ 2 mJ/pulse, 30 Hz) were performed using a dye laser (Lambda Physik FL3001) pumped by an excimer laser (Lambda Physik 103MSC). The time evolution of spectra was monitored by recording FIDs for a series of delay times (τ_d), ranging from 10 ns to 200 μs, between laser and microwave pulses. Signal intensities were obtained from the FIDs with the linear prediction–singular value decomposition technique[15] or by integration of the peaks in the frequency-domain spectra.

Results and Discussion

Extinction Coefficient of C_{60}^-. To obtain quantum yields of $^3C_{60}$ reductions, we have previously measured the extinction coefficients of C_{60}^- at its relatively weak absorptions in the visible.[2,16,17] In connection with current and ongoing studies, it is desirable to determine the extinction also for the strong peak at 1080 nm where there is less overlap with other transient spectra but for which only approximate and conflicting values are presently available.[9,10] We use, as before, the reaction $^3C_{60}$ + Am → C_{60}^- + Am$^+$, where Am represents the efficient quenchers tritolylamine (TTA) or tri-*p*-fluorophenylamine (TFPA), whose cation radicals have well-established extinctions, $\epsilon(TTA^+)_{680}$ = 26 200 M^{-1} cm^{-1} and $\epsilon(TFPA^+)_{645}$ = 26 600 M^{-1} cm^{-1} in benzonitrile.[2] The extinction of C_{60}^- is then obtained by comparing radical absorptions at 1080 and 680 (or 645) nm, measured on the same solutions at equal flash energies and corrected to take account of any overlapping radical formation and decay.[13] Absorbances measured at the amine cation peaks were corrected for small contributions from C_{60}^- at these wavelengths (ϵ_{645} ~ 1700 M^{-1} cm^{-1}; ϵ_{680} ~ 900 M^{-1} cm^{-1}). There is no ground state absorption (i.e., bleaching) beyond 630 nm. The values of $\epsilon(C_{60}^-)_{1080}$ thus found are 18 300 and 18 200 M^{-1} cm^{-1} (±5%), based on TTA and TFPA, respectively.

The C_{60}^- extinction coefficient was obtained also from kinetic data. Assuming a second-order back-reaction with rate constant k_2 for radical decay,[13] the slope, S_λ, of a plot of ΔD_λ^{-1} vs time following triplet disappearance is $k_2/\sum\Delta\epsilon_\lambda$, where $\sum\Delta\epsilon_\lambda$ is the total differential extinction coefficient at wavelength λ. Thus, in the C_{60}/TTA system,

$$\epsilon_{1080} = [S_{680}/S_{1080}]\sum\epsilon_{680}$$

Measured ΔD^{-1} vs time slopes of TTA^+ and C_{60}^- peaks are plotted in Figure 1. Using the extinction values of TTA^+ and C_{60}^- at 680 nm given above, the second-order plot in Figure 1 gives k_2 = (1.0 ± 0.1) × 10^{10} M^{-1} s^{-1}, in close agreement with values obtained previously using data at other wavelengths.[2] From this we then obtain $\epsilon(C_{60}^-)_{1080}$ = 19 500 M^{-1} cm^{-1}, in fair agreement with the result given above. This kinetic method is not subject to errors involving mismatch of initial triplet concentration on successive flashes where ΔD measurements

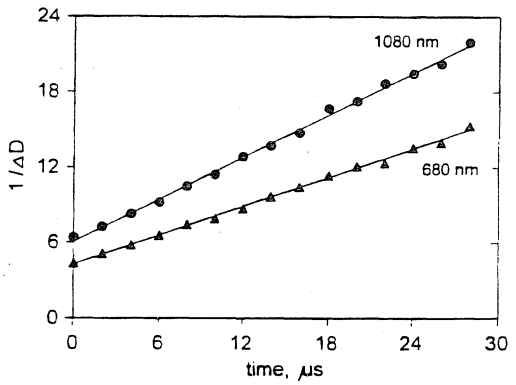

Figure 1. Second-order decay of radical ions produced by excitation of C_{60} (6 × 10^{-5} M) in the presence of tritolylamine (1.5 × 10^{-4} M) in benzonitrile at room temperature. ΔD^{-1} versus time at 680 nm (TTA^+) and 1080 nm (C_{60}^-).

are made at different wavelengths. However, we feel that the direct measurement of ΔD's is a more reliable procedure and take 18 300 ± 1100 M^{-1} cm^{-1} to be the preferred value. This may be compared with previously given values (M^{-1} cm^{-1}) from electrochemical preparation of C_{60}^- in the presence of electrolyte: 1.2 × 10^4 in benzonitrile,[9a] 2.0 × 10^4 in tetrahydrofuran,[9b] and 1.55 × 10^4 in methylene chloride.[9c] Values estimated from γ-radiolysis are in the range (3 ± 1) × 10^4.[10]

Reactions of $^3C_{60}$ with Chloranil. *Flash Photolysis.* In benzonitrile solution CA quenches $^3C_{60}$ with rate constant k_{CA} = (2.0 ± 0.3) × 10^7 M^{-1} s^{-1}. However, in this solvent, and on the 50 ns time scale, the expected C_{60}^+ cation radical absorption at 980 nm[10,11] is not seen. Moreover, any optical absorption by the presumed CA anion radical around 450 nm[18] is obscured by the strongly overlapping ground state absorption of CA itself. Thus, the detailed nature of this reaction in benzonitrile cannot be determined simply by flash photolysis. The absence of C_{60}^+ absorbance here may be related to the case of $^3C_{60}$ quenching by TCNQ, in benzonitrile, in which again neither C_{60}^+ nor $TCNQ^-$ absorptions are seen.[3] This has been attributed to formation only of a weakly polar triplet exciplex absorbing at shorter wavelength.[3]

Time-Resolved Magnetic Resonance (FT-EPR). More detailed information is given by FT-EPR observation of both $^3C_{60}$ and CA^- radicals. Figure 2a shows FT-EPR spectra from a solution of C_{60} (0.2 mM) with CA (9.9 mM) in benzonitrile for a series of delay times (10 ns–200 μs) between photoexcitation of C_{60} and a $\pi/2$ microwave pulse. In addition to the resonance peak from $^3C_{60}$ (g = 2.0012)[7,12] observed at early times, the spectra show a signal with g = 2.0057 assigned to the chloranil anion (CA^-). We confirmed the assignment by comparison with the spectrum from CA^- prepared by in situ electrolysis.

The time dependence of the intensities of the resonance peaks is displayed in Figure 2b. The signal from $^3C_{60}$ increases in intensity for $0 \le \tau_d \le 1$ μs as the triplet spin system relaxes to thermal equilibrium.[7,19] The signal from CA^- initially is in emission and becomes absorptive for $\tau_d > 5$ μs. The emissive signal can be attributed to spin polarization generated in the transient radical pair [C_{60}^+···CA^-] by the radical pair chemically induced dynamic electron polarization mechanism (RPM CIDEP[20]). Spin–lattice relaxation turns the signal from emission into absorption at longer delay times. As in the optical transient absorption measurements, no signal corresponding to C_{60}^+ is detected, nor is C_{60}^- detected with FT-EPR in reductive triplet quenching reactions.[7] In both cases this is perhaps due to a short T_2.

The time development of the intensity of the resonances is similar to that found in the study of reductive quenching of C_{60}

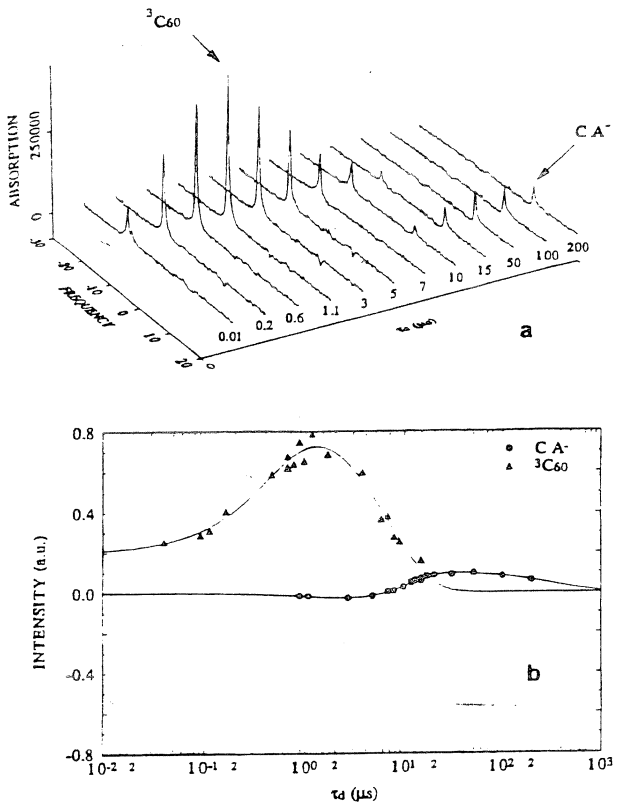

Figure 2. (a) Time evolution of the FT-EPR spectrum given by a solution of C_{60} (2×10^{-4} M) with CA (9.9×10^{-3} M) in benzonitrile following pulsed laser excitation of C_{60}. (b) Time profiles of the intensities of the $^3C_{60}$ and CA^- resonance peaks. The solid lines represent results of the data analysis described in the text.

triplets by hydroquinone and tritolylamine.[7] As discussed previously,[7,19] the time profile of the $^3C_{60}$ signal is determined by the spin polarization (P) with which the triplets are born, the spin–lattice relaxation rate (k_1^T), and the pseudo-first-order rate of triplet decay (k_d). A small second-order contribution to the triplet decay[19,21] is ignored. The solid line in Figure 2b gives the last-squares fit of the $^3C_{60}$ data based on this model. The analysis[7,19] gives the following data: $k_1^T = 2.7 \times 10^6$ s^{-1} ($T_1^T = 0.37$ μs), $k_d = (2.0 \pm 0.3) \times 10^5$ s^{-1}, and P (given as fraction of Boltzmann polarization) is 0.21. The values of k_1^T and P are in good agreement with previous results.[7,19] The decay rate is given by $k_d = k_0 + k_q$ [CA], where k_0 (0.4×10^5 s^{-1})[7] is the rate in the absence of quencher and k_q is the rate constant of electron-transfer quenching. Since [CA] = 9.9 mM, the triplet signal decay gives $k_q = (1.6 \pm 0.3) \times 10^7$ M^{-1} s^{-1}, in good agreement with the flash photolysis result.

The time evolution of the CA^- signal is described by a model[22] that takes into account rates of radical formation and decay as well as generation and decay of RPM CIDEP. The least-squares fit of the CA^- data, shown by the solid line in Figure 2b, gives a pseudo-first-order rate constant of radical formation of $k_f = (2.0 \pm 0.3) \times 10^5$ s^{-1} and a spin–lattice relaxation rate of 0.19×10^6 s^{-1} ($T_1^D = 5.3$ μs). This value of T_1^D is in agreement with that given by a direct relaxation measurement using the standard inversion-recovery method. The measured rates of $^3C_{60}$ quenching and CA^- formation are closely matched. It can be concluded that the FT-EPR data establish that C_{60} triplets are quenched oxidatively by CA giving CA^- free radicals.

Triplet quenching is expected to favor cage escape of products because of spin restriction on back electron transfer during the lifetime of the $^3[C_{60}^+ \cdots CA^-]$ radical pair. The yield of bulk CA^- can be derived from the magnetic resonance data since signal intensities are a measure of spin concentrations. The analysis of the time profiles of the $^3C_{60}$ and CA^- resonances makes it possible to calculate intensities that would obtain at thermal equilibrium in the absence of decay processes. If the CA^- concentration equaled that of the triplet precursor, the ratio of CA^- signal intensity over $^3C_{60}$ signal intensity at Boltzmann equilibrium would be 3/8, the ratio of magnetic moments. Experimentally, we find a ratio of ~0.076 so that only 20 ± 10% of the quenching events yield cage escape products. The uncertainty in this result is relatively large because of propagation of errors in fitting parameters. The rather low yield of cage escape products may be due to spin–orbit coupling in the chlorinated quinone anion radical.[23] It may be partly responsible for the failure to detect the C_{60}^+ cation with flash photolysis or FT-EPR.

ΔG^0 of the photoinduced electron-transfer reaction in benzonitrile (dielectric constant 26) can be estimated using the Rehm–Weller equation[24] given that the triplet energy (E_T) of C_{60} is 1.57 eV,[25-27] E_{ox}^0 of C_{60} is 1.76 V (SCE, in benzonitrile),[28] E_{red}^0 of CA is 0.07 V (SCE, in benzonitrile),[29] and assuming an acceptor–donor distance of ~7 Å.[1,2] With these values $\Delta G^0 \sim 0.04$ V. The low value of the electron-transfer rate constant (2×10^7 M^{-1} s^{-1}) derived from both flash and FT-EPR data is consistent with a very small thermodynamic driving force. The result may be compared with published data on reductive quenching. For the reaction of $^3C_{60}$ with tritolylamine in benzonitrile ($\Delta G^0 \sim -0.36$ V) the rate constant is 3.5×10^9 M^{-1} s^{-1},[2,7] and with diethylamine ($\Delta G^0 \sim -0.17$ V) Arbogast et al.[1] report 4.2×10^7 M^{-1} s^{-1}.

The rate constant of $^3C_{60}$ quenching by CA in toluene, determined by measuring the rate of decay of the FT-EPR signal from the triplet, is 0.6×10^7 M^{-1} s^{-1}. In this nonpolar solvent FT-EPR spectra only show the resonance peak from $^3C_{60}$. There is no evidence of cage escape product.

Flash Photolysis Study of Reactions of $^3C_{60}$ with Perylene. *Kinetics.* In benzonitrile solution Pe quenches $^3C_{60}$ with rate constant (1.4 ± 0.1) $\times 10^9$ M^{-1} s^{-1}, obtained from the decay of the 750 nm triplet absorption. The transient spectrum given in Figure 3 shows peaks at 1080, 555, and 485 nm which are unambiguously assigned respectively to the ion radicals, C_{60}^- and Pe^-,[30] and to the triplet, ^3Pe.[31,32] Thus, both electron- and energy-transfer reactions contribute to the quenching process:

$$^3C_{60} + Pe \rightarrow C_{60}^- + Pe^+ \quad (1)$$

$$^3C_{60} + Pe \rightarrow C_{60} + {}^3Pe \quad (2)$$

Reaction 1 can be followed most clearly at the absorption peak of C_{60}^-. Assuming pseudo-first-order radical formation and second-order radical decay (k_d),[13] we fit the 1080 nm transient profile with k_q ($=k_1 + k_2$) = (1.1 ± 0.3) $\times 10^9$ M^{-1} s^{-1}, in fair agreement with the measurement at 750 nm, and $k_d/\epsilon(C_{60}^-)_{1080}$ = (4.2 ± 0.5) $\times 10^5$ cm s^{-1}. With $\epsilon(C_{60}^-) = 18\,300 \pm 1100$ M^{-1} cm^{-1}, determined above, we obtain $k_d = (7.7 \pm 1.2) \times 10^9$ M^{-1} s^{-1} for the bulk radical recombination rate, very close to the diffusion-controlled value and comparable to that found[2] for reaction of C_{60}^- with TTA^-.

Quantum Yields. Nonlinear least-squares analysis of the transient profiles gives also the values of product absorbances (ΔD_λ^∞) corrected for decay during the formation period and corresponding to total product yields.[13] Quantum yields referred to the triplet are then given by

$$\phi = [\Delta D_\lambda^\infty(\text{prod})/\Delta D_{750}^0][\epsilon(^3C_{60})_{750}/\epsilon(\text{prod})_\lambda]$$

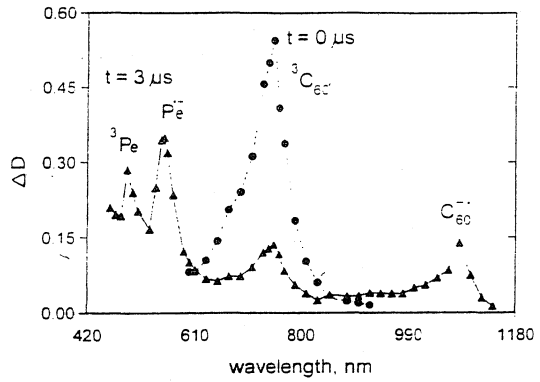

Figure 3. Time-resolved absorption spectra from a solution of C_{60} (~5×10^{-5} M) and perylene (5×10^{-4} M) in benzonitrile immediately (●) and 3 μs (▲) after flash.

TABLE 1: Data for Determination of Electron and Energy Transfer Yields of $^3C_{60}$ + Pe

wavelength (nm)	485	555	750	1080
transient absorbance	0.302[a]	0.303[a]	0.394[b]	0.122[a]
assignm	extinction coefficients, M^{-1} cm^{-1}			
$^3C_{60}$			16000[c]	
C_{60}^-	2500[d]	3800[d]		18300[e]
^{3}Pe	13400[f]	1900[g]		
Pe^+	5000[h]	50000[h]		

[a] ΔD_λ^∞, total product absorbance.[13] [b] ΔD^0, initial triplet absorbance. [c] Reference 2. [d] Reference 2. [e] This work. [f] Reference 31. [g] Reference 32. [h] Reference 30.

where ΔD^0_{750} is the initial absorbance of $^3C_{60}$. Since $\phi_T(^3C_{60})$ is close to unity,[8] these quantum yields may be taken to be essentially overall values.

Table 1 gives relevant data, including extinction coefficients at triplet and radical peaks, and average values of the ΔD's normalized to constant flash energy. The quantum yield of the electron transfer (LT) process, reaction 1, is determined directly from the initial $^3C_{60}$ absorption (ΔD^0_{750}) and total C_{60}^- absorption (ΔD^0_{1080}),[13] giving $\phi_{LT} = 0.26 \pm 0.03$. The quantum yield for the energy transfer (NT) process, reaction 2, was obtained from ΔD^∞_{485}, corresponding mainly to ^{3}Pe absorption. Corrections were made for absorption contributions at this wavelength (see Table 1) by C_{60}^-, derived from the 1080 nm measurement, and Pe^+, which was taken to be stoichiometrically equivalent to C_{60}^-. Corrections for C_{60} bleaching due to C_{60}^- formation were negligible. This gave $\phi_{NT} = 0.76 \pm 0.15$, in which the large uncertainty includes conservatively estimated errors in ϵ's as well as ΔD's. Finally, ϕ_{LT} was obtained also from the Pe^+ peak at 555 nm, corrected again for overlapping absorbances of C_{60}^- and ^{3}Pe. This method gave $\phi_{LT} = 0.20 \pm 0.07$, in reasonable agreement with the 1080 nm based value. Within the considerable uncertainty of these results, it thus appears that the total yield of energy transfer and bulk radical formation in the $^3C_{60}$ + Pe reaction is not far from unity. The result suggests that cage escape yield of radicals ions formed by reductive quenching of $^3C_{60}$ in this case is higher than that found (~0.3–0.4) in other $^3C_{60}$ charge-transfer quenching reactions.[2,33]

From the rate constant of overall quenching of $^3C_{60}$ by Pe, $(1.4 \pm 0.1) \times 10^9$ M^{-1} s^{-1}, and the quantum yields, we obtain $k_{NT} = (1.1 \pm 0.2) \times 10^9$ and $k_{LT} = (3.6 \pm 0.4) \times 10^8$ M^{-1} s^{-1} for the rate constants of energy and electron transfer, respectively. These rates may be compared with the ΔG^0 values of reactions 1 and 2. The triplet energies of $^3C_{60}$ and ^{3}Pe are 36.3[26,27] and 36.1 kcal/mol,[34] respectively, so that the energy transfer process is essentially thermoneutral. Its rate, slightly

TABLE 2

reactions	rate constants (M^{-1} s^{-1})[a] flash data	FT-EPR data	ΔG^0 (V)
$^3C_{60}$ + CA → C_{60}^+ + CA^-	2.0(0.3) × 10^7	1.6(0.2) × 10^7	0.04
$^3C_{60}$ + Pe → C_{60}^- + Pe^+	3.6(0.4) × 10^8		−0.13
$^3C_{60}$ + Pe → C_{60} + ^{3}Pe	1.1(0.2) × 10^9	1.3(0.2) × 10^9 [b]	0
$^3C_{60}$ + TTA → C_{60}^- + TTA^+	3.5(0.3) × 10^9 [c]	3.1(0.3) × 10^9 [d]	−0.36
^{3}Pe + CA → Pe^+ + CA^-		5.6(0.3) × 10^9 [e]	−0.5
C_{60}^- + CA → C_{60} + CA^-	2.5(1.0) × 10^9 [f]	4.4(0.3) × 10^9 [g]	−0.4
C_{60}^- + Pe^+ → C_{60} + Pe	1.2(0.2) × 10^{10} [h]		−1.52[i]
CA^- + Pe^+ → CA + Pe	1.3(0.2) × 10^{10} [j]		−1.14[i]

[a] Solvent benzonitrile, at room temperature. [b] Overall (energy and electron transfer) $^3C_{60}$ quenching rate constant derived from [Pe] dependence of $^3C_{60}$ resonance intensity. [c] From ref 2. [d] From ref 7. [e] From analysis of time profile of CA^- signal intensity, Pe directly excited with 440 nm laser light. [f] From effect of CA on decay of C_{60}^- under conditions where reductive quenching of $^3C_{60}$ by TTA is fast compared to electron transfer from C_{60}^- to CA. [g] From kinetics of CA^- generation upon excitation of C_{60} in the presence of TTA and CA, conditions as in *f*. [h] From second-order decay of C_{60}^- monitored at 1080 nm. [i] In benzonitrile with 0.1 M TBAHP. [j] From second-order decay of Pe^+ (cf. Figure 4C).

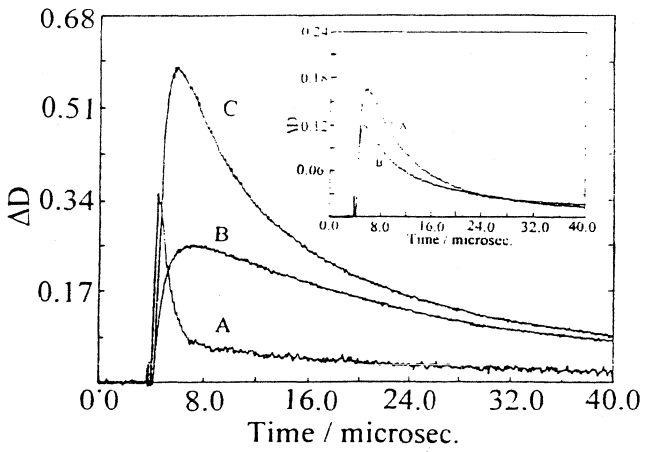

Figure 4. Flash transient time profiles of benzonitrile solutions of C_{60} (3×10^{-4} M) with Pe (6×10^{-4} M): A, At 750 nm ($^3C_{60}$); B, at 555 nm (mainly Pe^+); C, at 555 nm after addition of CA (6×10^{-3} M). Insert: A, 485 nm (mainly ^{3}Pe), solution as in A, B above; B, 485 nm solution as in C above.

below the diffusion-controlled value, matches that found for similar cases[35] and is consistent with the relation $k_{NT} = k_{dif}/[1 + \exp(-\Delta E_T/RT)]$.[35] The oxidation potential of Pe in benzonitrile measured relative to the reduction potential of C_{60} in the same solution is 1.52 V, directly giving ΔG^0 for the ground state electron-transfer reaction. Taking the interradical distance as ~7 Å,[1,2] we then obtain $\Delta G^0_{LT} \sim -0.13$ eV for the triplet quenching process.[24] Since a larger reorganization energy barrier is expected for electron transfer compared with energy transfer, the slower electron-transfer rate despite the more favorable ΔG^0 is reasonable.

Electron Transfer Mediated by $^3C_{60}$. *Flash Photolysis.* Addition of chloranil (CA) to the C_{60}/Pe system at relative concentrations such that primary quenching of $^3C_{60}$ occurs almost exclusively by reaction with Pe (see rate constants, Table 2) leads to the transient time profiles shown in Figure 4. We see (Figure 4B,C) a marked increase in the peak at 555 nm (Pe^+) and a decrease in the absorbance at 485 nm due to replacement of ^{3}Pe by weakly absorbing Pe^- and CA^- (Figure 4, insert). CA also causes more rapid disappearance of the C_{60}^- absorption at 1080 nm; in fact, with the conditions and time scale that apply for Figure 4, no C_{60}^- is seen at all. An associated formation of CA^- is demonstrated by EPR measurements described below. These results demonstrate the following

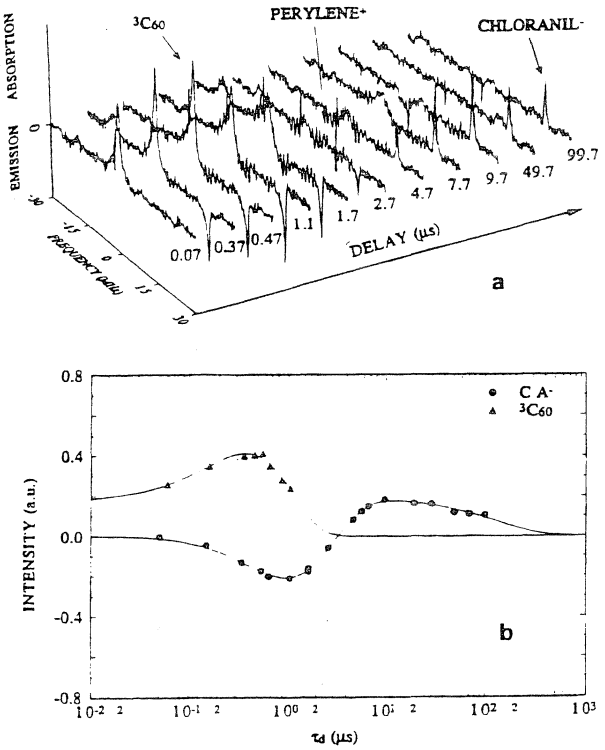

Figure 5. (a) Time evolution of the FT-EPR spectrum given by a solution of C_{60} (2.3×10^{-4} M), perylene (6.3×10^{-4} M), and CA (5.3×10^{-3} M) in benzonitrile following pulsed laser excitation of C_{60}. (b) Time profiles of the intensities of the $^3C_{60}$ and CA^- resonance peaks. The solid lines represent results of the data analysis described in the text.

secondary processes,

$$C_{60}^- + CA \xrightarrow{k_3} C_{60} + CA^- \quad (3)$$

$$^3Pe + CA \xrightarrow{k_4} Pe^+ + CA^- \quad (4)$$

in which C_{60}^- and ^3Pe are formed in the primary $^3C_{60}$ quenching reactions 1 and 2, respectively. The rate constant k_3, derived from the decay of 1080 nm absorbance as function of [CA], is $(2.5 \pm 1) \times 10^9\ M^{-1}\ s^{-1}$. The final decay of 555 nm absorbance is second order with rate constant $(1.3 \pm 0.2) \times 10^{10}\ M^{-1}\ s^{-1}$.

Under the conditions of Figure 4C, with almost total trapping of $^3C_{60}$ by Pe and of ^3Pe by CA, ΔD^{∞}_{555} is due to Pe^+ alone, and we obtain the overall yield of Pe^+, $\phi_{rad} = 0.62 \pm 0.04$. The contribution from the electron-transfer quenching of $^3C_{60}$ by perylene to ϕ_{rad} is ~0.26 (vide supra). The remainder is formed via the alternative route, energy transfer (2) followed by oxidative quenching of ^3Pe by CA (4). The value obtained earlier for the quantum yield of (2) $\phi_{NT} = 0.76 \pm 0.15$ so that the yield of (4) becomes 0.47 ± 0.10. Assuming reasonably that the unidirectional electron transfer in (3) occurs with unit efficiency, the flash photolysis data show that the overall yield of CA^- also must be ~0.62. FT-EPR measurements, which permit following the formation and decay of CA^- directly, support and extend these findings.

FT-EPR Results. Figure 5 shows a series of FT-EPR spectra given by a benzonitrile solution containing C_{60} (0.23 mM), Pe (0.63 mM), and CA (5.3 mM) excited with 532 nm laser pulses. A number of features distinguish these spectra from those given by C_{60}/CA (cf. Figure 2). (a) Both the rates of $^3C_{60}$ decay and CA^- formation have increased by the introduction of Pe even though the CA concentration has been reduced. (b) Additional

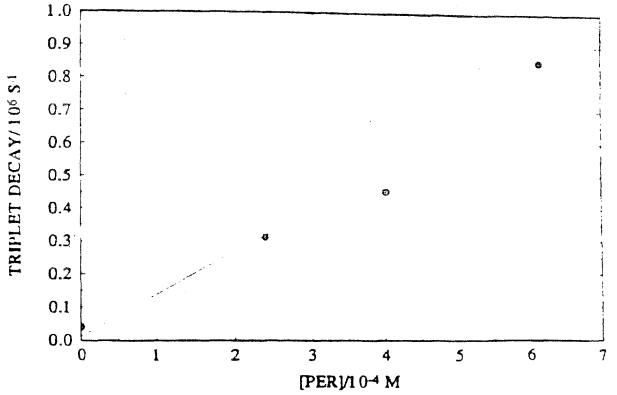

Figure 6. Rate of $^3C_{60}$ resonance peak decay as function of perylene concentration.

(weak) resonances due to Pe^+ are observed. (c) The intensity of the CA^- resonance has increased relative to the $^3C_{60}$ resonance.

In interpreting these results, we note first that the flash photolysis measurement of $^3C_{60}$ quenching by Pe is quantitatively confirmed by the dependence of the decay rate of the $^3C_{60}$ resonance on [Pe] (Figure 6) which gives an overall quenching rate constant of $(1.3 \pm 0.2) \times 10^9\ M^{-1}\ s^{-1}$, in good agreement with the flash photolysis value. Furthermore, the observation of resonance peaks due to Pe^- in the FT-EPR spectra is in accord with the photolysis finding that $^3C_{60}$ quenching by Pe occurs, at least in part, via the electron-transfer route (reaction 1).

Given the two mechanisms of $^3C_{60}$ quenching by Pe identified by flash photolysis, CA^- can be formed by (I) subsequent electron transfer from C_{60}^- (reaction 3, $\Delta G^0 \sim -0.4$ V) and/or (II) oxidative quenching of ^3Pe (reaction 4, $\Delta G^0 \sim -0.5$ V). From the fact that CA^- gives an emissive resonance at early times, we conclude that the dominant signal contribution is made by the ^3Pe quenching route (II). This conclusion is based on the following considerations. The spin polarization with which CA^- is born if formed via (II) can contain a triplet mechanism (TM) and a radical pair mechanism (RPM) component.[20] Since ^3Pe is formed by energy transfer from $^3C_{60}$, which initially carries little or no polarization,[7,19] the CA^- TM signal contribution must be absorptive but small since it cannot exceed the (triplet) thermal equilibrium value. On the other hand, spin state evolution in the radical pair $[Pe^+ \cdots CA^-]$ gives rise to an emissive signal contribution because $g(CA^-)(2.0057) > g(Pe^-)(2.002\ 57)$.[20] The magnitude of the RPM polarization is expected[22] to far exceed that given by the TM so that CIDEP will give rise to an emissive resonance peak. For the alternative reaction path, reductive quenching of $^3C_{60}$ followed by reduction of CA by the C_{60} anion, the spin polarization of CA^- is that carried over from C_{60}^-, and the TM contribution is absorptive for the reason given above. The RPM contribution is absorptive as well in this case since $g(C_{60}^-) < g(Pe^+)$.[20] Therefore, this route cannot account for the observed CIDEP effect.

The TM contribution is expected to be small for both reaction paths so that initial signal intensities will depend predominantly on RPM CIDEP. On the basis of the g values of the free radicals forming the radical pairs that are involved in CA^- formation, $[C_{60}^- \cdots Pe^+]$ and $[CA^- \cdots Pe^+]$, it can be concluded that RPM spin polarization generated by the pairs must be of similar magnitude. However, the contribution to the CA^- resonance by reductive quenching of $^3C_{60}$ by Pe followed by electron transfer from C_{60}^- to CA is expected to be strongly attenuated by the short spin–lattice relaxation time of the C_{60}

anion.[9b] This combined with the flash photolysis finding that energy transfer much exceeds electron transfer in the $^3C_{60}$ + Pe reaction leads to the conclusion that (I) makes only a minor contribution to the CA^- resonance for short delay times (i.e., before thermal equilibrium has been established).

The time profiles of the intensities of the $^3C_{60}$ and CA^- signals were analyzed quantitatively in order to derive values of the rate constants of the processes involved in the formation of the anion radicals. The analysis of the time evolution of the $^3C_{60}$ peak, as described earlier,[7,19] gives the value of the overall triplet quenching rate constant. The generation of CA^- involves contributions from routes I and II. An analysis of the time profile of the CA^- signal intensity in terms of a model that takes both these contributions into account is not feasible because of the large number of parameters involved. It is known, however, that (II) is the dominant path and in addition gives enhanced signal intensity because of spin polarization (vide supra). Therefore, a treatment based on the assumption that (I) makes a negligible contribution is expected to give reasonable results that can serve to establish that CA^- formation is a two-step process. The following conditions were applied in the numerical analysis of the data: (a) $^3C_{60}$ quenching by Pe (reaction 2) is a pseudo-first-order process ([Pe] $\gg$ [$^3C_{60}$]) and mainly determines the rate (k_{NT}) of decay of C_{60} triplets, (b) similarly, since [CA] $\gg$ [^{3}Pe], CA^- formation by electron transfer from ^{3}Pe (reaction 4) is pseudo-first-order (rate constant k_{LT}), (c) first-order chemical decay of CA^- (rate constant k_d). Actually, decay involves back electron transfer and is a second-order process. The error introduced by this simplification is not expected to affect values of rate constants that control time evolution during the first 10−20 μs, which are of primary interest here.

EPR signal intensity is proportional to the difference in population (n) of β and α spin states in CA^-. Given the approximations outlined above, the time evolution of n is given by

$$\frac{d}{dt}[n] = \alpha k_{NT}[^3\text{Pe}] + k_l^D(n_B - n) - k_d n \qquad (5)$$

In this equation, α represents CIDEP (TM and RPM) generating processes, $n_B = 0.75 \times 10^{-3}[CA^-]$ is the thermal equilibrium population difference, and k_l^D is the CA^- spin−lattice relaxation rate. A closed-form expression for the time evolution of n is readily derived given the proposed reaction scheme and specified conditions. Least-squares fitting of the experimental data to the theoretical expression is aided by the fact that values of rates k_{NT} and k_l^D are given by the time development of the $^3C_{60}$ resonance and relaxation time measurements, respectively. According to the model, by adjusting the relative concentrations of Pe and CA, triplet−triplet energy transfer (2) or electron transfer (4) can be made the rate-limiting step in CA^- formation. Time profiles of the resonances for these limiting conditions are shown in Figure 7. That $^3C_{60}$ quenching can be decoupled from CA^- formation by adjusting the concentrations so that quenching of ^{3}Pe is the rate-limiting step is evident in Figure 7b. The solid lines in Figures 5 and 7 give the calculated CA^- signal intensity profiles. Calculated and experimental data are in close agreement, providing additional support for the proposed mechanism. From the relative intensities of the $^3C_{60}$ and CA^- signals we calculate that 51 ± 15% of the triplets give rise to anion radicals. This result, within the uncertainty of both determinations, is comparable to the overall yield, $\Phi_{rad} = 0.62 \pm 0.04$, determined by flash photolysis (cf. Figure 4C). Therefore, compared to the direct oxidative quenching of C_{60} triplets by CA, the yield of free radicals has more than doubled.

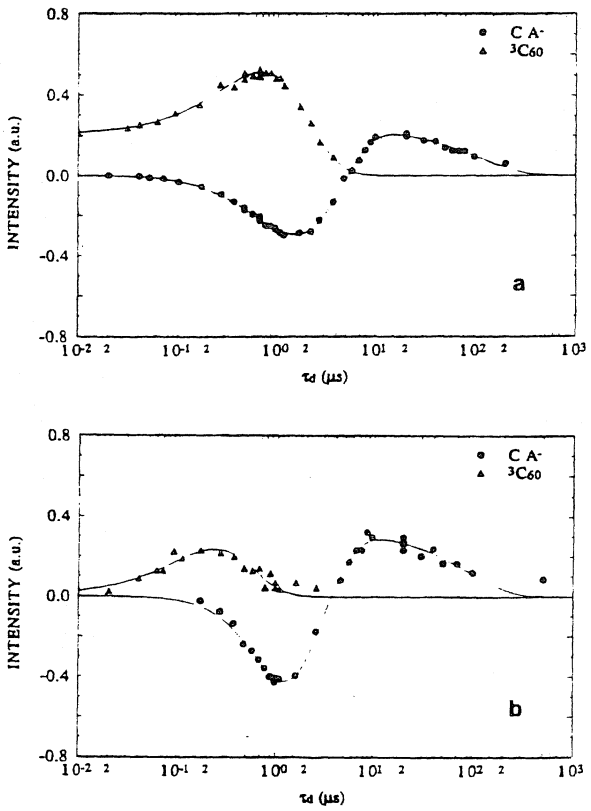

Figure 7. Time profiles of the intensities of the $^3C_{60}$ and CA^- resonance peaks given by solutions of C_{60} (2×10^{-4} M), Pe, and CA in benzonitrile: (a) Pe limiting, [Pe] = 4×10^{-4} M, [CA] = 4.1×10^{-3} M; (b) CA limiting, [Pe] = 2×10^{-3} M, [CA] = 3.3×10^{-4} M. The solid lines represent results of the data analysis described in the text.

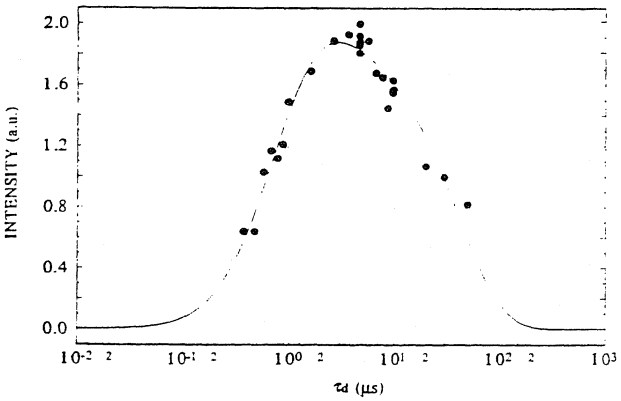

Figure 8. Time profile of the CA^- resonance peak given by a benzonitrile solution of C_{60} (2×10^{-4} M), tritolylamine (1.9×10^{-3} M), and CA (3.6×10^{-4} M) following laser excitation of C_{60}.

The C_{60}/TTA/CA System. The kinetics and spin dynamics of reaction 3 are conveniently studied with the C_{60}/TTA/CA system. Flash photolysis[2] and FT-EPR[7] measurements show that $^3C_{60}$ is reductively quenched by TTA at near diffusion-controlled rate. Therefore, in the C_{60}/TTA/CA (solvent benzonitrile) system, photoexcitation of C_{60} generates C_{60}^- and TTA^+ in the initial step. In a followup reaction CA^- is formed by electron transfer from C_{60}^-. Figure 8 shows that in this case the signal from CA^- is in absorption for all delay times in agreement with the CIDEP pattern predicted for this reaction sequence. In the initial triplet quenching step the C_{60} anion, which is not observed in the FT-EPR spectrum probably because of a short T_2, is formed with positive spin polarization stemming from TM and RPM CIDEP ($g(C_{60}^-) < g(TTA^+)$[36]). In the subsequent electron-transfer step, $C_{60}^- + CA \rightarrow C_{60} + CA^-$,

any spin polarization of the precursor is transferred to the quinone. Therefore, the CA^- resonance is expected to be in absorption.

The time profile of the intensity of the CA^- resonance was analyzed in terms of formation and decay steps taking spin polarization into account.[7]. The least-squares fit to the experimental data is given by the solid line in Figure 8.

Table 2 summarizes rate constants and yields measured in this work.

Conclusions

Flash photolysis and FT-EPR studies show that C_{60} triplets are quenched by chloranil. FT-EPR spectra establish that encounters between $^3C_{60}$ and CA in benzonitrile leads to formation of CA^- free radicals. The rate constant of the electron-transfer reaction (cf. Table 2) is some 2 orders below the diffusion-controlled limit which can be attributed to the small thermodynamic driving force. A comparison of $^3C_{60}$ and CA^- resonance peaks shows that only about 20% of the quenching events give cage escape products.

In benzonitrile solutions of CA with Pe (or TTA) and C_{60}, excitation with visible light initiates a fast and efficient reduction of CA. In the presence of Pe, the dominant reaction path is formation of ^{3}Pe by energy transfer from $^3C_{60}$ followed by oxidative quenching of ^{3}Pe by CA. In this process the yield of CA^- compared to that of the direct excited state electron transfer from C_{60} to CA is more than doubled. With the amine, reductive quenching of $^3C_{60}$ is followed by fast electron transfer from C_{60}^- to CA. It is noteworthy that C_{60} catalyses electron-transfer reactions that cannot be driven by visible light (TTA/CA) or would be very inefficient because of low triplet quantum yield[32] (Pe/CA). Since C_{60} absorbs light over a broad range of the visible spectrum and has a triplet quantum yield close to one, it may find application in solar-driven chemical reactions.

Acknowledgment. We much appreciate financial support for this work provided by the Division of Chemical Sciences, Office of Basic Energy Sciences, of the U.S. Department of Energy to the University of Massachusetts (DE-FG02-84ER-13242) and to Brandeis University (DE-FG02-89ER14072).

References and Notes

(1) Arbogast, J. W.; Foote, C. S.; Kao, M. *J. Am. Chem. Soc.* **1992**, *114*, 2273.

(2) Biczók, L.; Linschitz, H.; Walter, R. I. *Chem. Phys. Lett.* **1992**, *195*, 339; **1994**, *221*, 188. Biczók, L.; Linschitz, H.; Walter, R. I. *Res. Chem. Intermed.* **1994**, *20*, 939.

(3) Nadtochenko, V. A.; Denisov, N. N.; Rubtsov, I. V.; Lobach, A. S.; Moravskii, A. P. *Chem. Phys. Lett.* **1993**, *208*, 431.

(4) Michaeli, S.; Meiklyar, V.; Schulz, M.; Möbius, K.; Levanon, H. *J. Phys. Chem.* **1994**, *98*, 7444.

(5) Steren, C. A.; van Willigen, H. *Proc. Indian. Acad. Sci. (Chem. Sci)* **1994**, *106*, 1671.

(6) Steren, C. A.; van Willigen, H. In *Proceedings of the Symposium on Recent Advances in Chemical Physics of Fullerenes and Related Materials*; Kadish, K. M., Ruoff, R. S., Eds.; Electrochemical Society: Pennington, NJ, **1994**; p 818.

(7) Steren, C. A.; Levstein, P. R.; van Willigen, H.; Linschitz, H.; Biczók, L. *Chem. Phys. Lett.* **1993**, *204*, 23.

(8) Reference 2 and references therein.

(9) (a) Lawson, D. R.; Feldheim, D. L.; Foss, C. A.; Dorhout, P. K.; Elliott, C. M.; Martin, C. R.; Parkinson, B. *J. Electrochem. Soc.* **1992**, *139*, 268. (b) Schell-Sorokin, A. J.; Mehran, F.; Eaton, G. R.; Eaton, S. S.; Viebeck, A.; O'Toole, T. R.; Brown, C. A. *Chem. Phys. Lett.* **1991**, *195*, 225. (c) Kato, T.; Kodama, T.; Shida, T. *Chem. Phys. Lett.* **1993**, *205*, 405.

(10) Kato, T.; Kodama, T.; Shida, T.; Nakagawa, T.; Matsui, Y.; Suzuki, S.; Shiromaru, H.; Yamauchi, K.; Achiba, Y. *Chem. Phys. Lett.* **1991**, *180*, 446.

(11) Nonell, S.; Arbogast, J. W.; Foote, C. S. *J. Phys. Chem.* **1992**, *96*, 4169.

(12) Closs, G. L.; Gautam, P.; Zhang, D.; Krusic, P. J.; Hill, S. A.; Wasserman, E. *J. Phys. Chem.* **1992**, *96*, 5228. Regev, A.; Gamliel, D.; Meiklyar, V.; Michaeli, S.; Levanon, H. *J. Phys. Chem.* **1993**, *97*, 3671.

(13) Andrews, L. J.; Levy, J. M.; Linschitz, H. *J. Photochem.* **1976–77**, *6*, 335.

(14) Levstein, P. R.; van Willigen, H. *J. Chem. Phys.* **1991**, *95*, 900.

(15) de Beer, R.; van Ormondt, D. In *Advanced EPR: Applications in Biology and Biochemistry*; Hoff, A. J., Ed.; Elsevier: Amsterdam, 1989; Chapter 4.

(16) Dubois, D.; Kadish, K. M.; Flanagan, S.; Haufler, R. E.; Chibante, L. P. S.; Wilson, L. J. *J. Am. Chem. Soc.* **1991**, *113*, 4364.

(17) Kamat, P. V. *J. Am. Chem. Soc.* **1991**, *113*, 9705.

(18) Andre, J. J.; Weil, G. *Mol. Phys.* **1968**, *15*, 97.

(19) Steren, C. A.; van Willigen, H.; Dinse, K.-P. *J. Phys. Chem.* **1994**, *98*, 7464.

(20) McLauchlan, K. A. In *Modern Pulsed and Continuous-Wave Electron Spin Resonance*; Kevan, L., Bowman, M. K., Eds.; Wiley: New York, 1990.

(21) Dimitrijević, N. M.; Kamat, P. V. *J. Phys. Chem.* **1992**, *96*, 4811.

(22) Ebersole, M. H.; Levstein, P. R.; van Willigen, H. *J. Phys. Chem.* **1992**, *96*, 9311.

(23) Winter, G.; Steiner, U. *Ber. Bunsen-Ges. Phys. Chem.* **1980**, *84*, 1203 and references therein.

(24) Rehm, D.; Weller, A. *Isr. J. Chem.* **1970**, *8*, 259.

(25) Hung, R. R.; Grabowski, J. J. *J. Phys. Chem.* **1991**, *95*, 6073.

(26) Zeng, Y.; Biczók, L.; Linschitz, H. *J. Phys. Chem.* **1992**, *96*, 5237.

(27) v. d. Heuvel, D. J.; Chan, I. Y.; Gronen, E. J. J.; Schmidt, J.; Meijer, G. *Chem. Phys. Lett.* **1994**, *231*, 111.

(28) Dubois, D.; Kadish, K. M.; Flanagan, S.; Wilson, L. J. *J. Am. Chem. Soc.* **1991**, *113*, 7773.

(29) *Handbook of Photochemistry*; Scaiano, J. C., Ed.; CRC Press: Boca Raton, FL, 1989; a correction of 0.09 V has been applied to account for a change from acetonitrile to benzonitrile as solvent.

(30) Kuroda, H.; Sakurai, T.; Akamatu, H. *Bull. Chem. Soc. Jpn.* **1966**, *39*, 1893.

(31) Carmichael, I.; Helman, W. P.; Hug, G. L. *J. Phys. Chem. Ref. Data* **1987**, *16*, 239.

(32) Nakabayashi, K.; Toki, S.; Takamuku, S. *Chem. Lett.* **1986**, 1890.

(33) Biczók, L.; Linschitz, H.; Treinin, A. In *Proceedings of the Symposium on Recent Advances in Chemistry and Physics of Fullerenes and Related Materials*; Kadish, K. M., Ruoff, R. S., Eds.; Electrochemical Society: Pennington, NJ, 1994; p 909.

(34) *Handbook of Photochemistry*; Murov, S. L.; Carmichael, I., Hug, G. L., Eds.; M. Dekker: New York, 1993.

(35) Sandros, K. *Acta Chem. Scand.* **1964**, *18*, 2355.

(36) Neugebauer, F. A.; Bamberger, S.; Groh, W. R. *Chem. Ber.* **1975**, *108*, 2406.

JP960640H

KÖSZÖNETNYILVÁNÍTÁS

Ezúton is szeretnék köszönetet mondani BÉRCES TIBOR tudományos osztályvezetőnek, az MTA levelező tagjának, aki egész tudományos fejlődésem során már a kezdetektől meghatározó szerepet töltött be. Tudományos iskola teremtő munkája, hasznos tanácsai nélkül ez a disszertáció sem jöhetett volna létre. A tőle tanultak további munkám során is alapvető jelentőségűek.

Köszönöm MÁRTA FERENC akadémikusnak, az MTA Központi Kémiai Kutatóintézet igazgatójának, hogy munkám előrehaladását mindig figyelemmel kísérte, és tanácsaival segítette.

Ugyancsak köszönet illeti tudományos publikációim valamennyi társszerzőjét, akikkel együtt végzett munka nemcsak nagyon eredményes hanem élvezetes is volt.

Köszönöm az MTA Központi Kémiai Kutatóintézet Reakciókinetikai Osztálya valamennyi jelenlegi és korábbi dolgozójának bíztatását, segítségét és gyakorlati tanácsait.